THE MECHANICAL PROPERTIES AND FRACTURE OF URANIUM

A Thesis

presented in supplication for the degree of

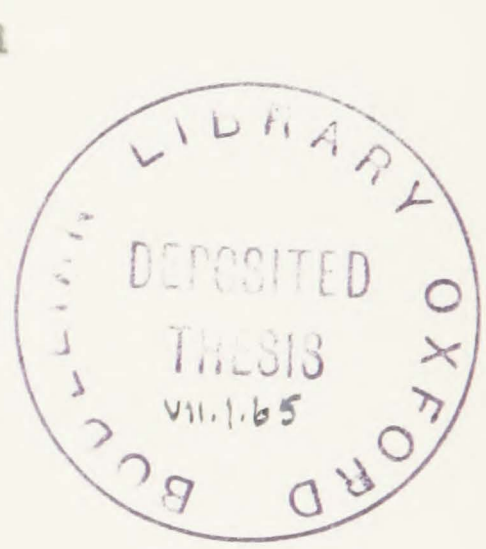
Doctor of Philosophy

in the University of Oxford

by

D.M.R.TAPLIN

St. Catherine's College



Trinity Term

1964

Department of Metallurgy

Parks Road Oxford

To my wife and children and

in remembrance of my mother

TABLE OF CONTENTS

ACKNOWLEDGEMENTS

ABSTRACT

I INTRODUCTION....1

II REVIEW OF PREVIOUS WORK....6
1. Crystallography of Uranium....6
2. Transformations in Uranium and its Alloys....8
3. Deformation Mechanisms in Uranium....15
4. Mechanical Properties of Uranium....20
5. Fracture of Uranium....23
6. Theories of Fracture....27

III SCOPE OF THE PRESENT WORK....38

IV MATERIALS....39
1. Technology of Fuel Rod Production....39
2. Composition of Materials....40
3. Preparation of Specimens....41

V APPARATUS AND EXPERIMENTAL TECHNIQUES....45
1. Thermal Treatment....45
2. Mechanical Treatment....48
3. Metallography....53

VI GENERAL METALLOGRAPHY....56
1. Examination of Second Phase....56
2. Grain Structure after Thermal Treatment....59
3. Structure after Mechanical and Thermal Treatment..68
4. Summary....74

VII FRACTURE BEHAVIOUR....76
1. Ductile Failure in Alpha....77
2. Intercrystalline Failure in Alpha....79
3. Cleavage Fracture in Alpha....87
4. Fracture of Alpha in Bending and Compression....95
5. Fracture in Beta....96

VIII MECHANICAL PROPERTIES....98
1. General Behaviour....98
2. Effect of Composition....106
3. Effect of Heat Treatment....110
4. Effect of Grain Size....123
5. Effect of Cold Work....135
6. Effect of Strain Rate....138
7. Effect of a Notch....140
8. Effect of Annealing Temperature....144

IX CONCLUSIONS....149

X REFERENCES....154

Tables I-XXV within the text; Figs 1-130 following....159

ACKNOWLEDGEMENTS

Firstly I should like to express my thanks to Dr J.W.Martin for the continual encouragement, help and advice that he has given throughout this work. I am also indebted to Professor W.Hume-Rothery for his interest and support.

This work has been made possible by the receipt of financial assistance from the United Kingdom Atomic Energy Authority and I am personally grateful for the bursary I received from 1961-1964.

The research programme was sponsored by Mr B.R.Butcher of AERE Harwell and I am grateful to him for the supply of materials, for providing experimental facilities in his section and for useful suggestions.

Finally I should like to thank my contemporaries, particularly Dr M.H.Lewis, in the Department of Metallurgy, University of Oxford, for many valuable discussions.

ABSTRACT

A study of the mechanical properties and fracture characteristics of four grades of reactor uranium has been carried out within the range -196°C and +800°C. Although the investigation is general and broadly-based without detailed examination of each aspect, particular emphasis has been placed upon the ductile/brittle transition which occurs at about room temperature.

Having considered the scientific and technological interest in this field of uranium metallurgy, there follows a comprehensive review of the relevant published work. This includes a discussion of previous reports upon the structure, transformation mechanisms, deformation, fracture and mechanical properties of uranium together with a survey of current theories of fracture.

The experimental work involved vacuum and lead bath heat treatment, tensile, notch, bend, compression and hardness testing followed by bright-field, polarized light and replica metallography.

An initial study of the microstructural effects of mechanical and thermal treatment showed how the required control of microstructural variables could be achieved. Additionally, this preliminary work suggested that the important criterion in grain-refinement upon beta-alpha quenching by alloying with iron and aluminium is the amount of dispersed network phase present which retards alpha grain growth. Contributory factors appear to be solution of these added elements in the beta phase and beta grain growth.

Three modes of fracture were observed in the alpha phase: crystallographic (low temperature), intercrystalline (in the region

of room temperature) and ductile (above room temperature). It is considered that the best explanation for the process of crystallographic failure (twin parting) is that it is nucleated at the apices of growing thick twins by a reaction involving emissary dislocations. Propagation is suggested to occur along the composition planes of the twins because these are the sites of structural distortion and stress thereby providing planes of inherent weakness in the lattice. Tests after thermal cycling established that an intergranular path of fracture is favoured because the anisotropy of thermal expansion gives rise to residual grain boundary stresses to a varying degree after most heat treatments thereby lowering the surface energy for fracture in these areas. Ductile failure occurred by the formation of cavities at cuboid inclusions which grew and, in the centre of the externally necked region, coalesced to form a macroscopic fissure which propagated outwards to cause failure. Below about 300°C cavity formation tended to occur at an early stage by cuboid cleavage, whilst above 300°C cavities tended to be formed at a later stage by inclusion/matrix parting.

The ductile/brittle transition may be attributed to increasing dislocation friction stress with decreasing temperature such that stresses at twin apices and composition planes are not readily accommodated and parting failure thereby facilitated. It is possible that with decreasing temperature there is a change in the electronic configuration to cause stronger covalent bonding and the transition can be explained in these terms.

All these changes in fracture behaviour are reflected in the tensile properties and consequently an explanation for the effect of temperature upon many of these properties follows. A number of variables were shown to lower the ductile/brittle transition temperature including:-

a) decreasing volume fractions of the finely dispersed intermetallic network (i.e. increasing purity),
b) decreasing grain size,
c) increasing amounts of cold-work or pre-strain,
d) decreasing strain-rate.

These effects can be mainly explained by invoking current theories of fracture. Additionally the transition temperature was shown to be sensitive to heat treatment. Heat treatment can cause variations in the surface energy for fracture at grain boundaries giving rise to intercrystalline embrittlement and promoting brittle fracture, thus providing an explanation.

The brittle (parting) fracture stress of polycrystalline alpha decreases progressively with decreasing temperature. This may be related to the anisotropic structure which results in a very low yield stress. No simple fracture stress/grain size (d) relationship was found but if account is taken of all the influencing factors in alpha uranium the results might be explained in terms of the usual $d^{-\frac{1}{2}}$ relationship.

Beta uranium was shown to be brittle both in the beta region (when fracture appears to take an intergranular path) and when retained to room temperature (and below) by quenching an iron and aluminium rich grade (when failure appears to be by crystallographic cleavage).

I INTRODUCTION

As a consequence of years of research the plastic behaviour of many metals under a variety of conditions is fairly well known and there exists some degree of understanding of the basic mechanisms. This work has, however, been largely restricted to metals with structures of high symmetry — cubic and hexagonal — and since the room temperature form of uranium is orthorhombic in which the atom bonds are partly covalent much interest is attached to its plastic behaviour. The research described in this thesis was undertaken with the object of investigating some of the properties of uranium and subsequently correlating the results with the behaviour of other metals. However, the work also has some technological relevance and to understand this it is appropriate to consider the practical applications of uranium: as fuel elements in nuclear reactors and in atomic weapons.

The essential requirement in these applications is a self-sustaining nuclear chain reaction (criticality) and this depends on neutrons not being lost from the fissionable material at a faster rate than they are generated. This is related to the mass and surface area of the material and the speed of the neutrons. The nuclear energy is made available in the form of heat and, according to conditions, this may be evolved at a controlled rate as in nuclear reactors, or with explosive rapidity, as in nuclear weapons.

Although other fissile materials can be produced by neutron absorption and decay processes, the only naturally-occurring nuclear fuel is the 235 isotope of uranium which constitutes about 0.7% of natural uranium. This material can only be made critical if in very large masses and in special conditions. Nevertheless it is important as a commercial reactor fuel.

Apart from the loss in activity due to burn-up of the fissile atoms, one of the major factors limiting the life of a fuel element is the dimensional stability of the uranium. During irradiation uranium suffers changes in length, surface wrinkling, general distortion and swelling. These effects must be curtailed otherwise puncturing of the protective sheath results with consequent attack by the coolant fluid and release of radio-active products. The first two phenomena are associated with physical changes in uranium produced by irradiation and thermal cycling, which is related to the anisotropy of the crystal structure. From a practical viewpoint, the solution to the problem is a random orientation of very fine grains which can be approximated by a heat treatment procedure. General distortion occurs as a result of relief of internal stresses produced during fabrication and irradiation. Swelling is partly accounted for by an increase in the total number of atoms present, particularly by the formation of bubbles of inert gases. The number of factors known, or suspected, to influence the swelling behaviour of uranium is very large. Structural and irradiation variables and a number of properties of the material are involved including yield strength, brittleness and tendency for intercrystalline cracking (Pugh 1960).

A study of the factors which influence these properties may be helpful in reducing swelling. Also, complex stresses of considerable magnitude arise in the fuel when it is in the reactor and the mechanical properties of uranium at both room and elevated temperatures are therefore important considerations in fuel element design. It is relevent to note that, although ceramics are likely to be the dominant fuel of the future because of increased reactor temperatures, metallic fuels will be important for many years to come (U.K.A.E.A. Annual Report 1963).

Atomic weapons development comes under the Official Secrets Act (1911-1939) but many of the problems are well known. Fully enriched uranium (U-235) is used, the amount quoted being 1-100Kg. One problem in any bomb (chemical or nuclear) is the containment of the explosion until the chain reaction develops fully. For this purpose a ductile material is required and commercial uranium exhibits a ductile/brittle transition at room temperature. If the factors which influence the transition were known and understood it might be possible to increase the ductility and hence solve some of the problems of containing the explosion. The most recent hydrogen bombs, which are detonated by a uranium bomb, are surrounded by natural uranium in which a further nuclear reaction develops producing an even greater destructive force. This material must also be ductile for maximum efficiency. Uranium also presents a number of difficulties during fabrication of weapon components and a knowledge of the mechanical properties may be helpful in this context.

Apart from the scientific and technological interest, a consideration of the present knowledge within the prescribed field is necessary before deciding upon a research programme. Although a great deal of information is available on the mechanical properties of uranium, the many influencing factors such as grain size, orientation, heat treatment, fabrication route and purity are unstated in much of the data and the remaining data is very inconsistent. This wide variation is perhaps explained by the ductile/brittle transition, since near room temperature the properties are changing rapidly; no systematic investigation of the transition had been reported. A comprehensive study of the mechanical properties of uranium with particular reference to the ductile/brittle transition was clearly needed. Previous work on fracture appeared to be limited to that of Davies (1962) who made a fractographic study of uranium but much of his work was on as-cast untreated material which is liable to gross inhomogeneity of structure. A study of fracture was therefore also necessary particularly the correlation of metallography of fracture with mechanical properties.

The general field of study decided, it was then important to consider how this could be best implemented within the limitations of the existing facilities. Uranium presents some hazards in handling since it is radioactive, pyrophoric and the oxide dust is toxic. The first limitation was upon specimen preparation which had to be carried out under special conditions at AERE Harwell. Consequently mechanical and thermal treatments were preferably carried out on the machined specimens. Secondly although super-

purity material would have been more suitable this could apparently only be supplied from France and became unavailable after the decrease in Anglo-French co-operation following the breakdown in Common Market negotiations. This was a considerable limitation for the material used was only commercially pure and contained about 5% volume fraction of inclusions. Also present were a number of defects in some of the material. The specimens used initially were either cut from longitudinally quartered cast bars (eliminating the axial pipe), which contained a small proportion of shrinkage porosity, or from rolled cast bars, which contained a high proportion of defects. Clearly the results obtained on this type of material are suspect. However, material cut from a large ingot and subjected to a rolling and annealing schedule became available for much of the work and specimens machined from this material were sound and the results obtained reliable.

With these prescribed limitations it was considered more valuable to make a broadly based general study rather than a detailed study of one aspect. A major drawback therefore, is that although the influence of a number of variables on the mechanical and fracture behvaiour have been examined, a detailed study of all the mechanisms involved has not been possible.

II REVIEW OF PREVIOUS WORK

1 Crystallography of Uranium

Pure uranium can exist in three allotropic modifications in the solid state and although there has been some diversity in the values of the transformation temperatures reported, these have now been established using re-melted high purity electrolytic material (Blumenthal 1960):-

alpha - beta : 667.7 ± 1.3°C

beta - gamma : 774.8 ± 1.6°C

gamma - liquid : 1132.8 ± 0.8°C

1-a Structure of Alpha Uranium

Early work suggested a cubic, then a monoclinic structure for alpha uranium but Jacob and Warren (1937) first described the orthorhombic structure which Lukesh (1949) confirmed and is accepted today. The arrangement of atoms, with the room temperature lattice parameters is shown in Fig.1. The structure bears some resemblance to that of a hexagonal metal except that successive layers of atoms in the basal plane are skewed back and forth in the [010] direction. However, the structure is better understood if it is considered as being made up of corrugated sheets of atoms. The interatomic distances within the sheets is about 15% less than between corrugations and hence the binding is stronger. Pauling (1948) has pointed out that the four nearest neighbours of any atom in the sheets show a marked resemblance to the trigonal bi-

pyramid structure of such strongly covalent compounds as PO_5, and Tucker (1950) has discussed the crystal chemistry more fully. He demonstrates that all the available evidence implies that the atoms within the corrugated sheets are bound together by covalent bonds and may be regarded as "giant molecules" which are themselves held together by metallic forces. This high degree of covalent binding is reflected in the very low solubility of many alloying elements even though they may have a similar atomic radius, and also in the low conductivity. It no doubt also has an influence on the mechanical properties since it tends to increase hardness and brittleness.

Alpha uranium also distinguishes itself from many other metals by exhibiting appreciable anisotropy of a number of properties. Extreme anisotropy of thermal expansion is notable amongst these and this is demonstrated in Fig.2 which shows that although the expansion in the [001] and [100] directions are similar, in the [010] direction there is a contraction with increase in temperature. Also, the total expansion is not linear: an inflexion occurs at 225°C. Some of the other physical properties also show inflexions near this temperature and the phenomenon is usually explained by proposing a change in the nature of binding at this temperature (Holden 1958).

1-b Structure of Beta Uranium

Although agreement has been reached on the general aspects of the structure of beta-uranium, the more detailed interpretation has caused some controversy and is not yet fully resolved. However

it is agreed that the structure is tetragonal with 30 atoms per unit cell (Fig.3). The disagreement arises between Tucker (1954) who considers that the least populated layers only are puckered and Thewlis (1954) who considers that all the layers are puckered. Beta also shows anisotropy in some of its properties though not to such a marked degree as alpha.

1-c Structure of Gamma Uranium

The high temperature allotrope has a body centred cubic structure (Wilson and Ruddle 1949) which is isotropic and has the most typically metallic properties.

2 Transformations in Uranium and its Alloys

Of major importance in the production of fuel elements is the heat treatment procedure which involves the beta→ alpha phase transformation. This has stimulated fundamental interest in the kinetics and mechanisms of transformations in uranium generally and consequently a considerable amount of research has been done, such that the mechanisms are now fairly well understood. Before discussing these in detail the terms used for the different modes of transformation will be defined to eliminate any confusion which might arise thereby. The term "diffusional" will be used to describe a transformation in which growth of the regions of product occurs by the capture of single atoms from the parent lattice by means of thermally activated jumps across the interface. A "martensitic" transformation will be used when growth proceeds by the systematic co-ordinated shear of large numbers of atoms in the

in the parent phase through small distances relative to their neighbours such that the parent lattice is transformed into the product without atomic interchange by diffusion.

2-a Beta→ Alpha Transformation in Pure Uranium

The mechanism of the beta→ alpha transformation in pure uranium has been variously described as:

(i) diffusional decomposition under all conditions,
(ii) martensitic under all conditions,
(iii) diffusional or martensitic depending upon the cooling rate.

In a study of the phase transformation temperatures as a function of cooling rate, Duwez (1953) found that both the transformations in uranium may be depressed with increased rates of cooling. This contrasted with the behaviour of other metals (titanium, zirconium, hafnium and thallium) which transformed martensitically and whose transformation temperatures were not affected by cooling rates (Duwez 1951). This led him to infer that the transformation in pure uranium was diffusional at all cooling rates. This interpretation was based upon older ideas that martensitic reactions are athermal and cannot be suppressed. Lehr and Langeron (1958) also favoured a diffusion controlled transformation from the observation that alpha single crystals could be grown by the phase transformation technique. The generalisation of this conclusion to all cooling conditions is invalid.

White (1955) first proposed that the beta→ alpha transformation in pure uranium was wholly martensitic by extrapolation of results obtained on a number of U-Cr Alloys. Conclusions obtained by this method of extrapolation are somewhat speculative.

Butcher (1957) also considered that the transformation was martensitic. By quenching a beta single crystal he demonstrated that the transformation showed a definite orientation dependence with a definite relationship between parent and product. The subsequent generalisation for all rates of cooling is not valid since the observations were made under restrictive conditions.

Bement and Wallace (1957) were the first to propose that uranium underwent a martensitic reaction upon rapid cooling but was diffusional on slow cooling. The difference in metallographic appearance after the two treatments suggested this: after rapid cooling the grain boundaries were jagged with a large amount of twinning and after slow cooling the grains had smooth boundaries with less twinning. They provided further evidence for two transformation mechanisms in the sharp inflexion which they found to occur in hardness versus cooling rate curve. Further evidence apart from that of Butcher (1957) that rapidly cooled pure uranium transforms martensitically was obtained by comparing the structure obtained with that obtained in an alloy known to transform martensitically (Holden 1958). The similarity is very marked.

To summarize, the observations are all consistent with the transformation being diffusional at slow cooling rates and martensitic at rapid cooling rates and this is generally accepted today.

2-b Alpha→Beta Transformation in Pure Uranium

Under conditions of rapid heating martensitic alpha appears to transform to beta by a simple crystallographic reversal of the beta→alpha shear. However, the transformation in conditions other than these is more complex. One important feature of the transformation which must be accounted for is that preferred orientation may persist in alpha after beta treatment (remanent texture). This phenomenon is most easily explained if the alpha→beta transformation is martensitic; preferred orientation would then be retained at rates high enough to ensure that the beta→alpha transformation is also martensitic. The disappearance of texture is then the problem, which is explained by rapid beta growth (Butcher and Baverstock 1960). Klepfer and Chiotti (1957) also interpreted their resistometric results as indicating that the alpha→beta transformation was at least partly martensitic. In a review, Burke and Dixon (1962) from theoretical consideration, concluded that the transformation was diffusional. This suggestion has been since substantiated by Barwood and Butcher (1963) who found no athermal component of transformation by a dilatometric method in direct conflict with the work of Klepfer and Chiotti. They found that the transformation was diffusional but that the last stages of transformation were extremely sluggish at low beta range temperatures. This result affords an explanation for remanent textures at these temperatures whereby they may be explained by incomplete transformation of the alpha-phase to beta. However, remanent textures have also been observed in worked uranium that has been treated at comparitively high beta temperatures.

Donze (1962) has explained this by postulating that domains of the original alpha exist in the beta phase after transformations and serve as nuclei for re-transformation. Evidence proposed for these thermo-dynamically unstable embryos is the observations that the temperature of the start of the beta→ alpha transformation was depressed by increased superheat in the beta range. Donze supposes that increasing the superheat would decrease the size of the alpha embryos and thus greater undercooling of the beta→ alpha change would be necessary for them to nucleate the alpha phase. This interpretation neglects the influence of beta grain growth which might lower the transformation temperature if alpha nucleating sites are predominantly at beta grain boundaries (Burke and Dixon 1962).

Burke and Dixon (1962) provided an alternative explanation. They suggested that remanent textures may arise because orientation relationships are possible in diffusional as well as martensitic transformations (e.g. the formation of WidmanstÄtten precipitates). This appears to be a more rational explanation although no supporting evidence for the hypothesis has been obtained.

In summary, it seems likely that the alpha→ beta transformation is diffusional under all conditions apart from the beta-alpha reversal of martensitic alpha.

2-c Gamma Transformations in Pure Uranium

The gamma to beta transformation in pure uranium appears to be a normal diffusional transformation based on metallography (Holden 1959). However, Klepfer and Chiotti's work indicates that at least coherent nucleation may be involved. It seems improbable from Duwez's work that any rate of cooling from the gamma phase will prevent the formation, in order, of beta then alpha in pure uranium since the range of temperature over which the beta phase exists increases with increased cooling rates.

2-d Transformations in Dilute Alloys of Uranium

The transformation kinetics of certain dilute alloys of uranium have been examined in considerable detail, notably U-Cr and U-Mo, but some study has also been made of a number of other dilute alloys (Jepson et al 1958). The transformation behaviour of these alloys is very similar in many respects, with minor modifications for the individual systems. The TTT diagram generally consists of two C's, differences existing in the shape of the C's, the temperature range covered by them and the transformation times. An example is shown schematically in Fig.4. taken from Butcher (962). The upper C is associated with a diffusional process and the lower C with a martensitic process. The martensitic transformation differs in a number of respects from the transformation in steel. The transformation is not necessarily athermal and with moderate cooling rates it can be suppressed to any temperature including room temperature. When a constant temperature is reached transformation does not begin immediately but after an incubation period

which varies with temperature. Also, the rate of growth is extremely slow compared to other shear transformations but is far too rapid at the low temperatures observed for diffusion to be a major factor. Holden (1953) has suggested a reason for the slow growth of martensite in uranium. In the growth of martensite in steel, simultaneous deformation of the parent matrix to relieve the stresses formed during transformation is possible because the matrix is of a ductile face-centred-cubic structure. However, the beta uranium matrix has few slip systems and the rate of growth is limited by repeated stress build-up and repeated twinning in the alpha plate. This model also explains the jerky growth reported by Mott and Haines (1954).

Increasing additions of alloying elements increase the range covered by the upper C at the expense of the lower C. This has been suggested to be due to the shear process being hindered by the presence of impurity atoms (Jepson 1958). In general, elements having a large difference in solubility between the beta and alpha phases (e.g. Fe, Cr, and Si) are much more efficient beta stabilizers than those elements still soluble to some extent in the alpha phase (e.g. Mo and Nb).

Some modifications occur, apart from those already mentioned in certain systems. In some U-Mo alloys Lehmann (1960) observed a marked Ms temperature similar to that observed in steels. In U-Cr alloys an intermediate reaction involving simultaneous lattice shear and short range diffusion has been observed (Dixon and Burke 1962). This results in a TTT diagram with 3 C's.

The gamma→ alpha transformation occurs in some alloys and may either be diffusional or martensitic (Holden 1958). Gamma→ alpha martensite, in contrast with beta→ alpha martensite grows very rapidly, presumably, by invoking the above model, because the matrix is a ductile body-centred-cubic structure.

3 Deformation Mechanisms in Uranium

3-a Alpha Uranium

In view of unusual crystal structure of alpha uranium, involving corrugated planes and covalent bonding it is perhaps not surprising that the plastic deformation is complex. Deformation can occur in alpha uranium by three mechanisms: slip, twinning and kinking, but before discussing these modes individually some general considerations of deformation is appropriate. Plastic deformation occurs by movement of dislocations in the lattice and during this process some of the atoms are moved from their stable positions relative to the adjacent atoms. In a typical metal, the bonding is such that the relative atom movements associated with plastic deformation does not reduce the strength of bonding. However, where the interatomic bonding is covalent and therefore directional the displacement leads to a decrease in the strength of the bond and the crystal may fracture. Therefore uranium, from this point of view occupies a position between a typical metal and a brittle covalent substance such as diamond or silicon.

A Slip

The predominant slip system in alpha uranium at room temperature has been independently shown to be {010}<100> by Cahn (1953) and Lloyd (1955). Reference to the crystal structure will show that this represents the relative slip of the corrugated planes of covalent atoms over one another. Cahn also observed a minor slip system on {110} and deduced that the direction was <110>. In addition to confirming many of Cahn's results, Lloyd also observed a minor slip system {011}<100> which was also observed by Calais et al (1960). However, Lloyd was unable to confirm {110} slip at room temperature and concluded that it must be a high temperature mode. This conclusion conflicts with the results of Calais et al (1960) who observed {110} slip at room temperature. Fine irregular cross slip attributed to {011}, {013} and {001} planes was found by each of the workers at room temperature.

Teeg and Ogilvie (1961) in a study of deformation in compression at -196°C found that the critical shear stress for {010}<100> slip increased substantially with decrease in temperature relative to the other mechanisms. {110}<001> slip was established as the main slip system operative at -196°C. This contrasts with the work of Lemogne and Lacombe (1963) who found that {010}<100> slip was the major system at -196°C in tests in tension and only occasionally observed {110}<001> slip. The slip systems active at 600°C have been determined by Chiswick, Lloyd et al (1958). The system predominating at room temperature was found to persist but a new system {001}<100> with a much lower critical shear stress

was observed. (This system only acts as a cross-slip system at room temperature). Also found to be operative at 600°C were the systems {110}<110> and {021}<112>.

The varied reports for {110} slip were resolved in a joint paper (Lloyd, Calais et al 1961) in which it was concluded that the {110} plane was active between -196°C and 600°C but that at high temperature it occurs in the <110> direction and at room and low temperature in the <001> direction.

Reference to the crystal structure will show that the important factor in deciding the slip mode in alpha uranium is not the closeness of packing, as it is in other metals, but the absence of covalent bonding and the straightness of atom rows. At higher temperatures the covalent bonds are more easily broken and this accounts for the increased number of slip systems, but a further factor may be the possible change in the nature of bonding mentioned earlier.

B Twinning

The twinning mode of deformation is probably more important in alpha uranium than slip. Although twinning presumably occurs by some dislocation mechanism there is an important difference between this process and slip; when twinning occurs the relative displacement of atoms does not significantly affect bonding between individual atoms as it does in slip. This factor probably accounts for the relative importance of twinning in uranium where directional covalent bonding exists.

Several twin systems have been observed both by Cahn and Lloyd at room temperature and these same systems have been found at -196°C by Lemogne and Lacombe. These are {130}, {172}, {176}, {112}, and {121}. Cahn found that twinning decreased at elevated temperatures but a more detailed study of the effect of increasing temperatures on twinning was made by Butcher (1959). He concluded that above a temperature of between 450°C and 500°C twinning is only rarely found, the exact temperature varying with strain-rate, being increased for fast strain rates. This is consistent with the belief that the critical shear stress for slip decreases significantly with increasing temperature whilst the critical shear stress for twinning in contrast, varies little with temperature. Also relevant is the observation of an increased number of operative slip systems at high temperatures such that the five independent slip systems postulated by Taylor (1938) to be necessary for homogeneous deformation of a polycrystal are available without recourse to twinning. The first factor assumes the acceptance of a critical shear stress concept for deformation twinning which may not be strictly valid.

The atom movements in uranium twinning have been considered in detail by Cahn (1953) and to some extent by Holden (1958). The atoms in the alpha uranium lattice are not brought to their final positions by the twinning shear, as in metals of higher symmetry, but have to undergo additional adjustments to find their correct place in the twinned lattice. For {172} type twinning one in four of the atoms fall into place without need for readjustment. A detailed examination of the movement of the atoms and the final

positions shows that there is slight structural distortion and hence the immediate vicinity of the composition plane must be under stress (Cahn 1953). The atom movements in {130} type twinning are more easy to picture and are shown in Fig.5: all the atoms readjust after the original twinning shear. All the atoms are in abnormal final positions in the immediate vicinity of the composition plane and the structural distortion in {130} twinning is greater than for {172}. The composition plane must therefore be under considerable stress. Presumably dislocations are required at the interfaces to accommodate the twin interface with least stress.

C Kinking

Kinking is a local bending of the lattice about an axis normal to the major slip direction and in uranium the many twins might be considered to interfere with kink band formation to its preclusion. However, there are directions in uranium where, in spite of the many available twinning systems, none will operate. Kinking is then observed normal to [100].

3-b Deformation of Beta and Gamma Uranium

Very little work has been carried out upon the plastic deformation of the high temperature phases of uranium. Polycrystalline beta has been found to be brittle both at beta phase temperatures and in alloyed uranium which has been quenched to retain beta to room temperature. Gamma uranium is very soft and presumably it has deformation systems normally operative in body-centred-cubic metals.

4 Mechanical Properties of Uranium

The mechanical properties of uranium have been extensively studied but these investigations have been predominantly for technological purposes. Specific information has been required for fuel element design and tests have been carried out over a range of temperatures in such conditions as "as-cast", "rolled and annealed" and "beta-quenched" for these purposes. The many influencing factors such as grainsize, preferred orientation and purity are rarely stated and with these major restrictions the results obtained are of limited value.

4-a Hardness

Gittus (1963) states that hardness is considerably increased when large amounts of impurity are present and suggests that this is due to beta-retention but the fine dispersion of intermetallics will also tend to increase hardness and this may be a more important factor. Apart from this variable, Holden (1958), reviewing the data, found little variation in hardness between "rolled and annealed", "as-cast" and "gamma-extruded"uranium. Hardness decreases rapidly with increasing temperature and at about 400°C there seems to be a definite inflexion in the curve, thereafter the hardness decreasing more rapidly. Holden suggests that this is due to grain boundary relaxation and the change in the predominant mechanism of deformation from twinning to slip, but one may again relate this to the proposed change in the nature of bonding with increasing temperature. An example of a hardness/temperature plot is shown in Fig 6 (Chubb 1953). These results also demonstrate that beta is relatively hard and that gamma is soft.

4-b Tensile Results

Polycrystalline uranium has a very low limit of proportionality (Foote (1956) quotes a value of 1 ton/sq in) and the elastic portion of the stress-strain curve is poorly defined. It is therefore difficult to judge the yield stress and published data on yield stresses are therefore particularly equivocal.

Lacombe et al (1958) suggest that during cooling from heat treatment or casting the large internal stresses which result from the anisotropy of thermal expansion cause the elastic limit to be exceeded. Thus, when the specimen is tensile tested it is immediately plastic. However, this takes no account of the very low resolved shear stress for {010}<100> slip which Lloyd and Chiswick (1955) determined to be 0.21 tns/in^2. Furthermore, as Friedel (1961) has suggested, polycrystals with anisotropic elastic constants (as uranium) will produce stress concentrations and thus plastic deformation should start fairly easily in grains oriented in such a way as to have lower effective elastic constants under the applied stress, than their neighbours. These factors perhaps provide a more satisfactory explanation for the low yield stresses observed in polycrystals of uranium. The last factor also provides an explanation for the observation recorded by Holden (1958) that deformation in uranium was localized and occurred in some grains more than others.

The effect of temperature on the tensile strength has been reported many times, after different treatments, but the general effects are very similar. The results of Sergeyev et al (1958) shown in Fig 7 have been chosen as representative. An increase in strength with rising temperature is observed with a peak at about 100°C followed by a marked continual decrease. Grainger (1958) suggests that the decrease is not linear, but that uranium retains its strength fairly well up to 400°C above which the strength falls rapidly. This observation may again be related to the possible change in the nature of binding and predominant mode of deformation. A sharp increase in strength is observed in the beta phase and a sharp decrease in gamma phase regions.

The ductility has been generally observed to increase with increasing temperature but not all workers have observed the sharply rising curve of Hueschen and Sanderson (1953) with a brittle transition temperature. These results (Fig 8) appear to demonstrate that increasing additions of impurity raise the transition temperature slightly. However, no information on other variables such as grain size was presented and the results are therefore of limited significance.

With further increase in temperature through the beta transus a sharp drop in ductility from about 60% elongation (alpha) to about 3% elongation (beta) is observed (McIntosh and Heal 1958).

Gamma is very soft and malleable but it has limited ductility: in this respect it has been compared to lead at room temperature. (It should be noted that the ductility continuity through the beta and gamma transitions shown in Fig.8 cannot be correct).

Regarding the ductile/brittle transition in particular, only investigations of the effect of hydrogen had been published. This work has been reviewed by Cotterill (1961). Davis (1956) showed that a critical low concentration of hydrogen (about 0.3 ppm) raised the transition temperature by about 400°. These results are summarised in Figs. 9 and 10. No satisfactory explanation for the phenomenon exists but it is relevant to note that the embrittlement occurs at very low hydrogen contents and that further increase in the hydrogen content has no effect (Fig.9). that no metallographic evidence of a second phase in embrittled specimens has been obtained and that the embrittling concentration does not vary significantly with temperature (Fig.9). These factors suggest that the effect is not due to diffusion of hydrogen in the uranium lattice (as is the case with steel) nor due to an embrittling phase (as is the case with titanium). Cotterill suggests that the effect may be due to the preferential solution of hydrogen in some unidentified impurity phase situated at the grain boundaries but no evidence to support this hypothesis has so far been obtained.

5 Fracture of Uranium

When this research began the only work which appeared to have been reported on the fracture of uranium, was that of Davies (1962) together with a number of references in reports concerned

primarily with other aspects (e.g. Cahn 1953. Holden 1958). However, since that date an extensive investigation of the fracture of single crystals of uranium at -196°C has been published (Lemogne and Lacombe 1963).

The first record of work on fracture of alpha uranium is that of Cahn (1953). At room temperature Cahn occasionally observed small cleavage facets on the fracture surface although a dull, irregular surface was generally produced. Sectioning of the cleaved grains showed long twins accurately parallel to the cleavage trace and close to this trace. The plane was identified to be (172) both from Laue patterns and from the geometry of twin intersections. Cleavage was thus shown to occur along the twin boundary. This type of failure is quite common and has been observed, for example, in calcite (Brezina 1880), zinc (Davidenkov 1933), magnesium (Reed-Hill 1957), tungsten (Woolf 1962) and uranium oxide (Robins 1963); it is particularly well known in mineralogy and the term "parting" has been reserved for it.

Davies (1962) made a general study of the characteristics of fracture in uranium and observed a number of different types including "cleavage", "intergranular", "transgranular-tearing" and "dimpled" He was able to relate metallographic observations of the fracture edge with fractography and established the characteristics of each of the above types. Davies went on to make some conclusions regarding nucleation and propagation of the cracks. The observation that the numerous cuboid inclusions cracked at small tensile elongations and that the propagating crack tended to pass through them, led

him to conclude that the above modes of fracture(with the exception of "dimpled" failure which occurred at elevated temperatures) were all nucleated at these cracked cuboids. These observations can be interpreted in terms of the propagating crack merely tending to pass through inclusions. This would be expected in any circumstances, since the cuboids are so numerous, but since the cuboids crack at an early stage, a propagating crack would tend to pass through them preferentially. Similar observations in beryllium containing cuboid inclusions have been interpreted in this way (Koda and Morozumi 1962).

The characteristics of "cleavage" in Davies' specimens were identical with those of Cahn; a bright facety surface was observed which fractography revealed to be smooth with regular steps; sectioning showed that the cleavage plane was parallel to twins and that it occurred along a twin/matrix interface. Notwithstanding this evidence, Davies concluded that the cleavage plane was distinct and that failure did not occur along a twin/matrix interface. The evidence he claimed for this is that the deformation twins in uranium are "pencil" shaped and so, he argued, if failure occurred along a twin interface the fracture surface would contain only a small proportion of smooth areas (associated with parting at the "pencil" twins) linked by irregular surfaces formed by shear. (He quoted Cahn (1951) as evidence for "pencil" twins but nowhere does Cahn appear to state that twins in uranium are pencil-shaped). Since Davies observed relatively smooth fracture surfaces with regular steps he concluded that the cleavage plane was distinct and merely

happened to be parallel to a twinning plane. Twins are lamellar or lenticular in shape and therefore the argument has no foundations. Also, the main twinning planes are not parallel to lattice planes and this alone is sufficient evidence that "parting" along a twin interface occurs rather than "cleavage" along a specific lattice plane (Cahn 1954).

Lemogne and Lacombe (1963) investigated the fracture of single crystals of pure uranium at -196°C. These authors observed twin/matrix parting in all cases, confirming the work of Cahn and the experimental observations of Davies. The fracture surface was found to correspond exactly with the twinning plane and in general, fracture occurred along the twin nearest normal to the tensile stress. Parting was shown to be easiest on the composition plane of {172} twins and more difficult on those of {112}, {130}, and {121} twins. No instances of {176} twin parting were observed. No explanation was offered.

Holden (1952) studied the fracture of single crystals of metastable beta uranium in a 1% chromium alloy. Fracture at room temperature was apparently by brittle cleavage, but the cleavage plane was not identified. McIntosh and Neal (1958) suggested that fracture in the beta range was intergranular and Davies carried out a number of experiments which tend to confirm this.

6 Theories of Fracture

The basic problem in fracture is to account for the order of magnitude difference between the observed and the theoretical breaking stress of solids. Griffith (1920) attributed the low strength of brittle solids prepared by normal methods to the presence of surface or internal flaws at which the stress concentration is of sufficient magnitude that the theoretical strength can be exceeded locally from quite a low applied stress. This view is widely accepted and the high strengths of glass fibres and metal whiskers may be cited in this context. Griffith extended this concept to a consideration of the growth of these cracks and by a method of energy balance developed the well-known expression:-

$$\sigma = \left\{\frac{E\ \gamma}{c}\right\}^{\frac{1}{2}} \qquad \ldots\ldots\ldots\ldots\ldots\ldots(1)$$

for the breaking stress σ of a brittle solid of Young's modulus E and surface energy γ containing a sharp crack of length c. Experimental confirmation has been obtained with glass fibres relating the stress and crack length.

The Griffith criterion only applies to elastic cracks in perfectly brittle solids and it cannot be applied to more ductile materials, owing to the greater amount of work required to fracture them. However, once nucleated, the criterion can be applied if the velocity of crack propagation is high enough and the surface energy γ is replaced by one commensurate with the work done in creating new

fracture surfaces of the type observed (Orowan 1948). This term, γ_e, is the effective surface energy for fracture and is much larger than the theoretical surface energy because it takes into account the deformation near the tip of the crack and it will vary with the heterogeneity of deformation.

Cracks of the size required by this theory could be produced in metals, for example during working operations, but the Griffith criterion cannot alone account for brittleness in metals. The following observations suggest that other factors are important:-

a) None of the terms in the Griffith equation vary significantly with temperature to account for a ductile/brittle transition.

b) Hahn et al (1959) showed that, at low temperatures small cleavage cracks formed in plastic yielded regions of a steel specimen but not in unyielded regions even though these had endured the same stress.

c) When the yield stress is increased, for example by fast straining (Owen 1959) or by irradiation hardening (Churchman et al 1957), the brittle fracture stress is often raised by the same amount.

d) The cleavage fracture stress varies in the same manner as the yield stress when temperature grain size and other variables are changed. Low (1956) showed that at -196°C the cleavage fracture stress and the ductile compressive stress varied linearly with the reciprocal of the square root of grain size. This suggests that grain size plays a part similar to crack length in the Griffith theory, as was suggested by Petch (1953)

It is clear from the evidence that plastic deformation accompanies fracture and consequently that slip dislocations must play some part in the fracture process. Because of these observations it is now believed that some dislocation process sets up stresses that are relieved by atomic separation instead of atomic slip with consequent crack formation.

Several mechanisms have been suggested for the process of converting glide dislocations into cavity dislocations and these are illustrated in Fig.11. The first suggestion, (11a) due to Zener (1948) was that sufficient stress concentration to start a crack could be produced by a pile-up of glide dislocations at an obstacle such as a grain boundary. This model appears to be inapplicable to single crystals and led to the suggestion by Cottrell (1958) that a crack could be produced at the intersection of two slip bands (11b). Crack nucleation at the intersection of twins was observed in molybdenum by Cahn (1955), and Hull (1960) made similar observations in silicon-iron and proposed the models illustrated in 11c(i) and 11c(ii). Sleeswyk (1962) criticized these models and proposed that the crack at the twin intersection was due to a reaction between emissary slip dislocations created at the twin tip (11c(iii)). Hull (1962) suggested however, that it is unlikely that two twins initiated in different parts of the crystal should meet in the way illustrated. He considered that the more general case (11d) whereby a twin meets a pre-formed twin is the most important mechanism. The stresses associated with the growth of a twin may also result in crack formation. Hornbogen (1961) suggested that when deformation twins form rapidly, they may produce a shock wave travelling ahead of the twin. Such a wave may be partially reflected at an obstacle which might then produce sufficiently high stresses to nucleate a crack. Also, residual strain is associated with the apex of a growing twin and if this is not relieved cleavage may start at the advanced edge of the twin lamella. This has been demonstrated to occur in calcite by Rose (1868): calcite is a material which parts along its twin composition plane with great perfection.

For the formation of cavity dislocations and a microcrack stress relaxation by slip must not occur; clearly if dislocations are produced very rapidly the crack might form and spread in a time too short to allow stress relaxation by slip in neighbouring regions. This situation is possible in metals with pronounced load drops, i.e. at impurity yield points or when deformation twinning occurs. This explains the identical variation of yield stress and brittle fracture stress with temperature in iron (Low 1956). A further observation is important: hydrostatic pressure has been shown to exert an influence upon brittleness. This implies that at the critical stage in the fracture process a crack must already be present. Accordingly, nucleation of microcracks is considered to be an easier process than their growth and consequently it is concluded that the stress to propagate the crack is the governing factor in brittle fracture. The question is then whether or not a crack formed by dislocation coalescence can spread catastrophically across the crystal as a cleavage crack. If it can brittle fracture ensues.

These considerations have been developed quantitatively by Cottrell (1958) for the occurrence of brittle rather than ductile fracture. Much of this theory is based upon the two empirical (Petch) relationships:-

$$\sigma_y = \sigma_i + k_y d^{-\frac{1}{2}} \quad \ldots\ldots\ldots\ldots\ldots\ldots (2)$$

and:-

$$\sigma_f = \sigma_i + k_y d^{-\frac{1}{2}} \quad \ldots\ldots\ldots\ldots\ldots\ldots (3)$$

where σ_y is the yield stress; σ_i the friction stress resisting the motion of unlocked dislocations arising from the Peierls-Nabarro

lattice stress, intersecting dislocations, lattice defects or impurities; d is the slip band length, where 2d may be taken as the grain diameter; k_y is a function of the stress to generate unpinned dislocations and σ_f is the cleavage fracture stress. Cottrell assumed that, under certain circumstances, some of the first slip dislocations coalesce to form a crack. The crack may then either propagate to cause fracture or be damped out by plastic deformation. The quantitative treatment based on a similar method of energy balance to that used by Griffith led to a criterion for fracture of the type:-

$$\left.\begin{aligned} (\sigma_i\, d^{\frac{1}{2}} + k_y) &= \beta\mu\gamma \\ \text{or equivalently;} & \\ \sigma_y\, k_y\, d^{\frac{1}{2}} &= \beta\mu\gamma \end{aligned}\right\} \qquad \ldots\ldots\ldots\ldots\ldots\ldots (4)$$

where β is equal to unity in a tensile test and to approximately 1/3 for a notched test (triaxiality); μ is the shear modulus and γ is the effective surface energy. This is a general equation for the propagation of a crack and certain practical conclusions can be drawn. The conditions for brittle fracture are that the right hand side of the expression is smaller than the left hand side. Since the parameters on the right hand side of the equations only vary slowly with temperature it is the way in which changes occur on the left hand side of the expressions which is the important criterion in determining the ductile/brittle transition.

Thus, in a given material, brittleness should be favoured by low temperatures and high strain rates because these give rise to large values of σ_i and k_y, although k_y may be temperature independent (Cottrell 1963). Since certain impurities raise the σ_i

and k_y contributions the presence of these impurities (either as precipitates or in solution) should also favour brittle fracture. Also σ_i becomes high as soon as there is a departure from typical metals to directionally bonded solids (cf. the structure of uranium). Anything which breaks up the slip path (i.e. reduces d) favours ductile fracture and on the brittle side of the transition Cottrell obtains the relation:-

$$\sigma_f (\sigma_f - \sigma_i) d = \beta u \gamma \quad \ldots\ldots\ldots\ldots\ldots\ldots (5)$$

for the effect of d on brittle fracture stress. This relation is similar to the Petch relation (3) and hence it is accounted for. Clearly other factors which reduce d, such as sub-grain diameter are relevant but these have not yet been fully explored.

This theory accounted for experimental observations in body centred cubic metals to a large degree of accuracy. However, Johnson (1963) has applied the theory to a number of later results and revealed significant variance with experimental observation. He makes some modifications to the theory based on the observations that, at and above the transition, a growing microcrack is unable to penetrate the region of "forced-slip" near the boundary of the grain in which it is nucleated. He postulates that the critical stage in the growth of a crack occurs when it penetrates the region of forced slip in the grain in which it nucleates and justifies this by arguing that these regions will have a higher effective surface energy than the body of the grain because more deformation systems are available to relax the stress concentration at the tip of the crack. As strain hardening proceeds in brittle specimens

the stress increases until at some stress the crack is able to propagate and the specimen fails. The fracture stress, he postulates, is then given by this modification of the Griffith equation:

$$\sigma = \left\{ \frac{E \gamma_d}{2\pi(d-d_o)} \right\}^{\frac{1}{2}} \qquad \ldots\ldots\ldots\ldots(6)$$

where d_o = distance from the tip of the crack to the grain boundary (forced slip region) and γ_d = the value of effective surface energy at the instant of propagation. He suggests that γ_d may change continuously during work hardening and therefore postulates no simple functional relationship between fracture stress and grain size.

If this modification to the Griffith criterion is accepted then Cottrell's equations will be modified and the Petch relationship ($\sigma_f \propto d^{-\frac{1}{2}}$) is no longer theoretically predictable. Johnson suggests that this relationship is probably an approximation valid only over a limited range of grain size and temperature.

Intergranular brittle fracture has been regarded as a special type of fracture but this distinction is not now considered valid. Whether or not a low temperature brittle crack propagates along a crystallographic plane or a grain boundary, appears to be controlled by which of these alternative routes has the lowest surface energy. For cleavage failure this term is equal to $2\gamma_s$ where γ_s is the energy per unit area of the cleavage surface. For intergranular fracture this is equal to ($2\gamma_s - \gamma_B$) where γ_B is the grain boundary energy per unit area, since the energy of the two new surfaces is partly offset by the energy of the grain boundary

along which fracture is taking place. McLean (1962) has shown that the surface energy of solid metals can be reduced by surface adsorption of an element in solid solution. Consequently if such a solute concentrates at grain boundaries by equilibrium segregation, the grain boundaries become preferred sites for fracture because γ_s is reduced. Another method of reducing the value of $(2\gamma_s - \gamma_\beta)$ is apparent. In materials such as beryllia, grain boundary stresses arise from the anisotropy of thermal expansion and are not relieved by plastic flow. These residual stresses will increase the value of γ_β thereby favouring intergranular cracking (Clarke 1964). Chang and Grant (1956) have suggested a mechanism for intergranular crack nucleation. They postulate that if one grain deforms more than its neighbour, and this additional deformation is not transmitted across the boundary between the two grains, stresses are created which may result in an intergranular crack.

Ductile fracture is distinguished from brittle fracture by the fact that whereas plastic deformation is not necessary during the propagation of a brittle crack, plastic deformation is necessary for the spread of a crack during ductile failure. Smith (1936) showed that, irrespective of the state of the material, more plastic strain is always needed to spread a ductile crack. The view now widely held is that this is not a true fracture (in the sense of tearing atoms apart) but is due to the geometry of plastic deformation as, for example, in simple necking where simultaneous shear on intersecting slip lines produces a knife-edge or point failure.

This is clearly true in the case of pure single crystals but in practice most ductile failures give much less than total reduction of area resulting in the well-known cup and cone fracture. The original suggestion by Tipper (1949) is now considered to be correct. She proposed that 100% reduction-in-area did not result because necking occurs simultaneously from several cavities inside the material associated with inclusions. Plateau et al (1957) showed that a ductile fracture surface had a characteristic dimpled appearance, each dimple was suggested to represent one of these cavities and rupture was deduced to have resulted from cavity coalescence.

A detailed study of ductile failure was made by Puttick (1959). He showed that voids were formed at oxide particles in copper during plastic deformation, either by separation of the metal from the inclusion or by fracture of the inclusion itself, due to the differing elastic and plastic properties of the inclusion and metal. With continuing deformation these voids grew and linked-up and upon external necking the cavities grew together in the necked region to form a macroscopic fissure which propagated outwards to cause failure. The final shearing at 45° to the tension axis appears to be achieved by propagation along a deformation band. Zener (1948) suggested that the final fracture follows a path of intense, localized and rapid plastic shear in which material is softened by the heat of plastic working. A similar model was proposed by Puttick (1960) who provided evidence for it by careful control of crack propagation to a very slow rate using a hard tensile machine. Under these circumstances the shear cone was eliminated.

This cavity growth mechanism, if correct, has two important consequences. Firstly, it suggests that if no inclusions were present, failure should occur by the specimen pulling apart entirely by the inward growth of the external neck: evidence for this is found in both copper and aluminium where with increasing purity increased reductions are observed. For example, OFHC copper necks down to 90% reduction-in-area whereas tough-pitch copper shows only 70% reduction (Cottrell 1959). Secondly, the critical condition should be independent of temperature being simply sufficient local plastic deformation to join the inclusion cavities together into a major crack. Also, if the stress system changes from uniaxial to triaxial, although the overall strain may change, the local deformation to cause cavity interlinkage should be the same. Both these effects are found in practice. Teed (1950) found that the reduction-in-area of pure aluminium remained close to 90% between 20°C and -183°C. Knott and Cottrell (1963) found that microhardness measurements on ductile fracture surfaces for a steel were the same in tensile and in notch tests.

This, then, is the general picture but some anomalies exist. These are mainly due to work by Beevers and Honeycombe (1962) who found no evidence of cavity formation in an investigation of ductile failure in high purity aluminium and copper. Fracture was found to be initiated by microcrack formation in coarse slip bands presumably, they suggested, by a dislocation mechanism. In contrast to the above contentions, this means that the reduction-in-area will be dependent upon temperature and evidence was provided for this. At 20°K very little reduction-in-area was found in super-purity aluminium and this

was attributed to the early formation of crack nuclei by avalanches of dislocations. These same authors also studied the ductile fracture of precipitation hardened Al-Cu single crystals. Again no cavities were observed. Just preceding fracture the deformation became localized to a single slip system producing a heavy deformation band through which the crystal fractured. Failure occurred without necking and at a critical resolved shear stress. These observations are not completely reconcilable with the former picture: it would appear that in some circumstances ductile fracture occurs by the linking together of dislocation cracks that have been unsuccessful in breaking out as cleavage cracks, as was suggested earlier by Mott (1953).

III SCOPE OF THE PRESENT WORK

The general outline of the work was given in Chapter I but having surveyed the literature it is now appropriate to detail the scope of the present work. This is as follows:

1. Establish the effect of temperature between -196°C and about 800°C on the mechanical properties of uranium in a metallurgical condition which is fully specified and not liable to inhomogeneity of structure.

2. Examine how the mode of fracture varies with temperature and metallurgical condition and correlate this with the mechanical properties and ductile/brittle transition. This section is facilitated by Davies' work of characterizing the fracture types.

3. Investigate the nucleation and propagation of the various fracture modes, particularly in the alpha phase.

4. Investigate the ductile/brittle transition in detail and determine unambiguously the factors which influence the temperature and characteristics of the transition.

5. Determine cleavage fracture stress versus grain size relationships with particular reference to the Petch $d^{-\frac{1}{2}}$ relationship.

IV MATERIALS

1. Technology of Fuel Rod Production

Mining of uranium bearing ores and concentration to ammonium diuranate is followed by the preparation of very pure compounds of uranium such as the oxide or fluoride. Maximum purity is achieved at this stage since further processing introduces impurities. These compounds are then converted to the metal, usually by a thermite reduction process. The material used in this work was produced by the reduction of the tetrafluoride with magnesium powder followed by direct casting into 8in diameter graphite moulds. Direct-casting has been developed recently to avoid the necessity of re-casting the thermite reaction product which introduces further impurities. Nevertheless, carbon is picked up from the graphite mould and small amounts of iron, aluminium and silicon from the magnesium. The direct-cast ingots are then remelted and cast into the 1.2in diameter fuel rods which are then heated into the beta-phase and water quenched to refine the grain structure. Small additions of iron and aluminium are sometimes made to the melt prior to casting to effect further grain refinement after beta-quenching.

Colloquial terms for the various grades of metal have become common usage in uranium metallurgy and will therefore be used. These are defined as follows: "virgin unadjusted" refers to direct cast material; "unadjusted" is material which has been remelted and cast into a fuel rod; "adjusted" is the same re-cast material with additions of iron and aluminium, and "doubly-adjusted" is again the same re-cast material which has twice the additions of iron and aluminium as "adjusted". All four grades were used in this work.

2 Composition of Materials

Analysis of each grade of material used was carried out at AERE Harwell and the results are presented in Table I. The materials will generally be referred to by their colloquial terms but they have also been given letters for easy reference in some diagrams.

Table I

		Virgin Unadjusted ("A")	Unadjusted ("B")	Adjusted ("C")	Doubly Adjusted ("D")
Carbon	ppm	300	570	590	780
Oxygen	ppm	100	400	300	900
Nitrogen	ppm	< 5	7	20	23
Hydrogen	ppm	<10	<10	<10	<10
Silicon	ppm	60	65	30	70
Iron	ppm	50	50	500	1000
Aluminium	ppm	10	50	250	500
Nickel	ppm	5	4	20	10
Magnesium	ppm	30	<10	<10	<10
Others	ppm	<50	<50	<50	<50

Some work was carried out on material from different batches of B, C and D but the variations in composition were minor and of no significance here. In view of the effect of hydrogen on mechanical

properties it was considered important to establish the effect of long vacuum anneals on hydrogen content. The results obtained indicated no significant variation: The hydrogen contents can therefore be assumed to remain constant throughout this work.

3 Preparation of Specimens

The most readily available material for this work was in the form of cast rods 1.2ins in diameter (i.e. reactor fuel rods). Initially it was intended to work solely with this type of material: any variables, whose effects might be studied, were to be produced by heat treatment. However, it soon became apparent that it was impossible to produce the required variables (particularly grain size) satisfactorily by this method. Cast fuel rods were still the only available material and a rolling and annealing schedule was consequently carried out upon a number of these. Due mainly to axial defects, this material was unsound and therefore not satisfactory. Fortunately a virgin direct-cast billet was eventually made available for the work and by careful preparation this material proved sound and entirely satisfactory. Nevertheless the amount was limited and it only became available at a comparatively late stage, therefore, an appreciable proportion of the work was carried out upon the other two types of material.

3-a Preparation from Cast Fuel Rods

The importance of preparation of specimens from cast rods lies only in the choice of material. Defects in the form of blow-holes, shrinkage porosity and segregation of inclusions existed

throughout the bars but the particular sites for these defects were the periphery and the axial pipe. Thus the fuel rods were quartered longitudinally (Fig.12) and tensile specimens, whose dimensions are given in Fig.13, machined from these quarters. In this way, the major defects associated with the axial pipe and the periphery were eliminated from the specimens.

3-b Preparation from Rolled Fuel Rods

In default of sound material mechanical and thermal treatments were carried out upon cast fuel rods. It was hoped that the axial pipe would weld-up and produce sound material from which different grain sizes could be produced after annealing rods which had had varying cold reductions. Adjusted material only was available and the rolling schedule that was carried out was as follows:

TABLE II

1.	Roll 1.23in - 1.003in at 300°C (10 passes)
2.	Anneal for 24 hours at 630°C
3.	Roll 1.003in - 0.501in at 300°C (34 passes)
4.	Anneal for 24 hours at 630°C
5.	Cut into five equal lengths and roll varying reductions at 300°C to: (a) 0.492in (b) 0.484in (c) 0.475in (d) 0.450in (e) 0.425in

Annealing was carried out in a vacuum furnace and rolling temperatures achieved by means of a salt bath. Tensile specimens were machined direct from these rods to the dimensions given in Fig.13. Unfortunately, examination of the material showed that it was unsound. Axial pipes, porosity and inclusions were present and these had often given rise to cracks during rolling (Figs. 14 and 15). The cracks produced perhaps resulted from the rolling temperature falling. This may be reflected in the large number of passes required for the reductions. Nevertheless, the tensile results were found to be reproducible, with some notable exceptions, and since75 specimens (which had cost about £10 each to produce) were available tests were carried out. Naturally the material was of little significance for investigation of fracture characteristics.

3-c Preparation from Virgin Direct-Cast Ingot

In the preparation of material from a direct cast ingot it was possible to implement both previous techniques for improving the soundness of the meterial. A cylindrical direct-cast ingot 8in in diameter and 9in long was made available for the work and great care was taken in deciding upon the best method of preparation. The cast billet was cut into six equal longitudinal segments and a rolling rod 1.25in in diameter machined from each segment (Fig 12). This procedure eliminated the axial and peripheral defects and considerably reduced any possible segregation effects. The rods were then subjected to a mechanical and thermal treatment to break-up the cast structure, weld-up any porosity and produce a fine uniform grain size. Three rods were then subjected to varying reductions so that a

variation in grain sizes could be produced after annealing. The details of the mechanical and thermal treatments are summarized in Table III.

Table III

1.	Roll 1.25in - 1.0in diameter at 600°C
2.	Anneal for 16hours at 600°C
3.	Roll 1.0in - 0.75in diameter at 300°C
4.	Anneal for 16hours at 600°C
5.	Roll 0.75in - 0.50in diameter at 300°C
6.	Anneal for 16hours at 600°C -- specimens machined from three rods at this stage
7.	Three rods then rolled different amounts (8%, 11%, 28%) at 300°C and tensile specimens machined

Annealing was carried out in a vacuum furnace and the rolling temperatures achieved by means of a salt bath. Tensile specimens of the dimensions shown in Fig 13 were machined from the rolled rods and microexamination showed that the material was sound and defect-free.

V APPARATUS AND EXPERIMENTAL TECHNIQUES

1. Thermal Treatment

The experimental work involved a considerable amount of varied heat treatment: fast and slow heating and cooling rates were required in an environment which afforded protection against oxidation of the uranium. For general treatments a horizontal vacuum furnace was constructed. The furnace unit consisted of a closed evacuated system surrounded by a Nichrome-wound furnace which was supplied with alternating current through a variable auto-transformer giving 0-240 volts. The temperature was controlled by an Ether Transitrol. A mercury microswitch relay was incorporated into the circuit such that the current was switched on and off across a rheostat. This ensured that the current fluctuated between two close values instead of between zero and that controlled by the transformer. A chromel/alumel thermocouple for this controller was situated in the maximum temperature zone on the outside of the tube and temperature control could be adjusted to give $\pm$ 20° up to 800°C. The full circuit diagram is shown in Fig 16.

The vacuum system for this furnace consisted of a 3 ft. long silica tube with a bore of 1.25in which was evacuated by means of an Edwards 1in oil vapour diffusion pump backed by an Edwards two-stage rotary pump. The furnace tube was sealed at each end with brass/wax seals onto which brass plates were bolted incorporating grooved 'O' ring seals. The ends of the tube were water cooled to prevent breakdown of the vacuum seals at high furnace temperatures. Through one seal the vacuum line passed and through the other an

'O' ring sealed 0.2in diameter silica thermo-couple tube passed. Attached to the tube was an alumina tray upon which the specimens were placed whose temperature could be measured directly by means of a platinum/platinum-13% rhodium thermocouple, which passed down the tube, and a portable potentiometer. The 'O' ring seal enabled the specimen-tray to be drawn out of or into the hot zone and thus both "furnace" and "air" heating and cooling of the specimens could be accomplished.

The pressure inside the furnace was measured by means of a Philips cold cathode ionization gauge and head. After construction the system was probed for leaks with ether, large leaks (greater than about 1 lusec) being detected by means of a discharge tube and Tesla coil and smaller leaks by using the Philips gauge. Eventually the total leak rate was reduced to less than about 10^{-1} lusecs and a dynamic vacuum of between 10^{-5} and 10^{-6} torr could be achieved after less than one hour's evacuation.

A vertically mounted vacuum furnace with a quenching arrangement was available for treatments requiring faster cooling rates. The furnace, vacuum system and method of temperature control were all very similar to that just described except that straight-through pumping was not possible because of the quenching system and consequently a satisfactory vacuum could only be achieved after a slightly longer pumping time. The specimens were held in a tungsten wire basket, (tungsten is almost inert to uranium) supported by a wire attached to a cylinder of soft iron which was retained in position

by a magnet. The bottom end of the tube was wax sealed and attached to a brass quenching pot which held either mercury or silicone oil as a quenching medium whose temperature could be controlled by surrounding the pot with liquids or liquid/solid mixtures in a Dewar flask. Quenching was carried out by removing the magnet and allowing the specimen to fall into the quenching medium. The furnace is illustrated in Fig 17.

During the course of the work it was necessary to heat specimens very rapidly to temperature, treat for very short periods and follow this by faster quenching than could be accomplished in the vertical vacuum furnace. This was possible only with a lead bath since resistance heating and argon-quenching of irregularly shaped specimens is not possible. A lead bath was therefore constructed using a Chronite 4in diameter by 6in deep pot, commercially pure lead and a Nichrome furnace winding. The same method of temperature control as above was used with the thermocouple, in an alumina sheath, dipping directly into the bath. A surface layer of carbon was maintained on the molten lead to minimize lead oxidation and the uranium specimens were coated with grease prior to immersion. On immersion the grease burnt leaving a protective adherent film which inhibited attack both in the lead and during the brief period of quenching.

Varied rates of quenching were achieved by employing different quenching media; some comparison between rates of quenching in these different media was required. The mechanism of quenching is complex and depends mainly on the stability and conductivity

of the vapour blanket formed around the specimen. Quenching rate thus depends not only on the conductivity of the medium but on a number of factors such as vapour pressure and it can only be satisfactorily determined empirically. Fortunately the temperature range in question has been studied in detail for steels and the results are directly applicable. Rate of quenching is compared with that of pure water at 0°C which is taken as unity and the comparative quenching rates for the media used are as follows - (taken from Metals Handbook 1948):-

1) 10% aqueous solution of NaCl at 0°C = 1.96
2) Water at 0°C = 1.00
3) Mercury at 0°C = 0.78
4) Silicone oil at 20°C (approximately) = 0.2
5) Still air at 20°C (approximately) = 0.03

For mercury quenching a mercury vapour gas-mask was worn to reduce the risk of poisoning.

Occasionally heat treatments were carried out in sealed silica capsules in the horizontal furnace and rapid cooling achieved by withdrawing the capsule from the furnace and quenching into water whilst breaking the capsule. Also, low temperature treatments were sometimes carried out in hot water and in liquid nitrogen.

2 Mechanical Treatment

2-a Tensile

Tensile testing was carried out on modified Hounsfield Tensometers. These are soft beam machines with limited accuracy but adequate for the general work involved here. Testing between -196°C

and 85°C was carried out on a horizontally mounted machine incorporating extension rods, chucks and an insulating vessel which held various liquids or liquid/solid mixtures at a constant temperature around the specimens. Temperatures were measured with a copper/constantan thermocouple and a portable potentiometer. The load was transmitted to a spring beam whose deflection was converted by means of a hydraulic piston to a movement of mercury in a calibrated glass tube.

For tests between 85°C and 800°C a vertically mounted Tensometer of the same type was used. Fig 18 shows a diagram of the tensile assembly. The system incorporated a Wild Barfield miniature Nichrome wound furnace, hot tensile chucks and extension rods. The specimens, chucks and extension rods were enclosed in a Ni-Co-Fe tube with cooling rings and seals at top and bottom; an oil bath at the bottom served as a moving gas-tight seal. Argon was passed through the tube and testing thus carried out in a protective atmosphere. Nickel radiation shields were used within the tube to minimize temperature gradients and temperature control effected by a similar method to that used for the furnaces. With the Tensometer in the vertical position the deflection of the beam could not be measured by the mercury piston but was measured directly with a micrometer dial gauge. Calibration of the beam deflection against dial gauge reading was carried out on the horizontally mounted tensometer. The deflection measured on the gauge was plotted against the load measured by the mercury column for each beam used and conversion factors determined. These were:-

2 ton beam: 0.100in (1 rev) ≡ 0.41 tons

1 ton beam: 0.100in (1 rev) ≡ 0.20 tons

and the graphs showed close agreement with linearity over the whole range

Since these factors differed widely from those determined in a previous study by a different author using resistance strain gauges, the calibration was checked at frequent intervals but it was found that the factors remained constant throughout experimental work extending over three years. In the vertical position an error in the factor can arise due to the weight of the chucks causing a reverse beam deflection. This is a zero error and should make little difference to the results but it was checked with mild steel tensile specimens. Specimens were tested to the U.T.S. on one machine, unloaded and tested on the other machine to the U.T.S. again and unloaded then returned to the original machine and tested again. This procedure was repeated a number of times with several specimens and the full stress/strain curves plotted. In no cases were discontinuities observed at the transfer points. Also identical specimens tested on different machines all had U.T.S. values within 5% of each other. These results demonstrated that there was neither a consistent nor a zero error between the machines that was of sufficient magnitude to be significant in this work.

The strain-rate was controlled on each machine by identical motor and pulley systems producing variable cross head speeds between 2.0in/min and 0.0078in/min. Unless otherwise stated the slowest strain-rate was used in this work (equal to 1.25% per minute)

The tensile specimens were standard no.13 Hounsfields (Fig 13) but for one section of the work notched tensile specimens were used The dimensions were identical with no. 13 Hounsfields with a 60°

angle notch, 0.02in deep, of root radius 0.010in, cut around the centre of the gauge length of the specimens.

The experimental error usually claimed for results obtained on Tensometers is ± 2% but the more conservative estimate of ± 5% only is claimed here.

2-b Bend

Bend testing between -196°C and 85°C was carried out using a Hounsfield Universal Bend Test attachment to the horizontally mounted machine (Fig 19). The attachment was surrounded by an insulating vessel which held various liquids or liquid/solid mixtures at a constant temperature around the specimens. For three-point loading the apparatus is as illustrated, but for four-point loading two further beams were assembled into positions C, the central beam then only acting as a guide. Positions A and B are for longer specimens.

Construction of the bending-moment and shear-force diagrams for three- and four-point loading illustrates the main differences between the methods (Fig 20). Clearly there is an advantage associated with four-point loading since there is a range of maximum strain and fracture tends to occur simultaneously at the two points of maximum shearing force. This gives greater scope for microexamination but at room temperature and above the apparatus could not accommodate the increased bending required for fracture except with very thick specimens. Three-point bending was therefore adopted

using rectangular beams of dimensions 2.5in by 0.1in by 0.3in cut from cast fuel rods. The beams were cut so that the axial defects were eliminated from the material.

A measure of ductility was possible from the angle of curvature at rupture and from the load/extension curve but a measure of strength is more difficult. The highest tensional stress in the beam section (S) determines rupture and is given by:-

$$S = M/Z$$

where M is the bending moment given by:-

$$M = PL/4$$

for a maximum load P and beam span L; and where Z is the section modulus given by:-

$$Z = bh^2/6$$

for a beam width, b and thickness, h. Hence,

$$S = 3PL/2bh^2$$

The point of highest stress is located at the intersection of the plane of load application (a-a in Fig.21a) with the bottom surface of the beam. When rupture occurs within the elastic range, S represents this stress (Fig 21b). However, when rupture occurs after appreciable plastic yielding the actual stress is no longer S but some lower value (Fig 21c) since the flexure formula is based on a stress distribution that increases linearly from the neutral axis to the outer fibre. Hence the stress calculation above is only approximate where the plastic deformation is appreciable.

2-c Compression

Compression tests were carried out between -196°C and 85°C using the Hounsfield Compression attachment and similar methods of temperature control. Only measurements of the decrease in length at fracture were made.

2-d Instron and Hardness

Some tests have been carried out using an Instron TM hard beam tensile machine. All standard accessories were used and it is therefore not proposed to describe these. Macro- and micro-hardness determinations were also carried out using a Vickers Macrohardness tester and the microhardness attachments on a Reichert microscope.

3 Metallography

As has already been mentioned, uranium presents some hazards in handling and many of these become apparent in metallographic preparation. The dust is toxic, pyrophoric and radioactive, and since no active laboratory was available in the Department much of the preparation was carried out at AERE Harwell to minimize these hazards.

Prior to mounting, the round tensile specimens were sectioned longitudinally under special conditions on a slitting machine at Harwell. The sections were then mounted in hard (black) bakelite. This mounting medium is particularly suitable for this work because it is sufficiently hard to preserve the fracture edge without recourse to nickel plating. However this was not always available and in

these cases, the fracture edge was nickel plated using an $NiSO_4$/NH_4Cl/H_3BO_3 plating solution and a very low current density, and the specimens mounted in diakon plastic. Mounting was followed by grinding under water with graded silicon-carbide papers (usually carried out at Harwell) followed by diamond polishing.

For inclusion identification no further preparation was necessary, apart from etching, but for grain structure examination normal etching techniques are of no value since grain contrast cannot be developed. Also, although uranium is anisotropic in many of its physical properties no grain contrast is revealed under polarized light. It is necessary to first develop an optically active surface whence contrast under polarized light is obtained. The grain contrast so produced is attributable to the production of an anisotropic oxide layer. A number of methods were investigated for the production of this surface including electropolishing and "attack-polishing" in a number of solutions. The method of attack-polishing described by Haddrell, Sykes and Mott (1956) was finally adopted. This involves mechanical polishing concurrently with chemical etching and results in anodizing of the surface to produce the required surface conditions. The mixture used was in the following proportions:-

50 grms	CrO_3
10 mls	HNO_3
40 mls	H_2O
5 grms	γ-Al_2O_3

Polishing was carried out with an automatic polishing machine on a Terylene Velvet cloth mounted in a Polythene bowl which contained the attack-polish solution. The cloth was welded to the underside

of a Polythene polishing disc which fitted into the bowl and a Polythene paddle directed the mixture onto the polishing disc (Fig 22). The Terylene remained unattacked and the gamma alumina became embedded in the fabric so that polishing occurred concomitantly with etching. The time required for polishing was approximately 15 minutes. Occasionally diamond instead of gamma-alumina polishing was used by embedding diamond paste into the polishing pad and using the mixture without gamma alumina. After preparation the best method of producing a stain-free microspecimen was found to be washing in soap and hot water followed by rinsing and drying with an air blast. The specimens oxidized fairly rapidly and were therefore only available for examination for a few hours before repolishing was necessary.

The fracture surface was also examined both by direct optical microscopy and, after two-stage carbon replication, by electron microscopy. The Davies (1962) technique of replication was adopted. This involved first obtaining a plastic replica by pressing the fracture surface into softened cellulose acetate strip and following this by gold-palladium shadowing and carbon evaporation. The plastic was then dissolved away leaving the carbon replica which was collected on microscope grids for examination.

VI GENERAL METALLOGRAPHY

The experimental results of this thesis are presented and discussed in three separate chapters; this is the first of these. Recorded here are the preliminary investigations which were undertaken to determine the feasibility of the original programme and those undertaken to establish the optimum treatment conditions, as well as a general study of the microstructural variables.

1 Examination of Second Phases

Probably the most important alloying characteristics of uranium are its tendency to form one or more intermetallic compounds with other elements and the very low solubility of alloying elements in the complex alpha and beta allotropes. The material used in this work contained significant proportions of carbon, oxygen, nitrogen, iron, aluminium and silicon (Table I). None of these elements is appreciably soluble in the alpha phase but they readily form compounds with uranium, and therefore exist as distinct phases throughout the matrix. The atomic weight of uranium is large compared with that of impurity atoms and therefore small weight percentages of these impurities appear as a large volume fraction of inclusions.

The most notable of these inclusions are cuboid in form and their appearance varies with the method of metallographic preparation. In the attack polished condition the cuboids were pale grey in colour but on immersion in 50% nitric acid they were stained

uniformly black although occasionally a "cored" structure was observed. The general distribution is given in Fig 23. The volume fraction varied between approximately 3% and 10% and the size between about 2 and 10 microns (side length). Sometimes the cuboid inclusions apparently develop a dendritic habit when molten and this is visible in Fig 23 but is more strikingly shown in Fig 24. These inclusions were originally identified as UC (Baenziger and Ruddle 1944) but later work suggested UO_2, UO and UN. The evidence for UC_2 was obtained from X-ray patterns of chemically extracted inclusions and Meredith and Waldron (1959) suggested that the UO_2 was formed on the surface of the extracted particles. The remaining conflicting conclusions are compatible in view of the isomorphous nature of UO, UN and UC and the cuboids are considered to be a complex designated U(O.C.N.). It has been suggested (Meredith and Waldron 1959) that this compound exists over a wide composition range as a result of intersolubility of the constituent elements. Thus, the impurities oxygen, nitrogen and carbon will all exist as this complex whose composition will vary with the relative concentrations. None of the heat treatments used in this work was found to affect the size or distribution of these inclusions.

Occasionally inclusions were observed which, from the work of Meredith and Waldron, were probably magnesium fluoride slag inclusions. Uranium hydride was not distinguished in any of the specimens and it therefore seems likely that the hydrogen content was too low. (It was hoped to obtain hydrogen analysis to an accuracy of better than 1 ppm but this is apparently not directly

possible in this country (Austing 1962). Construction and calibration of a hydrogen analysis apparatus was considered irreconcilable with the present programme of research).

The remaining elements present, iron, aluminium and silicon take the form of precipitates of the intermetallic compounds U_6Fe, UAl_2 and U_3Si. In the as-cast condition they exist as a fine network of particles unrelated to the alpha grain boundaries (Fig 25). Attempts were made to distinguish between the different types of intermetallic particles by selective etching techniques. These techniques were shown to be satisfactory (Jepson et al 1958) with U-Al, U-Fe and U-Si alloys where the particles were present in relatively large proportions but was found to be largely unsatisfactory with the materials used here. Thus, no technique was available to distinguish between the intermetallic compounds and moreover it was found difficult to evaluate or eliminate pitting effects.

It was originally intended that the distribution of these intermetallic phases should be a major variable in this work and a number of heat treatment schedules were investigated in the hope that they might indicate how control of distribution could be achieved. Equilibrium data indicates that aluminium and iron are soluble in the gamma phase up to about 0.5 wt% and therefore prolonged gamma treatments followed by a water-quench and alpha-anneal was considered as a possible method of varying the distribution. It was found that the intermetallics were partially retained in solution by gamma-quenching and also to some extent by beta-

quenching. This was followed by precipitation on alpha-annealing but random network distributions similar to that shown in Fig 25 resulted. Occasionally in some specimens, there appeared to be some tendency for grain boundary precipitation but the results were not reproducible. Many heat treatment variations were used but precipitation was in each case random. It was concluded that a study of the effects of second phase distribution on the mechanical properties and fracture of uranium would be more profitably carried out using material with higher concentrations of iron and aluminium. Alloys of this type were originally to be supplied but subsequently became unavailable and therefore a study of the effects of intermetallics distribution on the properties was not attempted.

2 Grain Structure after Thermal Treatment

Materials of grades B,C and D (Table I) were supplied in the as-cast conditions and since cast structures are liable to gross heterogeneities of both grain and precipitate structure, all specimens were subjected to a preliminary homogenizing treatment. This usually consisted of a long beta-anneal (48 hours at 720°C) followed by slow cooling to room temperature. At these cobling rates the beta→alpha transformation was diffusional and the resulting grain structure was coarse with smooth grain boundaries. The grains often contained deformation twins in the form of thin lamellae which result from the stresses arising from the anisotropy of thermal contraction of orthorhombic alpha. Fig 26 shows a structure with examples of such twins. Frequently only one family of twins was observed per grain but sometimes several families were found. The twins were very thin, usually not exceeding a width of 10 microns and were sometimes less than one

micron. At grain boundaries or other obstacles they usually tapered to a point and thus, if the twins were short and thick they were lenticular rather than lamellar shaped. When twins met each other they either tapered to a point and started afresh on the other side or intersected. Cahn (1953) has studied such twin intersections in uranium in detail and as a consequence it was sometimes possible to identify twin families from the geometry of intersections. Twins were also observed to divide (Fig 26) and often appeared to be grain boundary nucleated (which would be expected since the grain boundaries are the sites of the thermal contraction stresses). The twins seemed to readily incorporate cuboid inclusions during growth.

At increased rates of cooling from the beta the grain sizes became finer and more irregular in profile. At air-cooling rates only grade A material showed gross irregularity of profile (Fig 27) indicating significant contribution of the shear mechaniam of transformation at even this cooling rate. At fast cooling rates (oil-quenching) all grades of material exhibited the well-known jagged or feathery grain structure (Fig 28). The irregularity of profile increased with increasing cooling rates and there was a concomitant decrease in grain size. Doubly-adjusted material after high beta-treatment temperatures and rapid quenching (iced-brine) resulted in retention of the beta phase. This was followed by a slow isothermal shear transformation to alpha (Fig 29). This room temperature shear transformation usually resulted in widespread cracking of the specimens (Fig 30).

Gamma-quenching into iced brine of the purer materials resulted in similar structures to those observed on beta quenching but at the surface of doubly adjusted specimens the direct gamma-alpha transformation was observed (Fig 31). At the edge of the specimens can be seen a fine equiaxed grain structure which it is claimed results from the diffusional gamma→ alpha transformation whilst in the centre of the specimen, a structure similar to that observed upon beta quenching is found. This micrograph also gives some indication of how the transformation takes place (Grainger 1958): by the formation of martensite plates which then widen giving thick almost equi-axed feathery grains.

Since the fine equiaxed structure resulting from the gamma-alpha diffusional transformation only occurred at the surface in the fastest quenched material, the treatment could not be used in this work for the production of a range of grain sizes. However, the different grain sizes resulting from differential beta-quenching rates were studied as a possible method. Initially the grain sizes were determined in the materials B, C and D after various cooling rates and these are given in Fig 32. The cooling rates were not measured quantitatively but the results were reproducible.

It is not sufficient merely to test after different rates of quenching since other variables are present which may mask the effect of grain size so produced. These are, variation in precipitates (due to partial retention in solid solution after rapid cooling) and variations in grain profile (resulting from the varying

contributions of the shear and diffusional modes of transformation). It is possible to define a sequence of treatments which should eliminate any precipitation effects:-

1) Prolonged alpha anneal (100 hours at 625°C) which homogenizes and will precipitate all the intermetallics.

2) Very short beta treatment such that only sufficient time is given to achieve the required temperatures without any solution of intermetallics.

3) Varying rates of cooling from the beta-phase temperature.

The distribution and amount of precipitate should not change after treatment (1) and, within the limitations already defined, this was observed.

It is more difficult to eliminate the effect of grain shape. Alpha-annealing of the fast-quenched specimens resulted in recrystallization producing smooth grain boundaries without change in grain size (Fig 33). Tests on such specimens could be compared with tests on specimens with slow-cooled beta→ alpha diffusional structures. However, annealing of specimens cooled at intermediate rates resulted in no such recrystallization. Presumably insufficient strain was present for recrystallization at the maximum treatment temperature (660°C). Hence this procedure is not completely satisfactory because of the additional variation in grain profile between specimens.

As an alternative to eliminating the grain profile variable a heat treatment programme was devised, similar to that above, to isolate and investigate the effect of grain shape on the mechanical properties and fracture. Having isolated and studied its effect it might then be possible to examine the effect of grain size by the

above method and make appropriate allowance for any comcomitant effect of grain shape. This was attempted for the three cast materials: the treatments involved a preliminary alpha homogenising treatment followed by a short (75 second) beta treatment. No solution of the intermetallics could then occur in the beta to produce the possibility of a further, dispersion variable. After beta treatment the specimens were quenched and then annealed, either to recrystallize the specimens (at 625-650°C), or to strain-relieve without changing the grain shape (at 470-500°C). The hardness as a function of annealing time results are recorded in Fig 34. The tensile results which were obtained (Chapter VIII) indicated that the variation in grain shape in specimens of different grain size produced by differential quenching rates could influence the tensile results in a manner that could not be accurately compensated for.

The results of McIntosh and Heal (1958) suggested a second possible method of producing a range of grain sizes in cast material by heat treatment. They observed appreciable grain growth after beta-quenching followed by alpha-annealing. Specimens were therefore fast-quenched and annealed for various times at a number of temperatures. However, even after annealing for 175 hours at 640°C only recrystallization of the specimens without appreciable grain growth, had taken place and the method was therefore of no value.

A further method of varying the grain size was attempted. Presumably the alpha grain size must be effected by the original beta grain size: specimens were therefore alpha homogenized and subjected to isothermal beta anneals for varying periods and oil-quenched to establish the alpha grain size as a function of soaking

time. The grain sizes on transformation for the grades B, C and D are shown in Fig 35 and clearly there is an effect (longer beta treatment times result in increasing fineness of alpha grain size) but the grain size range possible from such treatments is too limited to be useful here.

Although grain size control of fuel rods is of great importance in nuclear technology, the fundamental reasons for the effect of iron and aluminium additions on grain refinement are not well understood (Butcher 1962). The present results may make some contribution to this field. It is relevant to note that grain refinement of reactor bars is achieved by quenching after only 15 seconds in the beta range. This is too short a time for appreciable solution of the additions but it does not eliminate the possibility that refinement is attributable to the elements in solution, rather than to the network dispersion, since after casting the elements are in supersaturated solid solution (Butcher 1962).

The results presented in Fig 32 merely demonstrate the well known effect semi-quantitatively but Fig 35 records effects which have not been previously reported.

a) An initial decrease in grain size with increasing soaking time in each alloy is observed which levels out to a plateau at approximately the same time in each alloy (5 hours).
b) After prolonged beta treatments of unadjusted material a further decrease in grain size upon transformation is observed with increasing soaking time.

The shortest treatment time was 1¼ minutes in the lead bath and the results of Dixon and Fern (1963) indicate that no appreciable beta solution of the intermetallics could have taken place after these

treatments. These workers have also shown that complete solution takes of the order of on hour at similar temperatures.

The initial decrease in grain size with increasing soaking time would appear to be related to solution of the intermetallics since both processes take approximately the same time. Additions of iron and aluminium in solution are known to lower the transformation temperature (Jepson et al 1958) and as a consequence a finer grain size would be predicted since the rate of alpha grain growth would be reduced. This provides an explanation for the initial decrease but this effect is small compared with the general influence of adjustment which exists even after only 1½minutes at temperature where solute effects are absent. The general effect of grain refinement must therefore be due only to the increasing amounts of dispersion network present.

Where a dispersion is random, increasing amounts tend to increase the recrystallized grain size because grain nucleation rather than growth is inhibited (Doherty and Martin 1963). However, this effect was not observed here: increasing amounts of the network dispersion resulted in a decreasing recrystallized grain size after coldwork. This may be attributed to the continuous nature of the dispersion (Fig 25) which might be expected to inhibit grain growth more profoundly. One can explain the transformation grain size effect in the same terms: increasing amounts of dispersed network (i.e. increasing iron and aluminium content) inhibit alpha grain growth and produce a finer grain size. Also nucleation of alpha from beta may be enhanced by increasing amounts of dispersion.

Grain growth of beta is suggested to occur after prolonged treatment to explain the second decrease in transformed grain size in unadjusted material. This is a reasonable speculation since the volume fraction of dispersion will be much less in this grade particularly after beta-solution and similar effects of the dispersion on alpha grain growth have been found (see section 3). Then, if alpha nucleating sites are predominantly at beta grain boundaries, beta grain growth will lower the transformation temperature reducing the rate of alpha grain growth and produce the observed grain refinement. This explanation is speculative and further experimentation is necessary to confirm this and the other suggestions. This was not attempted here because the grain size effect produced is of too small a magnitude to be useful in this work.

The microstructural effects of thermal cycling were investigated to a limited extent. The twins already discussed arise from the stresses due to the anisotropy of thermal expansion but the cumulative effects of a few thermal cycles was also examined. Specimens of unadjusted beta slow-cooled material were thermally cycled between 100°C and 350°C 10 times in the horizontal vacuum furnace by pulling in and out of the hot zone when the required temperature was achieved. The complete treatment took three hours. More twins were found after the treatment but no grain boundary effects were visible (e.g. rumpling) as is generally observed after many cycles (Foote 1956). Polished specimens were also examined after cycling 10 times between -196°C and 75°C. Twin traces were observed to have formed across several grains on bright field examination (contrast resulting from surface tilt) and an example is shown in Fig 36. Again no contrast at grain

boundaries was produced. An indication of the plastic strain produced by successive cycles was obtained from hardness determinations (Table IV).

Table IV

No. of cycles between -196°C and +75°C	Hardness V.P.N. (10Kg)
0	190
1	203
3	209
5	211
7	208
9	215
10	213
20	215

Notable in these results is that the hardness increases only slowly after the initial few cycles such that the increase produced in the first cycle is roughly equivalent to that produced between 1 - 10 cycles. The increase between 10-20 cycles is not sufficiently large to be satisfactorily detected by this technique. These results are similar to those obtained by Young, Gardiner and Rotsey (1959) using a more elegant technique for measurment of plastic strain.

Micro-hardness measurements across grains after thermal cycling gave no indication of any concentration of strain to grain boundary (or other) regions.

3 Structures after Mechanical and Thermal Treatment

It was clear from the results of the preceding section that heat treatment alone could not produce the required microstructural variables. Mechanical treatment followed by annealing was therefore investigated, firstly upon the machined test pieces.

Unadjusted specimens, after beta-quenching and alpha-annealing to produce a fine grain size, were strained controlled amounts at room temperature in the Tensometer and isothermally alpha annealed. The resulting grain sizes are given in Table V.

Table V

Tensile Strain (Elongation at 20°C)	Average Grain Size (diameter)
2.1	1.0mm
3.2	1.0mm
4.5	0.7mm
5.9	0.33mm
7.8	0.11mm

These results are satisfactory from grain size considerations but the cuboid inclusions cracked at about 3% plastic strain and the surface of the specimens was considerably roughened. Both the variation in surface condition and the cuboid cracking could mask any grain size effect and therefore the method was not considered to be satisfactory. Isochronal alpha annealing at various temperatures after 5% plastic strain, thus eliminating these variables, was therefore tried. The grain size results are recorded in Table VI.

Table VI

Alpha annealing time = 24 hours

Plastic strain = 5.2% elongation

Temperature of Annealing	Average Grain Size (diameter)
550°C	0.45mm
580°C	0.50mm
605°C	0.42mm
625°C	0.55mm
658°C	0.50mm

Clearly isochronal annealing is unsatisfactory since the maximum annealing temperature is limited to 666°C, the beta-transus, and at lower temperatures grain growth is negligible.

As a consequence of these findings AERE made available some adjusted cast fuel rods upon which a rolling and annealing schedule was carried out. The details of this schedule were given in Table II and from the rolled rods tensile specimens were machined and supplied The reductions in area varied between 3% and 30% and the grain sizes after annealing for 5 hours at 640°C are given in Table VII.

Table VIII

% Reduction in Area at 300°C	Grain Size (average diameter)
3.2	0.02mm
6.3	0.03mm
10.2	0.045mm
19.4	0.03mm
27.9	0.025mm

An example of a grain structure is shown in Fig 37. No appreciable grain growth after recrystallization was found to occur (e.g. after 100 hours at 650°C) and this and the small range of grain sizes produced can be attributed to the fine dispersion of intermetallics retarding grain growth. In addition, examination of the specimens revealed that the material was unsound. The axial pips had not welded-up on rolling and was sometimes 0.5mm in width (Fig 13). Porosity and large inclusions were also present which had sometimes given rise to cracks on rolling (Fig 14). Also occasionally a banded grain structure was observedwith bands of coarse and fine grains (Fig13'

This is a consequence of the heterogeneity of deformation which occurs in uranium (Foote 1956).

The consequence was that AERE finally made available a direct cast ingot of virgin unadjusted material. This ingot was prepared as outlined in Table III and the resultant material proved sound and defect-free. Also, it was of much higher purity than any of the other grades and thus grain growth was not retarded to the same extent. The grain size in the annealed condition prior to the final treatment was 0.03mm average diameter and a typical structure is shown in Fig 38. some rods of this material were rolled to varying reductions at 300°C and annealed at various temperatures to produce a wide range of grain sizes (Table VIII).

Table VIII

Treatment (24hr anneal)	Grain Size (diameter)
28% red'n / 496°C	0.01mm
28% red'n / 545°C	0.015mm
28% red'n / 613°C	0.04mm
28% red'n / 641°C	0.06mm
11% red'n / 496°C	0.03mm
11% red'n / 545°C	0.04mm
11% red'n / 613°C	0.07mm
11% red'n / 641°C	0.09mm
8% red'n / 496°C	0.03mm
8% red'n / 545°C	0.12mm
8% red'n / 613°C	0.14mm
8% red'n / 652°C	0.20mm

Typical grain structures are shown in Figs 39-41. Notable features arethe uniformity of grainsize, smooth grain profiles and absence of inclusions and defects.

Tensile specimens of this material prior to the above final reductions were also subjected to a strain anneal schedule (after Cahn 1951) to produce coarse grain sizes. Tensile specimens were plastically strained between 1% and 7% elongation at 85°C (this temperature chosen as a convenient elevated temperature which increases ductility and reduces the likelihood of cuboid cracking) and annealed for 3 hours at 640°C. The results are presented in Fig 42. Plastic strain of greater than approximately 3% was necessary to produce a homogeneous structure: at lower strains some very coarse grains were produced with regions of unchanged structure (Fig 43). The grain structures were similar to those shown in Figs 39-41 with equiaxed smooth profiled grains.

Specimens were also tested in the rolled condition and after annealing at a range of temperatures. Fig 44 illustrates the types of microstructure obtained. After the rolling treatment, the structure was very confused with elongated grains and many intersecting twins. After annealing at below the recrystallization temperature, a banded structure was developed, the bands being parallel to the direction of rolling. After annealing at 348°C, the microstructure was composed of approximately 25% recrystallized grains/75% deformed, and after annealing at 420°C, 50% of the microstructure was composed of recrystallized bands (Fig 44). The as-rolled structure was similar to that seen in the deformed bands of Fig 44. After beta annealing the grain structure was very coarse. These results are summarized in Table IX.

Table IX

Original grain size 0.03mm average diameter followed by rolling 28% reduction in area at 300°C.

Annealing Temperature ("air" cooled)	Grain Size (mms av. diameter)	Comments
as-rolled	unrecrystallized	deformed elongated grains corresponding to deformed zones in Fig 44.
242°C	unrecrystallized	
348°C	25% recrystallized	banded structure in direction of rolling corresponding to Fig 44.
420°C	50% recrystallized	
496°C	0.01	uniform equiaxed smooth profiled grains - corresponding to Figs 39-41.
545°C	0.015	
613°C	0.04	
641°C	0.06	some secondary recrystallization resulting in a heterogeneous grain structure.
680°C	0.75	beta transformed structure - corresponding to Fig 26.
752°C	0.9	

An example of a microstructure after 15% tensile deformation at room temperature is shown in Fig 45. With decreasing temperature the twins tended to be thinner and frequently deformation on only one family of twins was observed per grain. With continued deformation the twins became more profuse and tended to run into one another (Fig 46). Further features of mechanical twinning are shown within the micrographs referred to in the next chapter.

One important aspect which was not investigated directly was the effect of preferred orientation. Specimens machined from cast rods and heat treated should have random grain orientations. However, a pronounced texture develops in uranium after mechanical treatment and this is not removed by alpha-treatment but only by beta-treatment followed by slow cooling. Thus preferred orientations must be present in all the mechanically treated specimens but this will be constant in specimens given similar treatments. Nevertheless the overall effect should not be neglected.

4 Summary

1. The factor of controlling the distribution of second phase was investigated as a possible microstructural variable and although the study was not exhaustive sufficient knowledge was obtained for it to be considered that full exploration to control this variable was irreconcilable with the present programme. Material with a larger proportion of iron or aluminium would be preferable for the work and special etching techniques would have to be developed.

2. The microstructural variable of grain size cannot be satisfactorily isolated by heat treatment alone. However a variation in grain shape can be produced in which no variation in grain size or precipitate distribution is expected.

3. Some contribution to the grain size problem in uranium has been made. It seems likely that the important criterion of grain refinement by additions of iron and aluminium is the increasing amounts of network dispersion produced rather than a solution effect.

4. The beta→ alpha transformation can be suppressed by fast beta -quenching to 0°C. in doubly adjusted material to produce meta-stable beta which then slowly transforms martensitically to alpha.

5. The direct gamma→ alpha transformation was observed by fast gamma-quenching to 0°C in doubly adjusted material.

6. The microstructural effects of small numbers of thermal cycles are limited to twinning: no grain boundary effects were observed.

7. A satisfactory method of producing a range of grain sizes without any other influencing variable being present was found. This involved careful preparation of the original material followed by mechanical and thermal treatments.

8. The various microstructures obtained were characterized.

VII FRACTURE BEHAVIOUR

It has already been established that uranium exhibits a fracture transition from a ductile to a brittle behaviour in the region of room temperature. However, some of the detailed aspects of the transition were unknown and it was the function of the work described in this chapter to elucidate these.

Three distinct modes of fracture were observed in alpha uranium: above the transition a typically ductile failure occurred which with decreasing temperature changed to a cleavage type failure, but in the limited region of this transition intercrystalline failure was frequently observed. This behaviour is perhaps best summarized in terms of a classical fracture stress diagram (Fig 47). The intersections of the curves A (cleavage strength), B (grain boundary strength) and C (yield strength) represent the change in fracture mode. However, a sharp change of this type is not exhibited. Where there is little difference between the corresponding strengths, both types of failure are prevalent: the dotted lines have therefore been constructed to indicate these ranges. The fracture transition occurs concomitantly with a tensile transition and both are affected by many variables: these are more appropriately dealt with in the next chapter. Apart from the alpha fracture characteristics, some study of fracture in beta uranium was made.

1. Ductile Failure in Alpha Uranium

Above the ductile/brittle transition tensile elongations of between 15% and 60% were obtained depending upon temperature soundness, purity and other variables. To determine the detailed mechanism of failure, specimens were interrupted at various stages of tensile tests above the range of temperature within which the transition to brittleness occurred and examined metallographically. The following results were obtained, mainly with fine-grained virgin material since ambient temperature was within the ductile range:-

1) At elongations greater than about 2% at room temperature cuboid inclusion cracking was observed either by inclusion/matrix parting (Fig 48) or by cleavage of the cuboids (Fig 49). At higher temperatures (300°C) only occasional cracking of the cuboids was observed at these extensions but above about 10% elongation the majority of the inclusions were observed to have either parted or cleaved. With further increasing temperature the inclusions less frequently cleaved but holes were observed to form at inclusion/matrix interfaces after 15-20% elongation (500-600°C).

2) Increasing extension caused these cracks or holes to open up (Figs 49 and 50) until the microstructure contained a large number of elongated voids (Figs 51 and 52).

3) With continuing deformation these voids linked-up to form larger voids (Fig 53) and external necking of the specimen became appreciable.

4) At the centre of the neck a macroscopic fissure formed by cavity coalescence (Fig 54) which propagated outwards to cause failure (Fig 55). Fig 56 shows a replica of a fracture surface taken from a specimen which failed in this way.

These observations are very similar to those of Puttick (1959) in copper and are consistent with the more general theory of ductile fracture discussed in Chapter II. The inclusions

present in uranium which initiate void formation are larger and in greater number than those in copper. Hence many more voids are produced. Also, the number of slip systems operative in uranium at room temperature are limited and therefore void-formation occurs at an early stage because accommodation of the inclusions in the deforming matrix is less likely. This explains the effect of temperature upon cuboid cracking since at high temperatures further slip systems are active. Electron microscopy demonstrated that failure occurred by coalescence of cavities under the influence of a uniform plastic strain in the direction of the applied stress since equiaxed dimples were produced rather than parabolic cusps (Fig 56). The diameter of the dimples on the replica are approximately the same diameter as the voids produced by cuboid cracking.

At lower temperatures, material soundness was shown to have a profound influence upon ductility. Above about 300°C any major defect present merely opened up to form large internal necks and ductility was not appreciably affected. However, in the region of room temperature, the defects propagated as a crack taking a path through cracked cuboids to cause early failure (5-10% elongation). The material under investigation by Davies (1962) contained a high proportion of such major defects and it is claimed that this explains why he suggested that there were two distinct types of ductile failure; "tearing" below 400°C and "dimpled" above 400°C. The "dimpled" failure he described appears to be similar to that characterized above, except that he observed parabolic cusps as opposed to equi-axed dimples on the

fracture surface. This would be expected in unsound material because cavity coalescence would probably occur under the influence of a non-uniform strain and the voids would be distorted and appear as cusps (Beachem 1963). However, it is claimed that the "tearing" fracture observed by Davies was a consequence of cracks propagating from major defects. Davies contended that this "tearing" failure was caused by cracks propagating into the matrix from the cracked cuboids. No evidence that inclusion cracks initiated cracks in the matrix was obtained in the present examination of many specimens under a variety of conditions and it is suggested that Davies' results can be interpreted in terms of the propagating crack tending to take a path preferentially through the cracked cuboids.

It is therefore concluded that, in the absence of major defects, the only mode of failure in alpha uranium above the transition is by the cuboidal cavity coalescence characterized by Figs 48-56. This makes the reasonable assumption that uranium will always contain some cuboid inclusions.

2 Intercrystalline Failure in Alpha Uranium

At about room temperature a transition from the ductile failure described above to a predominantly intercrystalline failure described was observed. The amount of intercrystalline failure varied with metallurgical history but was observed to at least a small degree after most heat treatments. The gauge length

of specimens were examined after fracture and a number of features of intercrystalline cracking observed.

No satisfactory evidence was obtained of particular sites for the nucleation of intercrystalline fissures but there appeared to be some evidence that it occurred where a twin impinged upon a grain boundary (or the other way round) (Fig 57). Stresses are associated with the apices of twins and in favourable circumstances these could result in such crack nucleation. No evidence was found to support the hypothesis of Davies that intercrystalline failure was nucleated by cracked cuboids. Fig 58 shows the progress of a small microcrack along a boundary at room temperature. These microcracks tended to be arrested at grain boundary junctions in which a major change of direction was involved (Fig 58 and 59). and also at points where twins intersected the grain boundary (Fig 59). However the twins may have been a consequence of arrest of propagation or alternatively it is possible, as discussed, that the twins are the sites for the nucleation of cracks. Subsequent transgranular propagation of a grain boundary fissure was often observed (Fig 60). A typical fracture edge after this type of failure is shown in Fig 61. As is shown in this micrograph, the fracture was frequently "mixed" with vestiges of both ductile failure and twin-parting. Intercrystalline failure predominated down to about $-10^{\circ}C$ in many specimens but with further decreasing temperature brittle cleavage failure became the predominant mode. Occasionally, however, intercrystalline microcracks were observed down to $-95^{\circ}C$ (Fig 62).

It was originally tacitly assumed (Taplin and Martin 1964) that intergranular failure was due to impurity segregation since no evidence was found to suggest that a grain boundary precipitate could be the cause. The variation in prevalence of intercrystalline cracking with heat treatment with no observable change in precipitate distribution was considered to lend some support to the suggestion. Radioactive tracer analysis and surface energy measurements would be necessary to investigate this fully and it remains a possible explanation.

However, there is a further possible method of lowering the surface energy at grain boundaries to favour an intergranular path of fracture. The work done during grain boundary cracking (W) is given by:-

$$W = (2\gamma_s - \gamma_B) \qquad \ldots\ldots\ldots\ldots\ldots\ldots(1)$$

where γ_s is the surface energy per unit area of the fracture surface and γ_B is the grain boundary energy. γ_s may be reduced by impurity segregation but if γ_B is increased, grain boundary failure will also be favoured. This term can be increased in selected areas if there are residual stresses at the grain boundary and these can arise in alpha uranium due to the anisotropy of thermal expansion particularly if the strains are sufficient to produce plastic flow. The temperature increment to produce plastic flow during a heat treatment cycle has been shown by Young et al (1960) to be given by:-

$$\Delta T_p = \frac{Y(1+\nu)}{E\,\Delta\alpha} \qquad \ldots\ldots\ldots\ldots\ldots\ldots(2)$$

where ΔT_p is the temperature increment; Y is the yield stress;

E Young's modulus; ν Poisson's ratio and $\Delta\alpha$ is given by:-

$$\Delta\alpha = \alpha_a - \alpha_b \quad \ldots\ldots\ldots\ldots\ldots\ldots(3)$$

where α_a, α_b, and α_c are the coefficients of thermal expansion in the a, b and c directions and $\alpha_a \doteqdot \alpha_c \doteqdot +30^{\circ}C^{-1} \times 10^{-6}$ (mean) and $\alpha_b \doteqdot -5^{\circ}C^{-1} \times 10^{-6}$ (mean) (see Fig 2). For cycles of less than ΔT_p no plastic strain is postulated by the theory.

The value of ΔT_p is temperature dependent for not only do Y and E vary with temperature but $\Delta\alpha$ is strongly temperature dependent. For example, at room temperature $\Delta\alpha$ is approximately $+20^{\circ}C^{-1} \times 10^{-6}$ and at 500°C is $+60^{\circ}C \times 10^{-6}$ (see Fig 2). The consequence is that ΔT_p decreases with increasing temperature so that a smaller heat treatment cycle is necessary at higher temperatures to produce the same amount of strain.

The original results obtained (Taplin and Martin 1964b) were:-

a) Beta treatment and furnace-cool:- grain boundary cracking is only rarely observed.

b) Beta quench followed by alpha anneal and air-cool:- grain boundary cracking predominated within the limited transition temperature range.

After (a) few residual grain boundary strains would be present since beta treatment will remove any strains and subsequent furnace cooling will produce few strains; whereas after (b) strains will be introduced on beta-quenching and after alpha annealing and air cooling. It is suggested that the prevalence of grain boundary cracking after (b) is a consequence of the residual grain boundary

stresses lowering γ_B in selected areas. Some experiments were therefore devised to test this hypothesis by introducing additional boundary stresses by treatments which would by unlikely to produce impurity segregation effects at the same time. Unadjusted tensile specimens were subjected to the following consecutive treatments and some specimens tested after each stage:-

1) Beta Treatment: 48 hours at 720°C and furnace cool.
2) Alpha Cycle: 10 slow thermal cycles between 100°C-350°C.
3) Beta Treatment: 30 mins at 720°C and furnace cool.

Examination of sectioned specimens tested at a range of temperatures revealed that;

a) after 1) only rarely were intercrystalline cracks observed.

b) after 2) a considerable amount of intercrystalline cracking occurred within the temperature range 0°C -100°C;

c) after the final beta treatment 3), again only rarely were intercrystalline microcracks observed.

These results demonstrate that after alpha cycling grain boundary cracking is favoured but that this effect is removed by a short beta treatment and furnace cool. One cannot conclude unambiguously that this is due to residual grain boundary stresses and not due to solute segregation since diffusion of some impurities is still possible at 350°C. Some specimens were therefore alpha annealed after the initial beta treatment for 3 hours at 350°C - (about the same time at 350°C as the complete cycle treatment took) with both furnace heating and cooling, and tested. The specimens showed no tendency for intercrystalline failure and only rarely

were microcracks associated with grain boundaries observed at any temperature. This tends to confirm the suggestion that intercrystalline cracking is due to residual grain boundary stresses rather than solute segregation since the 350°C anneal should produce the same segregation effects as the 350°C cycle.

Nevertheless the hypothesis was subjected to further tests. Specimens were thermally cycled 10 times between 75°C (hot water bath) and -196°C (liquid nitrogen bath) after beta treatment and tested. The complete treatment took 40 minutes and the diffusion rate of most of the possible elements would be too slow to cause a lowering of γ_s. The time at 75°C was about 20 minutes and the increased diffusion rate above that at room temperature could only have any influence upon interstitials. Taking hydrogen as an example, where $D_o = 1.4 \times 10^{-3} cm^2/sec$ and $Q = 6400$ cal/g.atom are known (Davis 1956) diffusion distances can be approximated. A diffusion distance of the order of a grain diameter (0.1mm) is estimated for 20 minutes at 75°C so that solute segregation is possible. But at room temperature a similar diffusion distance is estimated to result after less than a day and therefore the cycling treatment should give no variation in segregation between that at room temperature.

After this cycling treatment intercrystalline microcracks were frequently observed in the range 0°C - 100°C but the embrittling effect was of a smaller magnitude than the effect of the 350°C thermal cycle. This is consistent with the theory since Δa is

approximately $+20^{\circ}C^{-1} \times 10^{-6}$ for the low temperature cycle and approximately $+35^{\circ}C^{-1} \times 10^{-6}$ for the 350°C cycle and thus the strain produced by the low temperature cycle will be considerably less. Also, the yield stress increases with decreasing temperature with similar consequences.

Finally specimens were cycled ten times between room temperature and -196°C and a similar but smaller grain boundary embrittling effect was produced - the smaller effect is readily explained in terms of decreasing stress with decreasing temperature increment of cycle.

Fig 63 shows an intercrystalline microcrack in a specimen tested after thermal cycling. Notable in this micrograph, apart from the fissure, are the twins which appear to be grain boundary nucleated. This is consistent with grain boundary strains being relieved by twinning and direct observations of plastic strain after thermal cycling were made. Hardness results after each cycle (Table VIII) show that a significant amount of strain is produced by even one cycle and that although thermal cycling produces a cumulative effect it is not additive. This means that even one heat treatment (particularly with rapid cooling) may give rise to sufficiently large residual stresses to cause grain boundary embrittlement. It should be noted however, that thermal cycling stresses cannot have been sufficient to cause actual grain boundary rupture for beta treatment completely restores ductility which would only be possible if the embrittlement was due to stresses rather than crack nuclei.

An effect of grain size upon the tendency for intergranular fissuring was found after identical final thermal treatments: a marked tendency for increased predominance of intercrystalline cracking with increasing grain size was observed. This would be expected if the thermal cycling model were valid but not if a solute segregation effect were: the magnitude of the residual boundary stresses would be expected to increase with increasing grain size thereby promoting intercrystalline cracking. Indeed the reverse effect might be predicted if intergranular failure were attributable to impurity segregation since the diffusion distance to grain boundaries is shorter in fine grained material. Some confirmation of this suggestion was found by counting the number of twinned grains and the number of twin families per grain in different grain sized specimens which had had identical heat treatments. The results are presented in Table X. (An appraisal of the micrographs referred to in Chapter VI demonstrates the effect quantitatively).

Table X

Grain Size (average diameter)	(A) Percentage of Grains with twins visible	Percentage of (A) with more than one family of twins visible
0.015mm	1%	10%
0.04 mm	15 %	25%
0.12 mm	60 %	30%
0.90 mm	80 %	40%

In conclusion it is contended that an intergranular path of brittle fracture is favoured because the grain boundary surface energy is lowered in selected areas by the residual grain boundary stresses which are present to a varying degreee after most heat treatments. This does not preclude an additional influence of impurity segregation.

3 Cleavage Fracture in Alpha Uranium

With decreasing temperature below ambient there was a gradual transition from predominantly intercrystalline to crystallographic failure (except in beta-treated and furnace cooled specimens in which very little intercrystalline cracking is observed). The features of the crystallographic failure were in all cases identical. Direct examination revealed a fracture surface which was "facety" and highly reflective in areas and with decreasing temperature the proportion of such areas increased. By estimating the percentage of these facety areas a quantitative measure of the transition behaviour could be made (cf Tipper 1962). Optical microscopy revealed distinct cleavage steps (Fig 64) and "river" markings (Fig 65); similar effects were observed upon electron metallographic examination of fracture replicas (Fig 66). These results demonstrated that the low temperature brittle fracture was characteristic crystallographic cleavage.

Bright field examination of sectioned specimens showed that the microcracks exhibited similar crystallographic characteristics (Figs 67 &68). The crack in Fig 67 appear to have been nucleated at a surface flaw. Under polarized light, grain contrast

indicated that the fracture edges associated with facety areas were accurately parallel to families of twin traces (Fig 69). Careful examination showed that failure coincided exactly with twin/matrix interfaces and that the cleavage steps were produced by the fracture path jumping from one twin interface to another (Fig 70). Fig 71 shows the same area as Fig 69 ground back approximately 0.1mm and comparison clearly demonstrates that the cleavage plane accurately follows the interface of twin lamellae in two dimensions, finally refuting the interpreting of Davies (1962).

These results established that the mode of low temperature brittle fracture in these specimens was identical with that first observed by Cahn (1953) and which is usually termed twin/matrix interface parting.

Cahn showed that only twin intersections involving {172} and {130} twins occur and by examining the geometery of twin intersections it was sometimes possible to identify a twin family as belonging to one or other of these. Such observations that were made in conjunction with fracture edges usually indicated that the main twin composition planes of parting involved either or both of these twins. A full investigation of the plane of parting is only satisfactory with single crystals since X-ray patterns from the facety areas are distorted due to the plastic deformation which accompanies the fracture process. In any event, this was rendered unnecessary here by the work of Lemogne and Lacombe (1963) who studied the fracture of single crystals of uranium at -196°C. These authors concluded that brittle failure invariably occurred

by parting along a twin composition plane and that {172} parting was easiest but that {130}, {121}, {112} twin parting were also observed. The above tentative conclusions are consistent with these findings. Re-examination of the atom movements in {172}and {130} twinning (Chapter II) shows that considerable stress is associated with the twin boundaries and one might therefore predict that these are planes of relative weakness in the lattice. The fact that more stress is associated with {130} than {172} twinning is difficult to reconcile with the observation of Lemogne and Lacombe (1963) that {172} parting occurs most easily. However, the explanation may lie in a study of the possible crack nucleation mechanisms.

A study of brittle crack nucleation is always difficult because the rate of propagation of a nucleated crack often approaches the speed of sound in the material. Thus sectioning of specimens after interrupting a low temperature test is rarely rewarding. This was attempted here but it was found to be consistently unprofitable. Examination of specimens after fracture however, occasionally revealed crystallographic microcracks. The following features were then observed:-

a) Load drops presumably associated with twinning always preceded fracture.

b) Arrested microcracks were observed in approximately 5% of the grains in the gauge length at temperatures near the transition but only very rarely below the transition. Most of these fissures were near the fracture edge.

c) Cracks were observed to be arrested at grain boundaries or, perhaps, in the regions of "forced slip" (Fig 72).

d) Small fissures were found on twin interfaces (Fig 73) and usually these were unrelated to twin intersections apart from that shown in Fig 74 in which one might

also, cracks tend to be on side of twin nearest fracture edge — ?

argue that propagation has been arrested at the intersections.

e) Some microcracks must have formed early in the process for they had opened-up into a narrow D shape (Fig 74). These microcracks appeared to have been arrested at the ends of the twin or at intersections.

f) These parting microcracks were more frequently associated with long rather than short and thick rather than thin twins and tended to be situated near the twin apices.

g) Cracks which might have been grain boundary nucleated with subsequent propagation along a twin interface were sometimes seen (Fig 73) and some cracks appeared to have been nucleated at surface flaws (Fig 67).

The consequences of b) and c) would appear to be that the critical stage of fracture is propagation and, in particular, propagation of a crack through a grain boundary similar to the behaviour of body-centred-cubic metals. One might then explain the fracture transition in this way. By invocation of the dislocation models of crack nucleation in metals it seems reasonable to assume that the mechanism here involves a twin interaction. No experimental evidence was found for crack nucleation at twin intersections and thus a mechanism involving a pile-up of slip dislocations at a twin boundary may be preferred, as suggested by Lemogne and Lacombe (1963). Leteurtre (1962) observed a reaction between {121} twins and {010} slip dislocations: the resulting dislocation is sessile and so can form an obstacle to further dislocation movement. Nucleation and propagation of a crack along this twin could then occur and no doubt similar reactions are possible to account for parting along {172} and {130} twins. A second possibility is that cracks are nucleated

at grain boundaries, due to residual grain boundary stresses, which then propagate along a twin. No doubt this model is operative but it is insufficient to explain all the available evidence for polycrystals and cannot operate in single crystals. Clearly sometimes cracks are initiated at macro-flaws but again this cannot always operate.

However, in the general context of fracture the brittleness of uranium may be more related to homopolar crystals such as germanium and, equally, heteropolar crystals such as calcite in which it has been pointed out that twin parting occurs with great perfection. In calcite, parting is thought to be directly related to the stresses associated with twin apices and a similar model may apply to uranium. Considerable stresses are associated with a growing twin; this accounts for the ridge shape of the growing lamellae in which the strain is relieved at the tip by dislocations, giving the familiar lenticular shape. However, there must also be elastic distortion of the lattice in front of the twin apex and the stresses associated with the advancing lenticule must be relieved. Cahn (1954) has discussed these mechanisms of stress-relaxation and cited the following:-

a) Relaxation by fracture near the tip of a twin band as observed in meteoric iron.

b) Relaxation by diffusion — only found after annealing (Hall 1954).

c) Twin bands in single crystals may be relaxed by bending of the specimen (Basinski and Christian 1954).

d) Relaxation by dislocation movement near the tip, observed by Jillson (1950) in zinc (by kinking) and in 3% silicon-iron as slip lines radiating from tapered twins (Hull 1961).

Only a) and d) are directly relevant and in the absence of d) local cleavage may start at the advanced edge of a twin. With decreasing temperature in uranium the stresses cannot be relieved so readily and the high stress-concentration may produce a local tensile stress large enough to overcome the cohesive force of the atoms to nucleate a crack. A twin would not necessarily stop once a crack formed and it might continue growing either with relief of stresses at the crack tips or by progressively extending the crack.

A simple dislocation model for crack nucleation may thus be unrealistic but can be attempted by assuming that an advancing deformation twin is preceded by slip dislocations in uranium. In a study of the phenomenon in alpha iron, Sleeswyk (1962) suggested that these dislocations are emitted from the tip of a propagating twin by the transformation of a twin dislocation into a slip dislocation. By the specific reaction cited every third twin dislocation was expected to dissociate to produce an emissary dislocation. The possibility then exists that cracks may be nucleated by the piling-up of emissary dislocations (Priestner and Louat 1963). Also, when the twin encounters an obstacle during growth that cannot be incorporated, the emissary dislocations can be expected to interact with the obstacle. If the obstacle is an inclusion, crack formation may result, as observed by Edmondson (1961) or, if the obstacle is a dislocation, a reaction to produce a crack may result.

Having made these speculations upon crack nucleation it is necessary to decide which is the most likely. The observation that cracks tend to be near the apex of long rather than short

and thick rather than thin twins suggests that a model involving pile-up of slip dislocations at a pre-formed twin is invalid for no effect would be predicted. On the other hand these observations would be expected with a model involving the stress-concentration at a twin tip. The stress concentration at a twin is related directly to the thickness (e.g. Hull 1962) and a dislocation reaction of emissaries would be more likely with thick twins since the number of emissary dislocations is proportional to twin thickness (Sleeswyk 1962) and also with long rather than short twins. The twinning shear of {172} twins is significantly less than other twinning shears and {172} twins are therefore predicted and found to be thicker than other twins (Cahn 1951). Hence crack nucleation is more likely at {172} twins which provides an explanation for the observation of Lemogne and Lacombe (1963) that {172} parting occurs most easily.

It is therefore tentatively concluded that the process of low temperature crystallographic failure in alpha uranium is nucleated at the apices of growing long thick twins by a reaction involving emissary dislocations. Propagation occurs along the composition plane of the twin because of its inherent weakness and the process may involve the linking up of cracks on nearby twins to produce cleavage steps. The propagation rather than the nucleation stage appears to be the limiting criterion of fracture in view of the arrested microcracks observed. not conclusive

In view of the many differences between the behaviour of uranium and that of body-centred-cubic metals one cannot perhaps directly invoke the theory for the transition in these metals.

The transition can still be explained in terms of increasing σ_i and decreasing number of slip systems with decreasing temperature. Stresses at twin apices are then not so readily relieved and crack nucleation and propagation is facilitated at low temperatures. Another approach is possible. Covalent substances such as germanium and diamond have been shown to exhibit a ductile/brittle transition (van Bueren 1960) and one might predict a similar behaviour in uranium. However, the transitions in these materials are at approximately 60% of the absolute melting point and in uranium the transition is much lower. Also, above the transition uranium behaves like a typical ductile metal. One might explain the transition therefore as being from a typical metal at high temperatures to a typical brittle homopolar substance at low temperatures. It is possible that with decreasing temperature there is a change in the electronic configuration to cause stronger covalent bonding and the ductile/brittle transition could be explained in these terms. This is extremely unlikely in other less-complicated structures but is conceivable in uranium. This is a speculative suggestion but difficult to disprove and therefore must remain a possibility.

None of the models preclude similar qualitative effects to those observed in other metals but these would not be predicted quantitatively by the Cottrell equations. For example, crack propagation will be arrested at lattice discontinuities (grain boundaries) increasing strain rate and alloying will increase σ_i and k_y favour twinning and promote brittle fracture; a notch will provide a stress concentration, all of which predict similar effects to those in body-centred-cubic metals.

4 Fracture of Alpha in Bending and Compression

There was no a priori reason for investigating the behaviour of uranium under bending or compressional stresses. At one stage of the work, super-purity material was to be available but this could not be machined into tensile specimens since this is a wasteful process and AERE would have hoped to re-use the material allotted to this work. Bend and compression testing was therefore developed, to examine the fracture behaviour of unmachined specimens. Although super-purity material never became available, in the course of testing the technique, some useful results were obtained on reactor grade material and some of these are recorded here.

Essentially the same behaviour was observed in bending as in tensile testing with a transition from a ductile to a brittle failure; this is exemplified in Fig 75 which demonstrates the angle of bending at fracture at a number of temperatures. Above 50-80°C no fracture was obtained at the limit of bending of the apparatus. At such temperatures the cuboids cracked and voids opened up (Fig 76). At lower temperatures some preference for grain boundary cracking was observed but with further decreasing temperature failure was typically crystallographic. Fig 77 shows a good example of cleavage steps. One notable feature of bend testing observed was that the transition temperature was lower than in tensile testing. This phenomenon has also been found in germanium (van Bueren 1960).

In compression no brittle failure was observed and the specimens barrelled out and fractured by shear at approximately

45° to the compression axis. The inclusions were profusely cracked after compression (Figs 78 and 79) and many subsidiary cracks were present (Figs 80 and 81). The main fracture path tended to pass preferentially through the inclusions.

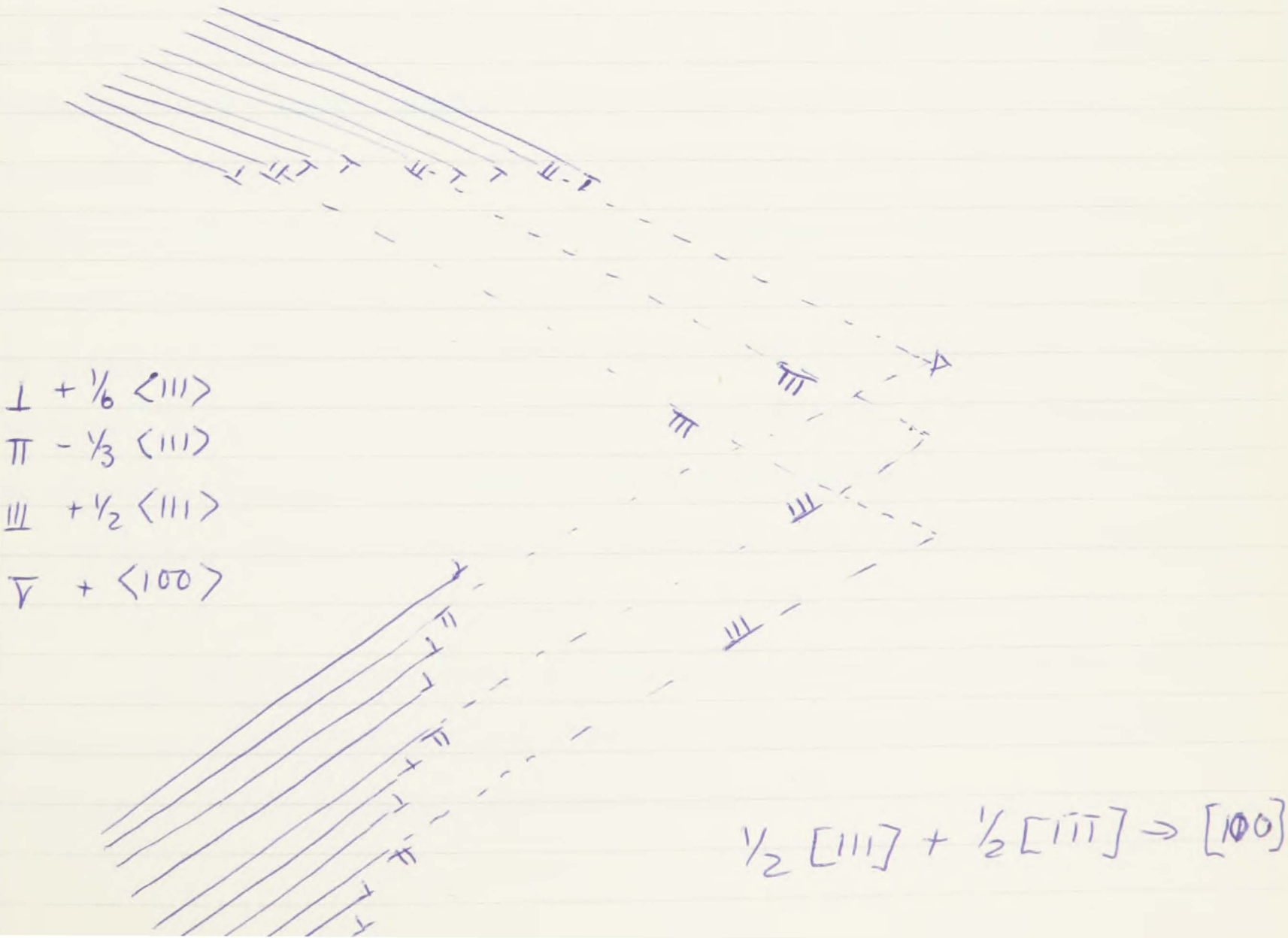
5 Fracture of Beta Uranium

It was considered that a study of the behaviour of uranium in the beta range under non-oxidizing conditions would be useful in confirming some of Davies' results. Oxidation occurs during tests in excess of 600°C in spite of precautions being taken to improve the protective atmosphere by flushing well with argon, having a slow rate of flow and ensuring that the gas seals were working efficiently. This oxidation might affect the results and a technique of evaporating a film of Gold-Palladium onto the surface of specimens prior to testing was used. The coating was adherent and non-porous, superior to nickel plating which was used by Hancock (1957) and enabled tests to be carried out at beta temperatures in an argon atmosphere without appreciable oxidation. A photo-micrograph of the coating after testing is shown in Fig 82. The results obtained tend to confirm those of Davies insofar as they are most satisfactorily explained by intercrystalline cracking. Microcracks were often observed at alpha grain boundaries whose shape suggested intergranular rather than transgranular brittleness (Fig 83). The cracks were invariably associated with the alpha grain boundaries showing that they were formed in the beta since during transformation grain growth would be halted at the cracks.

The emissary dislocation model of twin propagation is based on the generally accepted model of twin growth in which a twin lamellae in b.c.c. iron grows in its {112} habit plane by the expansion of 1/6 ⟨111⟩ twin dislocation loops on successive {112} planes, while the thickness of the lamella increases by the creation of new loops on adjoining {112} planes. When some 40 dislocation loops are piled up against each other, dissociation of twin dislocations on every third {112} plane occurs during further growth. The dissociations are of the type:-

$$\tfrac{1}{6}\langle 111\rangle \rightarrow \tfrac{1}{2}\langle 111\rangle - \tfrac{1}{3}\langle 111\rangle$$

Thus a 3-dim pile-up of 1/2 ⟨111⟩ "emissaries" gliding on {112} planes is created. Every third {112} plane is a slip plane on which an emissary dislocation is situated.



Preliminary work (Chapter VI) showed that beta could be satisfactorily retained to room temperature in doubly-adjusted specimens by rapid quenching after high beta temperature treatments. Specimens were quenched from 750°C into iced brine after 10 minutes at temperature and tested within 1½ minutes of quenching. The specimens were very brittle with large facety areas which suggested a large grain size with crystallographic failure. Examination of the fracture surface confirmed this (Fig 84). Similar specimens, preground, were quenched and immediately prepared for metallographic examination. 40 minutes after quenching the structure proved to consist of large grains of beta with a few areas of alpha (similar to Fig 29). The island areas of alpha produced were perhaps produced mainly by the strains associated with polishing (Dixon 1964). No cracks were found in these specimens but after about 10 hours, cracks were observed due to the strains associated with the shear transformation (Fig 85). Specimens tested 6 hours after quenching were very brittle and failed at very low stress levels and the fracture surface was irregular without bright facets. These observations tend to confirm that the structure was wholly beta on testing immediately after quenching. The results obtained are similar to those obtained by Holden (1952) on a retained beta structure ina quenched uranium-chromium alloy.

Fig 86 shows examples of fractured tensile specimens tested at various temperatures after a number of treatments which exhibit a number of the fractures discussed above.

VIII MECHANICAL PROPERTIES

1 General Behaviour

The succeeding sections of this chapter are concerned primarily with the effect of a number of variables upon the tensile properties of uranium between a wide range of temperatures. In this section the general effect of temperature upon the mechanical properties will be commented upon.

1-a Tensile

The material chosen to demonstrate the general effects of temperature was cast unadjusted uranium which had been beta-treated and alpha-annealed to produce a uniform smooth grain structure with a grain size of 0.1mm average diameter. The percentage elongation and reduction-in-area as a function of test temperature results are presented in Fig 87 and the U.T.S. and true fracture stress results in Fig 88. The fracture transition from a brittle to a ductile failure in the region of room temperature is seen to manifest itself clearly as a tensile transition over a similar range of temperature (this range of temperature will be referred to hereafter as the transition temperature). In later work the reduction-in-area was sometimes difficult to measure accurately because occasionally coarse-grained specimens reduced to an oval rather than a circular cross-section. This can be attributed to the anisotropic nature of alpha uranium which becomes an important factor at such large grain sizes. Also, the surface frequently became

roughened due to the heterogeneity of deformation. For this reason, and because it was the most accurately measurable parameter, elongation was chosen as the best indicator of the tensile transition. The peak in the fracture stress curve was occasionally used as an additional measure.

The ductility transition in the region of room temperature is clearly demonstrated in Fig 87. Above the transition the ductility rises gradually to the beta-transus with an inflexion in the reduction-in-area curve and a marked "dip" in the elongation curve at about 300°C. This effect can be related to the change in the ductile fracture behaviour at about this temperature: below 300°C the ductile-cavities tend to be formed at an early stage by cuboid-cleavage whilst above 300°C the cavities tend to be formed at a relatively late stage by separation at the cuboid/matrix interface. This is attributable to the decreased prevalence of twinning and increased number of active slip systems above 300°C which results in accommodation of the cuboids in the deforming matrix (Chapter VII). The total elongation measured in a tensile test is composed of the two contributory factors of uniform elongation and necking elongation. The uniform elongation is proportional to the rate of work-hardening (Orowan 1948) and since this falls with increasing temperature uniform elongation will also fall - that is, necking will begin at an earlier stage, as observed. The necking elongation on the other hand, is related directly to the reduction-in-area. This only increases gradually between 100°C and 300°C & since the uniform elongation decreases

markedly in this range one might expect a fall in the total elongation. Above 300°C however, the reduction-in-area increases rapidly with increasing temperature because of the later formation of ductile cavities and consequently one would predict a similar increase in necking elongation. Thus the fall in uniform elongation would be offset and an increase in the total elongation expected.

At the beta-transus there is a marked decrease in ductility demonstrating that polycrystalline beta-uranium is very brittle. In contrast gamma uranium is shown to be relatively soft and ductile.

Above the transition the fracture stress of uranium common with other metals, rises with decreasing temperature. Also, common with other metals exhibiting a ductile/brittle transition, it is accompanied by a large decrease in fracture stress (Fig 88). However, with continuing decrease in temperature the fracture stress in such metals usually drops to a value equal to the yield stress afterwhich the fracture stress increases because the yield stress is increasing with decreasing temperatures (e.g. Hahn et al 1959). This behaviour is not observed in uranium: the fracture stress falls progressively with decreasing temperatures below the transition. This must be related to the very low yield stress of polycrystalline alpha uranium which is due to the anisotropy of thermal expansion. The stresses at twin apices and interfaces will increase with decreasing temperature and in the effective absence of a yield stress the fracture stress would be expected to

fall progressively. Presumably single crystals at very low temperatures exhibit the more usual behaviour. It is relevant to note that Priestner (1962) found that the brittle fracture stress of Si-Fe decreased with decreasing temperature but this was not explained.

The U.T.S. results show similar characteristics except that with increasing temperature above ambient a strength plateau is observed between 100°C and 300°C. This is associated with an inflexion in the fracture stress curve and is related to the ductility effect at about this temperature. Above about 300°C many more slip systems are operative and twinning becomes decreasingly prevalent causing a rapidly decreasing strength. A similar behaviour was reported by Grainger (1958) but not by other workers (Chapter II). At the beta transus there is a discontinuous rise in strength, which falls with increasing temperature with a pronounced decrease at the gamma transus.

The shapes of the ductility (Fig 87) and fracture stress (Fig 88) against test temperature curves can thus be summarized as follows:-

a) The high temperature phase gamma is soft and has a low strength and high ductility.

b) Beta uranium is a complex structure with few slip systems and polycrystals are therefore brittle but of relatively high strength.

c) At high temperature alpha uranium has many active slip systems and failure occurs by coalescence of cavities formed by separation of the cuboid inclusions fron the matrix giving a high ductility and low strength.

d) Below about 300°C failure occurs by coalescence ofvoids formed at an early stage by cuboid-cleavage. The reduction-in-area decreases and ductility falls. The fracture stress increases as the critical shear stress for slip and the rate of work hardening increases.

e) With decreasing temperature below 300°C the reduction-in-area only falls slightly because of the earlier formation of ductile cavities and the uniform elongation before necking increases to give an increased total elongation. The fracture stress continues to rise but the U.T.S. exhibits a strength plateau before rising further. This is also associated with the progressively earlier formation of cavities by cuboid-cleavage.

f) With further decreasing temperature the critical shear stress for slip increases, the covalent nature of the bonding becomes more important and twinning predominates. The high stresses at growing twin apices are not readily relieved and the metal becomes brittle. Fracture occurs at a considerably lower stress.

g) At lower temperatures this process occurs at decreasing stress levels and gives decreasing ductility.

Doubly adjusted uranium fast beta-quenched to retain the beta phase is brittle. The properties at periods after quenching were (Table XI):-

Table XI

Time after Quenching	Fracture Stress 20°C	Elongation 20°C
1½ mins	18 tons/sq.in	1%
6 hours	3 tons/sq.in	NIL
24 hours	5 tons/sq.in	NIL

The extremely low fracture stress 6 hours after quenching is attributable to the cracks resulting from the stresses associated with the beta→ alpha shear transformation. These results tend to

confirm that the properties obtained immediately after quenching are valid. Similar specimens were therefore tested 3/5 minutes after quenching at anumber of temperatures and the results are recorded in Table XII.

Table XII

Test Temperature	Fracture Stress of Retained Beta
50°C	20 tons/sq.in
-10°C	20 tons/sq.in
-95°C	25 tons/sq.in
-196°C	28 tons/sq.in

Clearly the fracture stress increases with decreasing temperature as would be expected.

1-b Bend and Compression Testing

As was outlined in Chapter V the reasons for bend and compression testing were primarily to investigate their usefulness so that a method of examining the mechanical properties of super-purity material was available without incurring the machining losses necessary for the preparation of tensile specimens.

Load/extension bend test curves for adjusted beta-treated specimens at various temperatures are shown in Fig 89. From these results it is possible to obtain some measure of fracture stress and a direct measure of ductility - either from the extension or by measuring the angle of bending at fracture. Comparison of these results with tensile results obtained on the same material demonstrates that the transition temperature in bending is appreciably lower than in tension. This is also found in such materials as germanium (van Bueren 1961).

The only measurement made on compression specimens was the reduction in height at fracture. Crystallographic failure is observed in directionally bonded materials in compression but only shear failure at approximately 45° to the stress axis was observed here. The reduction in height was not affected appreciably by temperature within the range +70°C to -183°C and remained constant at about 30%.

1-c Hardness

The hardness versus temperature results have been adequately recorded above room temperature (Fig 6). Between -183°C and 100°C they are recorded in Table XIII.

Table XIII (Unadjusted)

β oil-quenched grain size 0.3mm		β furnace-cooled grain size 0.45 mm		β water-quenched and alpha-annealed grain size 0.1mm	
Temp	V.P.N.	Temp	V.P.N.	Temp	V.P.N.
100°C	225	100°C	203	100°C	188
20°C	238	20°C	212	20°C	195
0°C	245	0°C	210	0°C	210
-10°C	253	-10°C	215	-10°C	220
-23°C	265	-23°C	220	-23°C	218
-95°C	282	-95°C	245	-95°C	238
-183°C	343	-183°C	318	-183°C	310

Clearly hardness rises steeply with decreasing temperature, additionally it is worth noting that the hardness increase between -95°C and -183°C is greater than that between +100°C and -95°C. This might tend to confirm that a change in the nature of bonding occurs at low temperatures (Chapter VII). If this occurred progressively then this might contribute to the decreasing fracture stress with temperature behaviour.

2 The Effect of Composition

2-a Introduction

Four grades of uranium were available for this section but the virgin material was in a different metallurgical condition (rolled, as opposed to cast) from the other three. The investigation was therefore confined to specimens machined from unadjusted, adjusted and doubly adjusted quartered cast fuel rods. Examination of the analyses of these materials (Table II) shows that the only major variations in composition are iron and aluminium. These elements exist almost entirely as a fine network dispersion of the compounds U_6Fe and UAl_2. No heat treatment has been found to appreciably affect this network (Chapter VI).

It was found impossible to produce an identical grain size and structure in specimens of different composition so that its effect upon the properties could be studied in isolation. The same grain size in the different grades could be produced by differential beta-quenching rates (Fig 32) but this introduced a pronounced variation in grain shape and a possible, though undetected, variation in precipitate distribution. Specimens of different materials were therefore given identical treatments such that the only variable present apart from composition was grain size. Since the effect of grain size has been examined in isolation the results obtained here can be unambiguously interpreted.

2-b Results

Two heat treatments were investigated;

a) Beta-treatment - specimens of each grade were heat treated for 48 hours at 720°C in a dynamic vacuum and furnace cooled. The resulting grain structures were uniform, and equiaxed with "smooth" grain profiles.

b) Alpha-treatment - specimens of unadjusted and adjusted material were beta-quenched and then alpha-annealed for 24 hours at just below the beta-transus to produce a recrystallized, uniform smooth grain structure. The alpha treatment temperatures were, unadjusted: 650°C. adjusted: 640°C.

Examination of the microstructures of specimens after the different heat treatments indicated that there was no major difference in precipitate distribution and no preferential grain boundary precipitation was observed. The grain sizes for the different materials after these treatments are given in Table XIV.

Table XIV

Grade	Treatment	Grain Size (average diameter)
Unadjusted	Beta	0.45mm
Adjusted	Beta	0.30mm
Doubly Adjusted	Beta	0.12mm
Unadjusted	Alpha	0.10mm
Adjusted	Alpha	0.05mm

Recorded in Fig 90 are the percent elongation as a function of test temperature results for the three grades after beta treatment. These indicate that increasing iron and aluminium contents raise the tensile transition temperature but, as seen in the above table, with increasing iron and aluminium content the grain size after transformation is finer. However, as section 4 of this chapter shows the effect of decreasing grain size is to lower the transition and therefore the effect is real. In fact the variation in grain size would tend to reduce the magnitude of the observed effect. Clearly, therefore, increasing additions of iron and aluminium tend to raise the tensile-transition temperature. Examination of the specimens after fracture indicated that this tensile transition was in each case associated with a change in fracture mode from ductile to parting with little evidence of intercrystalline fracture at any temperature.

Fig 91 records that percent elongation versus temperature results after alpha treatment for unadjusted and adjusted material. A similar effect of iron and aluminium on the transition temperature is demonstrated, again the variation in grain size would tend to reduce the magnitude of the effect. However, a second effect is clear; a "stepped" transition is exhibited with a marked discontinuities at about 20% elongation. Examination of the fractures of specimens after this treatment showed that a considerable amount of intercrystalline cracking was occurring in the transition temperature range. Above and below the transition range ductile and cleavage failure predominated respectively. This behaviour contrasts strongly with the fracture behaviour of the beta treated specimens.

2-c Discussion

The effect of composition upon the tensile transition is difficult to explain satisfactorily because so little is known about the fine precipitates in uranium. There has been some suggestion (Dixon 1964) that after beta-quenching, and alpha-annealing there is some preference for precipitation of U_6Fe at alpha grain boundaries but this is not a marked effect. With increasing iron content this could favour grain boundary cracking. However, beta slow cooling was not shown to give this effect and therefore the phenomenon cannot be explained in these terms. Moreover, after beta-treatment little tendency for grain boundary cracking was observed and thus a solute segregation effect is also precluded.

The available evidence suggests therefore that it is just the increased volume fractions of dispersed phase which are giving rise to the increase in the transition temperature. It was suggested in Chapter VII that one mode of crack nucleation could result from the interaction of emissary twin dislocations with an obstacle such as a particle. This would be more likely with increasing amounts of iron and aluminium. Furthermore, σ_i is usually raised by increasing amounts of dispersed phase and this is likely here insofar as the hardness increases with increasing iron and aluminium (Fig 34). Relief of stresses at twin apices would then be more difficult and also, because of the reduced dislocation mobility, plastic flow to relieve the stresses at the tip of a growing crack

would be more difficult and consequently a crack would propagate more readily. Thus it is possible to provide explanations for the effect in terms of both crack nucleation and propagation being facilitated by the increasing volume fractions of dispersed phase. Nevertheless the suggestions must remain speculative without further experimental corroboration.

3 The Effect of Heat Treatment

3-a Introduction

In uranium different heat treatments frequently result in a variation in grain shape or profile between specimens. In view of this, it was important to establish the influence of this variable upon the mechanical properties. Before doing this it is necessary to firstly consider the general effects of heat treatment upon the mechanical properties.

The results of section 2 showed that different heat treatments alone could produce a variation in the tensile behaviour. This is clear if Fig 90 is compared with Fig 91: a considerable variation in the shapes of the curves is observed. The fracture behaviour also differed: the stepped transition (Fig 91) was associated with intergranular cracking whilst the smooth transition (Fig 90) was associated with a direct transition from ductile to parting failure.

Clearly the "stepped" behaviour may be attributed to grain boundary embrittlement and this process is summarized as a classical fracture stress diagram in Fig 92. Curve 'A' represents the cleavage strength, 'D' the yield strength and in the absence of intergranular embrittlement the grain boundary strength may be represented

by 'B' whence the transition is direct and "smooth" (Fig 90). In the event of intergranular embrittlement the grain boundary strength is lowered and may be represented by 'C' whence the transition temperature is increased and a "stepped" transition occurs (Fig 91). Since no grain boundary precipitation was observed, intercrystalline failure was originally tacitly assumed to be due to solute segregation lowering γ_s, the grain boundary surface energy (Taplin and Martin 1964). As was discussed in Chapter VII however, this effect of favouring an intergranular path of fracture can arise if the grain boundary energy γ_B is increased and the observed results can be explained in these terms. An experiment was devised to test this hypothesis.

3-b Thermal Cycling Investigation

The object of this experiment was to attempt to raise γ_B by thermal cycling and investigate its influence upon ductility in the absence of possible effects on γ_s. Specimens were given the following sequence of thermal treatments and some specimens tested at a number of temperatures after each stage:-

1) Beta-treatment: 48 hours at 720°C and furnace cool.

2) a) Alpha-cycle: 10 slow thermal cycles between 100°C and 350°C (total time = 3 hours).

or

b) Alpha-anneal: 3 hours at 350°C and furnace cool.

3) Beta-treatment: 30 mins. at 720°C and furnace cool.

The percent elongation results as a function of test temperature after these treatments are recorded within Fig 93. The results after 1), 2b) and 3) are shown to be coincident but after 2a) the

transition temperature is raised appreciably, and, as was discussed previously (Chapter VII) this was found to be attributable to intergranular cracking. It can be concluded that, firstly, the grain boundary embrittlement must be due to the thermal cycling since the anneal at 350°C has no detectable effect upon ductility and, secondly, subsequent beta-treatment removes the embrittlement indicating that the damage is not permanent (i.e. in the form of fissuring).

Tensile tests were also carried out on specimens thermally cycled similar temperature amplitudes at low temperatures. At these temperatures the rate of diffusion is considerably reduced. The two treatments after the initial beta treatment were:-

1) 10 cycles between +75°C and -196°C

2) 10 cycles between +20°C and -196°C

The elongation results are recorded within Fig 93 and it is clear that low temperature cycling produces similar embrittlement and under these conditions the possibility that a concomitant lowering of γ_s by impurity segregation occurs is eliminated.

The results of these experiments establishes unequivocally that grain boundary embrittlement with consequent raising of the transition temperature can be caused by an increase in γ_B in selected areas due to the anisotropy of thermal expansion of alpha uranium. The hardness results after successive cycles (Table VIII) demonstrate that this may be an important factor after even a single alpha cycle particularly with rapid cooling. Consequently the small amount of embrittlement existing after alpha-treatment

(Fig 91) as opposed to beta-treatment (Fig 90) is readily explained in these terms. The results do not however show that lowering of the grain boundary energy by solute segregation is absent after similar treatments: this may be a contributory factor in certain circumstances.

3-c Grain Profile Investigation

A Introduction

The influence of a variation in grain-shape upon the mechanical properties of unadjusted, adjusted and doubly adjusted materials prepared from quartered cast fuel rods was investigated. The preliminary work described in Chapter VI established experimental programmes to produce the microstructural variable alone by fast-beta quenching followed by strain-relieving (to produce the "irregular" grain profiles) or recrystallizing (to produce the "smooth" grain profiles). A further (third) grain profile was investigated in unadjusted material by quenching at a different rate.

All specimens were first subjected to a prolonged alpha homogenizing treatment of 100 hours at just below the beta-transus. To avoid solution and possible subsequent precipitation effects resulting from the solubility change upon transformation, a very short beta-treatment was used: 1½ minutes in a lead bath at 720°C was adequate time to reach temperature for the size of specimens used. After this treatment three batches of unadjusted specimens were treated as follows:-

a) Quench into 10%NaCl aqueous solution at 0°C and anneal for 25 hours at 470°C. This was the fastest quench and resulted in the most irregular grain profile. The heat treatment at 470°C strain-relieved the structure without recrystallization.

b) Quench into mercury at 0°C and anneal for 25 hours at 500°C. This was not quite as fast a quench and a somewhat less irregular profile resulted. The heat treatment at 500°C again strain-relieved without recrystallization.

c) Quench into mercury at 0°C and anneal for 25 hours at 650°C. In this case heat treatment caused recrystallization to a smooth grain structure.

Photomicrographs of the three grain profiles are shown in Figs 33, 94 and 95 which provide a qualitative comparison of the variation in irregularity. The squars of measurement of the average peripheries of the grain profiles gives some quantitative measure of the relative grain boundary surface areas and these are given in Table XV together with grain size and hardness results.

Specimens of adjusted and doubly-adjusted material were subjected to similar quenching and annealing schedules but only the two grain profiles which resulted from an iced brine quench were examined (i.e. recrystallized - "smooth", and strain-relieved - "irregular"). The final heat treatments and the resulting structures are also given in Table XV.

Table XV

Material (Grade)	Final Treatment	Grain Size (diameter)	Relative Grain Boundary Area	Hardness (10Kg)
Unadjusted	25h/650°C	0.1mm	1 (smooth)	194
Unadjusted	25h/500°C	0.1mm	1.54 (irregular)	210
Unadjusted	25h/470°C	0.1mm	1.84 (irregular)	215
Adjusted	25h/625°C	0.08mm	1 (smooth)	204
Adjusted	25h/470°C	0.08mm	1.65 (irregular)	226
D-Adjusted	25h/625°C	0.03mm	1 (smooth)	210
D-Adjusted	25h/470°C	0.03mm	1.75 (irregular)	238

The grain-sizes of specimens of the same composition but different grain profile were the same. However, although no difference in precipitate distribution between specimens was detected and even though precautions were taken against this event, it remained a possibility. Some solution of iron and aluminium may have taken place during the lead bath treatment and the final anneals could then give rise to variations in precipitate distribution. Dixon and Fern (1963) have shown that complete solution of the intermetallics takes approximately 20 minutes at the temperature used. Doubly-adjusted specimens were therefore given 20 minute lead bath treatments instead of 1¼ minute treatments and tested. Any difference due to precipitation should then be accentuated and the possible effect thereby examined.

It was also important to study the possible effects of different heat treatments themselves since the magnitude of residual grain boundary stresses could vary between specimens masking any possible grain shape effect. A complete recrystallizing treatment might be expected to remove all prior stresses and the magni-

tude of γ_B should therefore be relatively low in smooth grain-profiled specimens. On the other hand, after treatments to produce irregular grain profiles, one might expect the magnitude of γ_B to be relatively high. The following heat treatment schedules were devised to examine the influence of this factor:-

1. Unadjusted specimens were subjected to the following heat treatment schedule after the same alpha homogenizing and beta quench treatment as before and tested:
   a) Alpha cycle 10 times between -196°C and +75°C
   b) Either strain relieve at 500°C or recrystallize at 650°C for 25 hours.

The interceded alpha cycle here will produce increased grain boundary stresses and comparison of these results with those obtained without the alpha-cycle should indicate the effects of the final treatments upon existing grain boundary stresses.

2. Doubly adjusted specimens were heat treated to produce "smooth" grain profiles as before and then heated to 630°C in the lead bath (alpha-region) and brine-quenched followed by annealing for 25 hours at 470°C.

Tests after this treatment should demonstrate the effect of the boundary stresses present in irregular grain-profiled specimens in smooth grained specimens.

B Results

Percent elongation and U.T.S. results over the temperature range investigated for unadjusted material are recorded in Figs 96 and 97. Fig 98 indicates how the effect of temperature influences the fracture mode: the onset of brittle fracture (i.e. first sign of facety areas) is taken as a measure of the transition temperature. In each graph the increase in the ductile/brittle transition temperature with increasing irregularity of grain profile is clearly

demonstrated. Examination of the fractured specimens showed that the tensile transition was associated with the usual ductile to cleavage change with some intercrystalline failure in the limited range of the transition after all treatments.

Examination of the stress/strain curves indicated that the metal with the more irregular grain profiles had higher rates of work hardening (Fig 99).

The effect was also investigated by bend testing in unadjusted material and the angle at fracture results which are presented in Table XVI demonstrate the same general effect.

Table XVI

Temperature	Angle at Fracture	
	"Smooth" Grains	"Irregular" Grains
-183°C	0°	0°
-10°C	20°	10°
0°C	30°	25°
22°C	75°	45°
80°C	75°	60°

No effect of grain shape in similarly treated unadjusted specimens tested in compression was found (Table XVII).

Table XVII

Temperature	% reduction in height	
	"Smooth" grains	"Irregular" grains
-183°C	33%	40%
0°C	40%	30%
22°C	30%	40%
70°C	45%	35%

These same general effects were observed in both adjusted and doubly adjusted material. Tables XVIII and XIX demonstrate the effect in adjusted material:-

Table XVIII

Test Temperature	% Cleavage (Facety Areas)	
	Smooth grain Profiles	Irregular grain Profiles
0°C	100%	100%
22°C	90%	100%
82°C	50%	100%
180°C	0%	50%
240°C	0%	0%

Table XIX (Adjusted)

Test Temperature	% Elongation	
	Smooth Grain Profiles	Irregular Grain Profiles
0°C	4%	3%
22°C	7%	5%
82°C	15%	8%
180°C	21%	10%
240°C	24%	19%

The percent elongation results for doubly adjusted material are recorded in Fig 100. The U.T.S. and fracture mode results demonstrated the same effect. In both these materials the rate of work hardening in the specimens with irregular profiles was markedly greater than in smooth grain profiled specimens (Fig 99). No difference in sub-structure between specimens with different grain profiles was detected.

Also recorded in Fig 100 are the percent elongation results of doubly adjusted specimens given the 20 minute lead bath treatment (open points). Clearly any precipitation effect is

negligible. However, the results given in Table XX and XXI when compared to Figs 96 and 100 respectively show that the effects of residual grain boundary stresses cannot be neglected as an additional influencing factor.

Table XX (Unadjusted)

Test Temperature	% Elongation	
	Smooth grains and interceded cycle	Irregular grains and interceded cycle
0°C	7%	-
20°C	16%	3%
52°C	21%	5%
81°C	24%	10%
125°C	-	16%

The above results if compared with the results recorded in Fig 96 demonstrate that although prior thermal treatment strain has little effect upon the properties if recrystallization follows, the anneal treatment at 470°C does not completely remove prior residual strain.

Table XXI (Doubly Adjusted)

Test Temperature	% Elongation after smooth profile treatment plus a-quench and 470°C anneal
85°C	3%
208°C	4%
254°C	6%
315°C	18%

The results in Table XXI, if compared with those in Fig 100, demonstrate that the different treatments themselves cause a similar, if not greater, variation in ductility, without any difference in grain profile.

C Discussion

An apparent influence of grain profile upon the ductile/brittle transition is shown to exist in all three materials and the results of the precipitation experiment (Fig 100) do not refute this. However, it would appear from the results presented in Tables XX and XXI that the effect can be explained in terms of a variation in effective grain boundary surface energy caused by the different treatments used. The observation that the concomitant fracture transition was substantially from ductile to cleavage failure does not alter this. In all cases some intercrystalline cracking was found, and, as was discussed in Chapter VII

grain boundary fissures can propagate along twin boundaries giving a predominantly crystallographic failure.

This does not preclude an additional influence of grain profile and the results presented in Figs 96-98 on unadjusted material might suggest that an effect exists. A small but significant difference in transition temperature is apparent between the two irregular grain profiles (illustrated in Figs 94 and 95). Since the treatments used to produce the two irregularities of grain profile only differed slightly the results cannot be explained satisfactorily in terms of residual grain boundary stress. The effect might then be explained in terms of crack nucleation being more likely with increasing irregularity of grain profile.

3-d Summary

1) Small difference in prior heat treatment can have a profound influence upon the tensile and fracture behaviour of uranium.

2) This phenomenon has been established to be partly due to residual grain boundary stresses which arise during heat treatment owing to the anisotropy of thermal expansion, lowering the effective grain boundary energy with consequent intergranular embrittlement.

3) The apparent effect of grain shape, whereby increasing irregularity raises the transition temperature, can be largely explained in terms of a variation in grain boundary energy produced by the different heat treatments.

4 The Effect of Grain Size

4-a Introduction

The microstructural variable of grain size has a major influence upon the mechanical properties and fracture of many metals and it is therefore of particular importance to determine its effect upon the behaviour of uranium. Previous work appears to be limited to that of Loy (1962) who found that "beta-annealed" material which was coarse grained was less ductile and had a higher transition temperature than "alpha-rolled" material which was fine-grained. As the preceding section demonstrates, such methods of obtaining a variation in grain size are unsound because of the other microstructural variables introduced. The main object of this section was therefore to determine the effect of grain size upon the tensile and transition behaviour with particular reference to the relationship between cleavage fracture stress (σ_f) and $d^{-\frac{1}{2}}$ and between transition temperature (T_c) and $\log_e d^{-\frac{1}{2}}$.

As already discussed, the grain size variable proved difficult to isolate and some of the tensile results obtained on cast material, for example after different rates of beta-cooling and after strain-annealing, are suspect. In addition the adjusted rolled fuel rods were metallurgically unsound and consequently these results are equivocal. Therefore only the results obtained on the virgin ingot will be considered in detail here.

4-b Results

A Unadjusted Heat Treated

Unadjusted as-cast specimens were heat treated as follows to produce a variation in grain size with a uniform smooth structure:

a) Beta-treated: furnace cool after 48 hours at 720°C grain size 0.45mm average diameter.

b) Alpha-annealed: beta quench and recrystallize anneal for 24 hours at 650°C - grain size 0.10mm average diameter.

The percent elongation versus test temperature results are recorded in Fig 101. Within the range investigated there appears to be no significant variation in the transition temperature.

B Adjusted Rolled

The tensile results obtained upon the two widest grain sizes obtained after the adjusted fuel-rods rolling and annealing programme are shown in Figs 102 and 103. Each point is the avetage of at least two tests and the limits have been constructed to indicate the range obtained. Nevertheless because of the unsoundness of the material the results cannot be completely relied upon, but apparent in both the elongation (Fig102) and fracture stress (Fig 103) curves is that an increase in grain size tends to raise the transition temperature. The same characteristics of the fracture transition were observed with intercrystalline failure in the transition range (Fig 104) and crystallographic failure at low temperatures (Fig 105) with the same effect of grain size upon the fracture-transition temperature as on the tensile transition temp-

erature so the observed grain size effect is probably qualitatively valid.

C Virgin Rolled

The bulk of the work was carried out upon virgin rolled material subjected to the rolling and annealing schedule described in Chapter VI (see Table VIII). Since a number of grain sizes were produced from each rolling reduction it was possible to compare the effect of grain size upon ductility both after identical mechanical treatment and after identical thermal treatment. No variation in properties between specimens given different prior treatments but resulting in the same grain size was found. The collected results for the effect of grain size between 0.01mm and 0.20mm diameter upon the room temperature ductility are presented in Fig 106. Decreasing grain size considerably increases ductility.

The effect of grain size upon the tensile transition behaviour within the range 0.015 to 0.20mm average diameter is demonstrated in Figs 107 to 109. The ductility and strength transitions illustrated were accompanied by the usual fracture transition from ductile to intercrystalline to parting failure. The effect of grain size within this range upon the transition behaviour is small but it is clear that decreasing grain size lowers the transition temperature both from the elongation (Fig 107) and the fracture stress (Fig 108) curves.

The true brittle fracture stress at -196°C was determined for the complete range of grain sizes and these are plotted against the reciprocal of the square root of the grain diameter in Fig 110. The relationship is clearly not linear; representation of the rolling reductions prior to annealing on the graph shows that there is no additional effect of either prior mechanical or thermal treatment. This scatter of results could arise in the event of non-axial alignment of the tensile grips which might cause high local stresses at the surface. This is quite possible with the machine used and although this is unimportant where significant plastic deformation takes place before fracture, at -196°C the specimens break with negligible plastic extension. Accordingly the true brittle fracture stress has also been plotted against $d^{-\frac{1}{2}}$ at four higher temperatures where some plastic deformation occurs before brittle fracture so that any effect of non-alignment is eliminated. These results are recorded in Fig 111 and it is again shown that σ_f is not directly proportional to $d^{-\frac{1}{2}}$. One can go further than this; no simple relationship between brittle fracture stress and grain size is apparent at all.

D Virgin Strain-Annealed

The virgin rolling and annealing schedule provided a wide range of grain sizes in isolation of other variables. However the maximum grain size was limited and coarser grained specimens were produced by a strain-anneal treatment. Perhaps the results obtained after such a treatment cannot be directly related to the virgin-rolled results because possible differences in texture and other variables exist.

The treatments chosen after the preliminary work outlined in Chapter VI were 3½% and 5½% tensile strain at 85°C upon the rolled and annealed material of grain size 0.03mm average diameter. After recrystallization for 3hrs at 640°C the resulting grain sizes were:-

3½% strain : 0.90mm average diameter
5½% strain : 0.25mm average diameter

The percent elongation correction factors calculated for the specimens strained the above amounts were within the experimental error of the Tensometer. No corrections were there-fore made.

The tensile results obtained on these two grain sizes are recorded in Figs 112 and 113 and the fracture results in Table XXII.

Table XXII

Temperature	Grain Size Average Diameter	Predominant Fracture Mode
-95°C	0.25mm	twin parting
	0.90mm	
20°C	0.25mm	parting/interxtalline
	0.90mm	twin parting
85°C	0.25mm	intercrystalline
	0.90mm	parting/interxtalline
175°C	0.25mm	ductile
	0.90mm	interxtalline/ductile
250°C	0.25mm	ductile
	0.90mm	

The same general effect of decreasing grainsize increasing the ductility and strength and lowering the transition temperature is observed but the effect between 0.25mm and 0.90mm here is much greater than that between 0.015mm and 0.20mm as shown by comparison of these results with Figs 107 and 109. Estimates of the transition temperature over the complete range are plotted against $d^{-\frac{1}{2}}$ in Fig 114 demonstrating this. The relationship is approximately linear below a grain size of 0.20mm diameter whilst above this value the transition temperature rises steeply. If there are differences apart from grain size between the rolled and strain-annealed specimens this variation can be eliminated by approximating the results obtained on 0.25mm grain size strain-annealed specimens to those obtained on 0.20mm grain size rolled specimens. A large effect still remains.

If a plot of $\log_e d^{-\frac{1}{2}}$ against transition temperature is made then the graph for the complete range is similar to Fig 114. However the plot between 0.20mm and 0.015mm grain size of the rolled material shows good agreement with linearity (Fig 115) as predicted (e.g. Petch 1959).

A transition grain size can be obtained at a number of temperatures by plotting $d^{-\frac{1}{2}}$ as a function of elongation (Fig 116). At 20°C the transition is at about $d^{-\frac{1}{2}} = 2$, and this value increases (grain diameter decreases) to about $d^{-\frac{1}{2}} = 6$ at 0°C.

4-c Discussion

A brief appraisal of the grain size results would indicate that the usual effects of this parameter are found in uranium. The ductility and strength are increased with decreasing grain size, the ductile/brittle transition temperature is lowered and ductile/brittle transition grainssize which varies with temperature is found. However, some of the details of the results show considerable variance from the observations and theoretical predictions for metals such as iron.

The room temperature ductility is strongly grain size dependent:-

0.01mm diameter : 48% elongation

0.90mm diameter : 4% elongation

Clearly the major influencing factor here is that the transition temperature is lowered by decreasing grain size. However, at higher temperatures where this is no longer important a similar effect is observed. As shown in Fig 109, the rate of work hardening increases with decreasing grain size and consequently the uniform elongation increases to explain the behaviour in the usual way.

Notwithstanding Johnson's amendments to the Cottrell theory it is usually argued that the fracture stress should depend on $d^{-\frac{1}{2}}$ because the length of Griffith microcracks is limited to the grain size. The basis of this argument is that a crack will be able to grow across a grain at a stress lower than that required to force it through the boundary. The extent to which residual boundary

strain arising from anisotropic thermal expansion influence this relationship has been examined by Clarke (1964) in detail. With some approximations a $d^{-\frac{1}{2}}$ relationship is also predicted and observed in beryllia.

The relationship in uranium is complicated by all these factors but additionally it is necessary to consider the meaning of the parameter d. Usually the only important barriers to crack propagation in materials are grain boundaries but twin boundaries may also act in a similar manner. It is therefore relevant to examine whether twins vary in number in different grain sized specimens. These results are given in Table X. Clearly the number of twins varies considerably with grain size: the number increasing with increasing grain size. However, in the majority of these grains twinning was observed on only one family of planes. Consequently the grains are only sliced-up rather than fragmented. This means that the twins will have no influence as barriers to crack propagation in directions parallel to the twins. Nevertheless, if twin boundaries do act as barriers to crack propagation the effect will be to reduce the effective value of d with increasing grain size. An alternative effect of twin boundaries is possible though; since twins provide planes of relative weakness in the lattice, the presence of long straight twins may facilitate crack propagation rather than hinder it.

In view of these conflicting considerations the usual parameter of grain diameter was taken as a measure of d and the possible influence of the above factors taken into account in the interpretation of the results obtained.

Only the grain sizes obtained by the virgin rolling and annealing schedule are included in the fracture stress versus $d^{-\frac{1}{2}}$ plots since tensile-straining of the specimens after machining could introduce flaws (either surface or internal) which might affect the fracture stress. Preliminary appraisal of the graphs shown in Figs 110 and 111 indicates that the $d^{-\frac{1}{2}}$ relationship is not obeyed. The scatter of Fig 110 might be attributable to grip non-alignment but the plots at higher temperatures, (Fig 111) are still not linear and their lack of uniformity at different temperatures suggests that if any relationship exists it is not simple.

If account is taken of the twin boundaries as barriers in Fig 11[illegible] then, since the number of twins per grain increases with increasing grain size (Table X) the departure from linearity is accentuated still further. However, it seems more likely that these twins will facilitate crack propagation particularly just below the transition temperature: with decreasing temperature the effect of the twins on promoting crack propagation will become progressively less important.

The proportion of twinned grains is only appreciable where $d^{-\frac{1}{2}} < 3$ and thus at these grain sizes the fracture stress would be considerably reduced particularly just below the transition temperature. It is not possible to determine the effects of these considerations quantitatively but examination of Fig 111 will show that qualitative correction for the effects might result in a linear relationship between brittle fracture stress and $d^{-\frac{1}{2}}$.

Further effects are important. The model developed for beryllia (Clarke 1964), which is particularly relevant in view of its anisotropy of thermal expansion, assumes that:

1) the intercrystalline microcracks will not propagate transgranularly until they have grown to a size commensurate with the grain diameter;
2) the boundary stresses due to residual strain are independent of grain size.

Experimental observations cited in Chapter VII show that these assumptions are not valid in uranium. Both these effects will tend to lower the fracture stress markedly with increasing grain size. Correction for these factors in Fig 111 would also tend to produce a linear relationship between fracture stress and $d^{-\frac{1}{2}}$.

The transition temperature also exhibits no simple relationship with grain size (Fig 114) except below a grain size of 0.20mm where a linear relationship between $\log_e d^{-\frac{1}{2}}$ and transition temperature is found (Fig 115). Perhaps the results are fortuitous but the close agreement with linearity suggests that the slope is real.

Cracks have been observed to be arrested at grain boundaries (e.g. Fig 72) and consideration of the brittle fracture phenomenon in uranium suggest that propagation of a crack to a size commensurate with the grain diameter would be particularly easy since straight twins running completely across grains are frequently observed. (e.g. Figs 26 and 46). Thus a crack would tend to propagate rapidly along a twin composition plane to the grain boundary where growth would be restricted by the boundary imperfections, orientation change and lack of a suitable twin/matrix interface.

Clearly, in uranium this is not the only influencing factor. With increasing grain size the magnitude of residual boundary stresses increase (Chapter VII). The results of Table XI suggest that after the treatments used, boundary stresses are only significant above a grain size of about 0.1mm average diameter. Below this grain size these boundary stresses are probably unimportant and the major influencing factor is probably arrest of propagation at a grain boundary. Consequently a plot similar to that obtained in other metals might be expected and would explain the linear relationship in Fig 115.

With increasing grain size above this value the effective grain boundary strength will decrease considerably causing severe embrittlement. This would raise the transition temperature appreciably giving the observed effect (Fig 114). The observation that intercrystalline cracking is more frequently observed with increasing grain size (Chapter VII) and the "stepped" transition of Fig 112 reminiscent of those discussed in Section 2 (Fig 91) lend support to this suggestion. Clearly this second effect of grain size cannot be extrapolated to single crystals for here no grain boundary embrittlement is possible. Consequently the dotted line in Fig 114 has been constructed to suggest the effect of further increasing grain size.

It is possible to explain the effect in terms of a critical grain size being equal to the Griffith crack length. If this effect were valid the critical grain diameter would presumably be

0.20mm but further increasing grain size should have no effect on the transition temperature which is not found.

The transition grain size results presented in Fig 116 are mainly explained in terms of grain boundary embrittlement by residual grain boundary stresses arising from the anisotropy of thermal expansion. These stresses increase with increasing grain size, but are only significant at about $d^{-\frac{1}{2}} = 2$, consequently a transition grain size is found at this value (100°C, 50°C and 20°C). At lower temperatures (0°C), failure is predominantly by parting and a transition is also found but this is less marked and is with the stress to propagate a cleavage crack through a grain boundary as in other metals.

4-d Summary

1) The room temperature ductility of uranium is strongly grain size dependent. This can be explained in terms of the increased rate of strain-hardening and decrease in transition temperature with decreasing grain size.

2) No simple fracture stress/grain size relationship was found but if account is taken of all the influencing factors in uranium the results might be explained in terms of the usual $d^{-\frac{1}{2}}$ relationship.

3) With decreasing grain size the ductile/brittle transition temperature is lowered. Below a critical diameter of about 0.20mm a linear relationship between transition temperature and $\log_e d^{-\frac{1}{2}}$ is found and can be explained in terms of arrest of crack propagation at grain boundaries and the greater likelihood of parting crack formation with increasing grain size. Above this grain size, residual boundary stresses become of increasing importance, cause grain boundary embrittlement and a markedly increased transition temperature

5 The Effect of Cold Work

5-a Introduction

The usual effect of cold work upon the tensile properties of metals is to increase strength and decrease ductility. However in body-centred-cubic metals the ductility is sometimes increased due to a lowering of the ductile/brittle transition temperature (Lement et al 1963, Wain et al 1963). The influence of this variable upon the mechanical properties of uranium has been investigated and the major results are recorded here. Tensile specimens were tested after rolling 28% and 11% reduction at 300°C and after pre-straining 12% in tension at 85°C and 245°C. Bend tests were also carried out on beams rolled 30% at approximately 100°C.

5-b Results

The influence of 11% reduction at 300°C upon the ductility transition behaviour is demonstrated in Fig 117 and similar results for 28% reduction are recorded in Fig 118. Fig 119 demonstrates the effect of 28% rolling reduction on the tensile strength. Above the transition temperature the usual effect of decreasing ductility and increased strength is observed, but below the transition ductility is increased and a progressive lowering of the fracture transition temperature was observed but in worked specimens no intercrystalline cracking was detected and brittle facets were small and difficult to distinguish.

After pre-straining 12% at 85°C in tension little effect upon the transition behaviour was observed but straining at 245°C resulting in a significant lowering of the transition temperature as shown in Table XXIII:

Table XXIII

Test Temperature	Annealed Elongation	Elongation after 12% tensile pre-strain at 245°C
50°C	55%	42%
20°C	46%	38%
0°C	18%	27%
-23°C	5%	12%
-95°C	1%	3%

Unadjusted bend-test beams 0.14in thick rolled 30% to the same thickness as the annealed beams at 100°C showed a similar effect:

Table XXIV

Test Temperature	Angle at Fracture	
	30% Pre-strained at 100°C (rolling)	Annealed
80°C	55°	75°
20°C	50°	75°
0°C	40°	30°
-10°C	30°	20°
-95°C	10°	5°
-183°C	0°	0°

The grain structure after deformation is found to be very confused with profuse twinning and many intersecting twins and the original grain boundaries can rarely be distinguished (e.g. Fig 44).

5-c Discussion

In body-centred cubic metals the effect similar to that observed here is usually attributed to the formation of a dislocation substructure thereby reducing the parameter d in the Cottrell equation. This is also possible here but transmission microscopy of uranium after similar treatments to those above (Douglass and Bronisz 1963) indicates that the formation of such a substructure is unlikely here. However, a similar "grain-size" effect is caused by the "fragmentation" of the grains by twinning. The twins are irregular, intersecting and often twinned themselves and in these circumstances will provide effective barriers to crack propagation. Also, straight twins are rarely observed and no easy paths for propagation will exist. It is difficult to obtain a satisfactory estimate of the d parameter in these structures but from this work, and the thin foils of Douglass and Bronisz, it would appear to be less than a micron after 28% reduction. If the linear plot of Fig 115 is extrapolated to this value of d a transition temperature similar to that observed (Fig 118) is predicted.

This would appear to provide a satisfactory explanation for the experimental observations but an effect upon the residual grain boundary stresses might also be expected. Rolling would tend to eliminate these stresses and consequently the transition temperature would be lowered by raising the effective "grain boundary strength"

The following considerations provide explanations for the observations presented in Tables XXIII and XXIV. Tensile strain at relatively low temperatures (85°C for example) results in "slicing" rather than "fragmentation" of the grains by the twins (Fig 45) and consequently little effect upon the transition behaviour might be expected. However, rolling is a more complex process of deformation, more twinning systems are found at similar temperatures and fragmentation of the grains occurs, lowering d and thus the transition temperature.

A similar general effect to that recorded here (Taplin and Martin 1964b) was reported at about the same time (Bolton and Tilbury 1964) where it was suggested that the formation of a dislocation cell-structure might be the cause.

6 The Effect of Strain-Rate

6-a Introduction

The influence of a variation in strain rate from 1.25%/minute (cross-head speed = 0.0078in/minute) to 320%/minute (cross-head speed = 2in/minute) upon the tensile behaviour was examined in virgin rolled material of annealed grain size 0.03mm average diameter. For a full investigation of strain-rate further orders of magnitude strain-rate differential would have been necessary and consequently detailed conclusions cannot be made here.

6-b Results

The principal results (the two widest rates of strain tested) are recorded in Figs 120 and 121. The usual overall influence of increasing strain-rate lowering ductility and raising the fracture stress is observed. It is also clear that increasing strain-rate raises the ductile/brittle transition temperature. Notable also in Fig 121 are the facts that the transition is much more sharp at high rates of strain and that the brittle fracture stress appears to be decreased with increasing strain-rate.

6-c Discussion

The general effect of increasing strain rate is to increase the lattice friction stress (e.g. Campbell and Harding 1962) reduce dislocation mobility and favour twinning (Cahn 1951). The expected consequence would be an increase in the transition temperature and a fall in the brittle fracture stress which is consistent with the present observations. Stroh (1957) predicted a linear relationship between the logarithm of strain-rate and the reciprocal of the transition temperature. Such a relationship was found here for four strain rates within the above limits but the range is too narrow to permit reliable deductions.

7 The Effect of a Notch

7-a Introduction

Tensile testing at low temperatures sometimes resulted in fracture of the specimens across the shoulders as shown in Fig 86. This behaviour was tacitly assumed to be attributable to the material being extremely notch-sensitive below the transition. Clearly the notch brittleness would have to be severe to account for the behaviour for not only is the magnitude of the stress concentration associated with the shoulder low but the cross sectional area is double that in the gauge length (Fig 13). No information was available on this aspect and it was decided to make a limited investigation of the notch tensile behaviour to determine whether this assumption is valid.

A notch, to the dimensions given in Chapter V, was machined around the centre of the gauge length of a number of virgin rolled specimens which had an annealed grain size of 0.03mm average diameter. A tensile test with such a specimen shows whether or not a material is prone to brittle fracture in the presence of a stress concentration ("notch-sensitive"). The triaxiality of stress introduced by the notch raises the value of the longitudinal stress at which yielding occurs. Thus the entire flow curve of a notched specimen is raised and the fracture strain lowered. A notch also produces an increase in the local strain-rate near the notch which was considered by Stroh (1957) to be the most important influencing factor.

The percent elongation of a notched specimen when compared to that of an un-notched specimen sometimes gives an indication of the notch sensitivity but a more accurate and valid indication is given by the Notch Strength Ratio which is defined as:-

$$N.S.R. = \frac{\text{Maximum load/original C/s area at notch}}{\text{U.T.S. of an un-notched specimen.}}$$

If the N.S.R. is less than unity the material is said to be notch brittle (Dieter 1961). This parameter can exceed unity by an appreciable amount because of the triaxial stresses at the root of a notch.

7-b Results and Discussion

The notch tensile behaviour was examined in the treated condition (double oil-quenched from 600°C) and in the as-machined condition to determine whether any effect of prior heat treatment existed. The treatment used introduces residual grain boundary stresses but at the grain size used these are of a small magnitude. Heat treatment may also relieve internal machining stresses and result in thermal stresses due to the variation in cooling rate with change in section. The elongation results are presented in Fig 122 and the shapes of the curves appears to indicate that a notch raises the transition temperature considerably. However, the notch ductility transition is not associated with a ductile to crystallographic fracture transition, but with the gradual chahge that occurs in the ductile behaviour at about 300°C. Normal tensile tests above 300°C give rise to large amounts of necking due to the much later formation of ductile cavities and consequently above such an increased notch dutility results causing the "transition".

The notch strength ratios for the two series of specimens are plotted against test temperature in Fig 123. Above room temperature the NSR is considerably greater than unity and this falls gradually with decreasing temperature to about 20°C at which point a marked decrease in the parameter is observed. This corresponds with the normal tensile transition and the inferehce is that the notch does not appreciably affect the transition temperature and only below the normal tensile transition is uranium notch sensitive. On the brittle side of the transition, the NSR falls to a relatively high plateau in the as-machined specimens which indicates only moderate notch sensitivity. At all temperatures the NSR is lower in heat treated specimens but this is particularly so below the transition. Since no difference in grain structure exists between the specimens this is suggested to be due to the heat treatment causing rdief of internal stresses and thermal contractional stresses in the region of the notch. Grain boundary stresses are predicted to be negligible with the small grain size involved and no preference for intergranular cracking was observed and consequently any such effect must be mihor.

Metallographic examination of heat treated but untested specimens showed twins in the region of the notch but almost none in as-machined specimens. This provides some evidence for the

suggested effect. Profuse twinning was also found in the region of the tensile shoulder after heat treatment whilst the rest of the specimen remained relatively twin-free. Such a region is illustrated in Fig 124. Notable also in this photomicrograph is the fact that the majority of the twins run in one macroscopic direction (normal to the axis). This would not be expected of grain boundary stresses but is possible with thermal/machining stresses. The high magnitude of these stresses compared to similar effects in other metals must be a further manifestation of the anisotropy of thermal expansion. The presence of these twins will lower the fracture stress in these areas by providing sites for easy crack nucleation and propagation, particularly at low temperatures.

7-c Conclusions

Uranium is only moderately notch sensitive at low temperatures and fracture in the tensile shoulder at these temperatures may be attributed to thermal and internal machining stresses causing profuse twinning in such regions during heat treatment thereby promoting fracture. The brittleness of irregular-shaped machined components of uranium is therefore sensitive to heat treatment.

8 The Effect of Annealing Temperature

8-a Introduction

Previous work has indicated that the temperature of annealing deformed uranium can have a profound influence upon ductility. De Libanati and de Tanis (1962) found that partially recrystallized alpha uranium obtained on annealing at 350°C, was much more ductile than material fully recrystallized at 630°C. This phenomenon was investigated over a wide temperature range and the results are described in this section.

8-b Results

The main results were obtained on specimens machined from virgin material rolled 28% reduction at 300°C and annealed at varying temperatures for 24 hours but some results obtained on specimens from material rolled 11% and 8% are also presented.

Figs 125 and 126 demonstrate the effect of annealing temperature between 500-650°C on some properties after 11% and 8% reduction. The observations can be explained mainly in terms of increasing grain size since, except after annealing at 500°C the specimens were fully recrystallized.

The effect of annealing temperature between 240°C and 750°C was investigated on material rolled 28% reduction. Fig 127 shows the effect of annealing temperature on % elongation and % reduction in area at fracture. Good reproducibility was obtained and the shapes of the curves are real. The % elongation curve shows two peaks, one ate about 350°C and one at 500°C but in the reduction in area curve there is a single broad maximum. These conrasting ductility effects are attributable to the specimens after annealing at temperatures below 420°C exhibiting local necking: above 450°C the specimens fractured without appreciable necking. To indicate more clearly the ductility behaviour here a "Necking Parameter " has been introduced. The reduction in area which would have taken place if all the elongation measured were uniform, without necking, can be calculated from the relationship (Taplin 1961):

$$\frac{1}{R} = \frac{1}{E} + 1$$

R is the reduction-in-area and E is elongation. The"necking parameter" is the difference between this calculated value for the reduction and the measured reduction-in-area. The parameter is recorded against annealing temperature in Table XXV.

Table XXV

Annealing Temperature	Necking Parameter (x)
as received	1.5
242°C	1.2
348°C	5.0
420°C	7.8
490°C	0.9
545°C	0.5
613°C	0.2
641°C	0.5
680°C	3.2
752°C	3.8

The above table demonstrates that necking is a maximum at 420°C and comparison with Table IX shows that this is associated with the partially recrystallized structures.

The hardness and U.T.S. results are recorded in Fig 128 and indicate that the decrease in hardness and strength is progressive and continuous. Fig 129 demonstrates the effect of annealing temperature on the true fracture stress. In all three graphs the predominant mode of fracture and the phase at the

annealing temperature are indicated. Examples of the different stress/strain curves obtained are shown in Fig 130. 'A' is as-received material, 'B' is annealed at 420°C (banded, partially recrystallized structure) and 'D' is annealed at 680°C (coarse-grained-beta treatment). The increased necking observed after annealing at intermediate temperatures is demonstrated and it is also shown that the high necking parameter obtained after beta annealing and testing is anomalous and probably due to the ovality of section produced. The grain structures after annealing were given earlier in Table IX.

Although the room temperature fractures obtained were frequently mixed two changes in the predominance of fracture modes was observed with increasing annealing temperature in the range investigated:-

1) In specimens annealed at temperatures below 450°C a ductile failure predominated whilst after annealing above 450°C (and air-cooling) an intercrystalline failure predominated.

2) The second change in fracture mode occurred at the alpha/beta transformation temperature: specimens annealed above the beta-transus fractured mainly by twin parting.

8-c Discussion

Cold work has already been shown to lower the ductile/brittle transition temperature and this was attributed mainly to a decrease in the parameter d. Annealing at temperatures up to 420°C results in recovery with partial recrystallization in bands which rarely

exceed 0.05mm in width. This structure still has a low d value and the residual grain boundary stress effect will be negligible, consequently the transition temperature will still be low. Thus, the increased ductility can be related to the softening accompanying recovery. Significant softening begins at about 300°C (Fig128) and this is associated with increased necking which causes the rise in the reduction-in-area curve and the small increase in total elongation (Fig 127). After annealing at 420°C the rate of work-hardening is lowered significantly such that necking starts at an earlier stage thereby lowering the total elongation but the reduction-in-area is increased. After annealing at 500°C recrystallization is complete and the fine-grained structure results in a high elongation but the ductile/brittle transition temperature is raised and fracture occurs without necking: a decrease in the reduction-in-area therefore occurs. With further increasing annealing temperature to the beta-transus the grain size increases, raising the transition temperature and lowering the rate of work hardening with a consequent fall in ductility and strength. A very coarse grain structure results from beta annealing and the transition temperature is raised appreciably giving a discontinuous decrease in ductility and strength.

IX CONCLUSIONS

In the preceding chapters alpha uranium has been shown to exhibit properties, a number of which are uncommon amongst metals. This is perhaps not unwarranted in view of the low orthorhombic symmetry with corrugated planes, covalent bonding and high degree of anisotropy. Also, the unusual transformation behaviour gives rise to some distinctive alpha grain structures. Many of the properties, and in particular the fracture characteristics can be explained in terms of these, or related, considerations. From an understanding of the fracture behaviour an explanation for many of the mechanical properties then follows.

In particular the following conclusions may be enumerated:-

1. It is suggested that the important criterion in grain refinement upon beta-quenching by alloying with iron and aluminium is the increasing amounts of dispersion network present which retards alpha grain-growth. Contributory factors are solution of these elements in the beta and beta grain-growth which both occur with increased beta soaking times and both lower the transformation temerature thereby refineing the alpha grain structure.

2. The beta phase can be retained to room temperature by fast beta-quenching doubly adjusted material. The direct gamma→alpha transformation is observed in this material upon fast gamma-quenching.

3. A variation in grain size between specimens can only be produced in isolation of other variables by mechanical and thermal treatments.

4. It is suggested that the process of low temperature crystallographic failure in alpha uranium is nucleated at the apices of growing long, thick twins by a reaction involving emissary dislocations. Propagation occurs along the composition plane of twins because there are the sites of structural distortion and stress, therefore providing planes of inherent weakness in the lattice. This fracture process may involve the linking-up of micro-cracks on nearby twins to form cleavage steps.

5. In the region of room temperature intercrystalline cracking was frequently observed in alpha. Tests after thermal cycling established that this is due to the surface energy for fracture being lowered in selected areas at grain boundaries by the residual stresses which are present there to a varying degree after most heat treatments because of the anisotropic thermal expansion.

6. The prevalence of intergranular embrittlement was found to be sensitive to heat treatment and grain size.

7. With increasing temperature a transition from a brittle to a ductile behaviour was observed. Ductile failure occurred by the formation of cavities at cuboid inclusions which grew and, in the centre of the externally necked region, coalesced to form a macroscopic fissure which propagated outwards to cause failure. Below about 300°C cavity-formation tended to occur at an early stage by cuboid-cleavage whilst above 300°C cavities tended to be formed at a late stage by inclusion/matrix parting.

8) This change in the ductile fracture behaviour is reflected in the tensile properties and is associated with plateaux at about 300°C in the ductility and strength versus temperature graphs. It can be related to the change in the predominant mode of deformation from twinning to slip at about this temperature which results in accommodation of the inclusions in the deforming matrix.

9) The ductile/brittle transition behaviour in the region of room temperature may be attributed to decreasing dislocation mobility with decreasing temperature such that stresses at twin apices and composition planes are not so readily relieved and parting failure thereby facilitated. It is possible that with decreasing temperature there is a change in the electronic configuration to cause stronger covalent bonding and the transition could be explained in these terms.

10) The ductile/brittle transition occurs at a lower temperature in bending than in tension.

11) Increased volume fractions of the finely dispersed intermetallic network causes an increase in the ductile/brittle transition temperature. This is suggested to be due to the raising of σ_i by the dispersion.

12) The ductile/brittle transition temperature is lowered by decreasing grain size and a transition grain size is found. Below a grain size of about 0.20mm the effect is small and may be related to the increasing arrest of propagation at grain boundaries and the decreasing likelihood of parting crack formation with decreasing grainsize. Above this grain size increasing grain size causes a

large increase in the transition temperature. This is suggested to be due to residual grain boundary stresses which become an important factor at large grain sizes cause intercrystalline embrittlement and provide long straight twins thus facilitating brittle fracture.

13) Increasing amounts of pre-strain cause a marked decrease in the transition temperature. This is suggested to be due to a "grain size" effect caused by the dissection and fragmentation of the grains by twins.

14) The apparent effect of grain shape, whereby increasing irregularity of profile raises the transition temperature, can be largely explained in terms of the different heat treatments used causing variations in grain boundary surface energy.

15) An increase in strain-rate raises the ductile/brittle transition temperature.

16) The brittle (parting) fracture stress of polycrystalline alpha uranium decreases progressively with decreasing temperature This may be related to the anisotrppic structure which results in a very low yield stress.

17) No simple fracture stress/grain size relationship was found but if account is taken of all the additional influencing factors in uranium the results might be explained in terms of the usual $d^{-\frac{1}{2}}$ relationship.

18) Alpha uranium is only moderately notch sensitive at low temperatures and fracture in the shoulders of tensile specimens at these temperatures may be attributed to thermal and internal stresses causing twinning during heat treatment thereby promoting fracture.

19) The room temperature ductility of uranium is strongly grain size dependent. This is explained in terms of the increased rate of strain-hardening and decrease in the transition temperature with decreasing grain size.

20) Meta-stable beta fails by crystallographic cleavage at room and lower temperatures.

21) The cleavage fracture stress of meta-stable beta increases with decreasing temperature.

22) Some confirmation that fracture in the beta-region takes an intercrystalline path was obtained.

X REFERENCES

American Society of Metals 1948 Metals Handbook, A.S.M., New York

Austing C.E. 1962 Private Communication, AERE

Baenziger N.C. & Ruddle R.E. 1944 U.S.A.E.C./ANL/JJK/24

Barwood I.F. & Butcher B.R. 1963 J.Nucl.Mat., 8, 232-240

Basinski Z.S. & Christian J.W. 1954 Acta Met., 2, 148.

Beachem C.D. 1963 Trans.A.S.M., 56, 318.

Beevers C.J. & Honeycombe R.W.K. 1962 (Phil.Mag., 7, 763 / Acta Met., 10, 17

Bell R.L. & Cahn R.W. 1953 Acta Met., 1, 752

Bement A.L. & Wallace W.P. 1957 U.S.A.E.C./HW/51084

Blumenthal B. 1960 J.Nucl.Mat., 2, 23-30

Bolton J.D. & Tilbury P.D. 1964 Private Communication, AWRE Aldermaston, (also J.Inst.Met., 92, 59)

Brezina A. 1880 Verh.Geol.Reichsanstalt Wien, 45

Burke J. & Dixon P.H. 1962 J.Nucl.Mat., 7, 38-45

Butcher B.R. 1957 J.Nucl.Energy, 1, 273-278

Butcher B.R. 1959 Nuclear Power, 3, 105

Butcher B.R. & Baverstock D. 1961 J.Nucl.Mat., 3, 30-40

Butcher B.R. 1962 Symposium on Uranium and Graphite, Inst.Met. London,1962, Paper I, 1.

Cahn R.W. 1951 AERE/MR/744

Cahn R.W. 1953 Acta Met., 1, 53 and AERE/MR/740

Cahn R.W. 1954 Advances in Physics, 3, 202

Cahn R.W. 1955 J.Inst.Met., 83, 493

Calais D., Lacombe P. & Simenel N., 1960 J.Nucl.Mat., 2, 325

Campbell J.D. & Harding J. 1962 Response of Metals to High Velocity Deformation, 51, Interscience, New York

Chang H.C. & Grant N.J. 1956 J.Metals, 8, 544-551

Chiswick H.H., Dwight A.E., Lloyd L.T., Nevitt M.V. & Segler S.T. 1958 Second Geneva Conference, 15/P/713

Chubb W. 1953 U.S.A.E.C./B.M.I./X/112

Churchman A.T., Mogford I.L. & Cottrell A.H. 1957 Phil.Mag., 2, 1271

Clarke F.J.P. 1964 Acta Met., 12, 139

Cotterill P. 1961 Prog.Mat.Sci., 9, 201

Cottrell A.H. 1958 Trans.AIME, 212, 192

Cottrell A.H. 1959 Swampscott Conference on Fracture (Ed.B.L. Averbach et al.) P.20., New York: Wiley

Cottrell AH. 1963 Proc.Roy.Soc., A, 276, 1

Cottrell A.H. 1963 The Relation between the Structure & Mechanical Properties of Metals, 2, 457, H.M.S.O., London

Davidenkov N.N., Kolenikov A.F. & Federov K.N. 1933 J.Exp.Theor. Phys., (Moscow), 3, 350

Davies D.M. 1962 D.Phil. Thesis, Oxford

Davis W.D. 1956 U.S.A.E.C./KAPL/1548

Dieter G.E. 1961 "Mechanical Metallurgy" McGraw-Hull, New York

Dixon P.H. & Burke J. 1962 Symposium on Uranium & Graphite, Inst. Met., London, 1962, Paper 2, 9

Dixon P.H. & Fern F.H. 1963 Anglo-French Conference of the Physical Metallurgy of Uranium, Bournemouth, Feb.1963, Paper 7.

Dixon P H. 1964 AERE Private Communication

Doherty R.D. & Martin J.W. 1963 J.Inst.Met., 91, 332

Donze G. 1962 J.Nucl.Mat., 5, 150-152

Douglass D.L. & Broniez S E. 1963 Trans.AIME, 227, 1151

Duwez P. 1951 } Trans.AIME, 191, 765-771
} J.Appl.Phys., 22, 1174-1175

Duwez P. 1953 J.Appl.Phys., 24, 152-156

Edmondson B. 1961 Proc.Roy.Soc., A, 264, 176

Foote F.G. 1956 Progress in Nuclear Energy, Series V, 1, 99

Friedel J. 1961 Electron Microscopy & Strength of Crystals, ed.G.Thomas & J.Washburn: John Wiley (1963)

Gardner H.R. & Riches J.W. 1960 Trans AIME, 52, 728

Gittus J.H. 1963 "Uranium": Butterworths, London

Greenwood G.W. & Quarrell A.G. 1954 J.Inst.Met., 82, 551

Grainger L. 1958 "Uranium & Thorium": Newnes, London

Griffith A.A. 1920 Phil.Trans.Roy.Soc., A, 221, 163

Haddrell V.J., Sykes E.C. & Mott B.W. 1956 J.Inst.Met., 84, 112

Hahn G.T., Averbach B.L., Owen W.S. & Cohen M., 1959 "Fracture": Wiley, (New York), 91

Hall E.O. 1954 "Twinning": Butterworths, London

Hancock N.H. 1957 AERE, M/R, 1156

Holden A.N. 1952 Acta Cryst., 5, 182

Holden A.N. 1953 Acta Met., 1

Holden A.N. 1958 "Physical Metallurgy of Uranium": Addison-Wesley, New York

Hornbogen E. 1961 Trans.AIME, 221, 771

Hueschen R.E. & Sanderson M.J. 1953 U.S.A.E.C./HW/27082

Hull D. 1960 Acta Met., 8. 11

Hull D. 1962 Interscience, New York, Seattle Conference on Fracture of Solids

Jacob C.W. & Warren B.E. 1937 J.Am.Chem.Soc., 59, 2588-2591

Jepson M.D., Kehoe R.B., Nichols R.W. & Slatterly G.F. 1958 Second Geneva Conference, 6, 42

Jillson D.C. 1950 Trans.AIME, 185, 599

Johnson A.A. 1962 Phil.Mag., 7, 177

Johnstone W. & Gilman J.J. 1959 J.Appl.Phys., 30, 129

Klepfer H.H. & Chiotti P. 1957 U.S.A.E.C. /ISC/893

Knott J.F. & Cottrell A.H. 1963 J.Iron & Steel Inst., 201, 249

Koda S. & Morozumi S. 1962 J.Nucl.Mat., 6, 5

Lacombe P. & Calais D. 1958 Second Geneva Conference P/1258/3-13

Lehmann J. 1960 J.Nucl.Mat., 2, 152

Lehr P. & Langeron J.P. 1958 Rev. Met., 4, 829

Lement B.S., Passmore E.M., Kreder K. & Vilke I. 1962 Manlabs Inc. Mass. USA, MOA/P/108311/6

Lemogne A. & Lacombe P. 1963 J.Nucl.Mat., 8, 116

Leteurtre J. 1962 J.Nucl.Mat., 6, 338

Libanati N.A.(de) & de Tanis S.V. 1962 Compt. Rend., 255, 2435

Lloyd L.T. & Chiswick H.H. 1955 Trans. ASM, 203, 1206

Lloyd L.T. & Lacombe P., Calais D. & Simenel N. 1961 J.Nucl.Mat.3,241

Low J.R. 1956 "Deformation and Flow of Solids", Verlag, Berlin

Loy B. 1963 International R & D Ltd Research Report

Lukesh J.S. 1949 Acta Cryst., 2, 420

Marsh D.M. 1962 Seattle Conf. on Fracture, 119, Interscience, N.Y.

McIntosh A.B. & Teal J. 1958 Second Geneva Conference P/49/413

Mclean D. 1957 "Grain Boundaries in Metals" OUP, London

McLean D. 1962 "Mechanical Properties of Metals" Wiley, New York

Meredith K.E. & Waldron M.B. 1959 J.Inst.Met., 87, 321

Mott B.W. & Haines H.R. 1954 Rev. Met., 51, 9

Mott N.F. 1953 Proc.Roy.Soc. A 220, 1

Orowan E. 1948 Rep.Progr.Phys., 12, 165

Owen W.S. 1959 Swampscott Conf. on Fracture, 147, Wiley, New York

Pauling L. 1948 "Nature of the Chemical Bond" Ithaca, New York

Petch N.J. 1953 J.Iron & Steel Inst., 174, 25

Petch N.J. 1958 Phil. Mag., 3, 1089

Plateau J., Henry G. & Crussard C. 1957 Rev. Met., 54, 200

Priestner R. 1963 Seattle Conf. On Fracture, 455, Interscience, N.Y.

Priestner R. & Louat N. 1963 Acta Met., 11, 195

Pugh S.F. 1960 UKAEA/AERE, R/3458

Puttick K.E. 1959 Phil. Mag., 4, 964

Puttick K.E. 1960 Phil. Mag., 5, 759

Reed-Hill R.E. & Robertson W.D. 1957 Acta Met., 5, 728

Rose G. 1868 Phys. Abhandl. Kon. Acad. Wiss. , 57, Berlin

Sergeyev G.Y., Titova V.V., Nikobeva Z.P., Kapetlsev A.M. & Kolobneva L.L. 1958 Second Geneva Conf. P/2307/25

Sleeswyk A.W. 1962 Acta Met., 10, 705

Sleeswyk A.W. 1962 Acta Met., 10, 803

Smith C.S. & van Wagner R.W. 1936 Proc. A.S.T.M., 36, 263

Stroh A.N. 1957 Advances in Physics, 6, 418

Taplin D.M.R. 1961 DipTech Thesis, Birmingham C.A.T.

Taplin D.M.R. & Martin J.W. 1963a Anglo-French Conf. on Physical Metallurgy of Uranium, Bournemouth, Paper 10 (AERE)

Taplin D.M.R. & Martin J.W. 1963b J.Nucl. Mat., 10, 134

Taplin D.M.R. & Martin J.W. 1964a J.Nucl. Mat., 11, 268

Taplin D.M.R. & Martin J.W. 1964b J.Less-Common Metals, 6, (5)

Taplin D.M.R. & Martin J.W. 1964c J.Less-Common Metals, 6, (6)

Taylor G.I. 1938 J.Inst.Met., 62, 307

Teed P.L. 1950 "The Properties of Metallic Materials at Low Temperatures": Chapman & Hall, London.

Teeg R.C. & Ogilvie R.E. 1961 J.Nucl.Mat., 3, 81

Thewlis J. & Steeple H. 1954 Acta Cryst., 7, 323

Tipper C.F. 1949 Metallurgia, 39, 133

Tipper C.F. 1962 "The Brittle Fracture Story": Cambridge

Tucker C.W. 1950 Trans. ASM., 42, 762

Tucker C.W. 1954 Acta Cryst., 7, 752

U.K.A.EA. 1963 Annual Report, H.M.S.O., London

van Bueren H.G. 1960 "Imperfections in Crystals": Amsterdam: North-Holland Publishing Company

Votava E. & Sleeswyk A.W. 1962 Acta Met., 10, 965

Wain H.S., Johnstone S.T.M. & Henderson F. 1963 J.Inst.Met., 91, 41

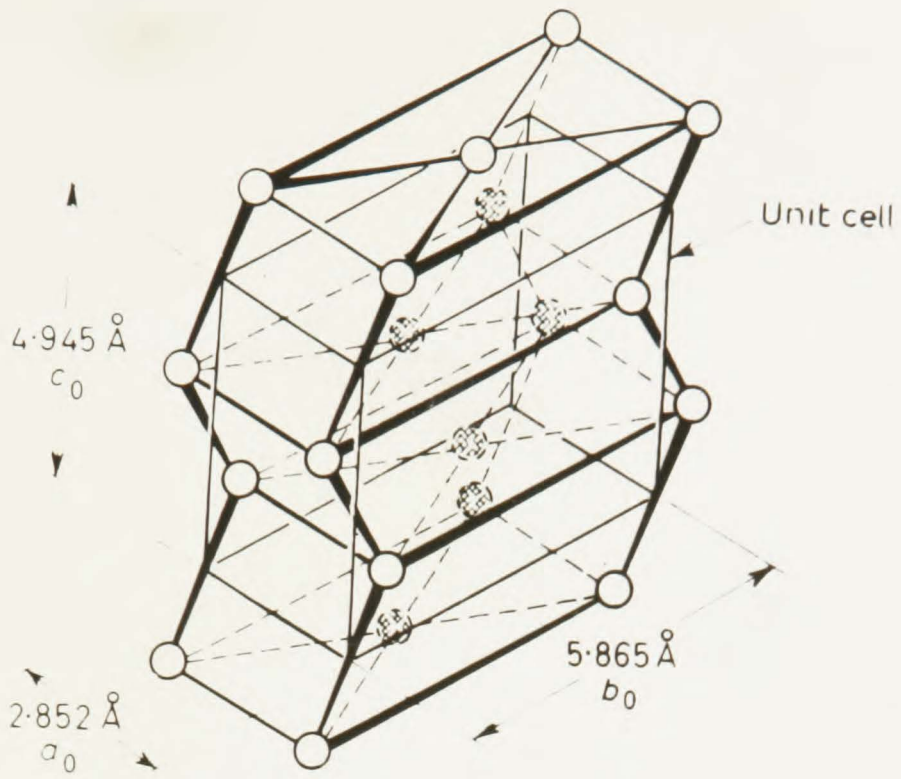
White D.W. 1955 J.Metals, 7, 22

Wilson A.S. & Ruddle R.E. 1949 Acta Cryst., 2, 126

Woolf U.E. 1962 Trans AIME, 224, 327

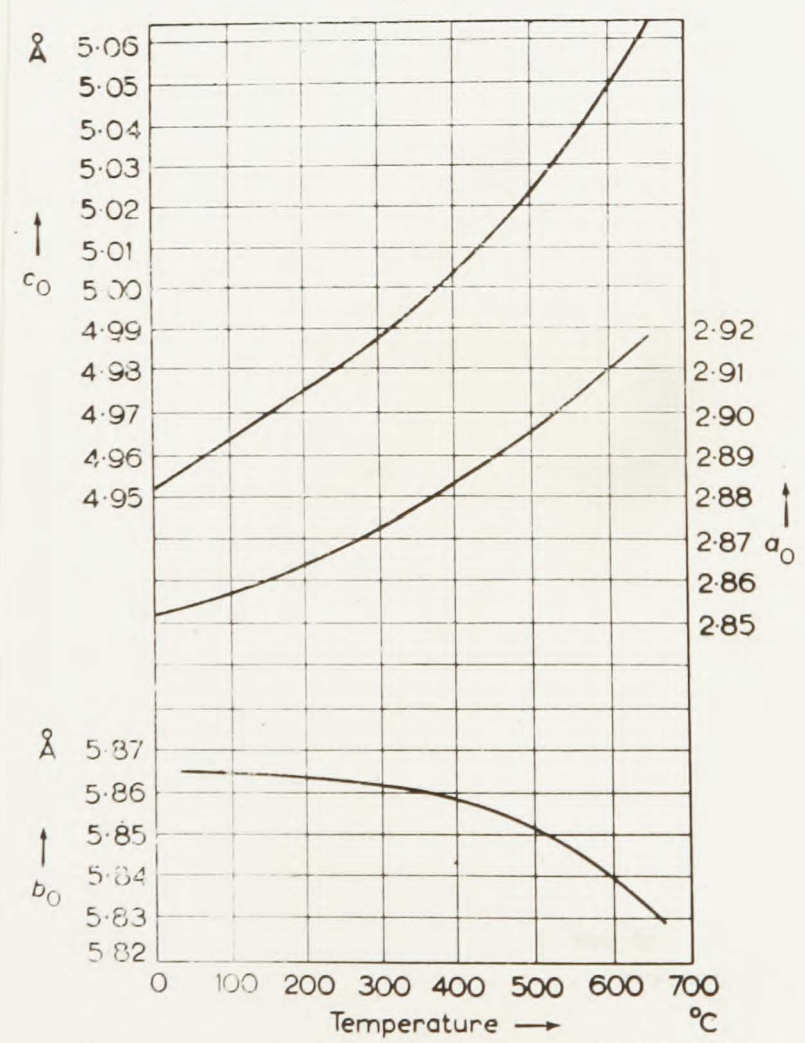
Young A.G., Gardner K.M. & Rotsey W.D. 1960 J.Nucl.Mat., 3, 234

Zener C. 1948 "Fracturing of Metals", Cleveland: ASM



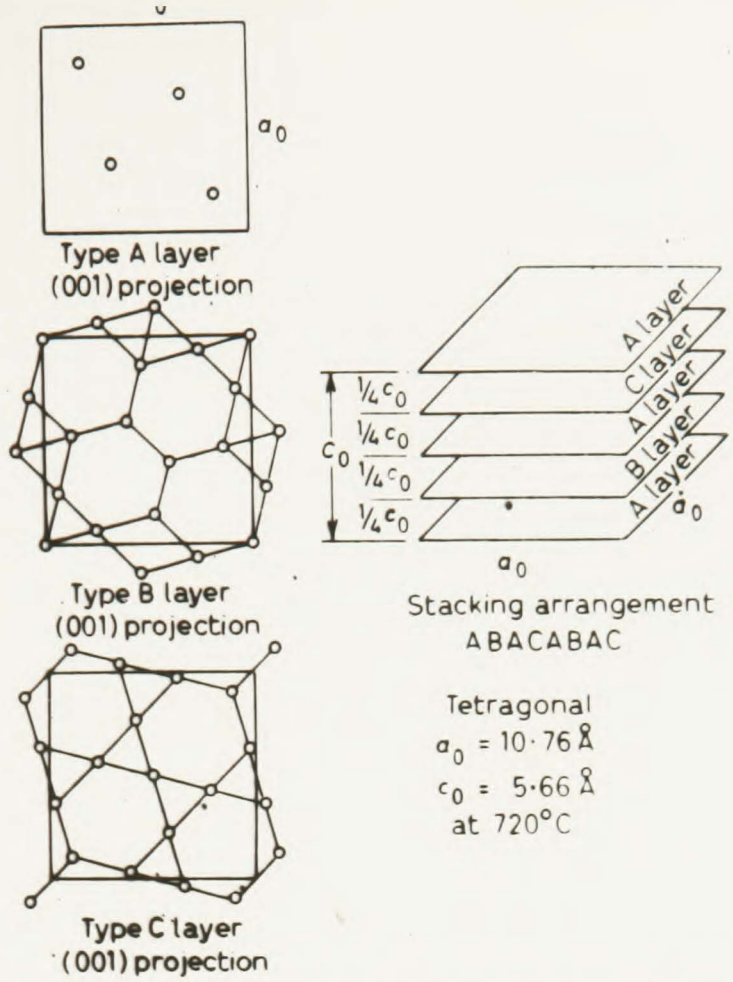
Crystal structure of alpha-uranium (from **A. N. HOLDEN**[34]*, by courtesy of Addison-Wesley Publishing Company, Inc.)*

FIGURE 1



Unit cell dimensions of alpha uranium as a function of temperature.
(BRIDGE, SCHWARTZ & VAUGHAN, 1956.)

FIGURE 2



Crystal structure of beta-uranium (from W. D. WILKINSON *and* W. F. MURPHY[6]*, by courtesy of Van Nostrand Co., Inc.)*

FIGURE 3

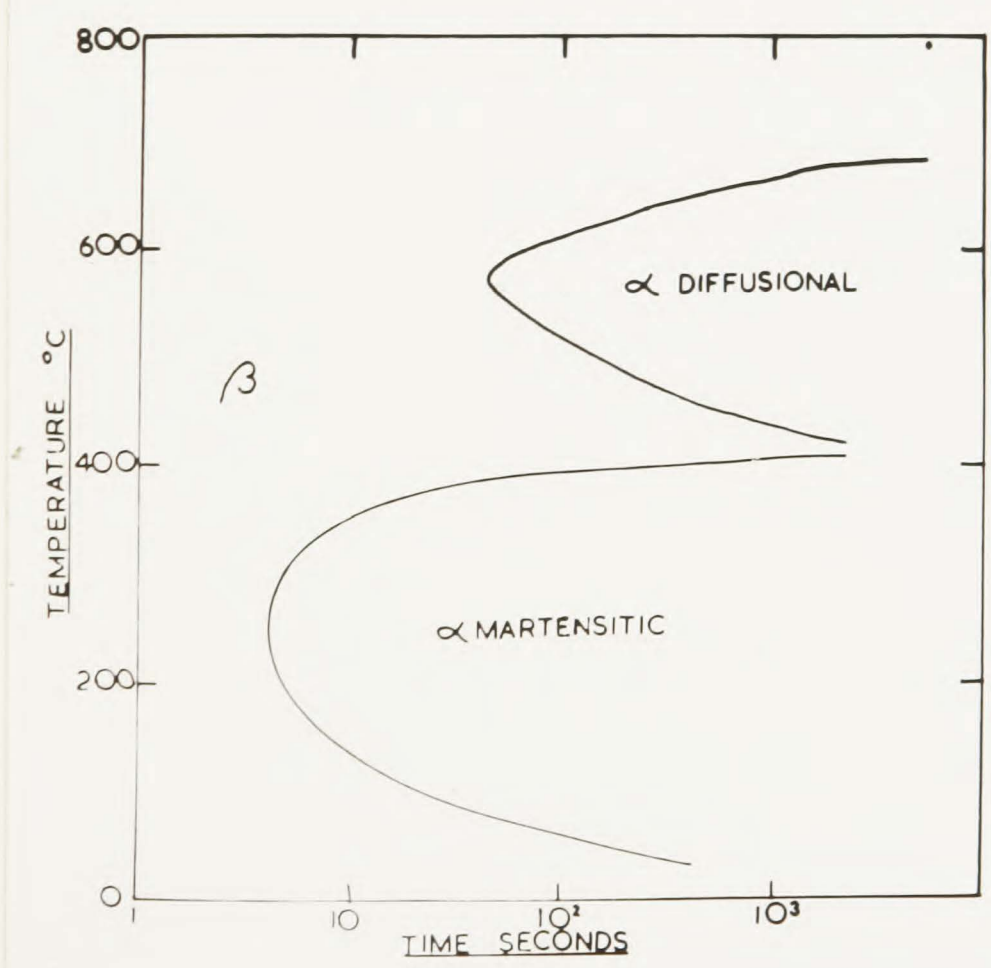
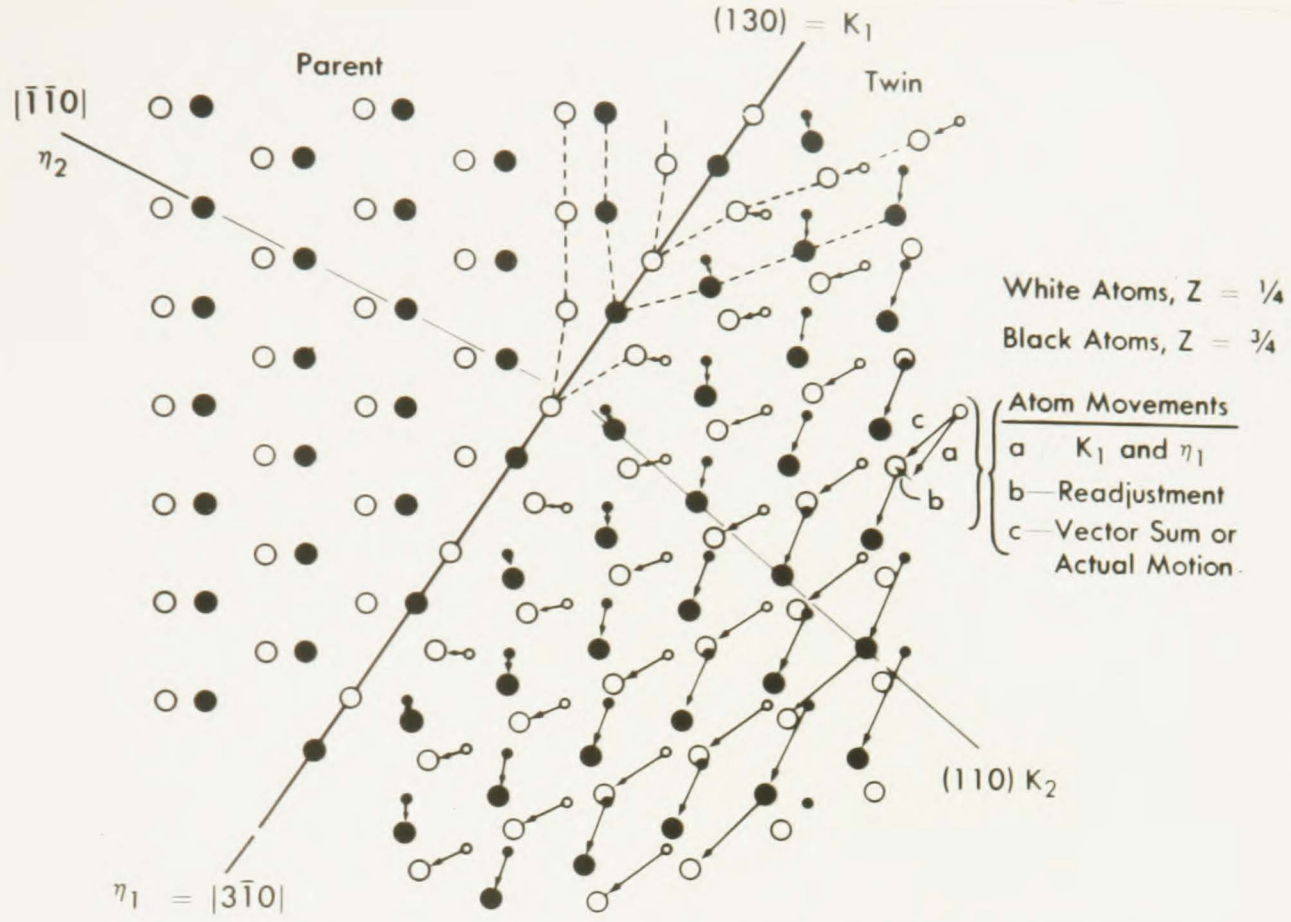


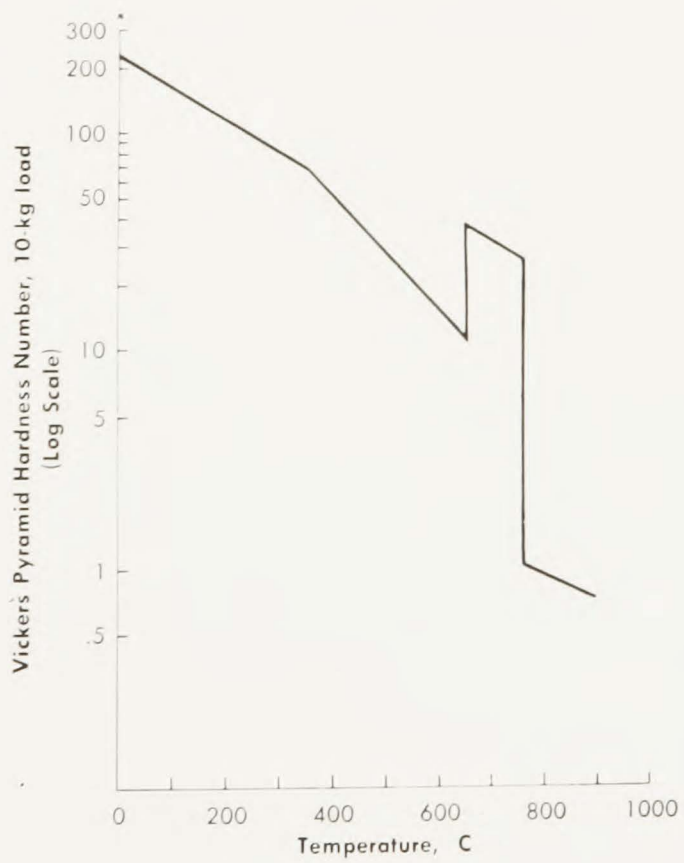
FIGURE 4

Schematic TTT diagram for a dilute alloy of uranium (after Butcher 1962).



Atom movements for {130} twin in alpha uranium.

FIGURE 5



Hardness of uranium as a function of temperature.

FIGURE 6

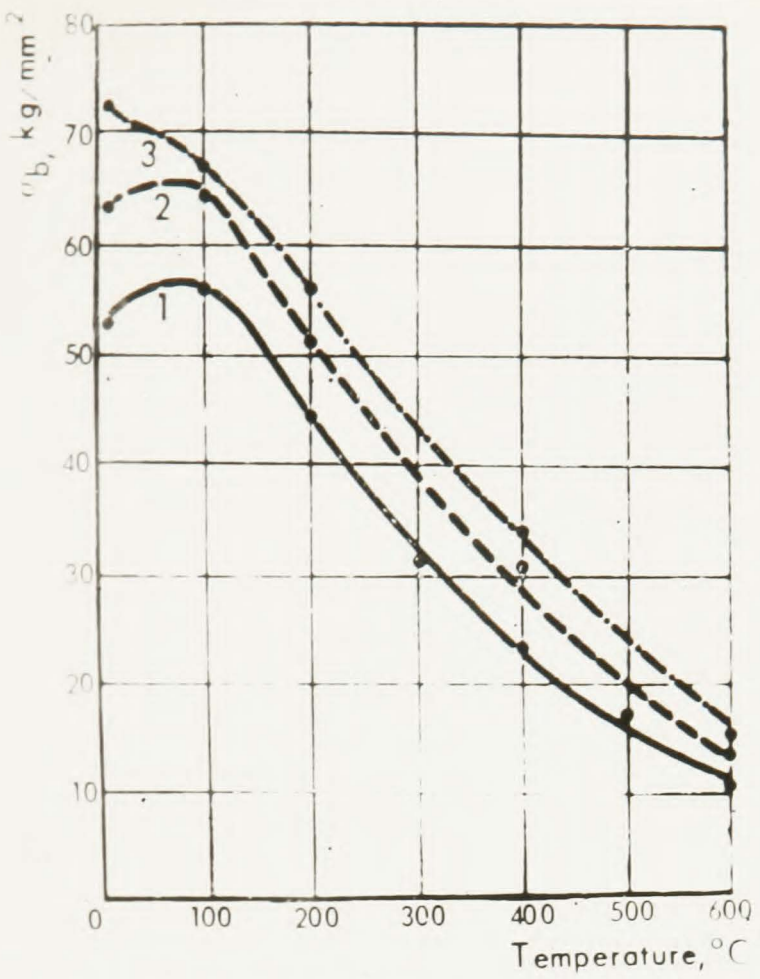
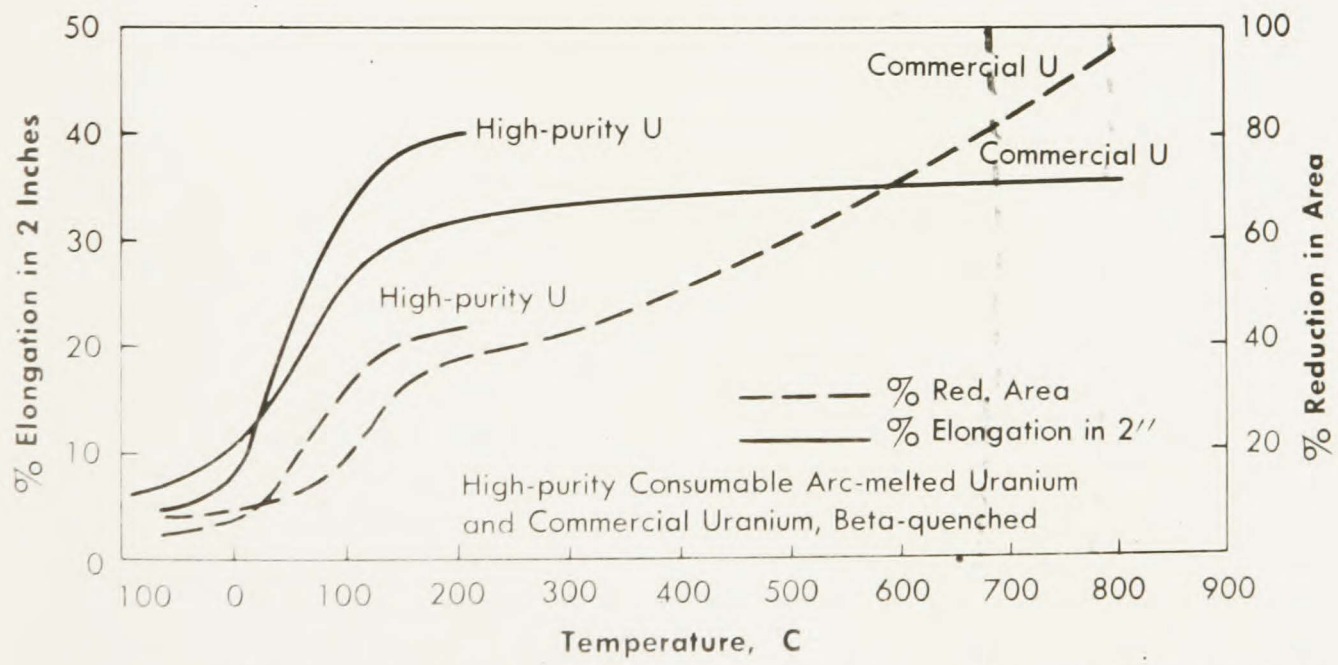


Figure 8. Change in tensile strength of cast and quenched uranium as a function of temperature of the test (metal from one melt) 1—cast uranium; 2—uranium quenched from the γ phase 3—uranium quenched from the β phase

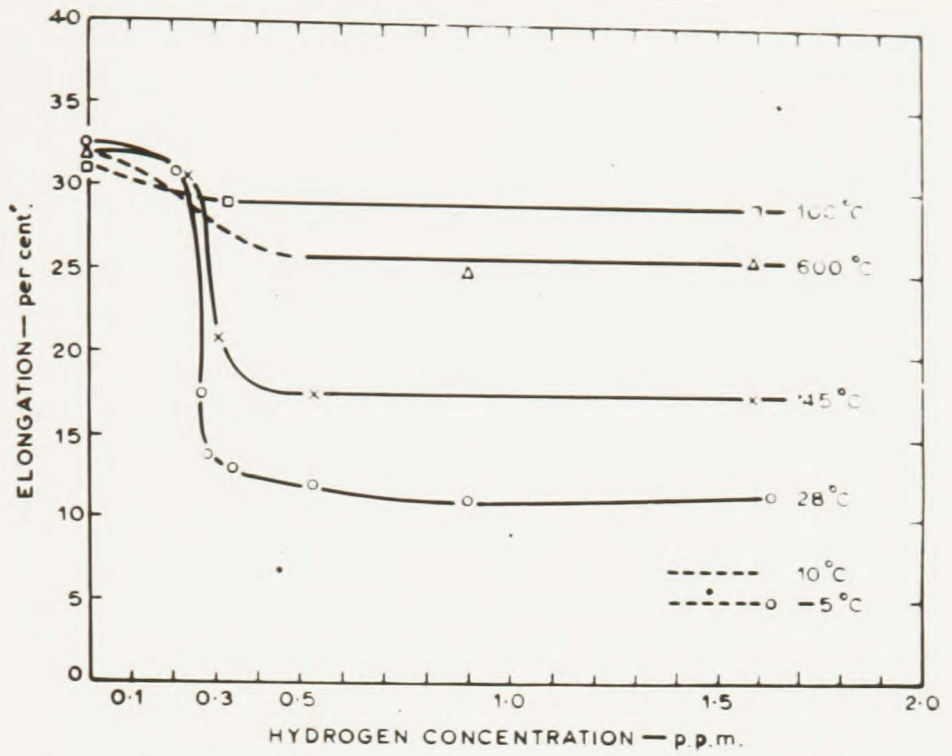
FIGURE 7



. Effect of testing temperature on the ductility of beta-treated and quenched uranium.

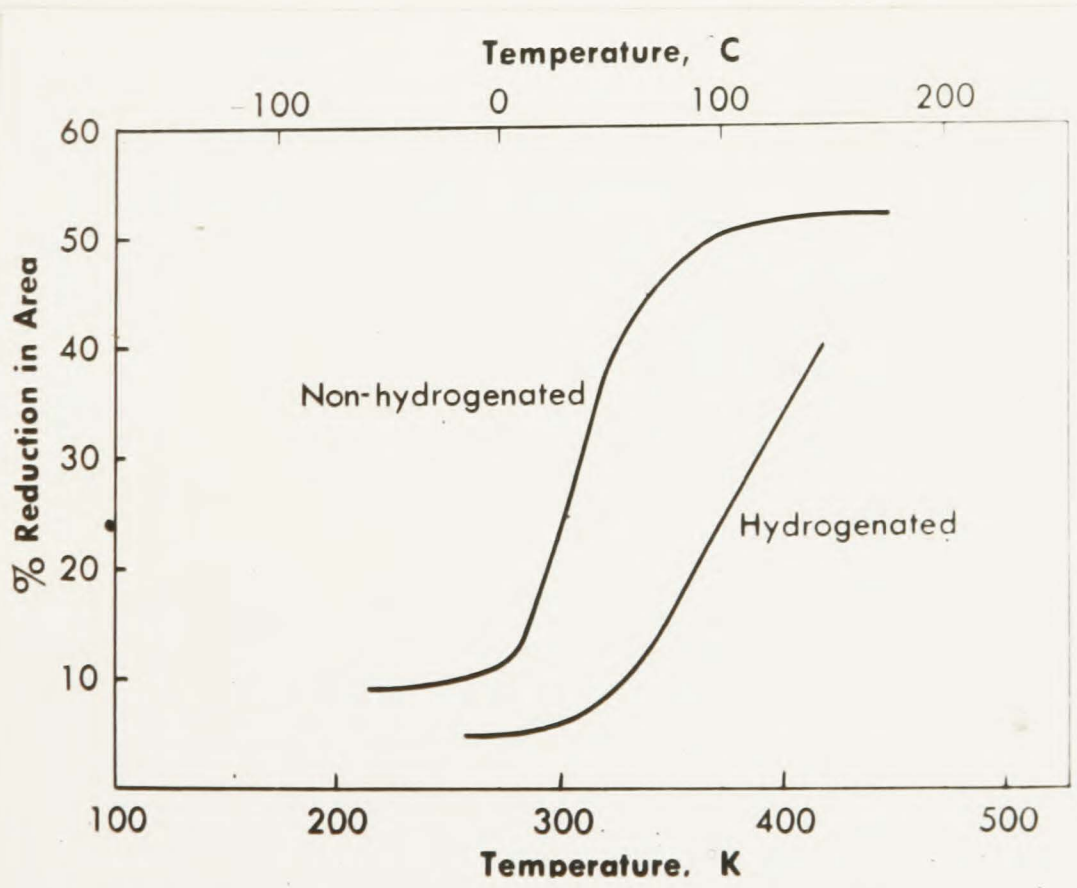
FIGURE 8

Note that the continuities through the beta and gamma transi cannot be correct.



Effect of hydrogen content on elongation at various temperatures of testing. Strain rate, 0·025 in./min.; specimen length, 1 in

FIGURE 9



Effect of hydrogen on the brittle transition of uranium

FIGURE 10

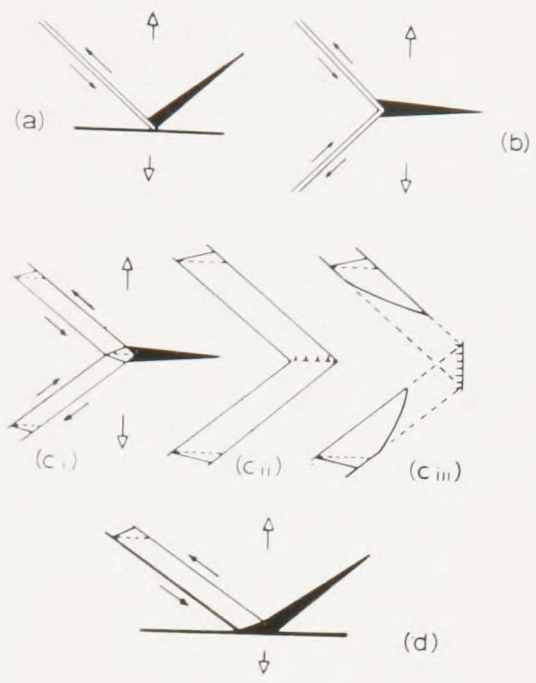
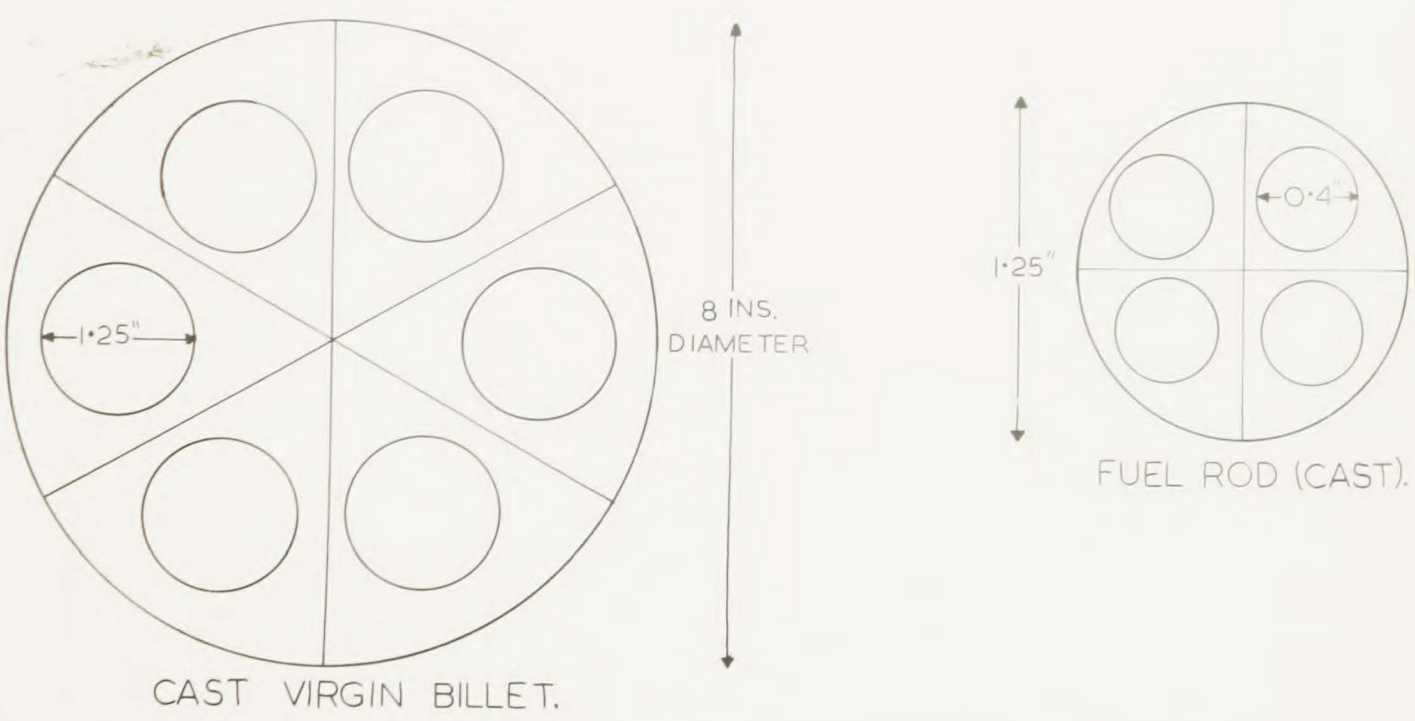


Fig. 1. Mechanisms proposed for the nucleation of cracks in body-centered cubic metals: (*a*) Zener mechanism; (*b*) Cottrell mechanism; (*c*) twin intersection mechanisms for twins meeting at their tips; (*d*) twin intersection for a growing twin meeting a preformed twin.

FIGURE 11



(a) (b)

FIGURE 12

Demonstrates the mode of sectioning of a direct-cast ingot for the production of rolling rods (a), and the mode of sectioning fuel rods for machining tensile specimens (b).

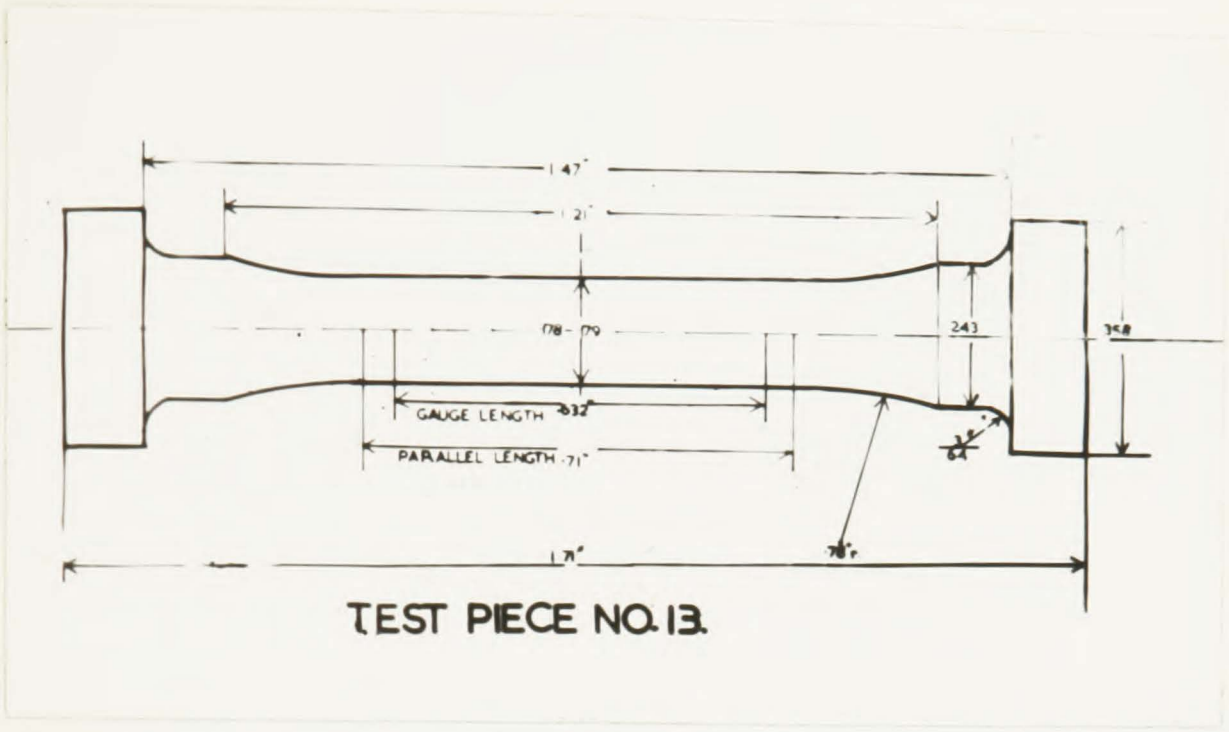


FIGURE 13

Dimensions of Tensile Specimens.

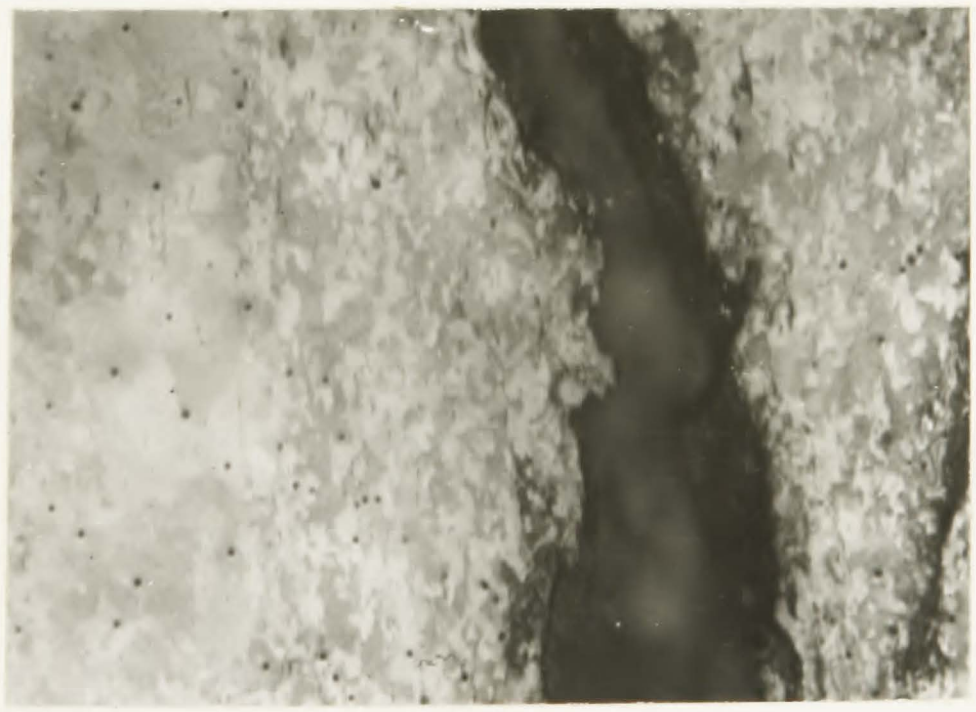


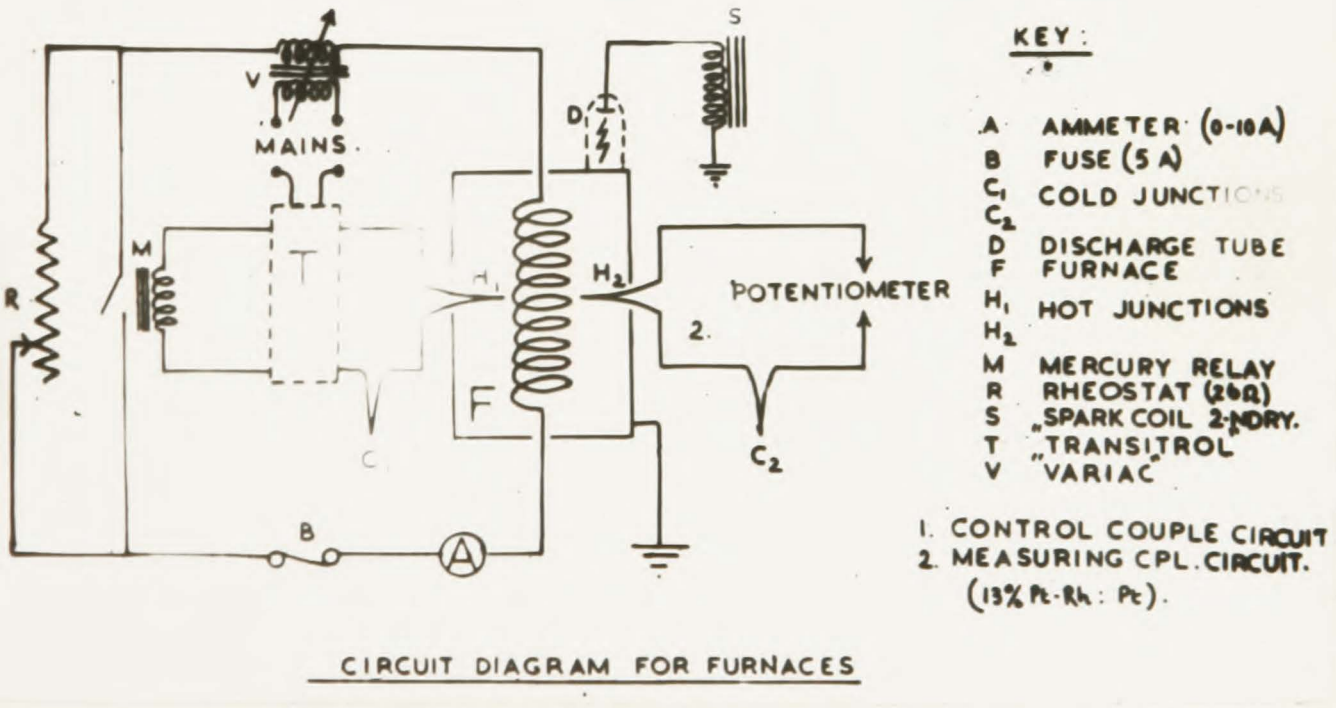
FIGURE 14 x50

Axial pipe and banded grain structure in rolled adjusted fuel rod.



FIGURE 15 x140

Porosity, inclusions and rolling crack in adjusted rolled fuel rod.



CIRCUIT DIAGRAM FOR FURNACES

FIGURE 16

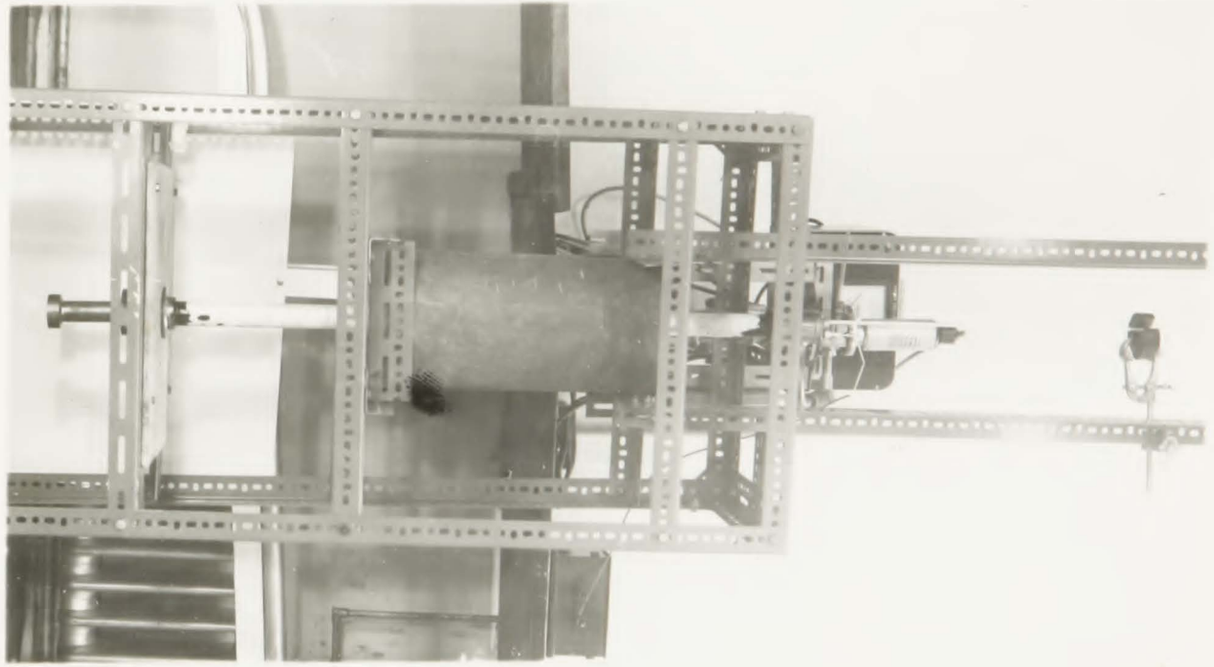


FIGURE 17

Vertical vacuum quenching furnace.

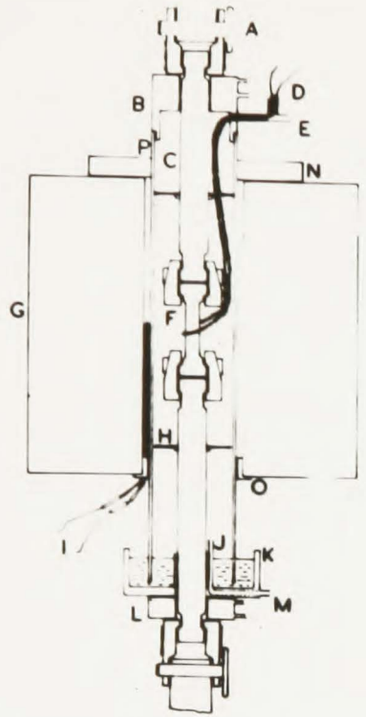


FIGURE 18

Elevated temperature tensometer.

High temperature tensile tester showing modifications.

A - 13/14 Tensile Chucks
B - Water cooled Brass ring also incorporating argon and thermocouple inlets.
C - Wm. Jessop G 18/B Extension Rods.
D - Thermocouple leads for measuring temperature of the test
E - Argon inlet
F - Wm. Jessop G 34, high temperature tensile chucks and uranium No. 13. tensile test piece
G - Heating unit
H - Nickel radiation shield
I - Thermocouple leads to Transitrol controller
J - Copper pipe outlet for argon and leading to waste
K - Brass oil bath
L - Water cooled brass ring
M - Argon outlet
N - Refractory insulator
O - Refractory insulator
P - Nickel/Cobalt/Iron alloy tube threaded to the brass ring B and suspended in the oil in the bath K

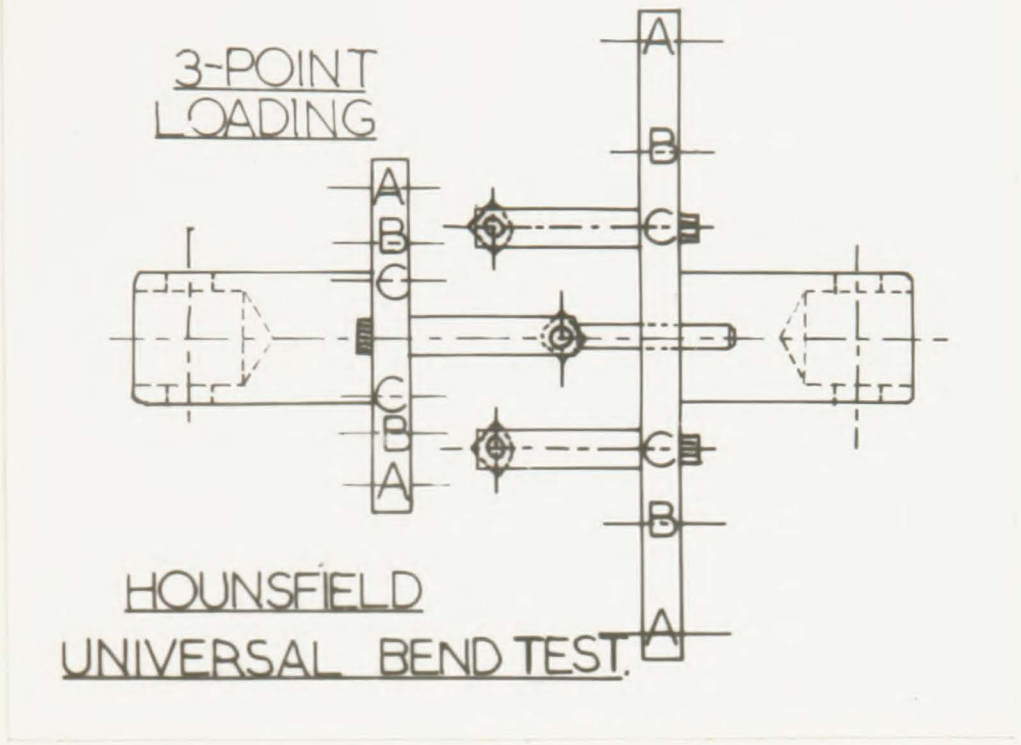


FIGURE 19

Bend-test attachment for Tensometer.

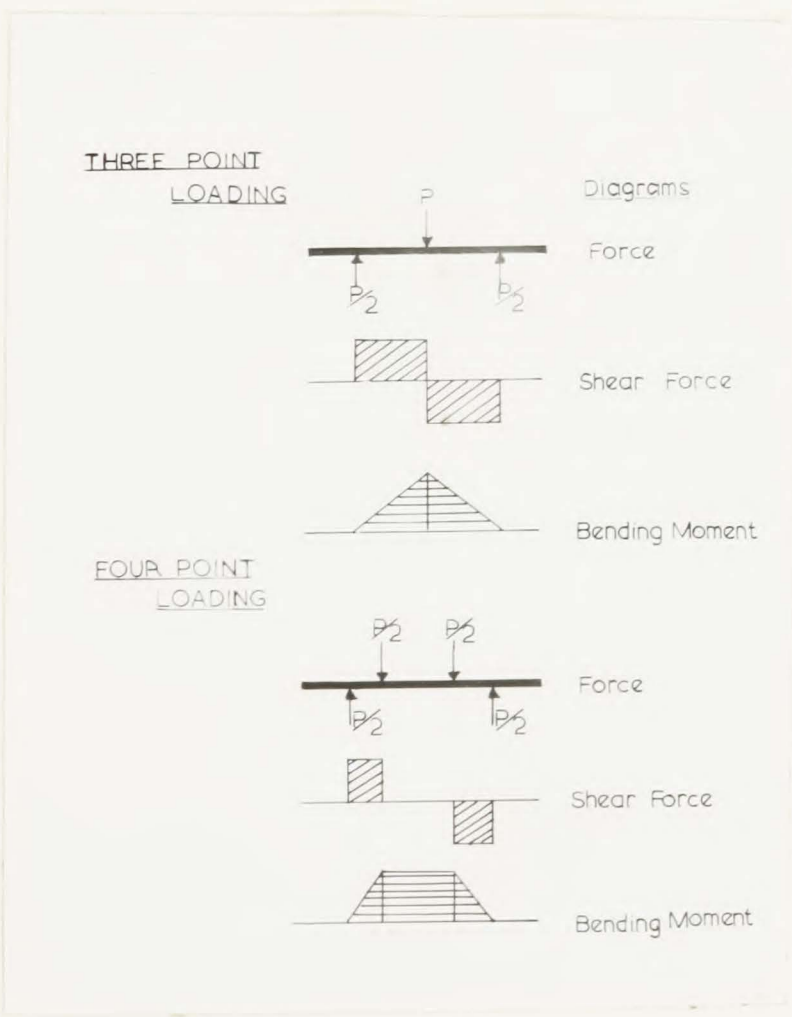


FIGURE 20

Bending Moment and Shear Force diagrams.

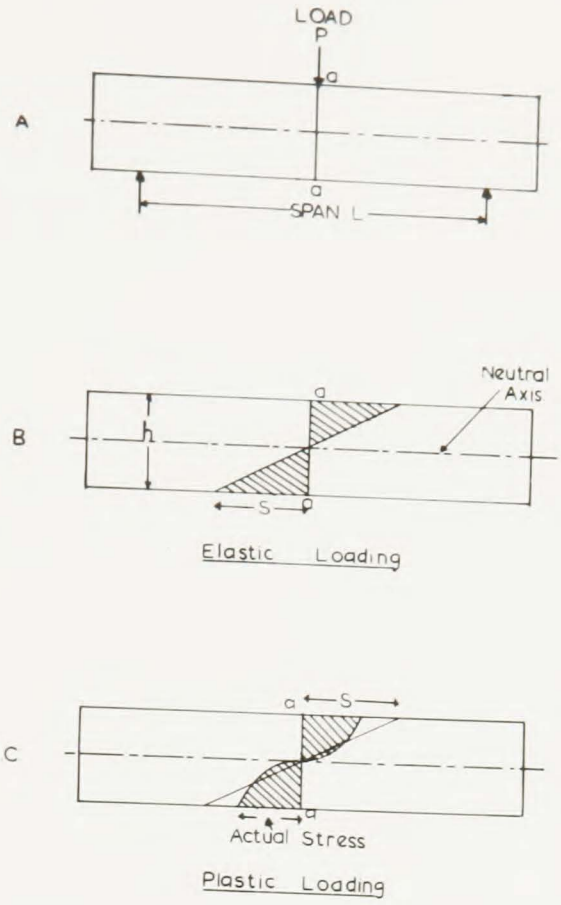
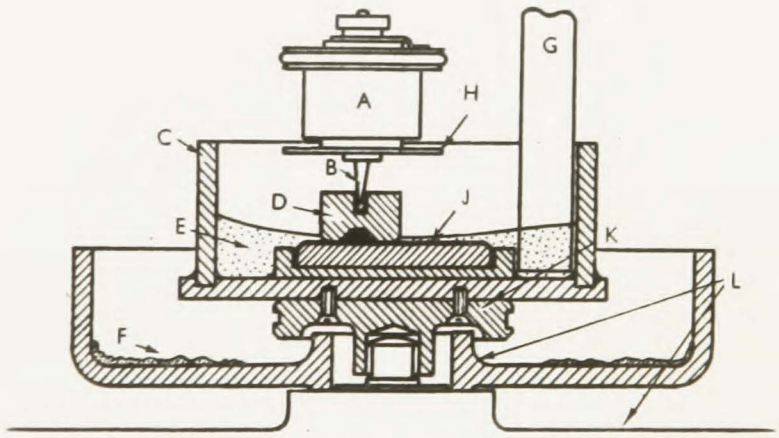


FIGURE 21

Stress distribution in bending.



—Attack-Polishing Bowl Fitted to an Automatic Polishing Machine.

KEY.

A Polishing head.
B Stainless-steel pin.
C Rotating Polythene bowl; welded construction.
D Mounted specimen.
E Acid solution and abrasive.
F Sodium carbonate to prevent acid attack in case of spills.
G Static Polythene anti-swirl plate.
H Polythene splash disc.
J Terylene-covered Polythene disc.
K Standard 3½-in.-dia. brass lapping wheel.
L C.T.S. automatic polishing machine.

FIGURE 22



FIGURE 23 x 270

General distribution of cuboid inclusions

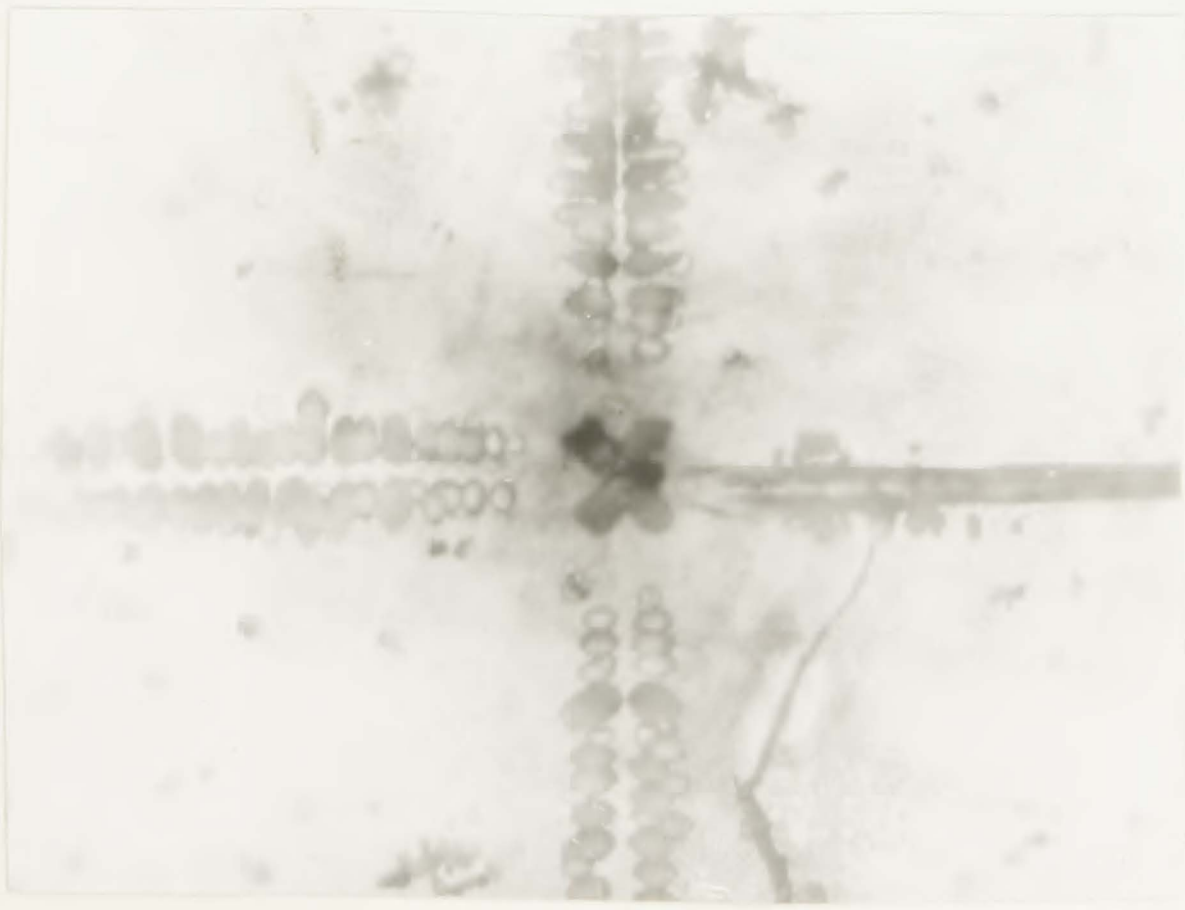


FIGURE 24 x1200

Dendritic carbide.

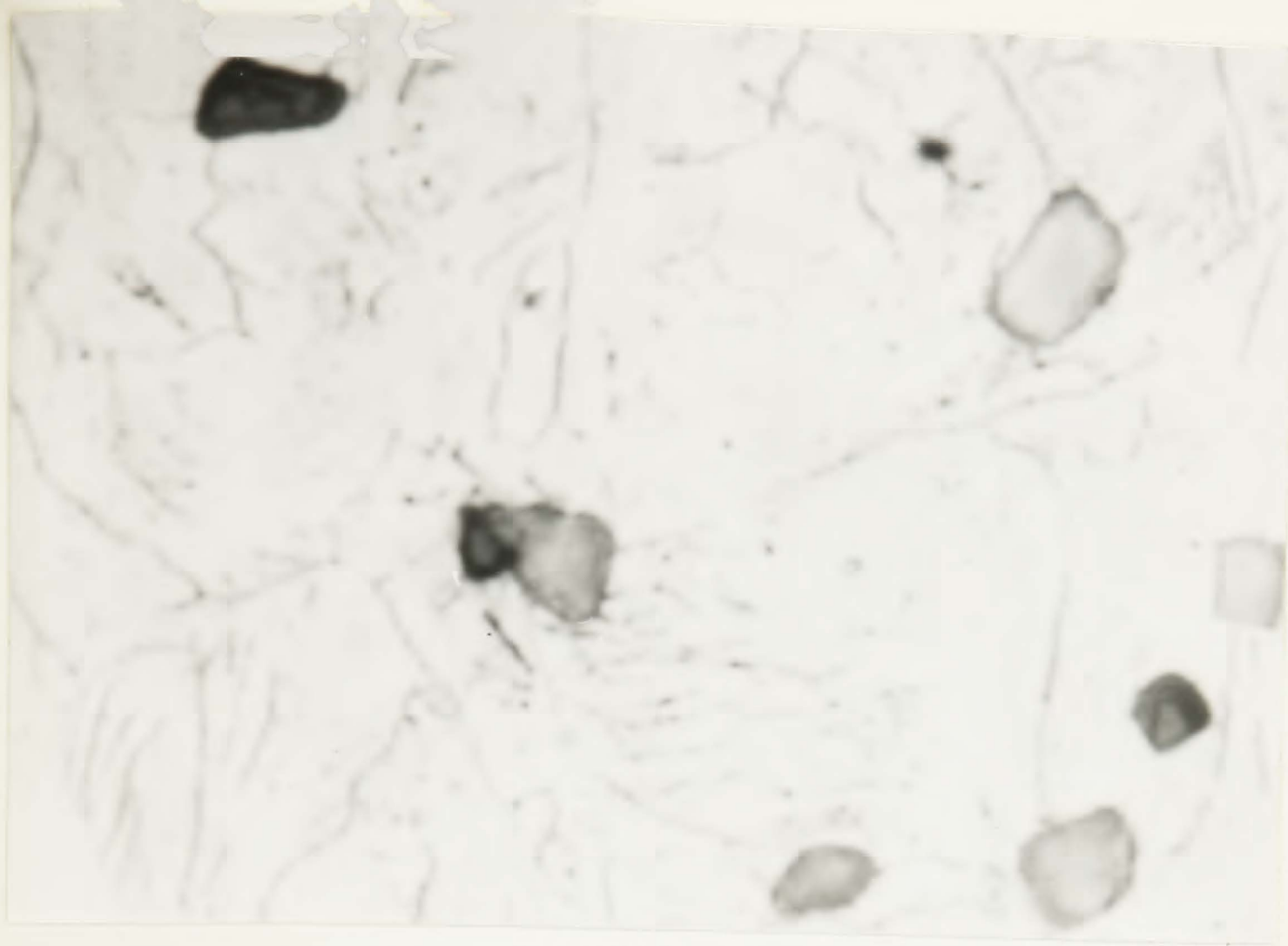


FIGURE 25 x2100

Fine network distribution of intermetallic compounds with cuboids.



FIGURE 26 x435

Examples of twins formed during cooling due to the anisotropic thermal contraction stresses.



FIGURE 27 x95

Jagged grain structure resulting from air cooling virgin material from the beta.



FIGURE 28 x72

Jagged grain structure resulting from oil-quenching adjusted material from the beta.



FIGURE 29 x220

Doubly-adjusted material fast beta-quenched. Coarse grained metastable beta partically transformed to alpha.



FIGURE 30 x120

Doubly-adjusted material fast beta-quenched. Transformed to alpha at room temperature with widespread cracking.

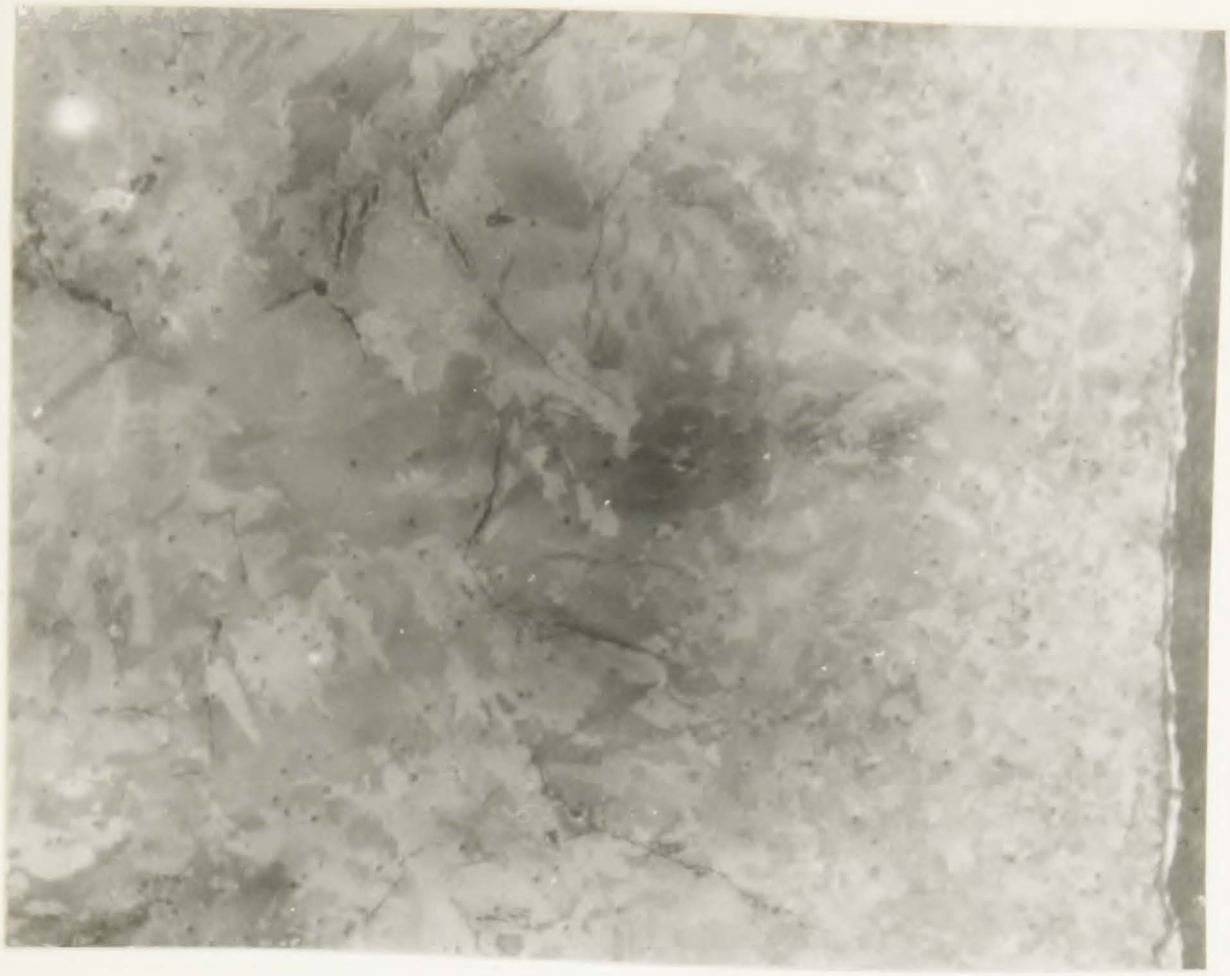


FIGURE 31 x75

Doubly-adjusted material fast gamma-quenched. The structure is interpreted as a diffusional product of the $\gamma \rightarrow \alpha$ transformation at the surface and a martensitic product of the $\gamma \rightarrow \beta \rightarrow \alpha$ transformation in the centre (as Fig.30).

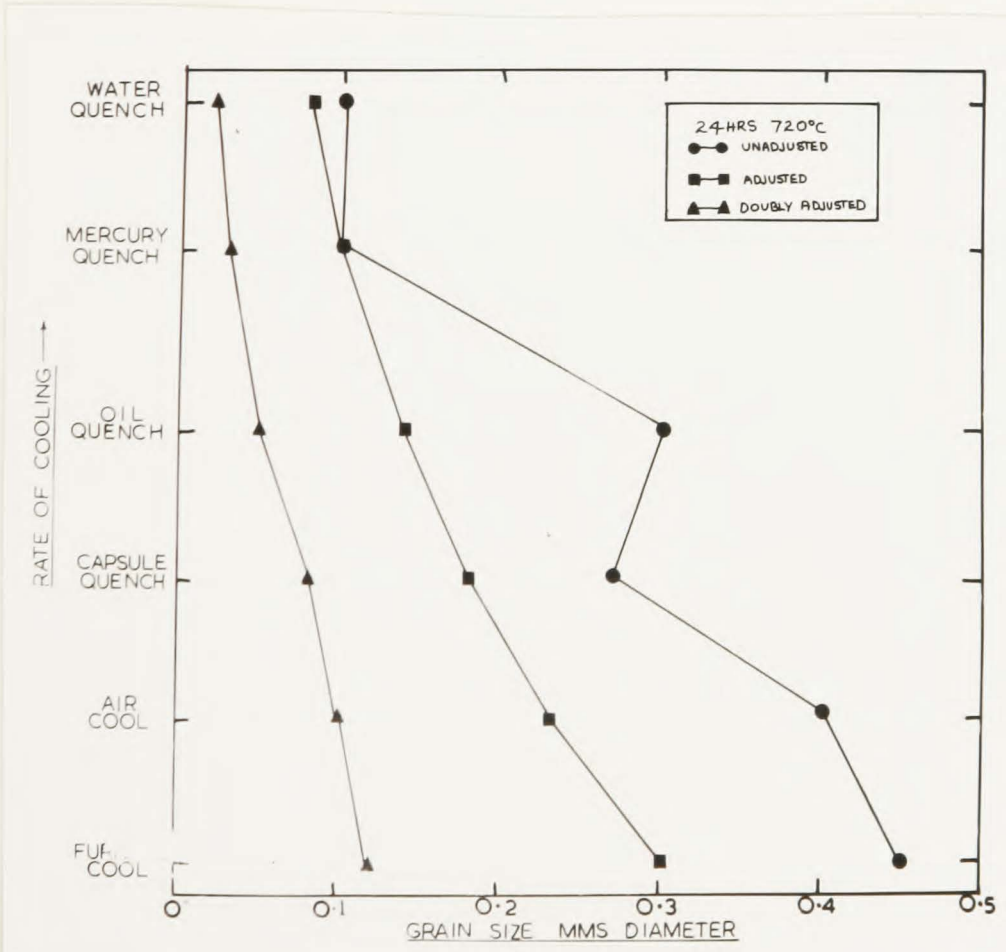


FIGURE 32

The effect of cooling rate on the transformed grain size of alpha.



FIGURE 33 x390

Unadjusted material fast beta-quenched and recrystallized at 650° C.

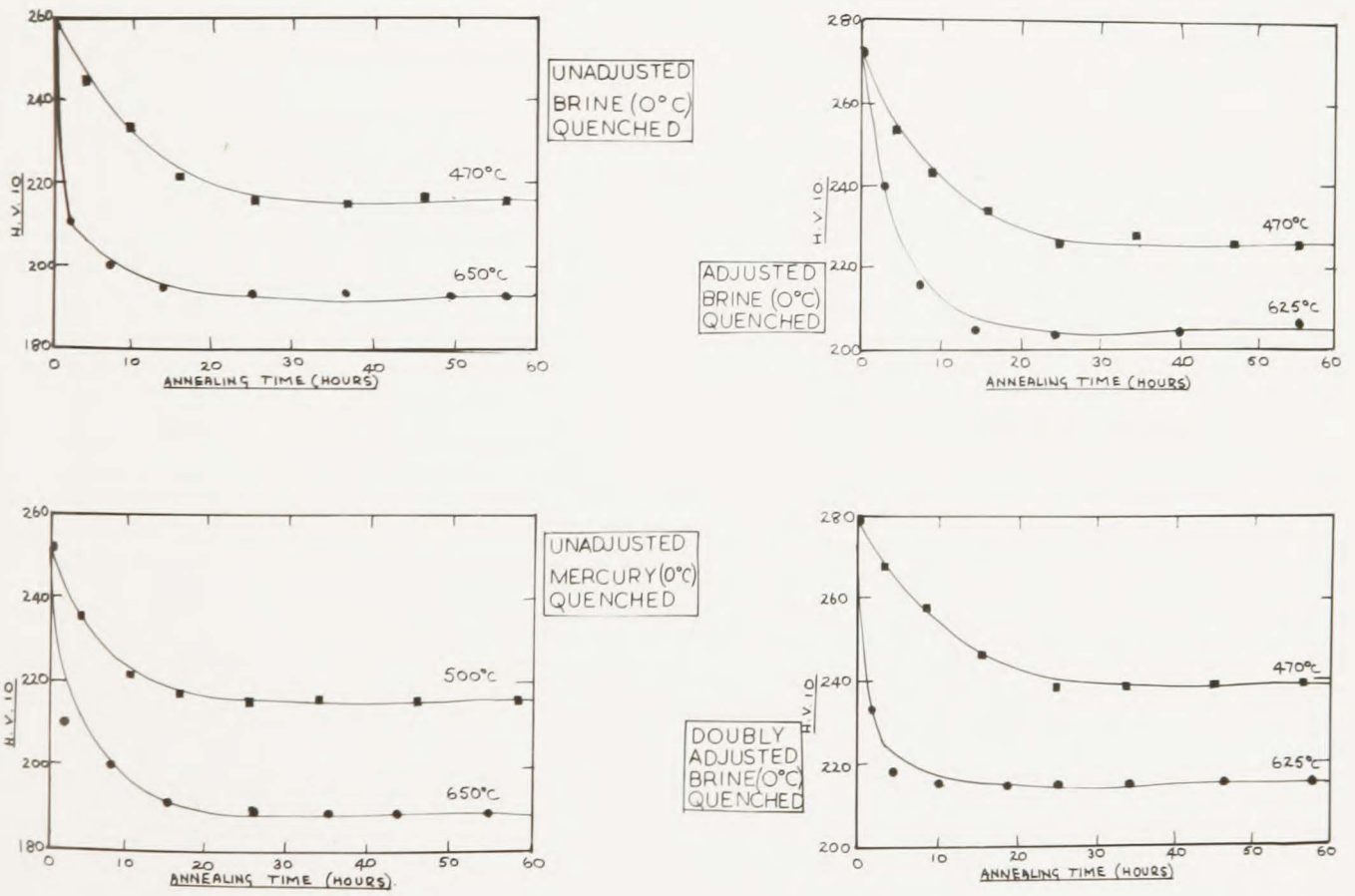


FIGURE 34

V.P.N. softening curves upon annealing after fast beta-quenching the three cast grades.

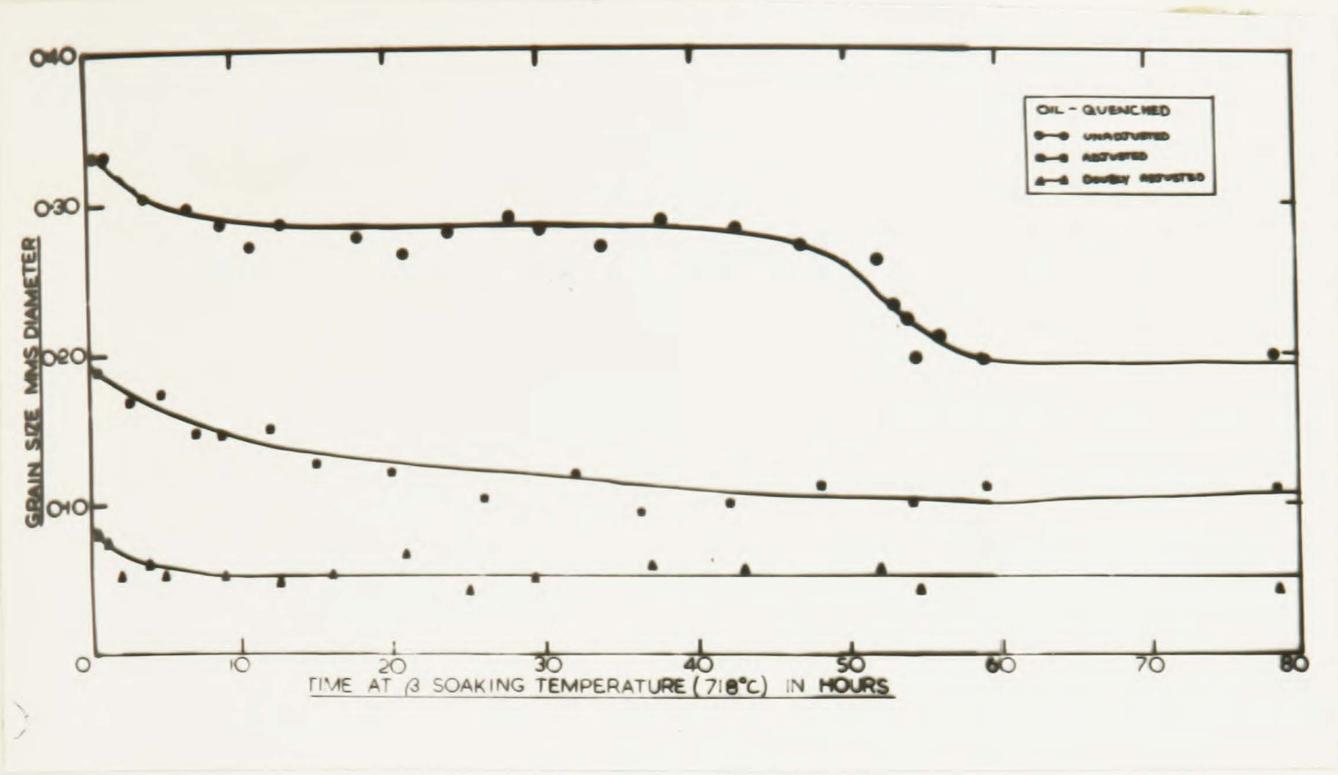


FIGURE 35

Alpha transformed grain size as a function of beta soaking time at 718°C.



x180

FIGURE 36

Twins formed during thermal cycling between -196°C and 75°C (contrast resulting from surface tilt).

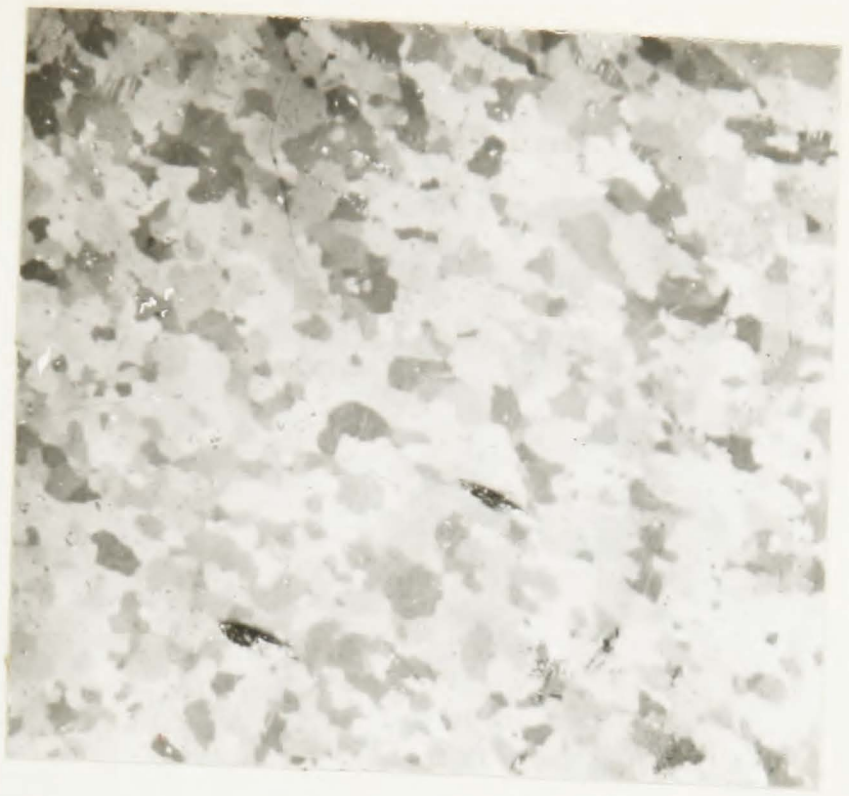


FIGURE 37 x120

Grain structure of adjusted rolled material.



FIGURE 38 x190

Grain structure of virgin material prior to final treatments: grain size 0.03mm.



FIGURE 39 x180

Virgin material, 8% reduction and 24hrs 613°C: grain size 0.14mm.



FIGURE 40 x165

Virgin material, 11% reduction and 24hrs 545°C: grain size 0.04mm.

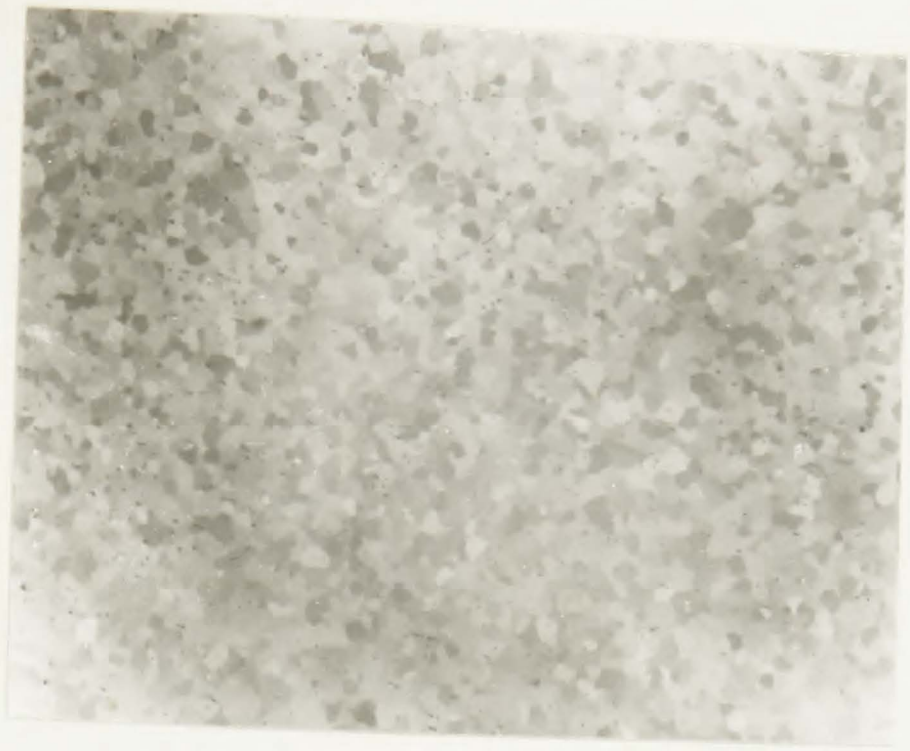


FIGURE 41 x180

Virgin material, 28% reduction and 24hrs 496°C: grain size 0.01mm.

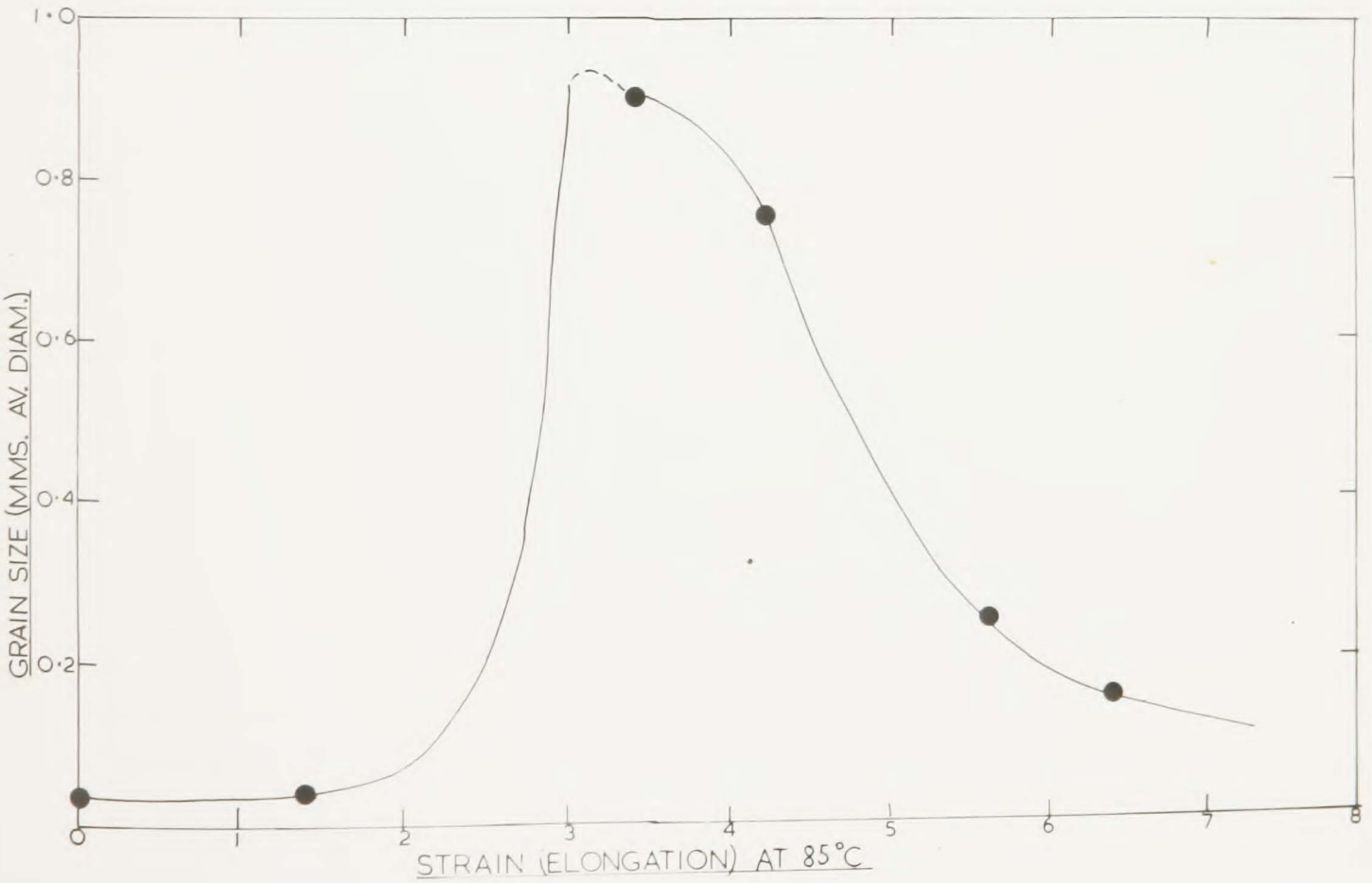


FIGURE 42

Tensile strain at 85°C as a function of Grain Size after annealing for 3hrs at 640°C (virgin).



FIGURE 43 x110

Heterogeneous grain structure resulting in virgin material after 3% tensile strain plus 3hrs at 640°C.



FIGURE 44 x720

Virgin material rolled 28% and annealed for 24hrs at 420°C showing banded structure (rolling direction vertical).



FIGURE 45 x230

Unadjusted material, 15% tensile deformation at room temperature.



FIGURE 46 x410

Unadjusted material deformed at -10°C.

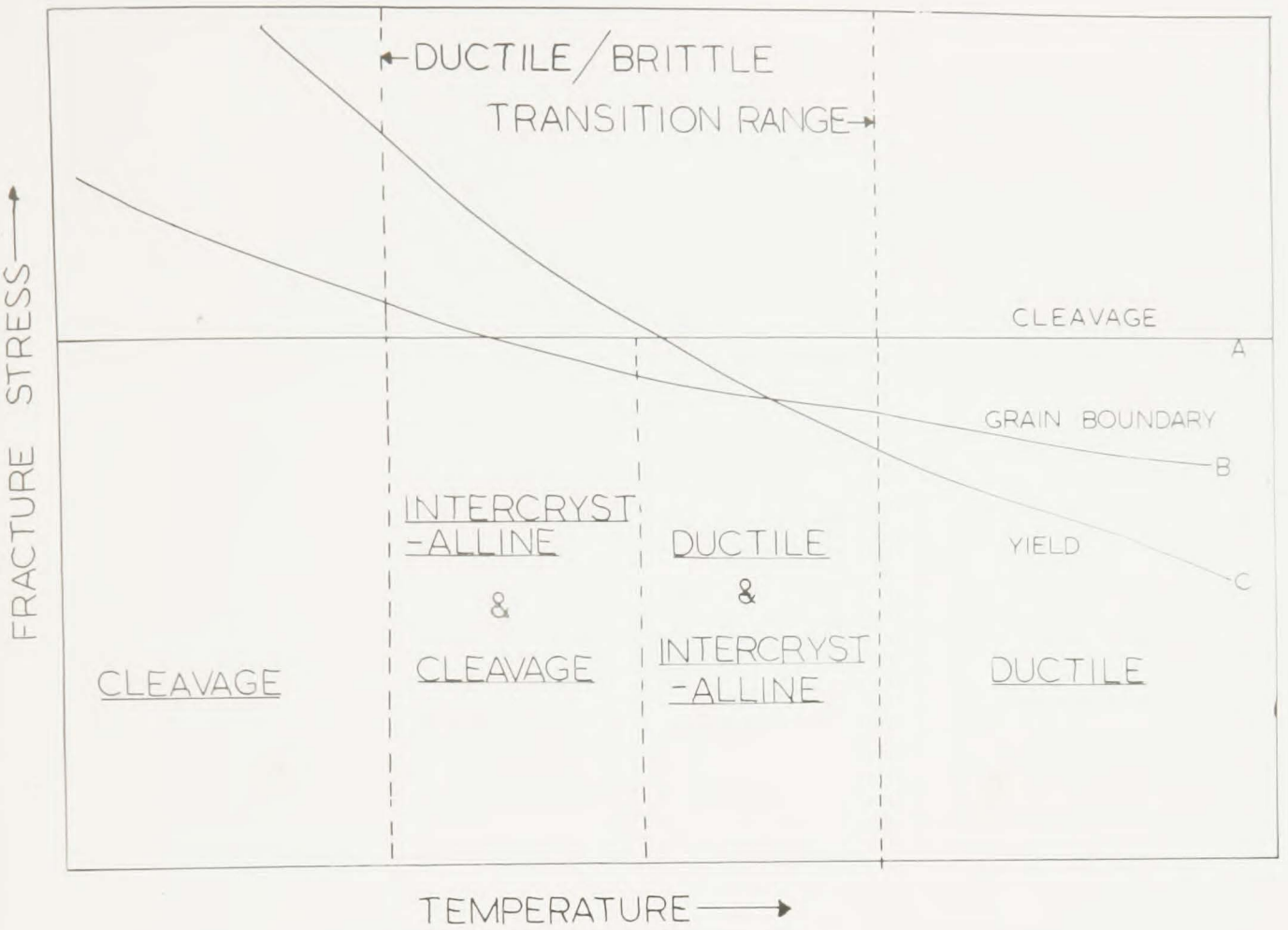


FIGURE 47

Schematic Classical Fracture Stress Diagram.



FIGURE 48 x2200

Virgin material, demonstrating cuboid/matrix separation.



FIGURE 49 x1950

Virgin material interrupted at 25% elongation (85°C) showing both cuboid cleavage and void formation.



FIGURE 50 x1760

Virgin material interrupted at 32% elongation (410°C) showing void formation at inclusion/matrix interface.



FIGURE 51 x890

Virgin material tested to 40% elongation at room temperature showing elongated voids



FIGURE 52 x430

Tested at 50°C — many elongated voids



FIGURE 53 x460

Voids coalescing in necked region



FIGURE 54 x325

Macroscopic fissure at centre of neck



FIGURE 55 x150

Ductile Fracture Edge



FIGURE 56 x2600

Replica of the fracture surface of a specimen which exhibited ductile failure showing equi-axed dimples

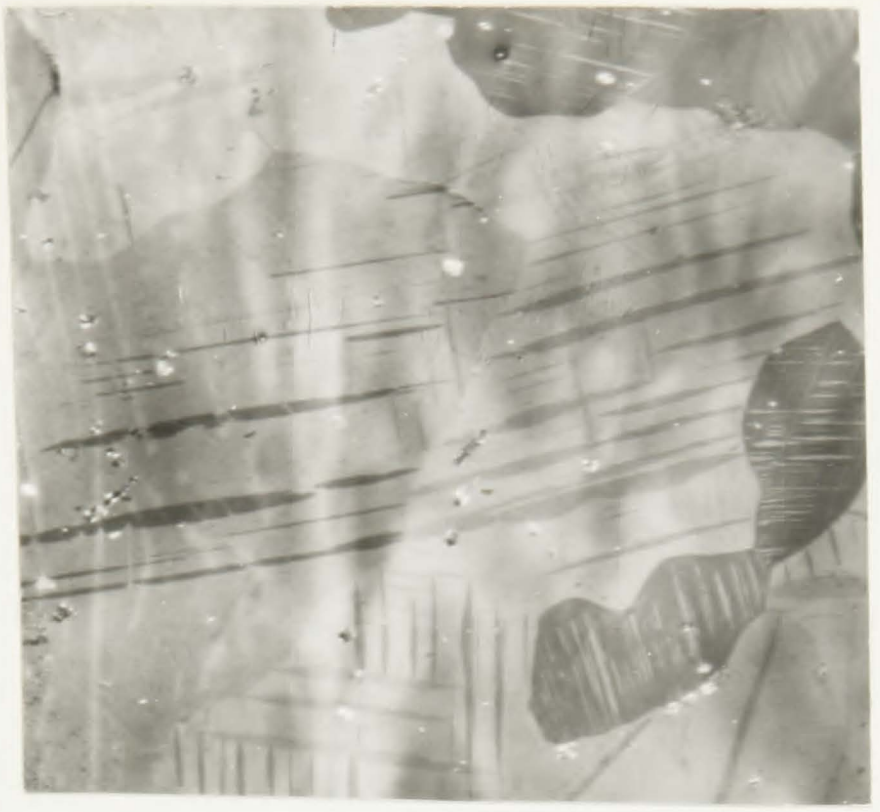


FIGURE 57 x435

Intercrystalline microcracks (X)

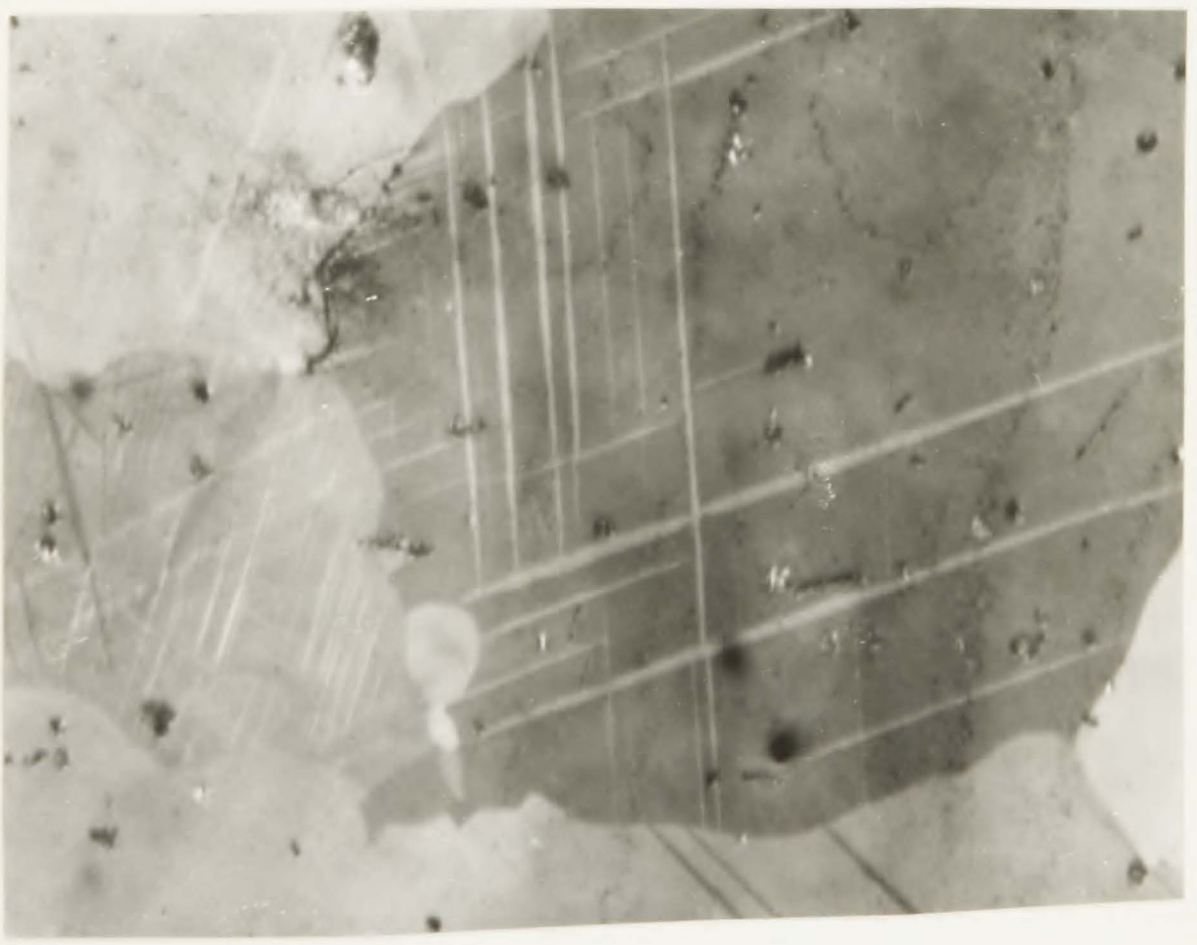


FIGURE 58 x125

Intercrystalline cracking (X)



FIGURE 59 x220

Intercrystalline cracks arrested at grain boundary junctions and (?) twins (X).

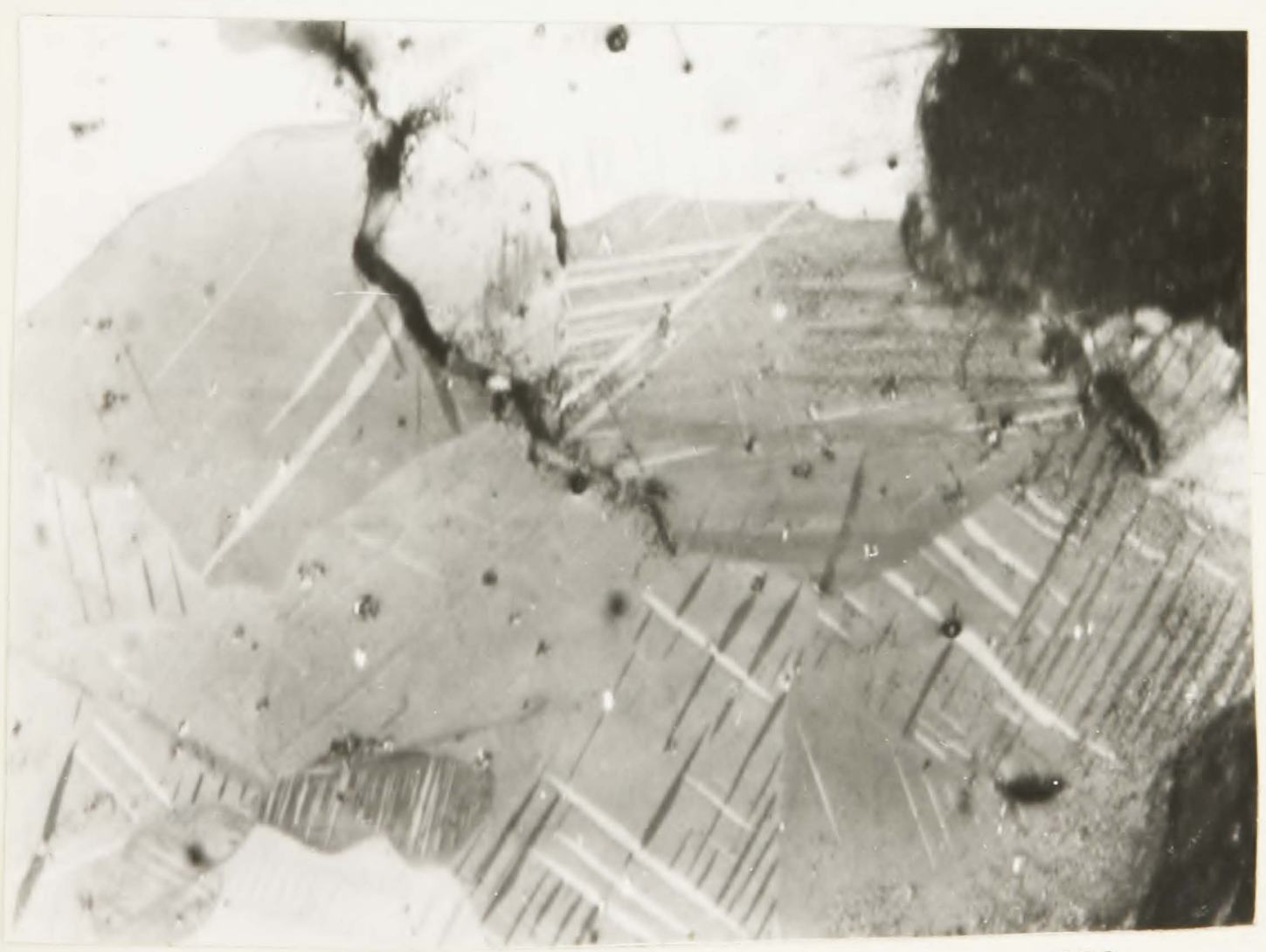


FIGURE 60 x360

Intercrystalline cracking.



FIGURE 61 x230

Mixed fracture edge with vestiges of intercrystalline, cleavage and ductile failure.



FIGURE 62 x1390

Intercrystalline fissure after testing at -95°C.



FIGURE 63 x500

Intergranular cracking after thermal cycling (X)



FIGURE 64 x720

Cleavage steps on Fracture Surface



FIGURE 65 x670

Cleavage Fracture Surface



FIGURE 66

Replica of Cleavage Fracture Surface.



FIGURE 67 x95

Characteristic crystallographic cracking



FIGURE 68 x310

Crystallographic microcracking

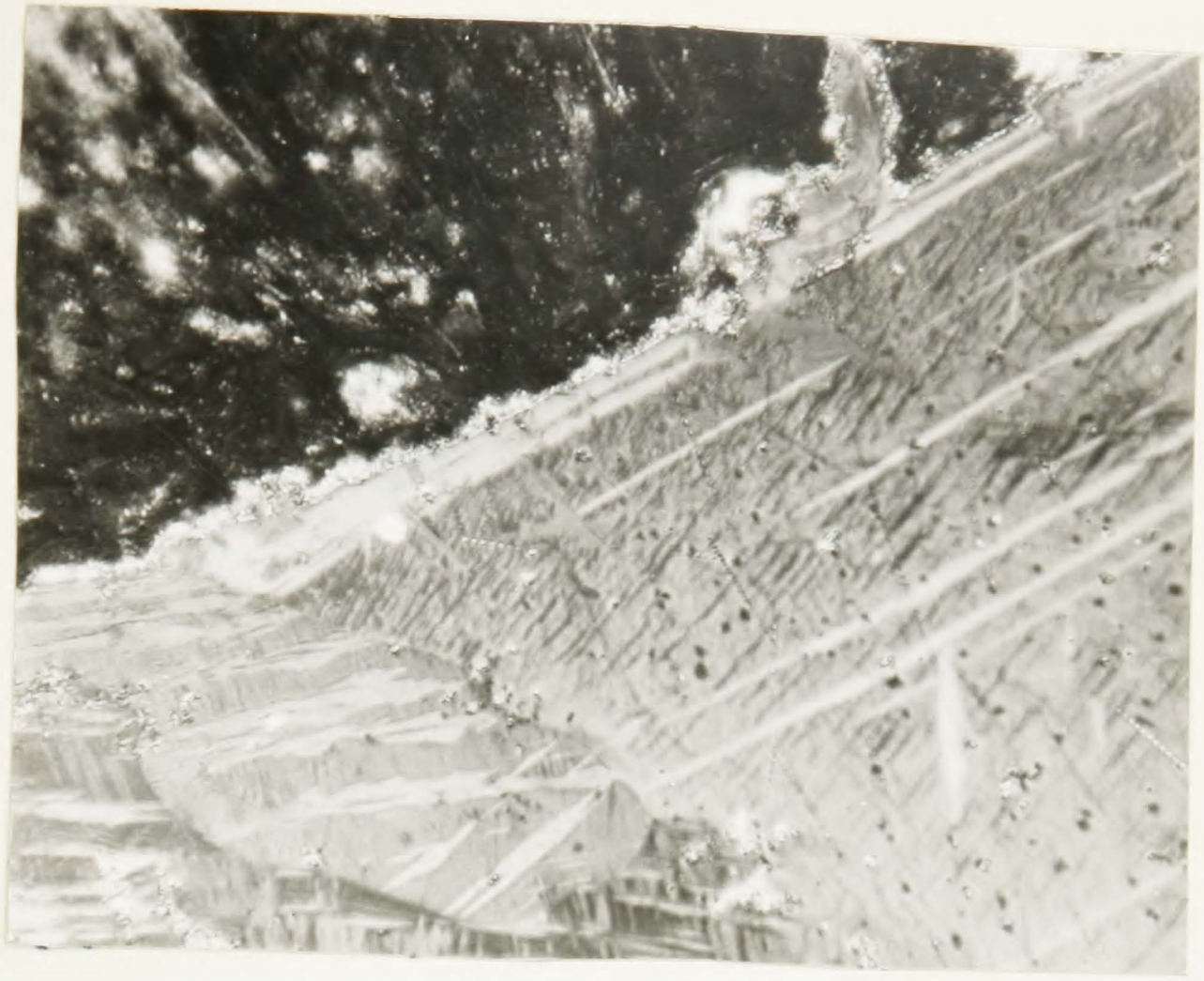


FIGURE 69 x840

Twin/matrix interface parting



FIGURE 70 x1260

Cleavage step formation



FIGURE 71 x790

Same area as Fig 69 ground back 0.1mm



FIGURE 72 x580

Doubly-adjusted material with irregular grain profile tested at 85°C. Crack arrested at grain boundaries.



FIGURE 73 x290

Twin/matrix failure with microcracks (X)

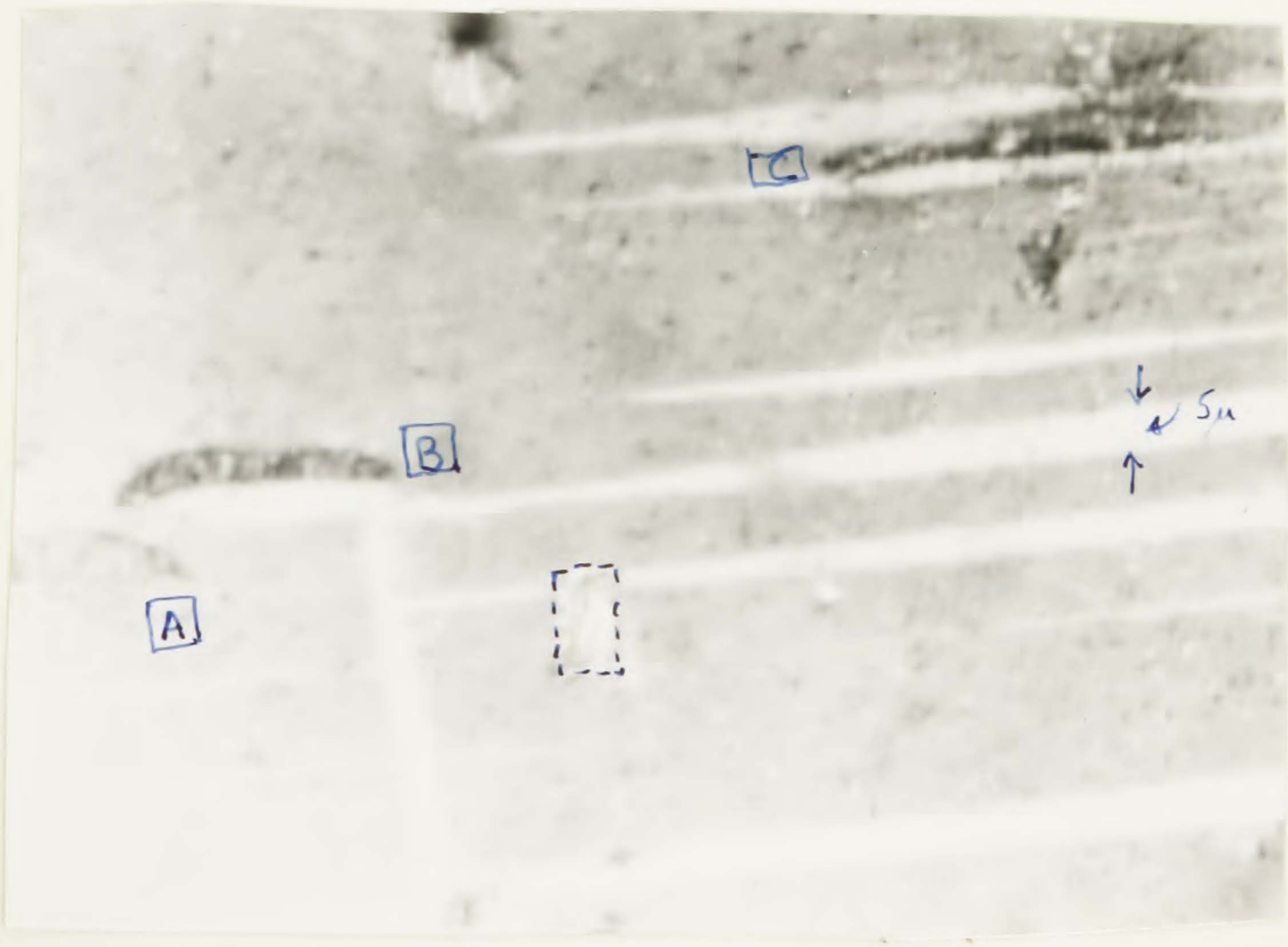


FIGURE 74 x1320

Parting microcracks (X)

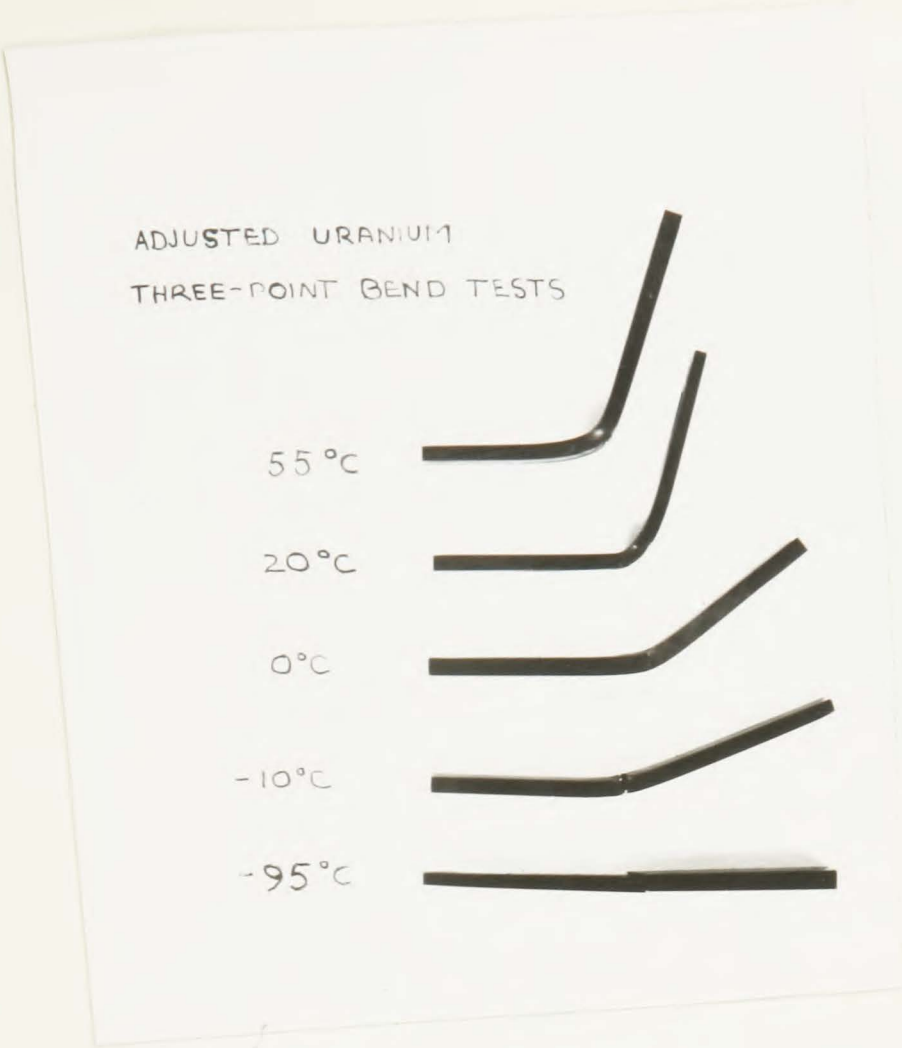


FIGURE 75

Failed bend-test beams



x770

FIGURE 76

Cuboid cleavage and void-formation in bending



FIGURE 77 x350

Cleavage steps produced in bending



FIGURE 78 x620

Cracking of inclusions in compression



FIGURE 79 x1470

Cuboid cracking in compression



FIGURE 80 x130



FIGURE 81 x490

Major compression crack at 45° to stress direction.



FIGURE 82 x1250

Protective Gold-Palladium coating after beta-testing



FIGURE 83 x175

Shape of cracks after beta-testing



FIGURE 84 x450

Metastable beta fracture surface in doubly-adjusted material fast quenched and immediately tested — cleavage.



FIGURE 85

x150

Cracks in partially transformed beta.

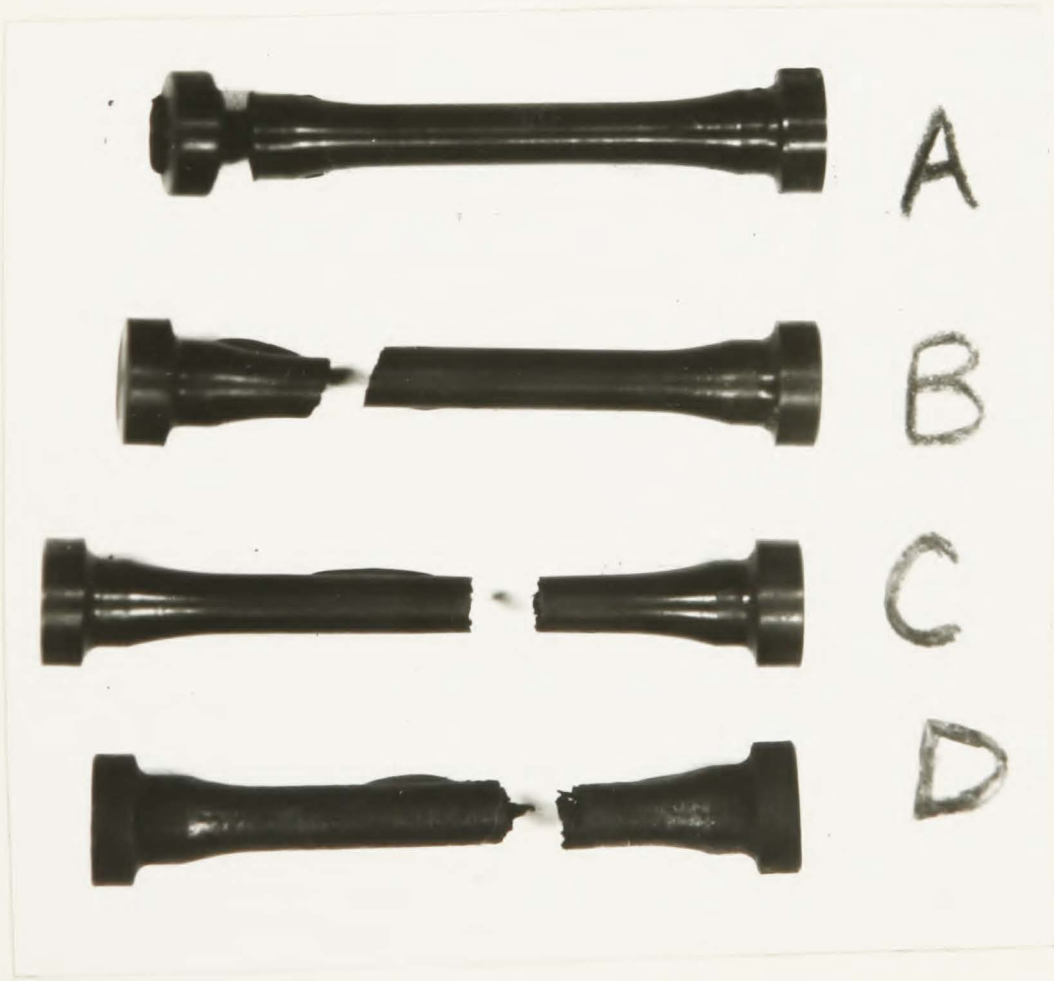


FIGURE 86

'A' - tested at -196°C and fractured in shoulder; 'B' - unadjusted, tested at 20°C; 'C' - virgin, tested at 20°C; 'D' - virgin, fractured at 720°C (beta)

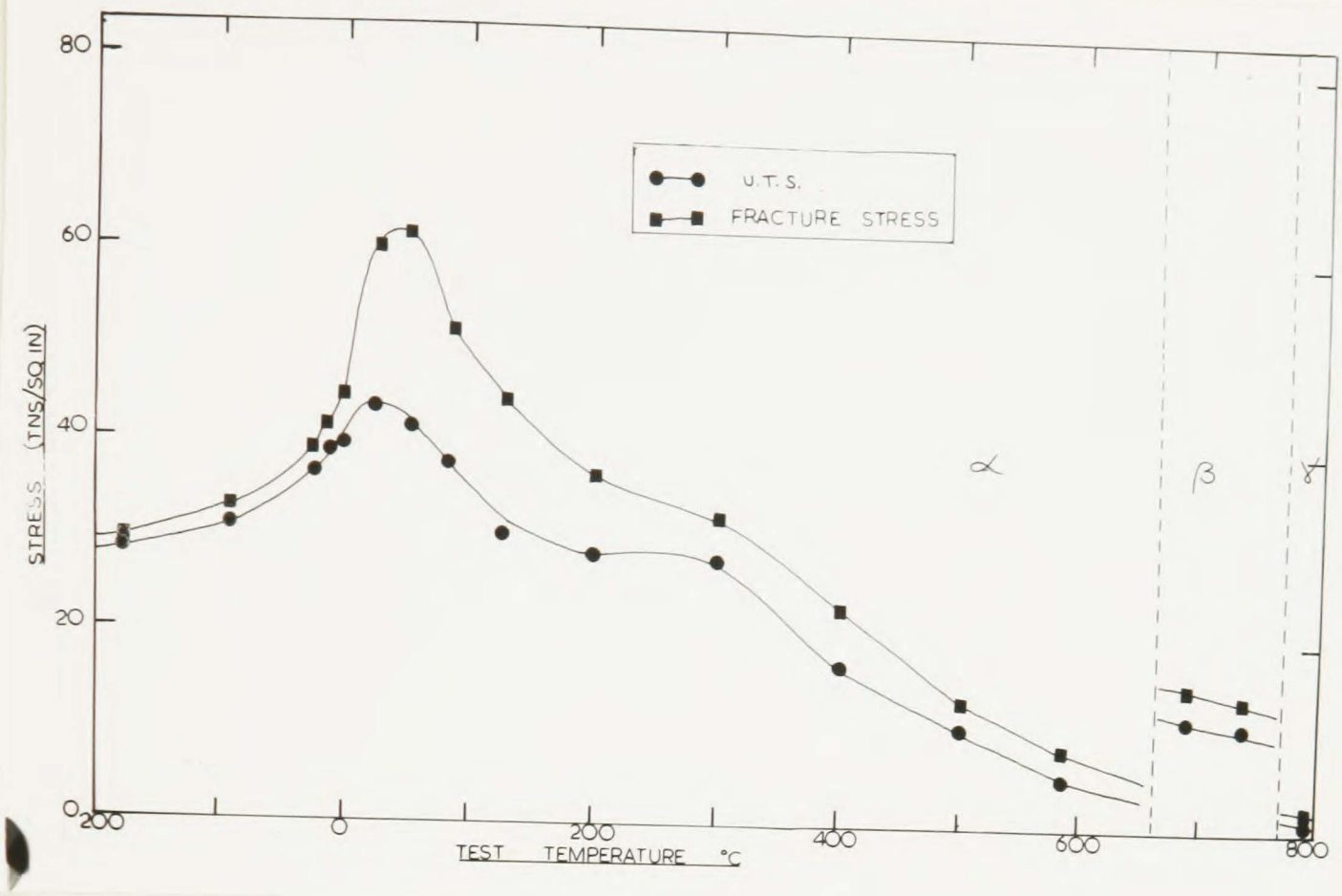


FIGURE 87

Ductility as a function of test temperature for unadjusted material

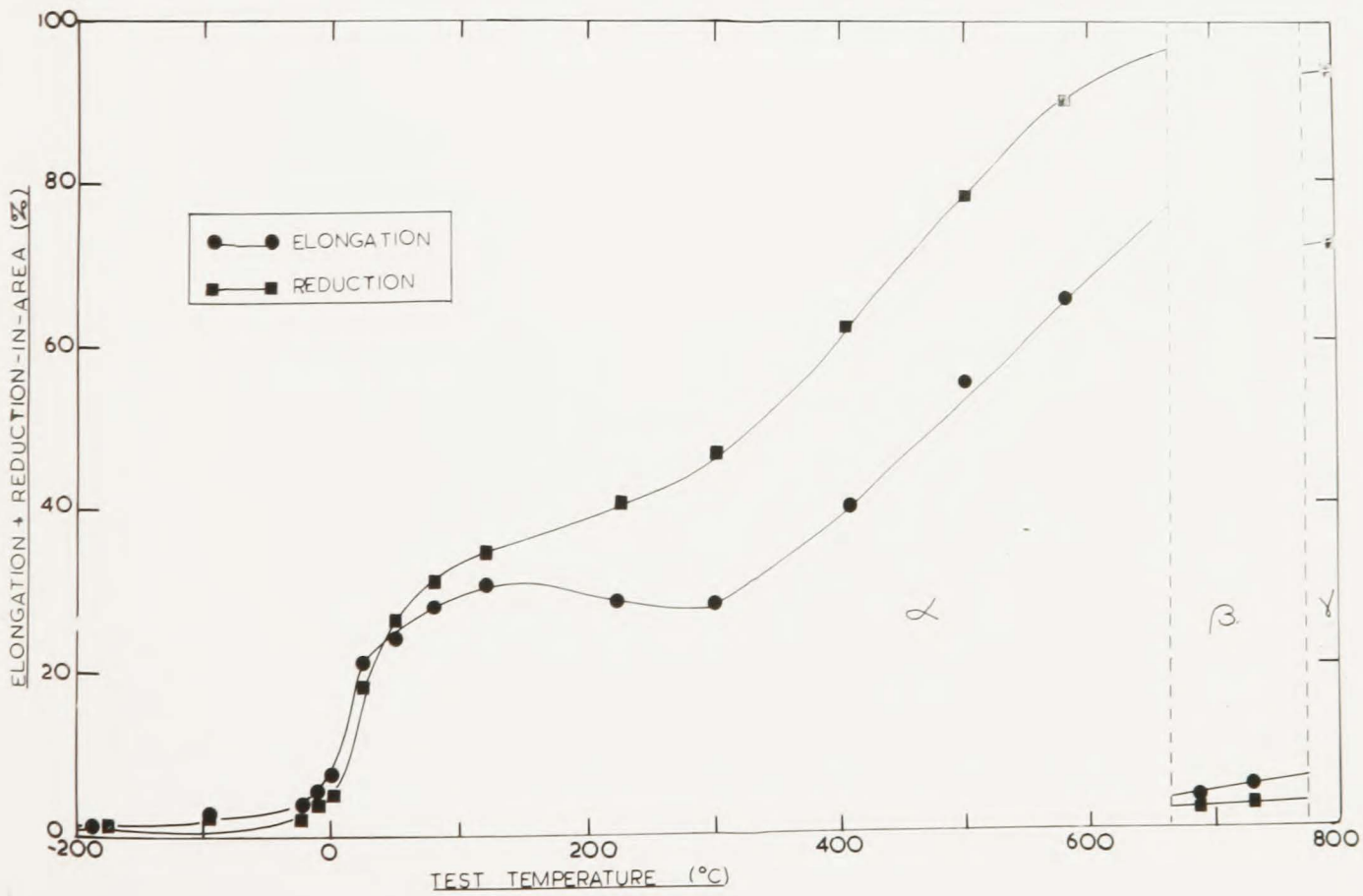


FIGURE 88

Strength as a function of test temperature for unadjusted material

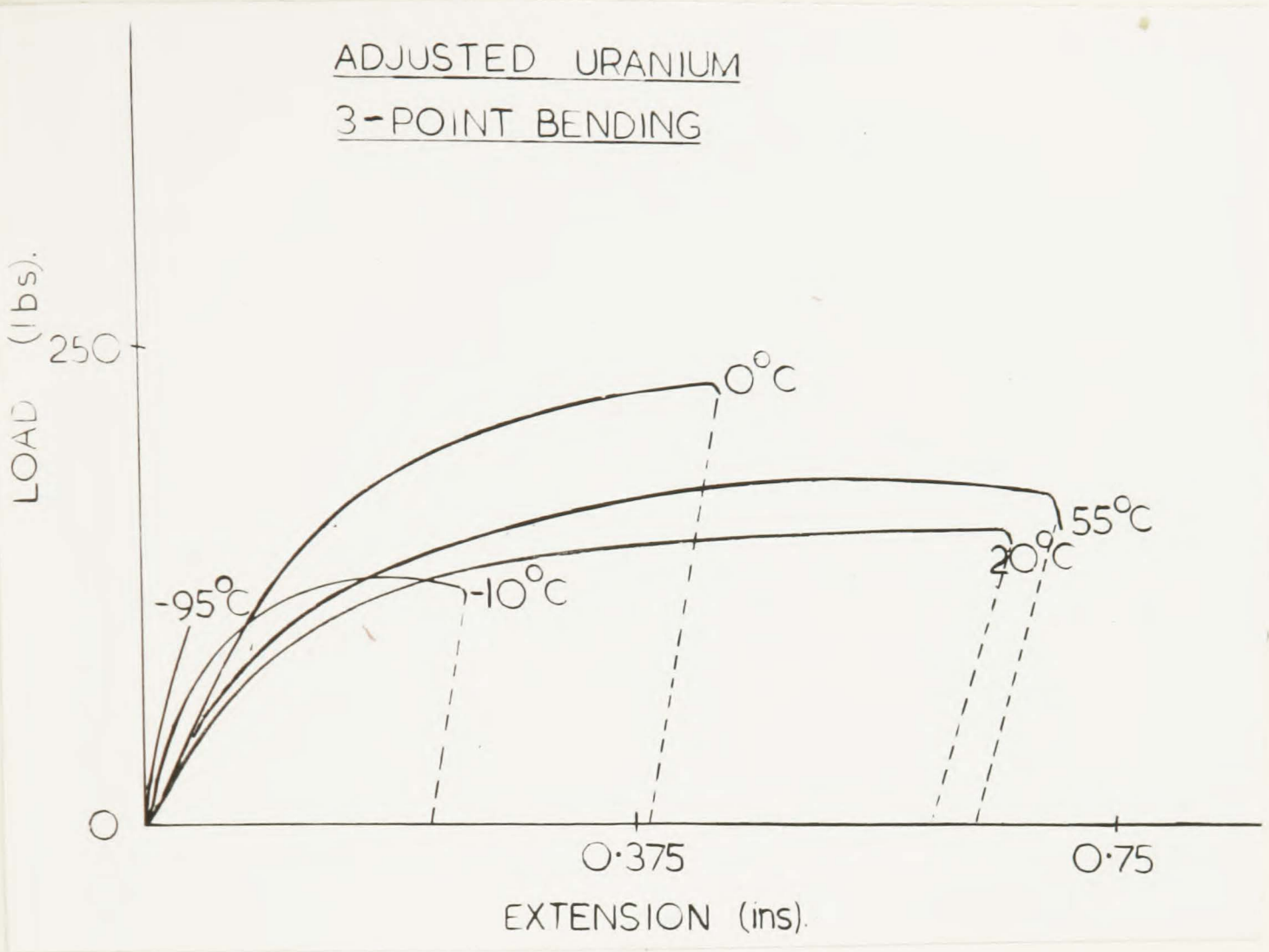


FIGURE 89

Load/extension curves in bending (adjusted material)

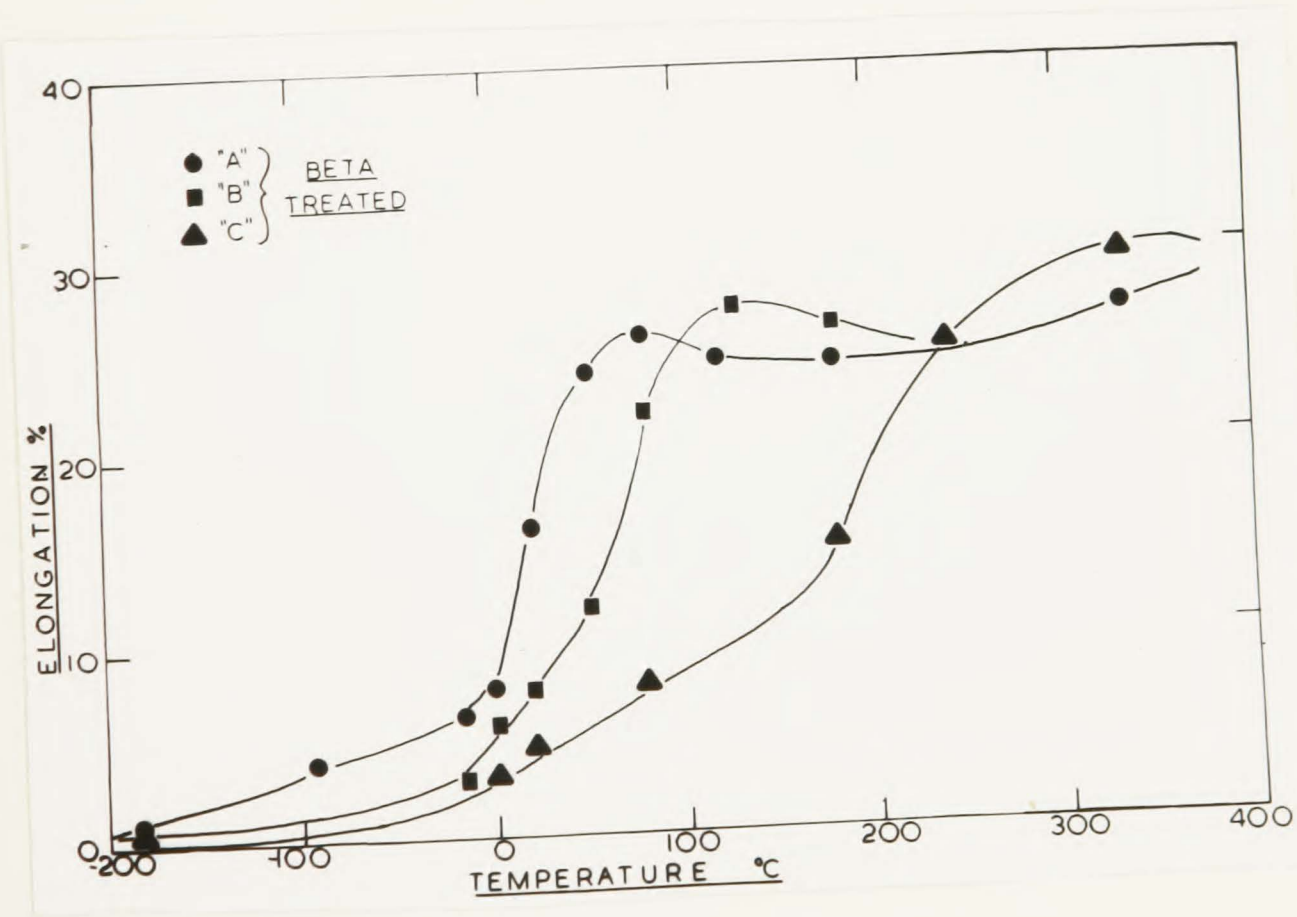


FIGURE 90

Elongation as a function of test temperature for the three cast materials "A" - unadjusted; "B" - adjusted; "C" - doubly-adjusted; after beta-treatment.

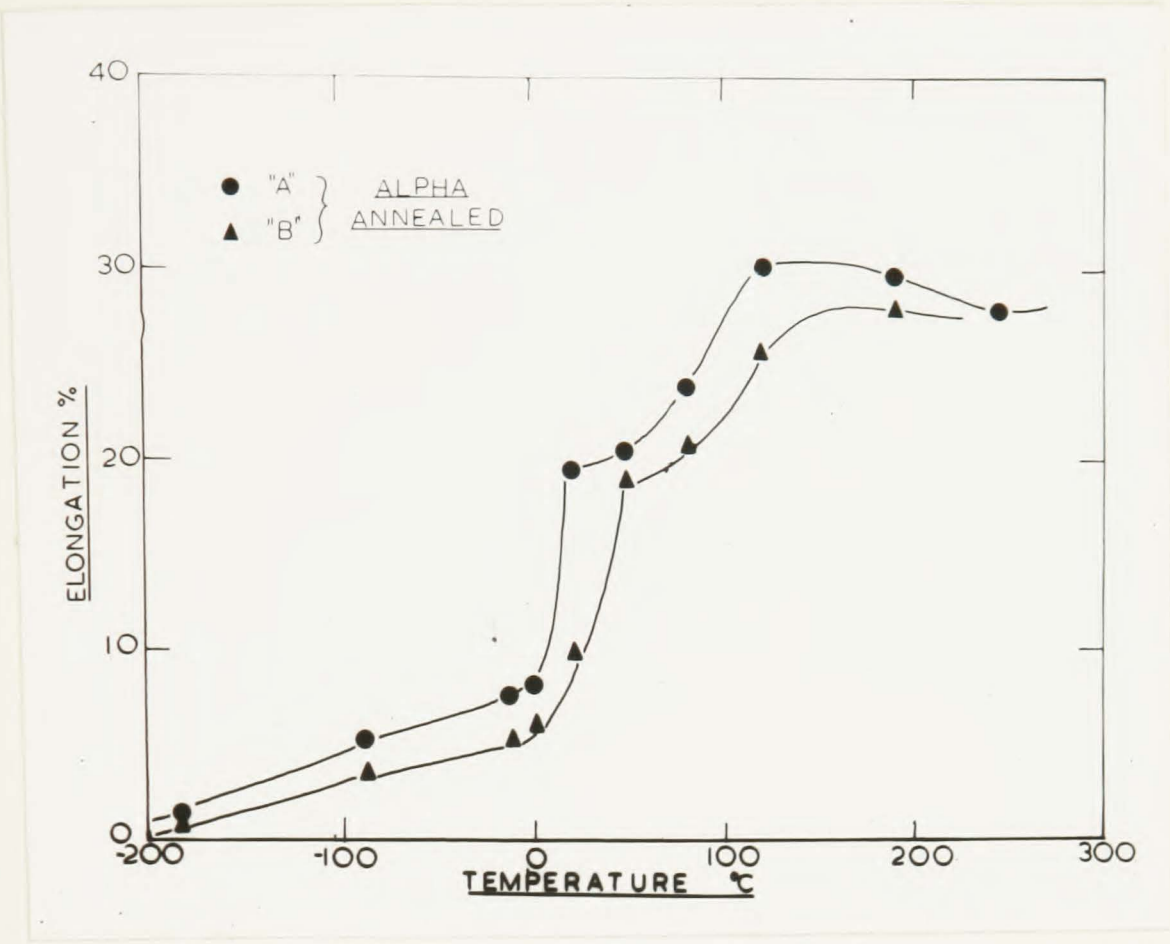


FIGURE 91

Elongation as a function of test temperature for "A" - unadjusted; "B" - adjusted; after alpha-treatment.

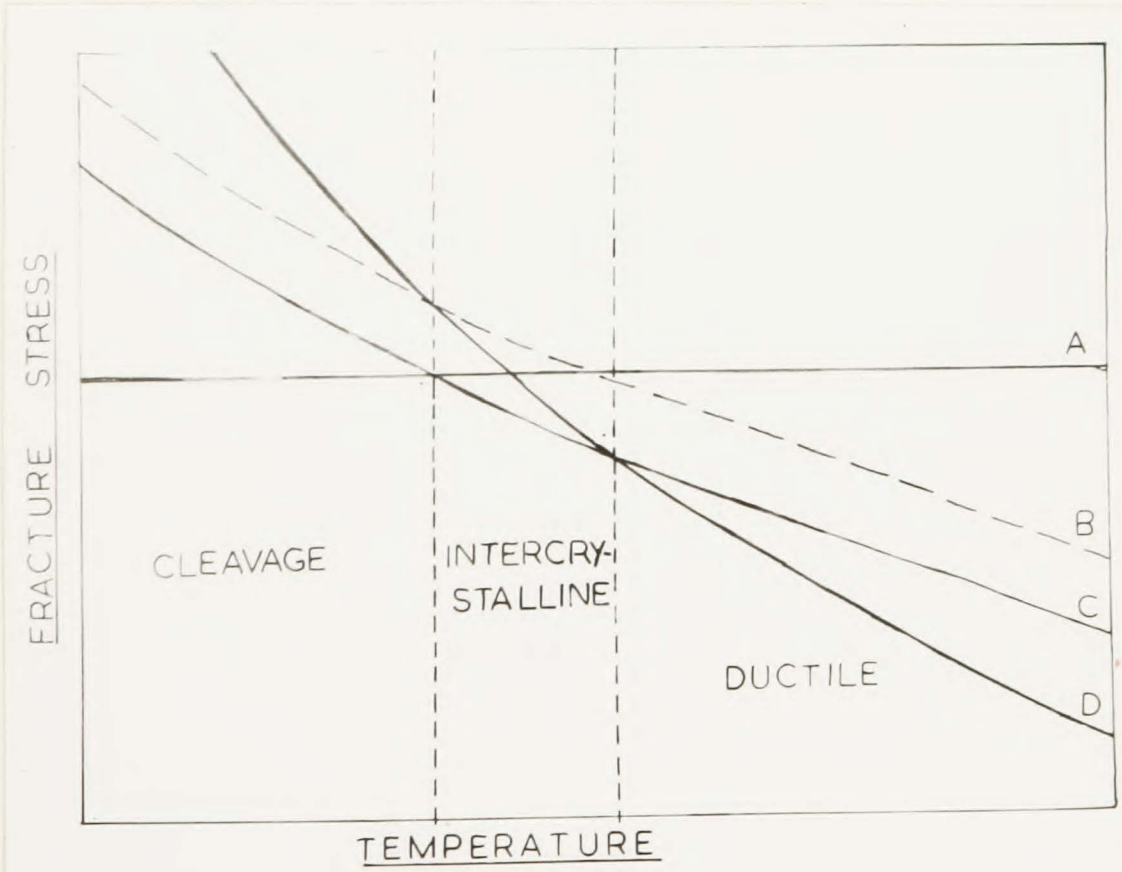


FIGURE 92

See text for explanation.

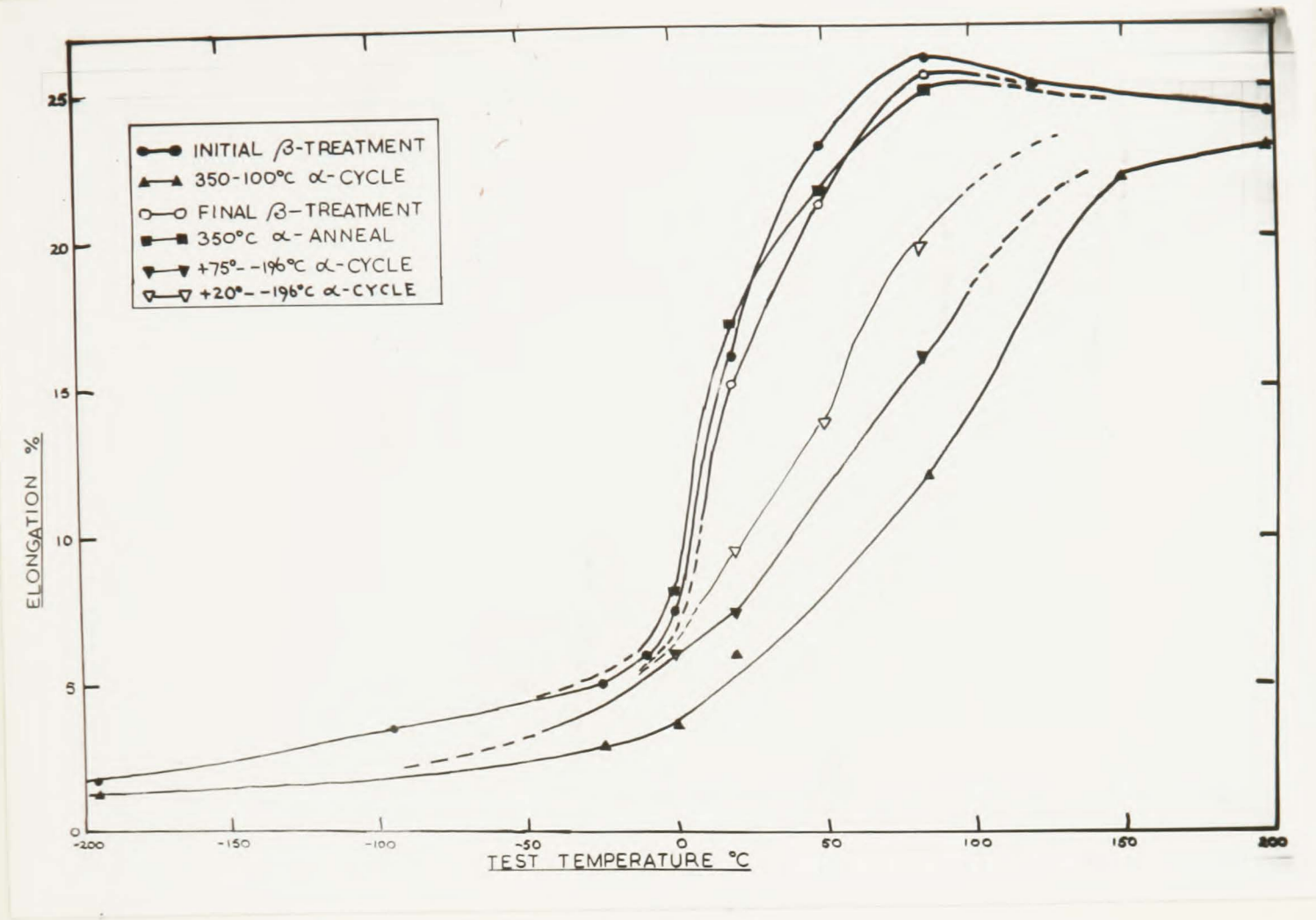


FIGURE 93

Elongation as a function of test temperature after a number of thermal cycling treatments



FIGURE 94 x395

Unadjusted material mercury quenched and strain-relieved



FIGURE 95 x485

Unadjusted material brined quenched and strain-relieved.

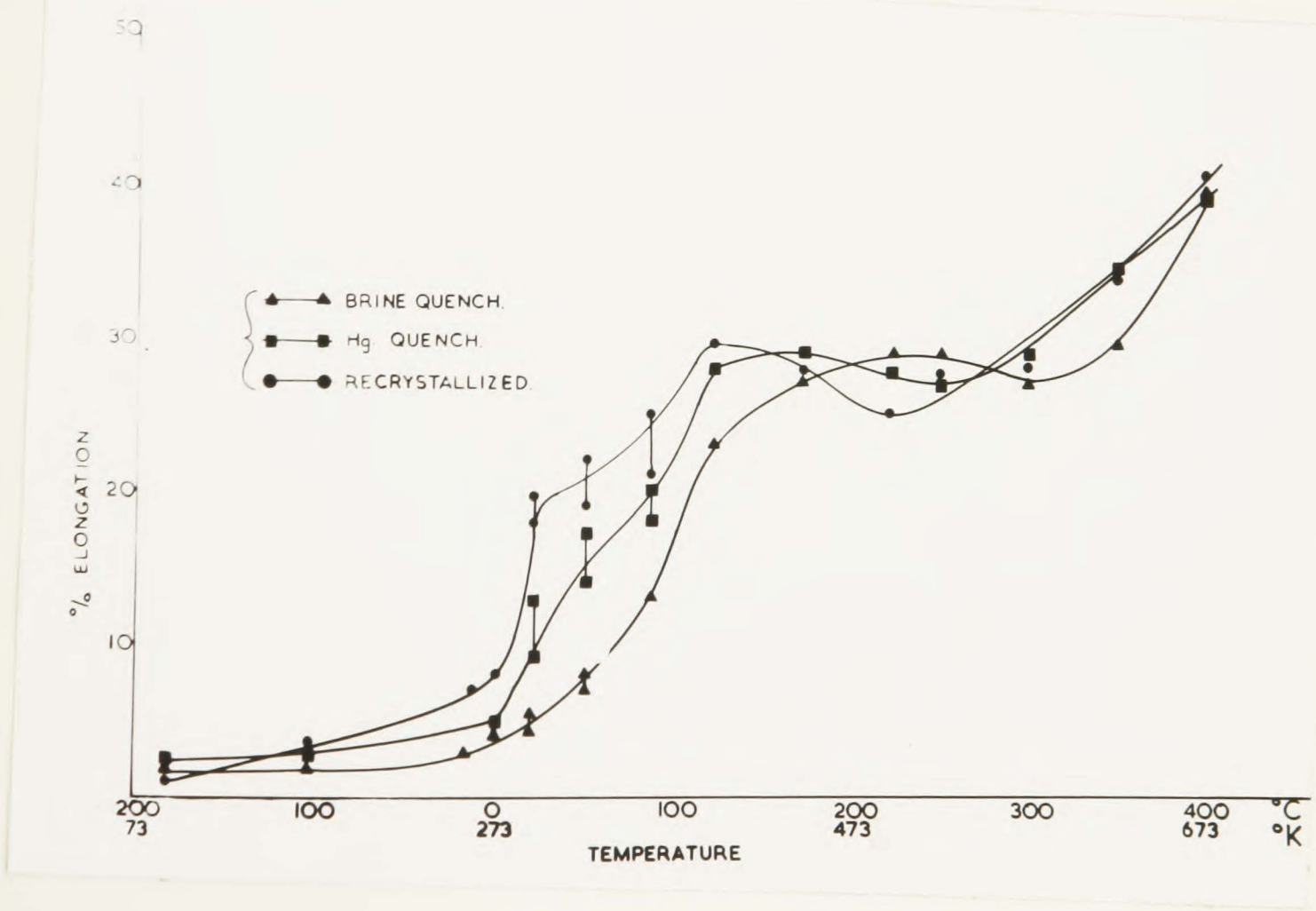


FIGURE 96

Elongation as a function of test temperature in the Grain Shape Experiment.

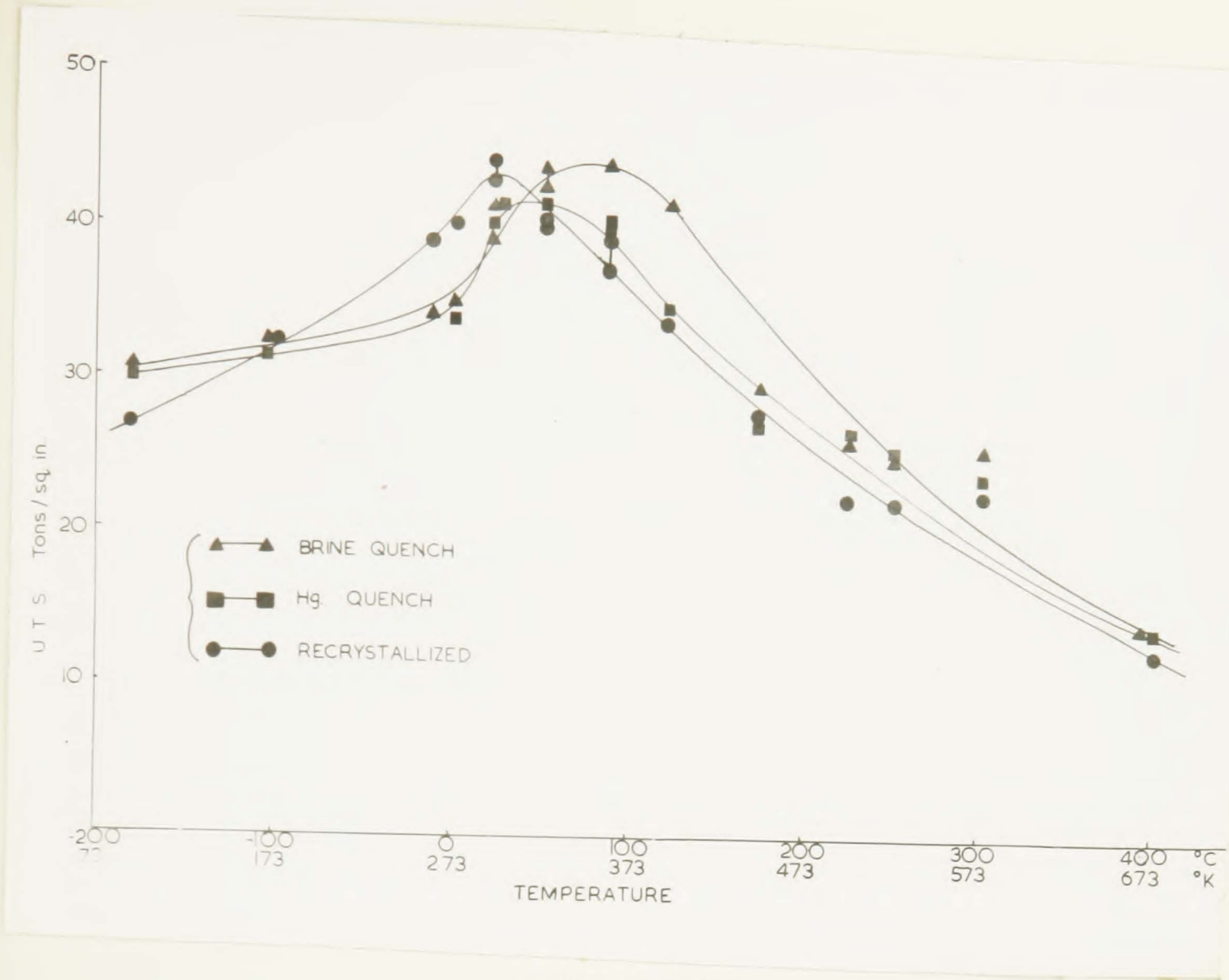


FIGURE 97

U.T.S. as a function of test temperature in the Grain Shape Experiment

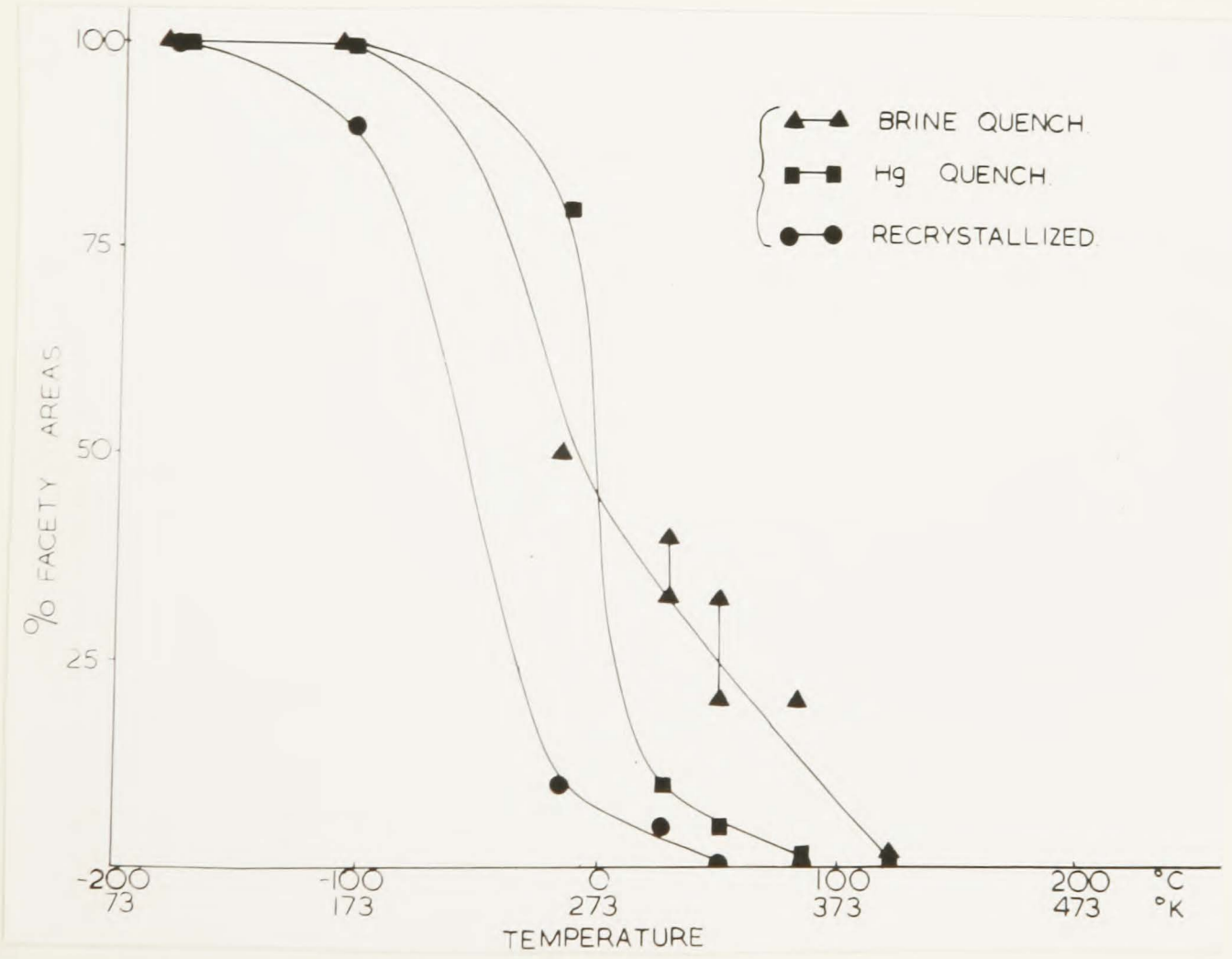


FIGURE 98

% cleavage fracture as a function of test temperature in the Grain Shape Experiment.

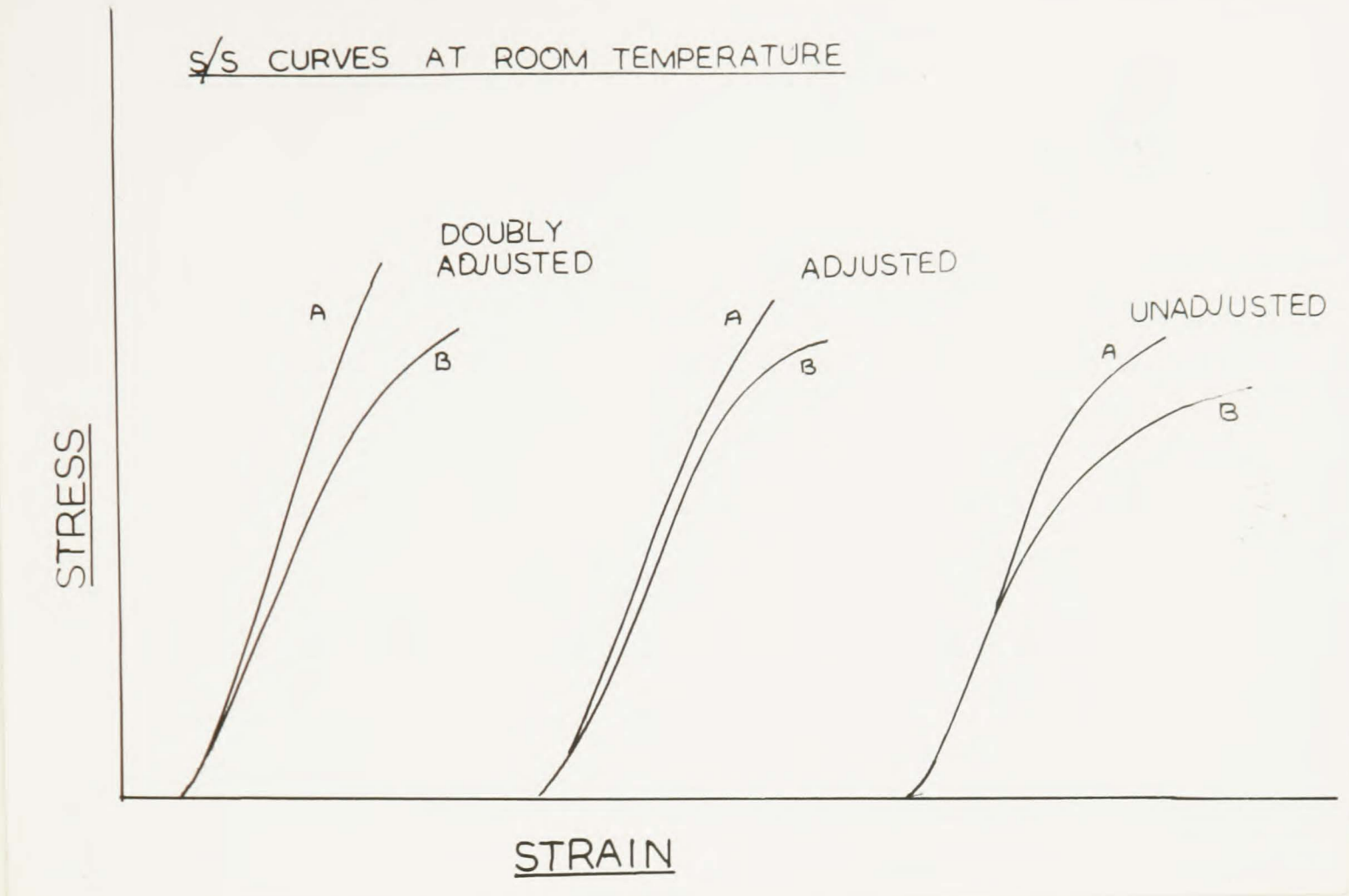


FIGURE 99

Stress/strain curves in three materials at room temperature. In each case "A" corresponds to irregular grain profiled material and "B" to smooth grain profiled material.

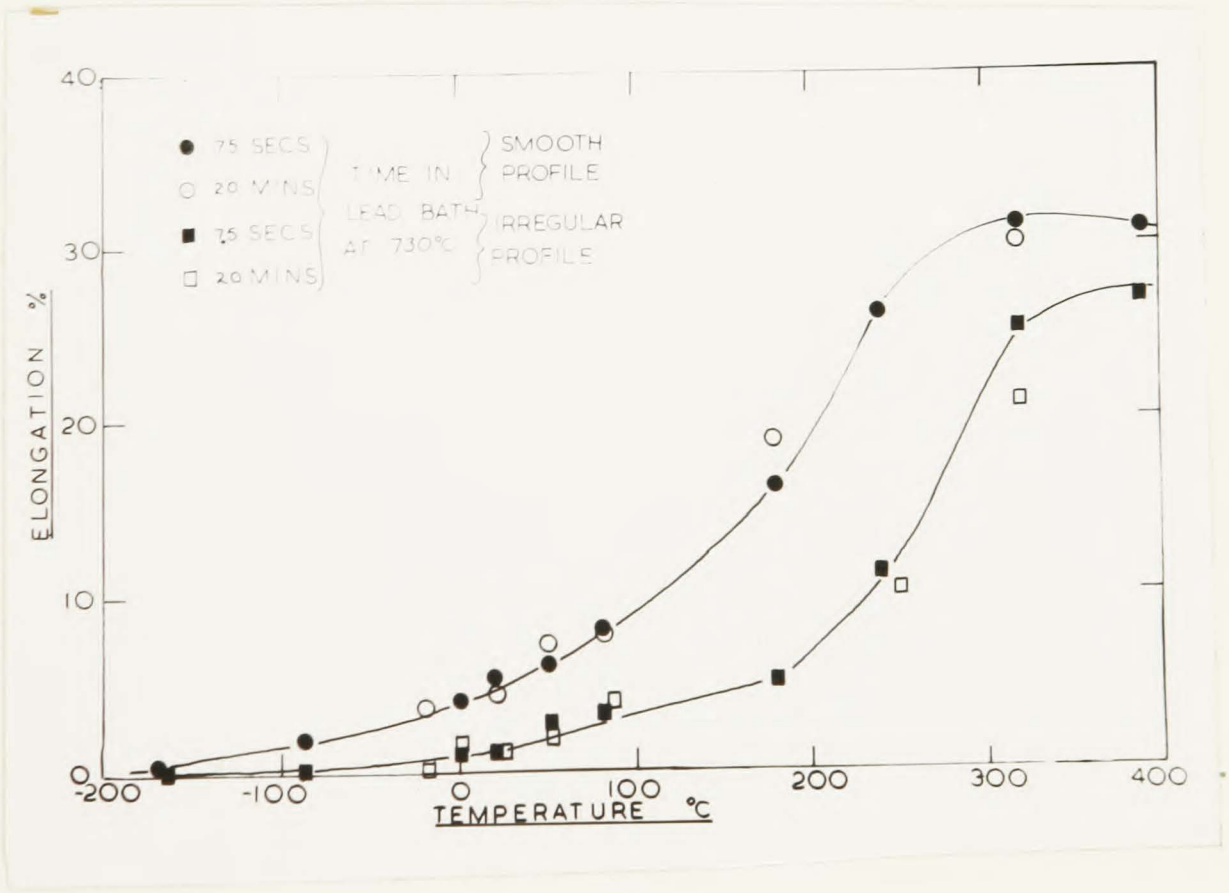


FIGURE 100

Elongation as a function of test temperature for doubly adjusted material after different lead bath treatments in the grain shape experiment.

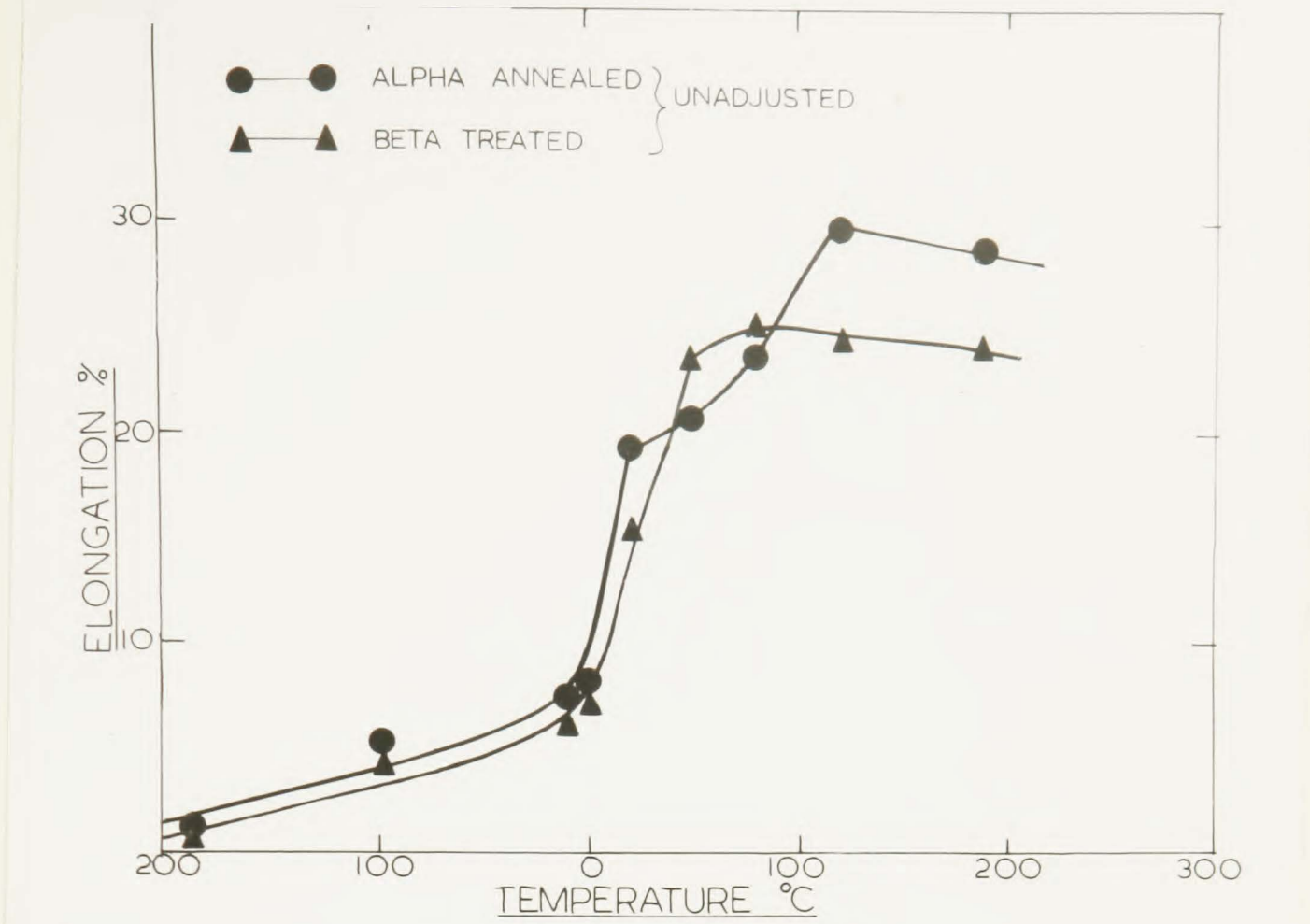


FIGURE 101

Elongation as a function of test temperature for unadjusted material after alpha treatment (g.s. 0.10mm) and beta treatment (g.s. 0.45mm).

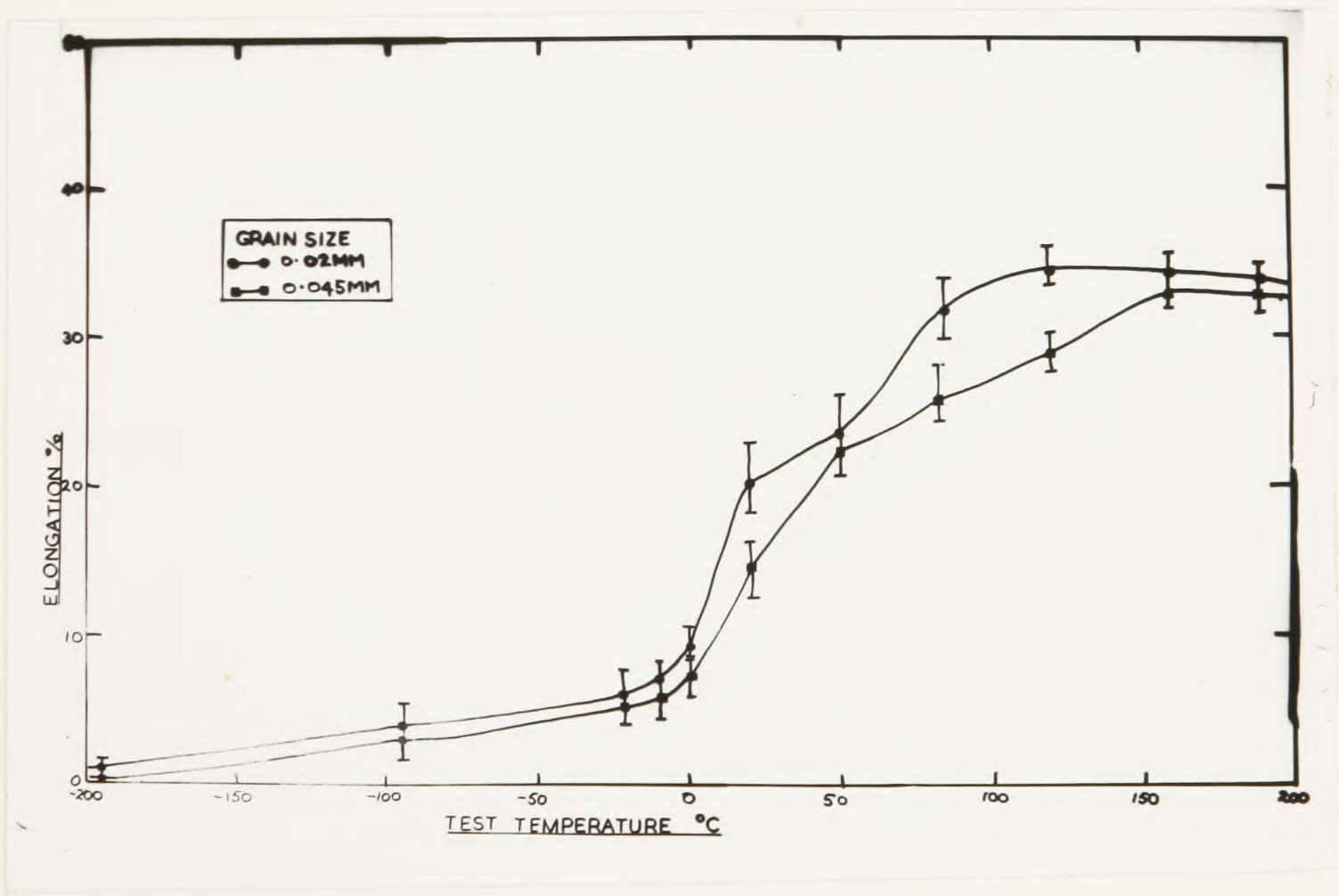


FIGURE 102

Elongation as function of test temperature for adjusted rolled material of two different grain sizes.

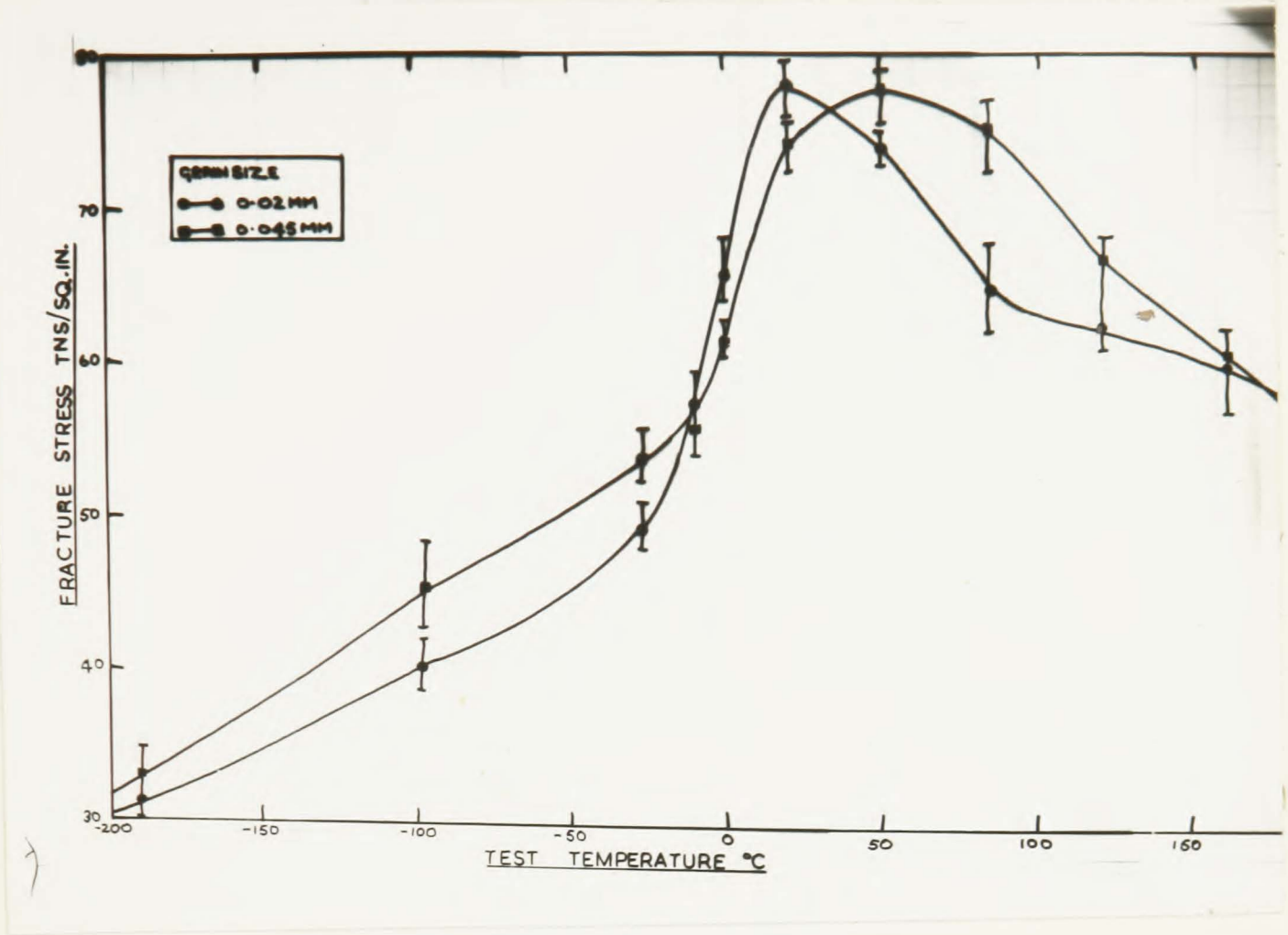


FIGURE103

Fracture stress as a function of test temperature for adjusted rolled material of the two grain sizes indicated.



FIGURE 104

Intercrystalline cracking in adjusted rolled material.



FIGURE 105 x660

Crystallographic cracking in adjusted rolled material

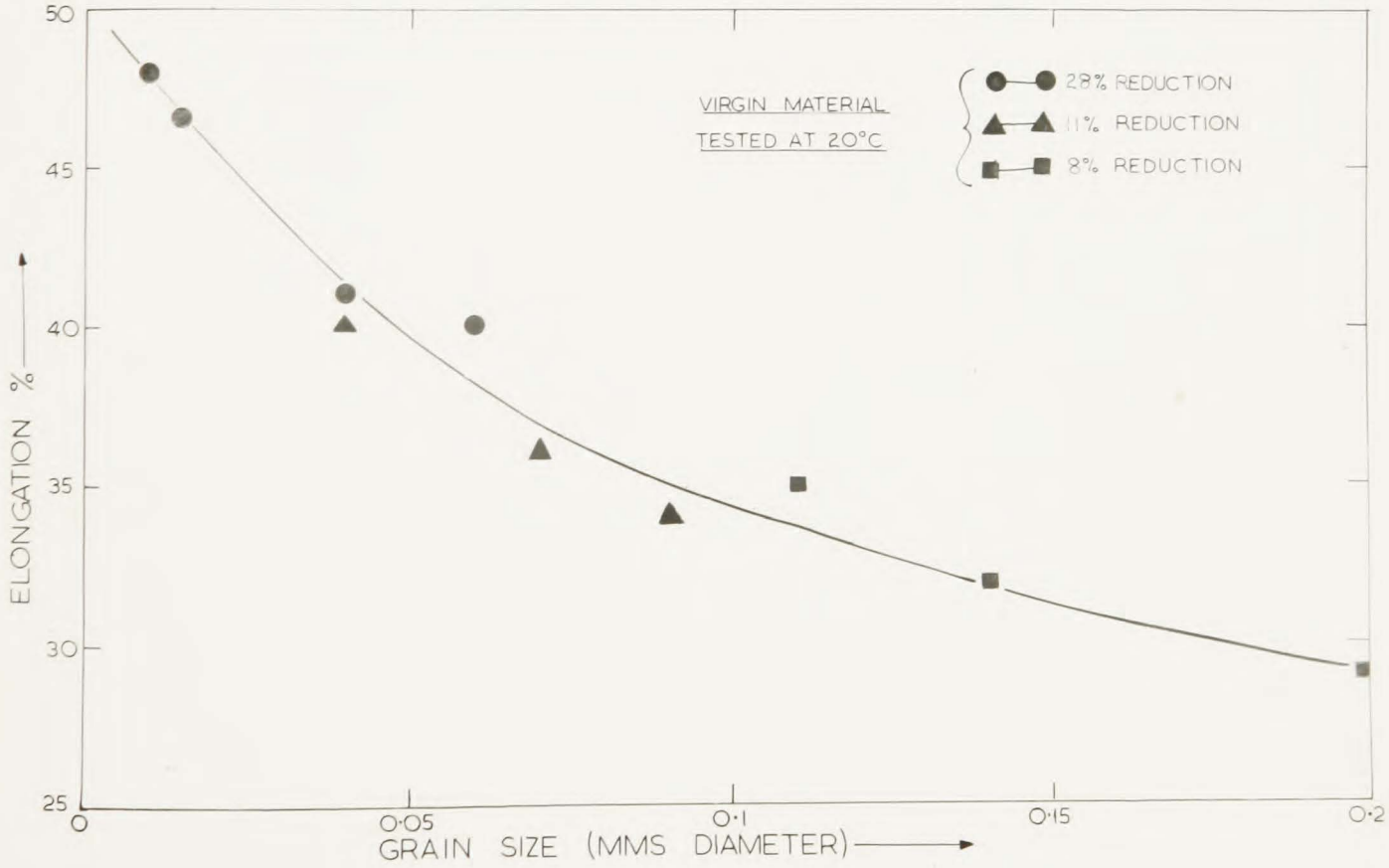


FIGURE 106

Elongation at 20°C as a function of grain size in virgin unadjusted material with prior mechanical treatment indicated.

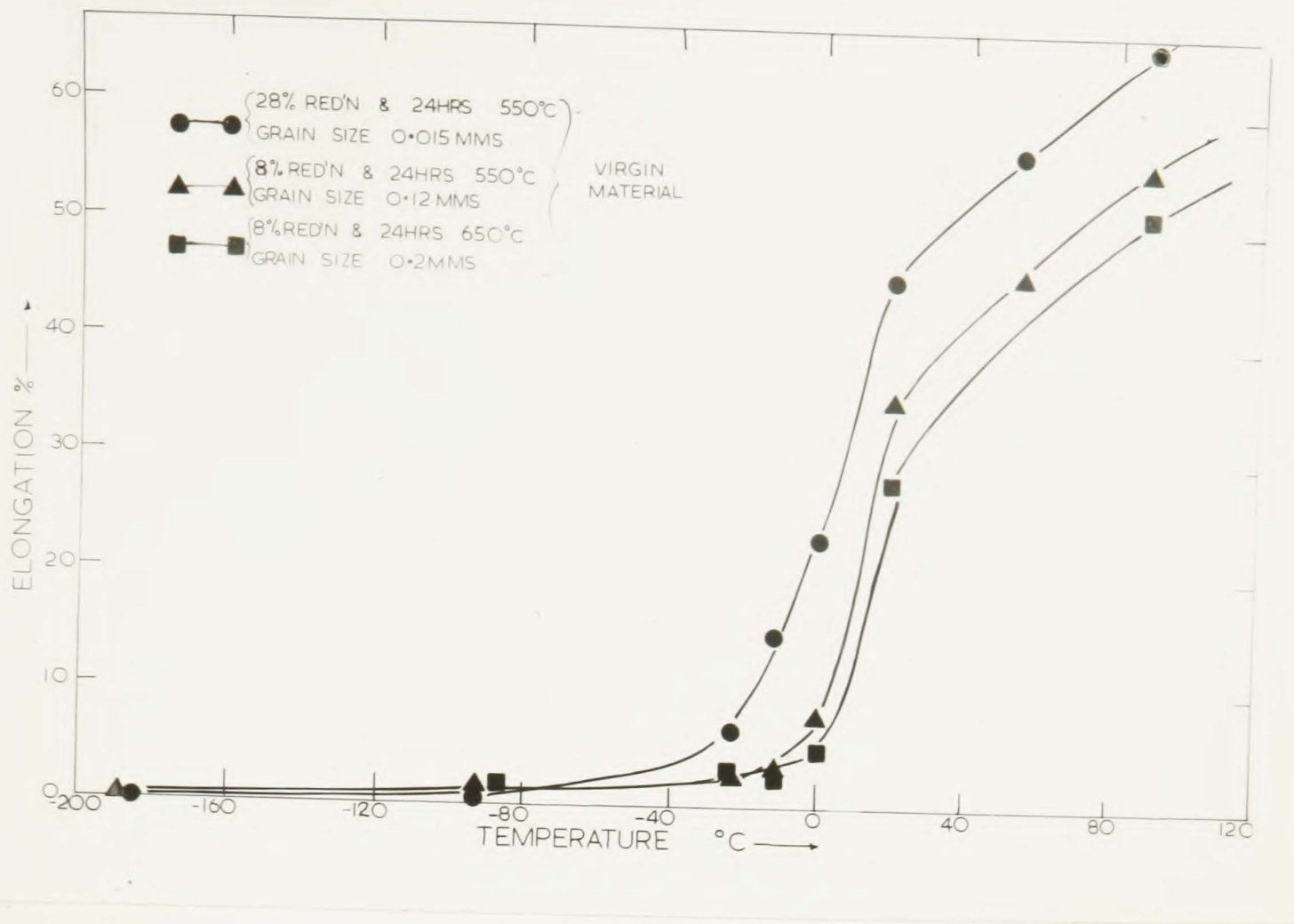


FIGURE 107

Elongation as a function of test temperature for three grain sizes in virgin material

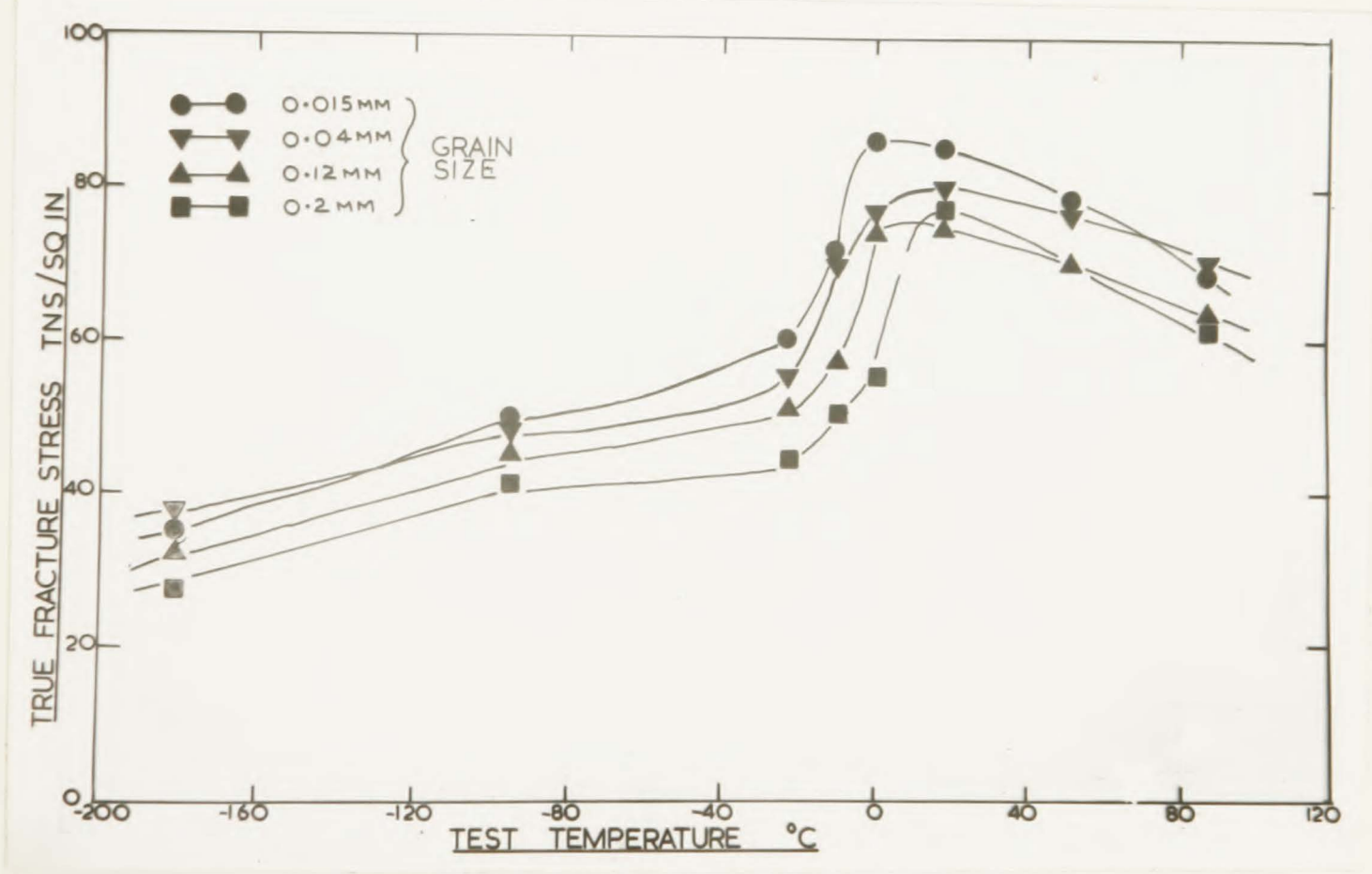
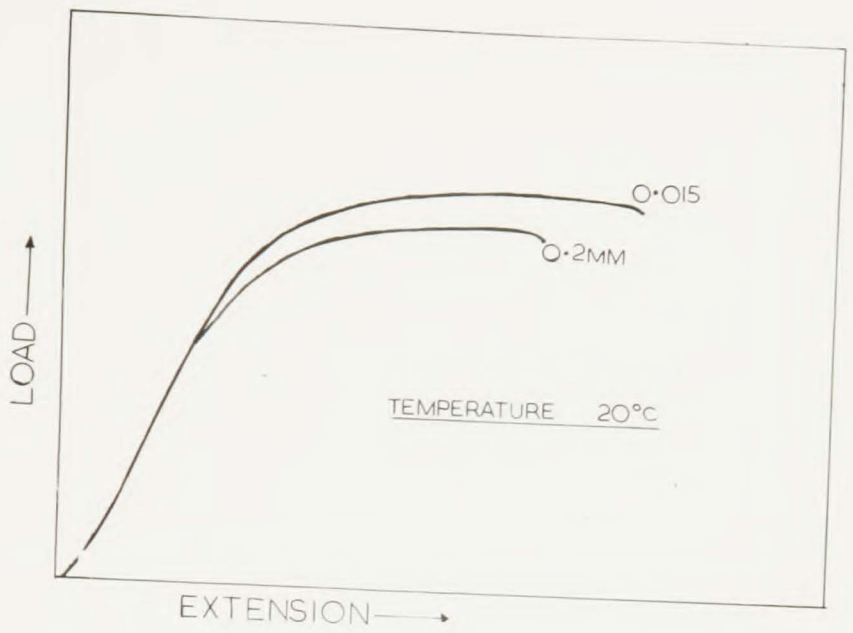


FIGURE 108

Fracture stress as a function of test temperature for four grain sizes in virgin material.



VIRGIN MATERIAL DEMONSTRATING THE EFFECTS OF GRAIN SIZE & TEMPERATURE ON THE LOAD/EXTENSION CURVES.

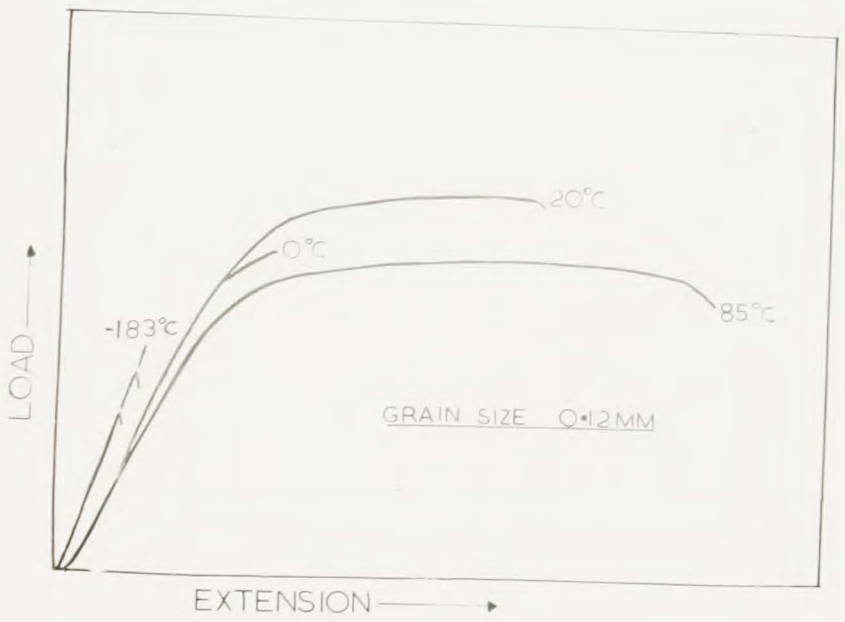


FIGURE 109

Load/extension curves for virgin rolled material showing the effect of grain size within the range 0.015 - 0.20mm at 20°C and the effect of temperature in the range -183°C - +85°C for a grain size of 0.12mm.

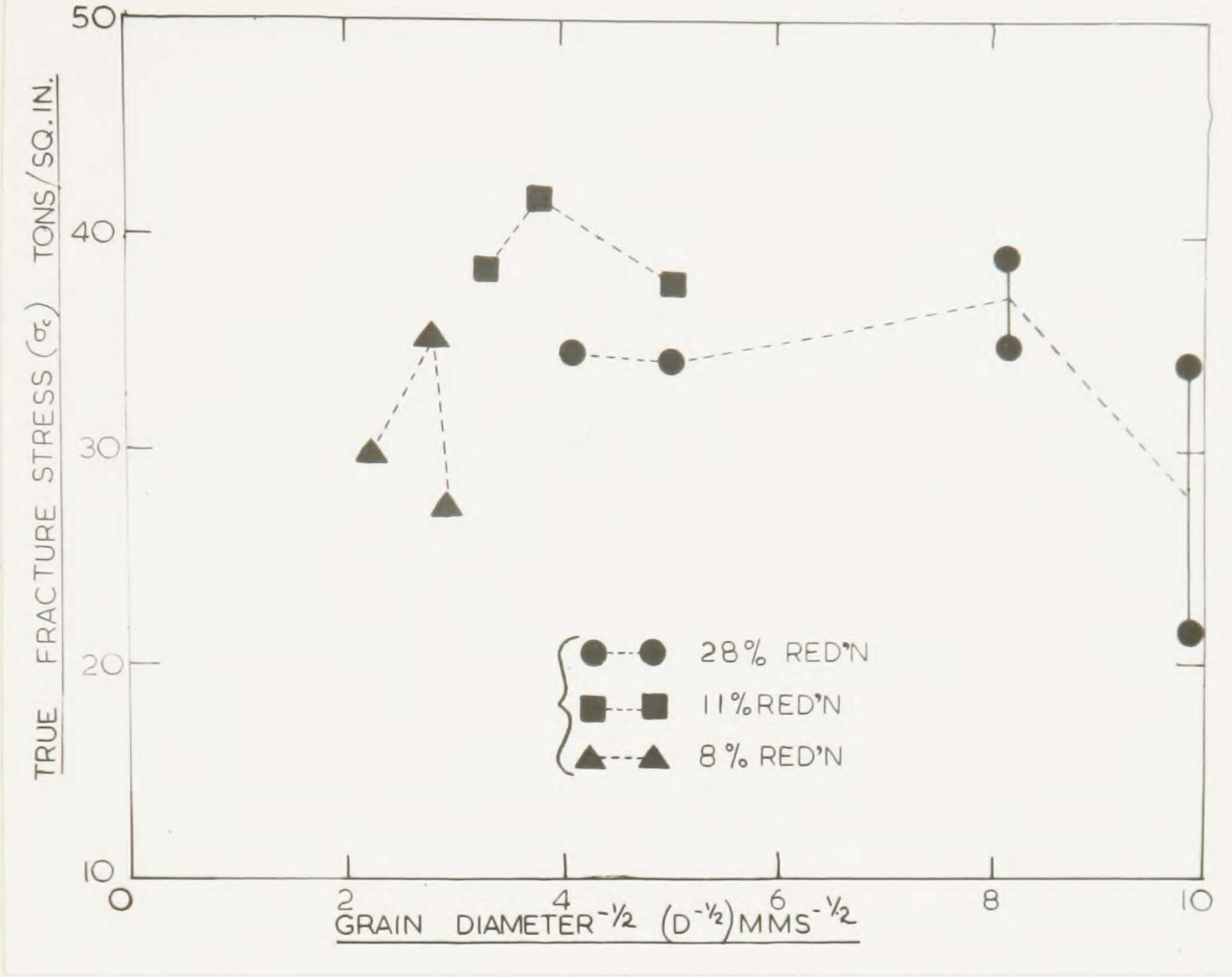


FIGURE 110

Fracture stress at -196°C as a function of $d^{-\frac{1}{2}}$

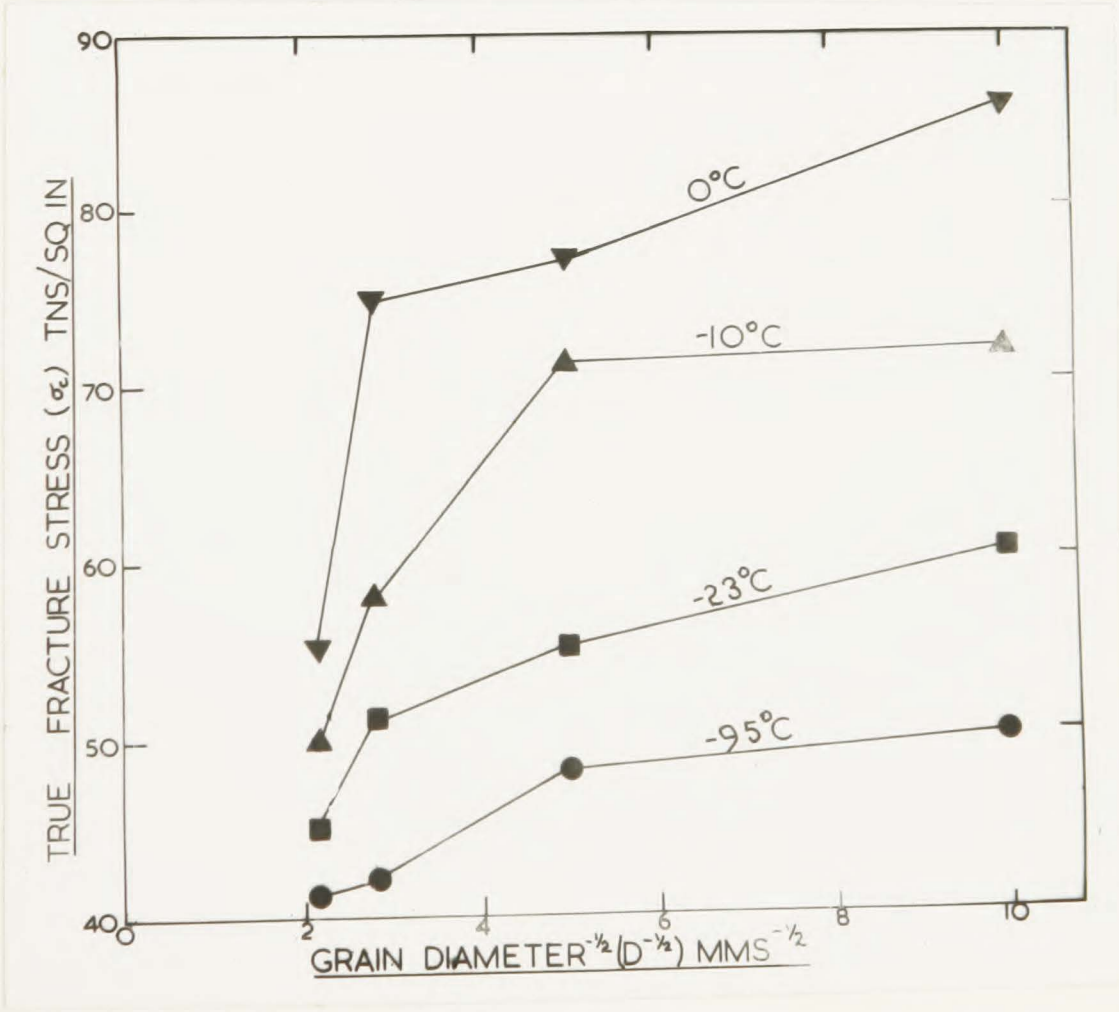


FIGURE 111

Fracture stress at 95°C, -23°C, -10°C and 0°C as a function of $d-\frac{1}{2}$

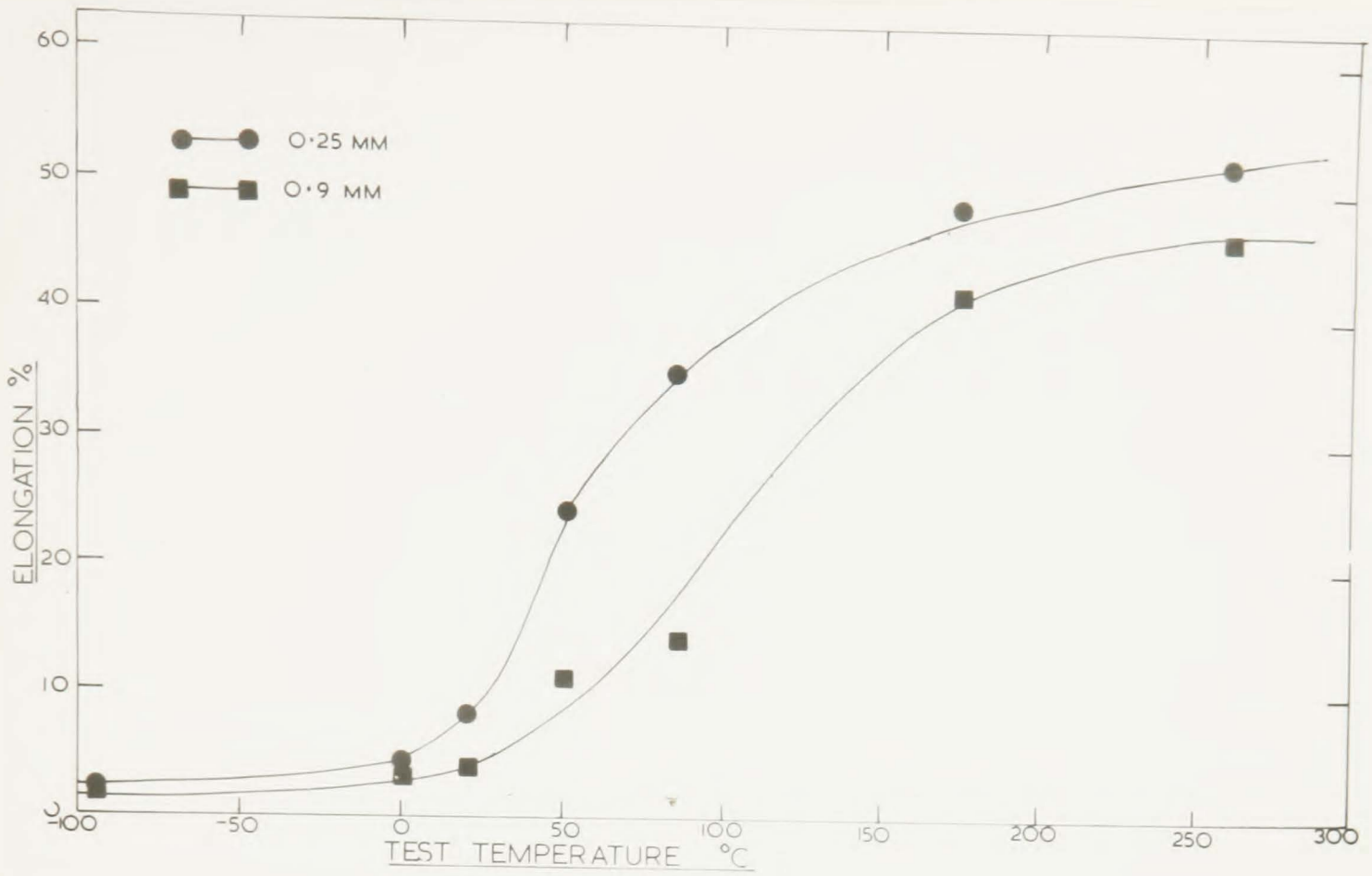


FIGURE 112

Elongation as a function of test temperature for two grain sizes after a strain-anneal treatment upon virgin material

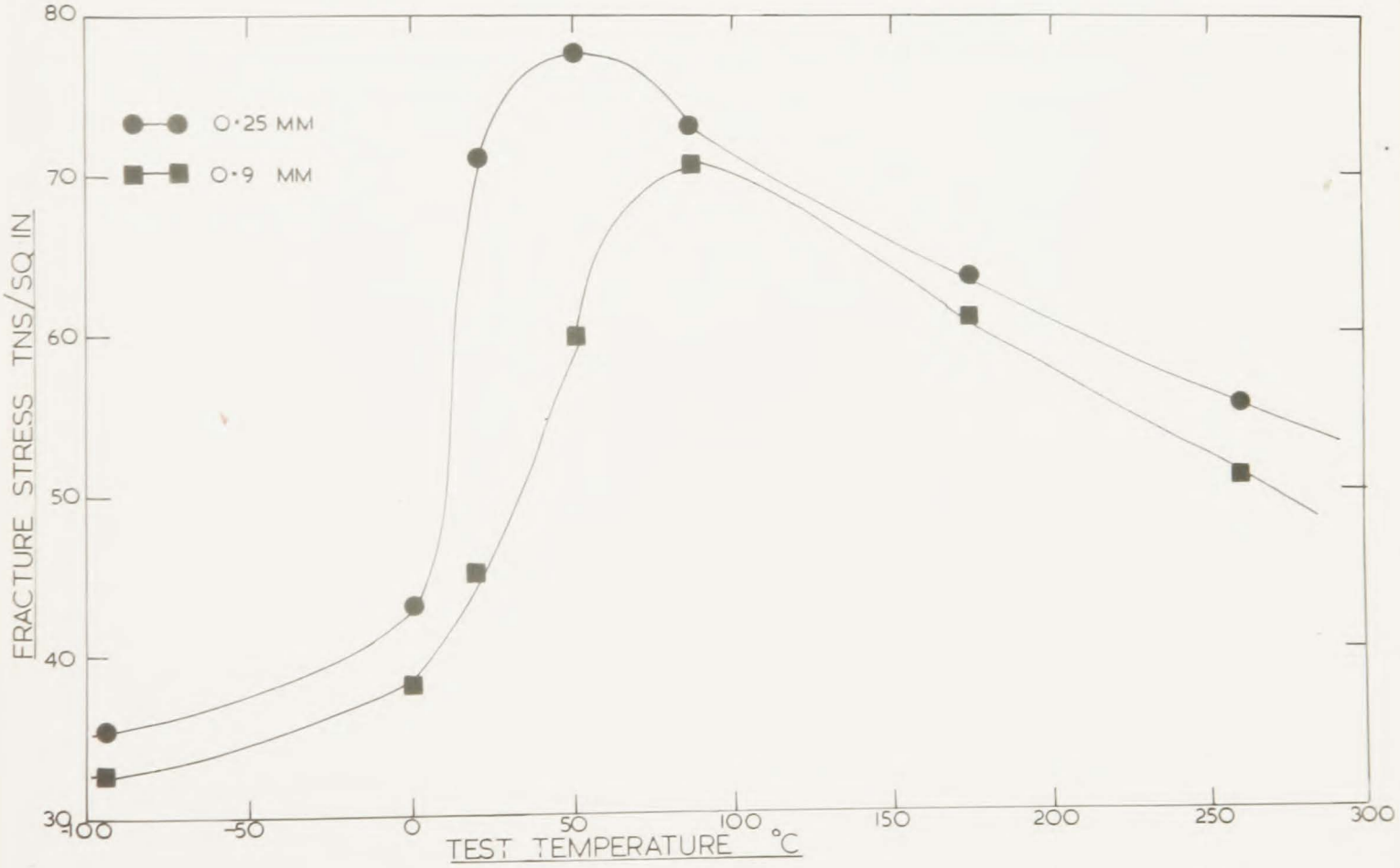


FIGURE 113

Fracture stress as a function of test temperature for two grain sizes after a strain-anneal treatment upon virgin material

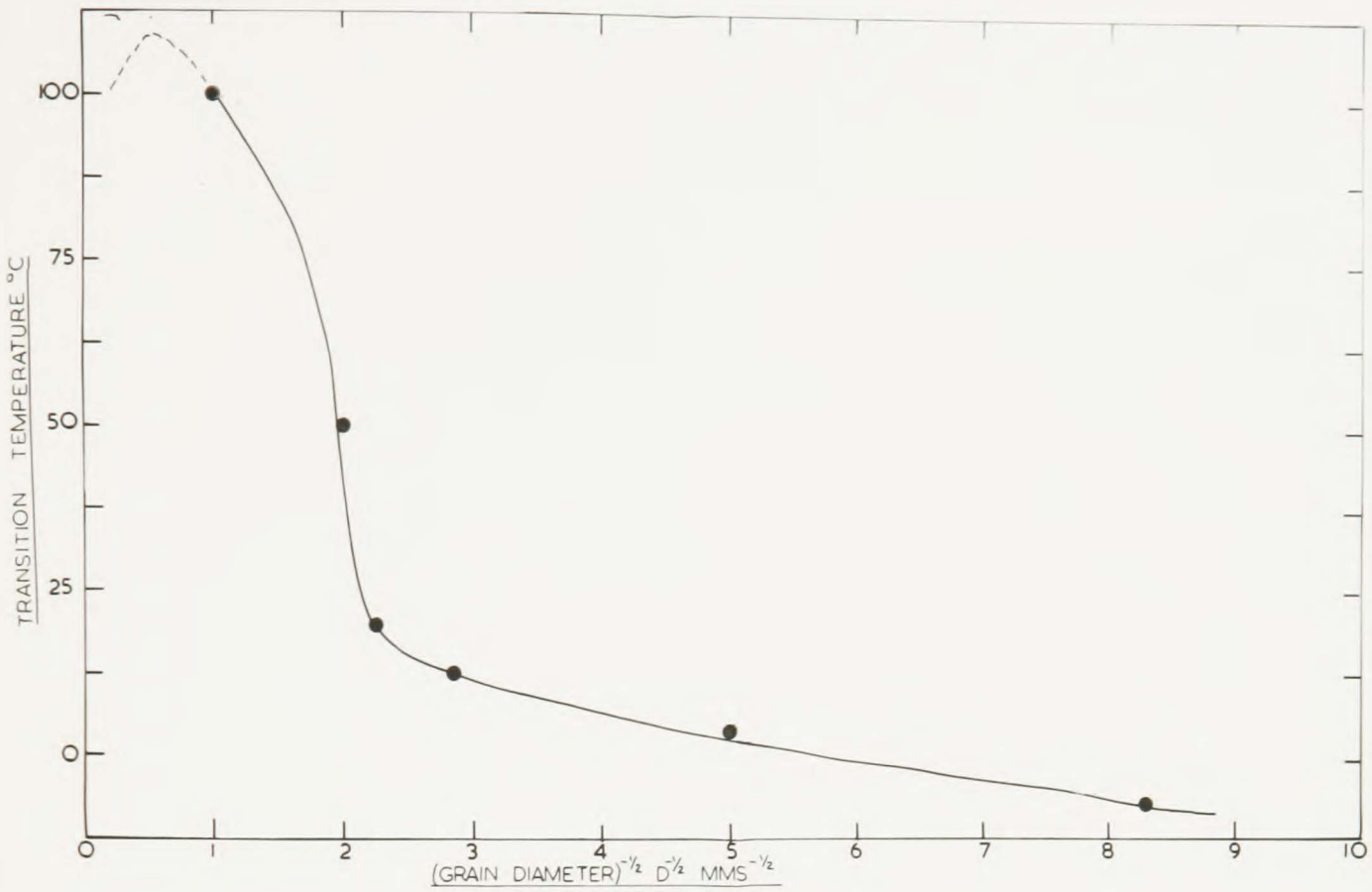


FIGURE 114

Ductile/brittle transition temperature as a function of $d^{-\frac{1}{2}}$

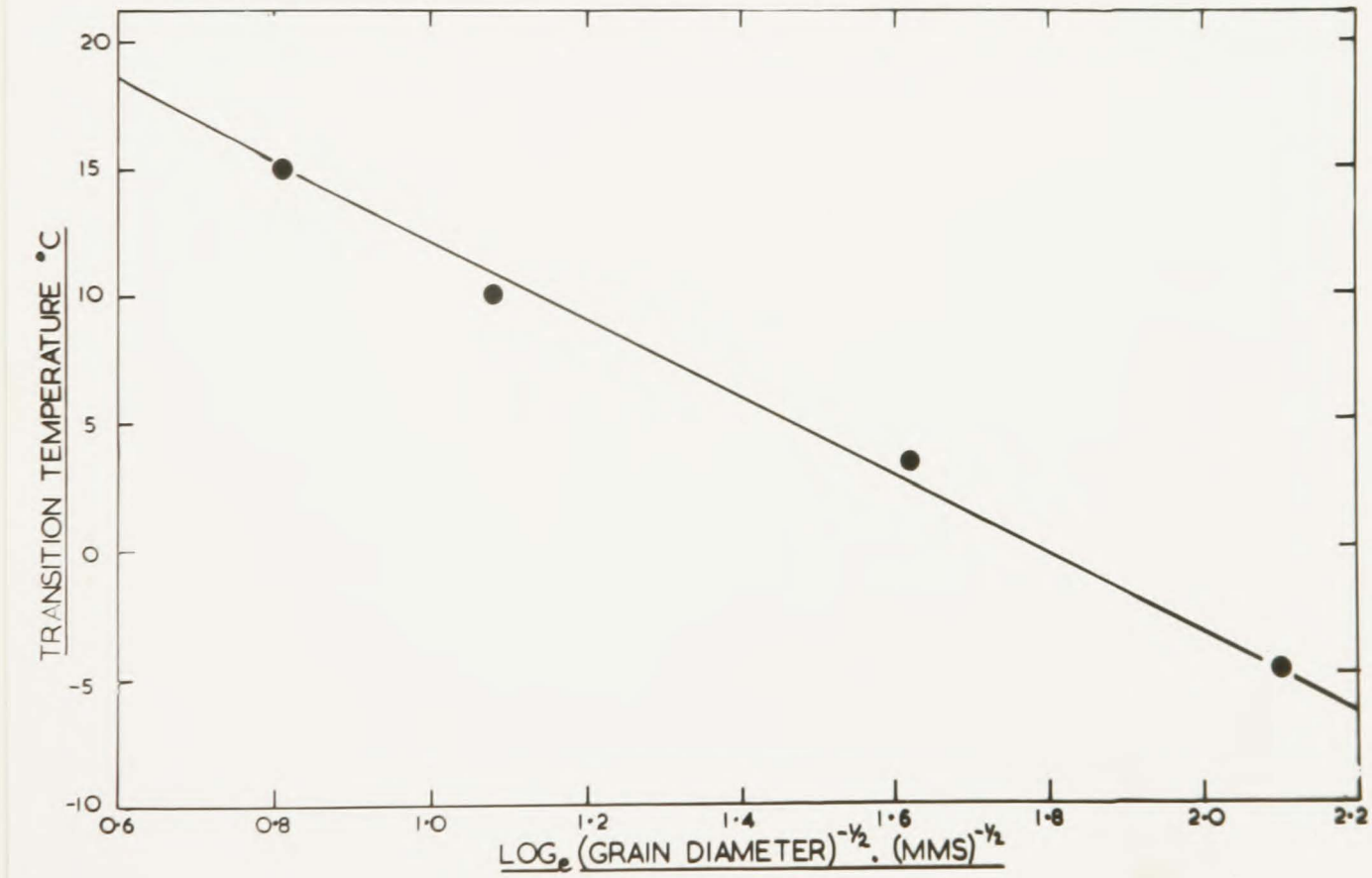


FIGURE 115

Ductile/brittle transition temperature as a function of $\log_e d^{-\frac{1}{2}}$ within the range 0.01 - 0.20mm diameter.

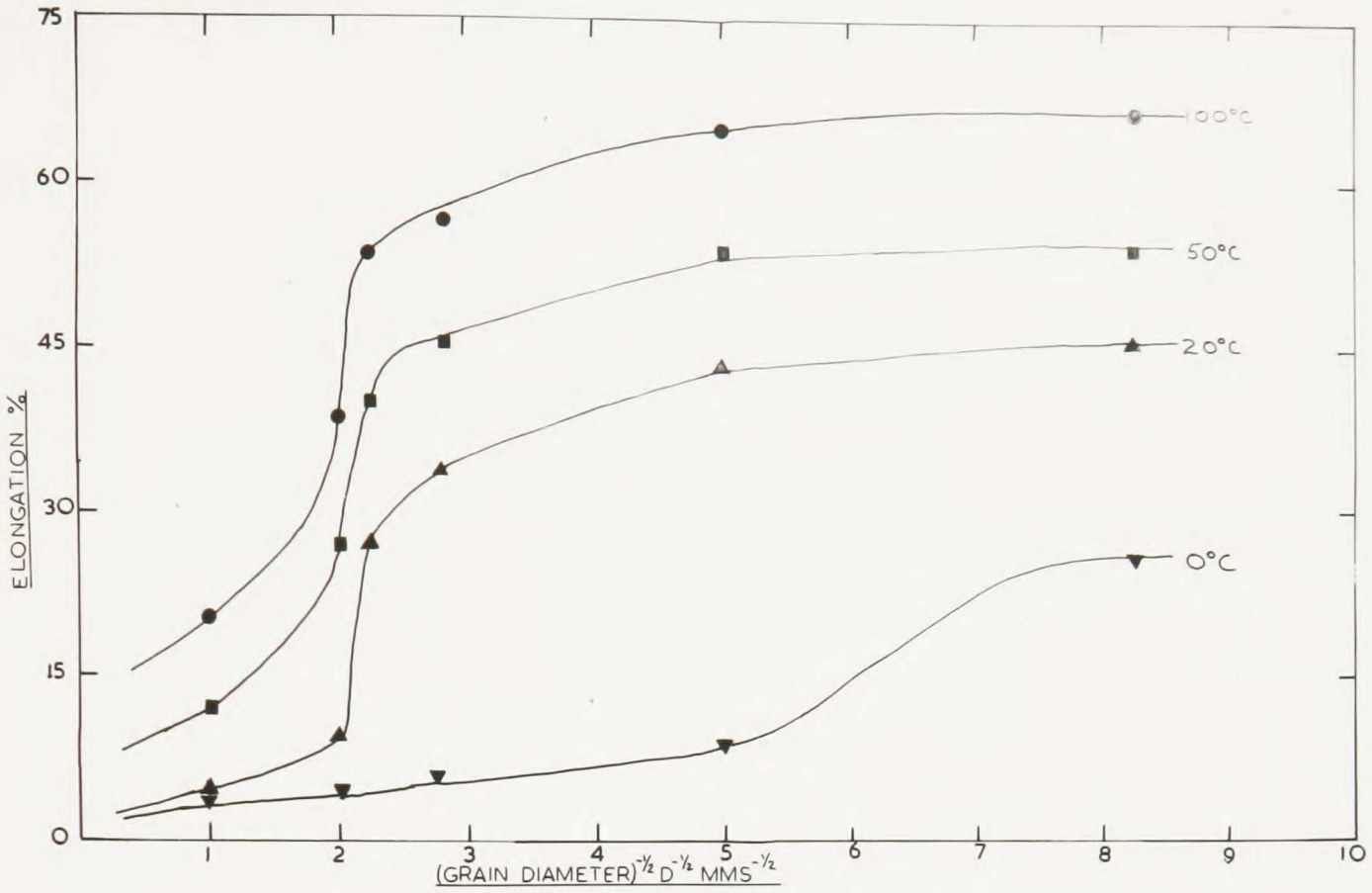


FIGURE 116

Elongation as a function of $d^{-\frac{1}{2}}$ for virgin material

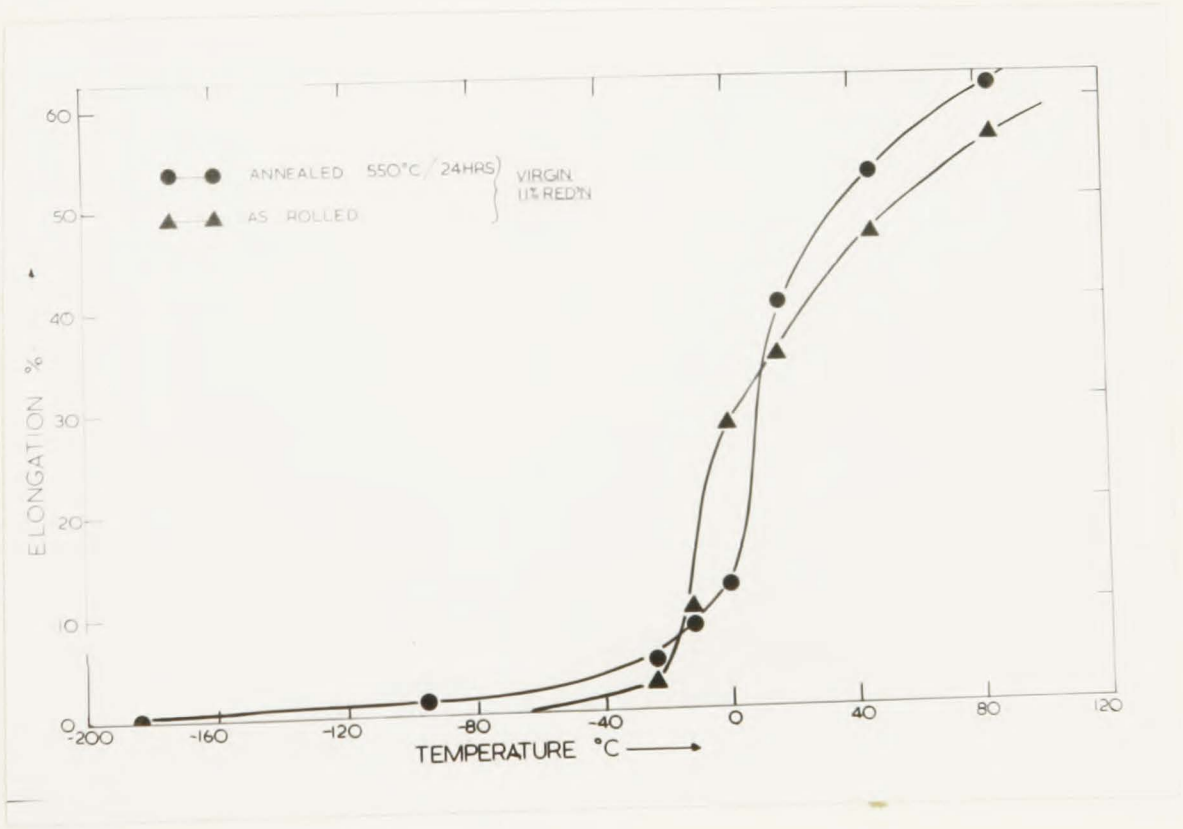


FIGURE 117

Elongation as a function of test temperature showing the influence of 11% rolling reduction on the transition.

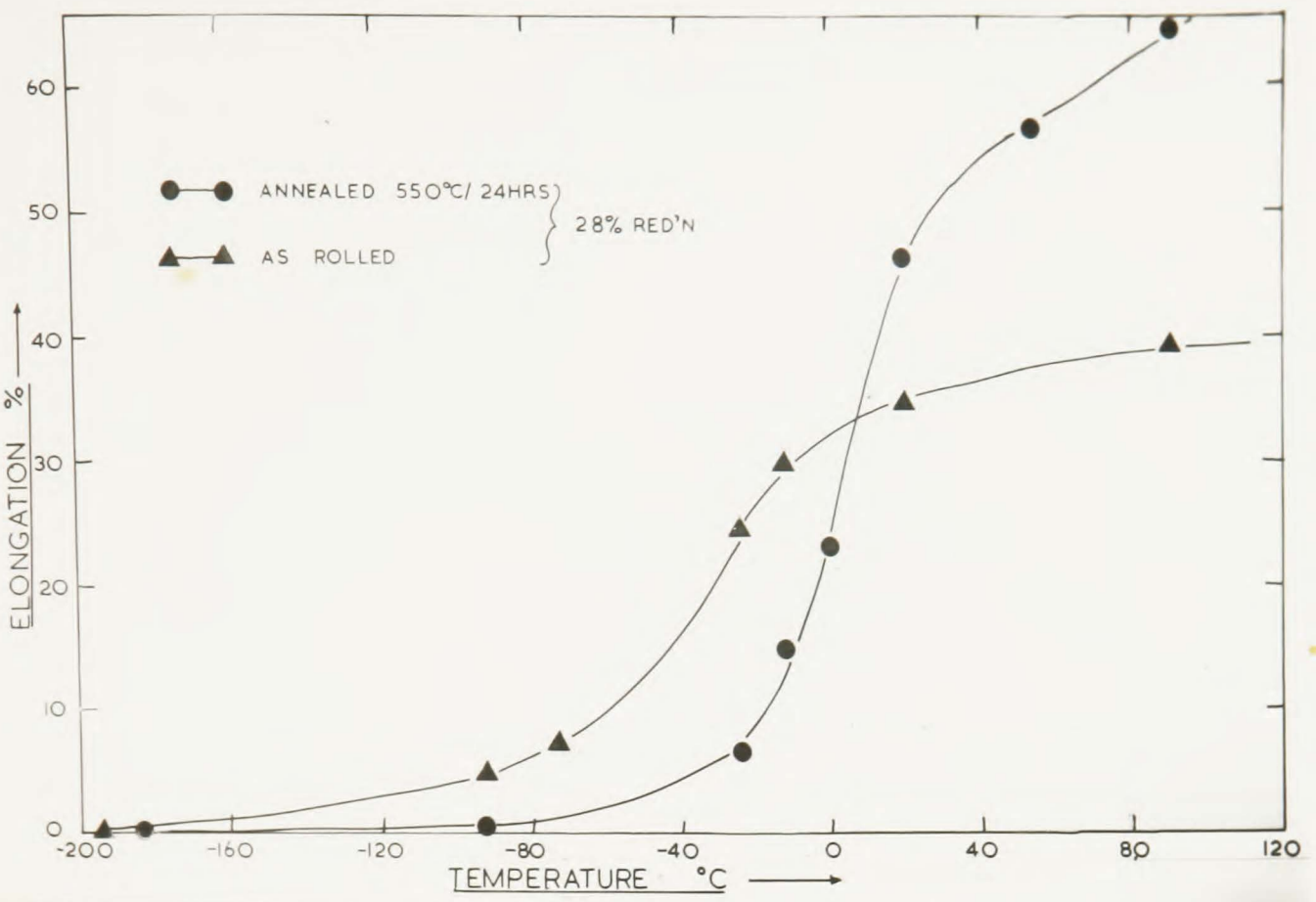


FIGURE 118

Elongation as a function of test temperature showing the influence of 28% rolling reduction on the transition.

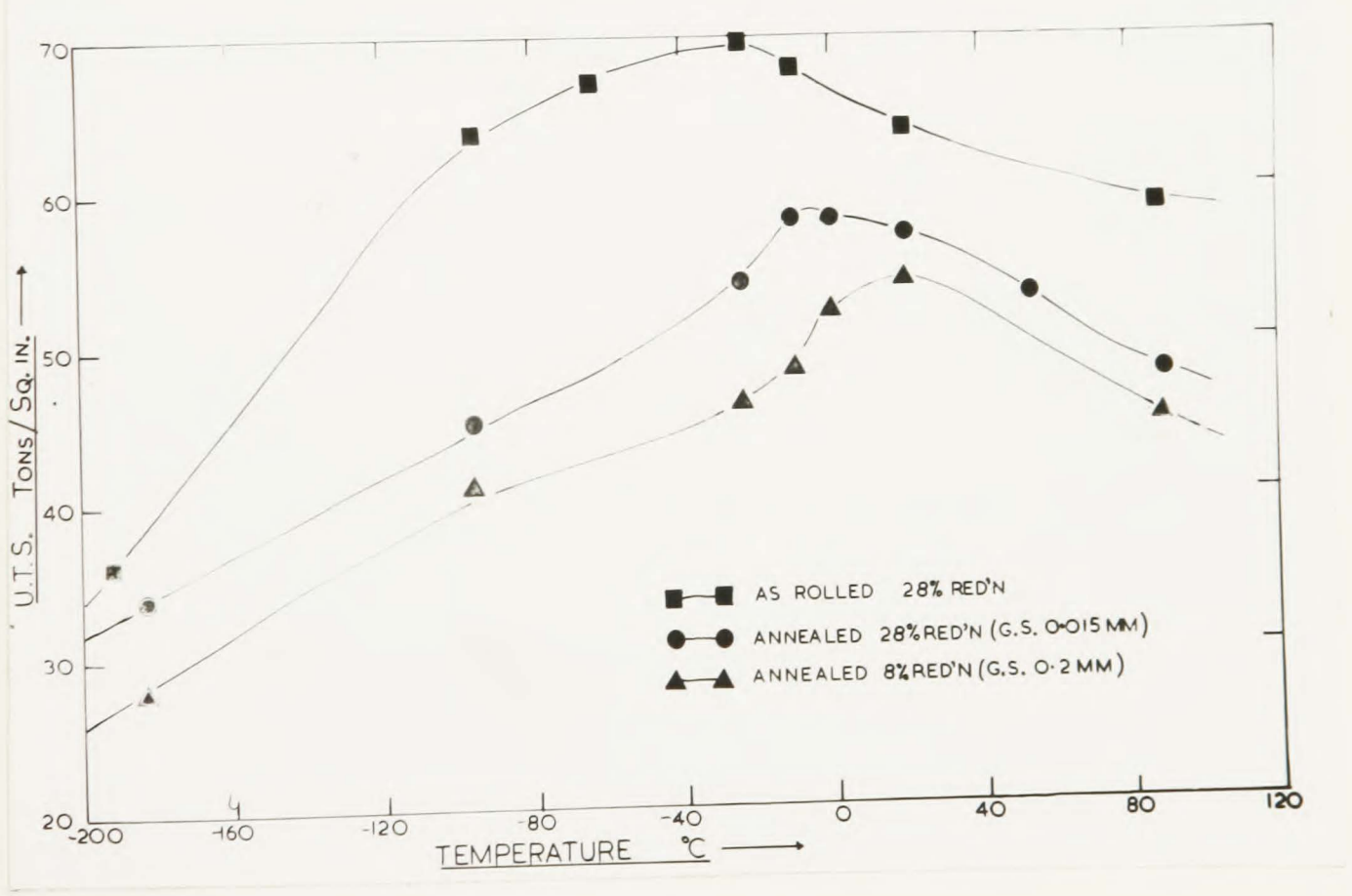


FIGURE 119

U.T.S as a function of test temperature showing the effect of grain size and cold work.

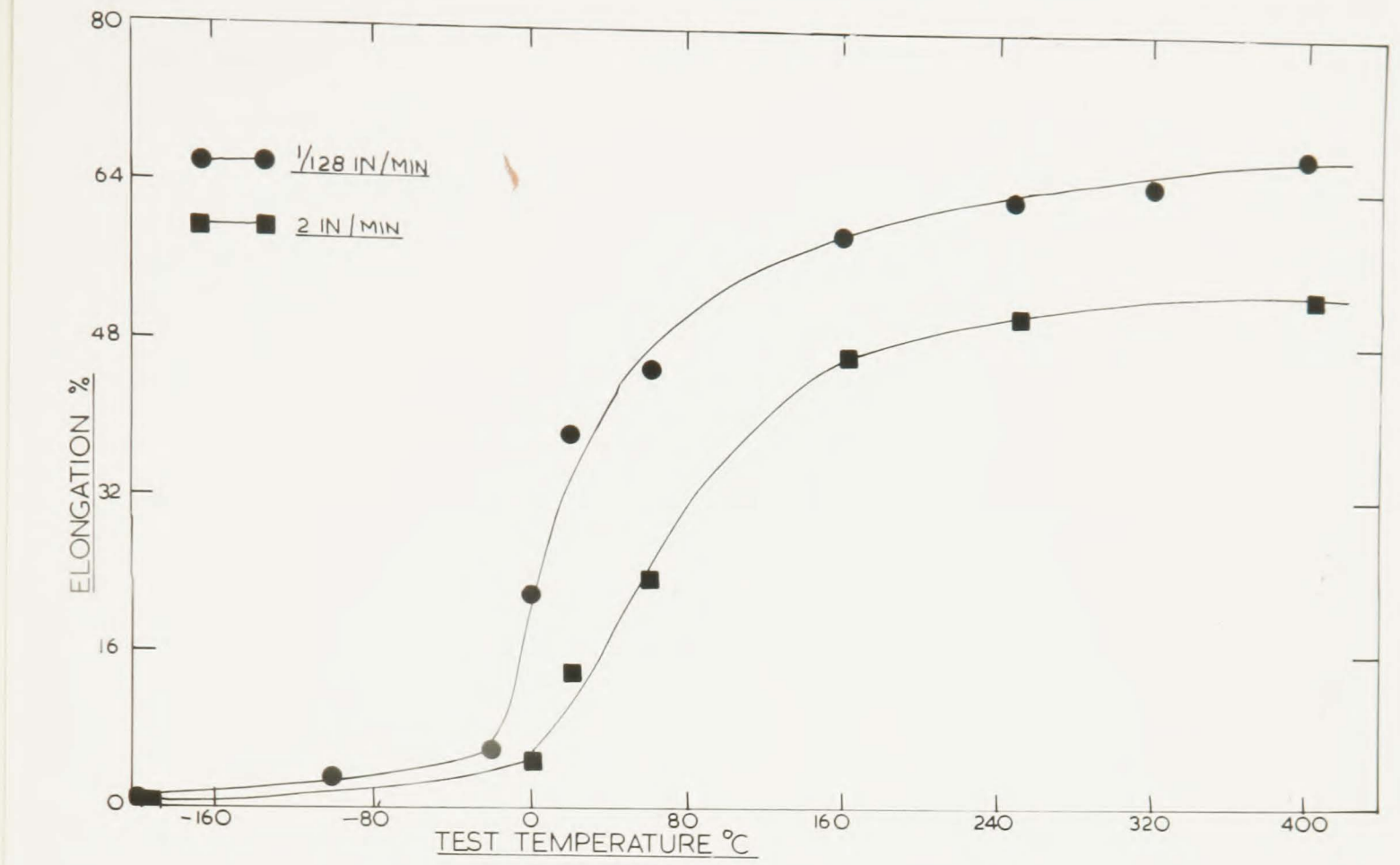


FIGURE 120

Elongation as a function of test temperature showing the effect of strain rate on the transition.

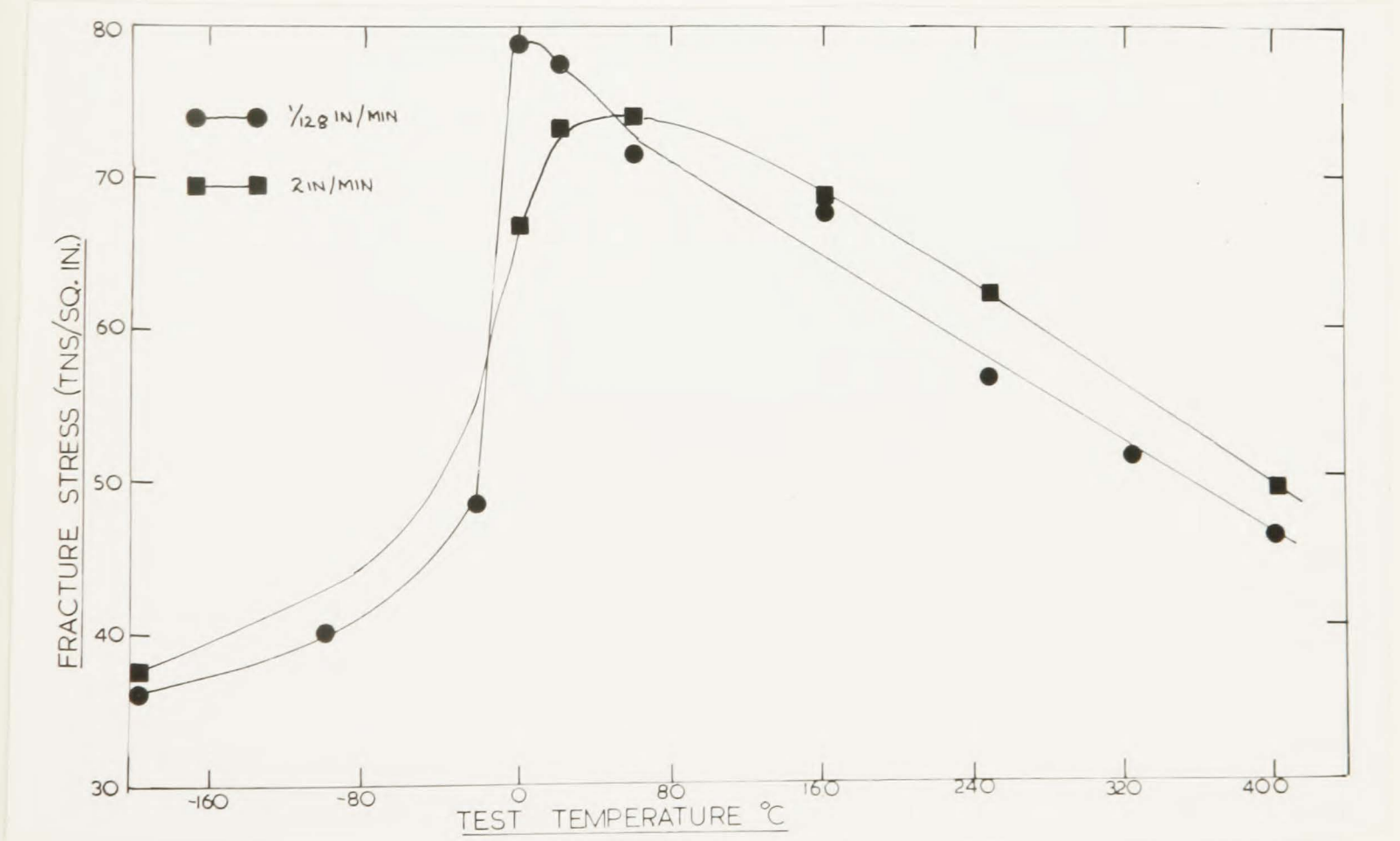


FIGURE 121

Fracture stress as a function of test temperature showing the effect of strain-rate.

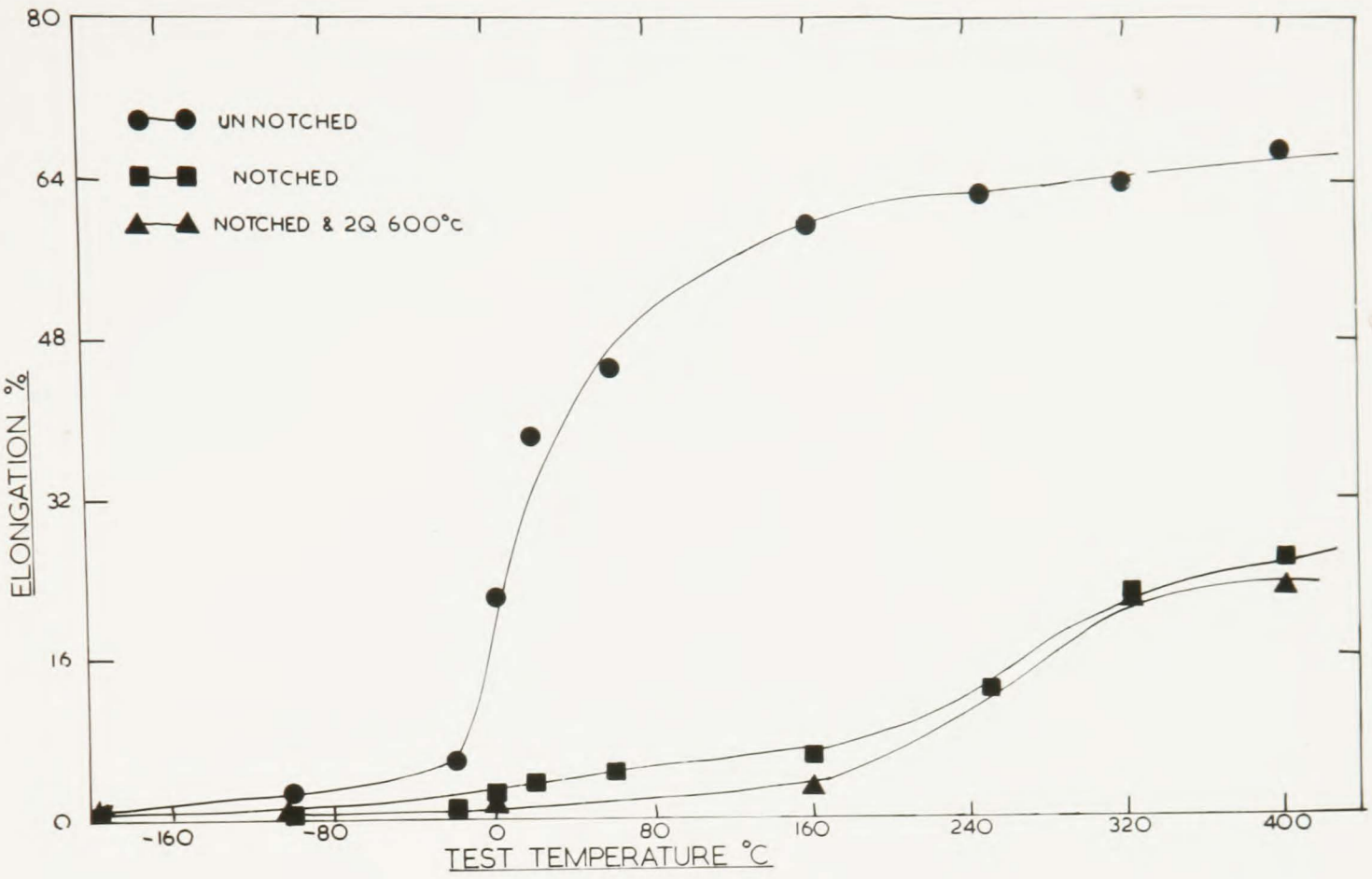


FIGURE 122

Elongation as a function of test temperature showing the effect of a notch.

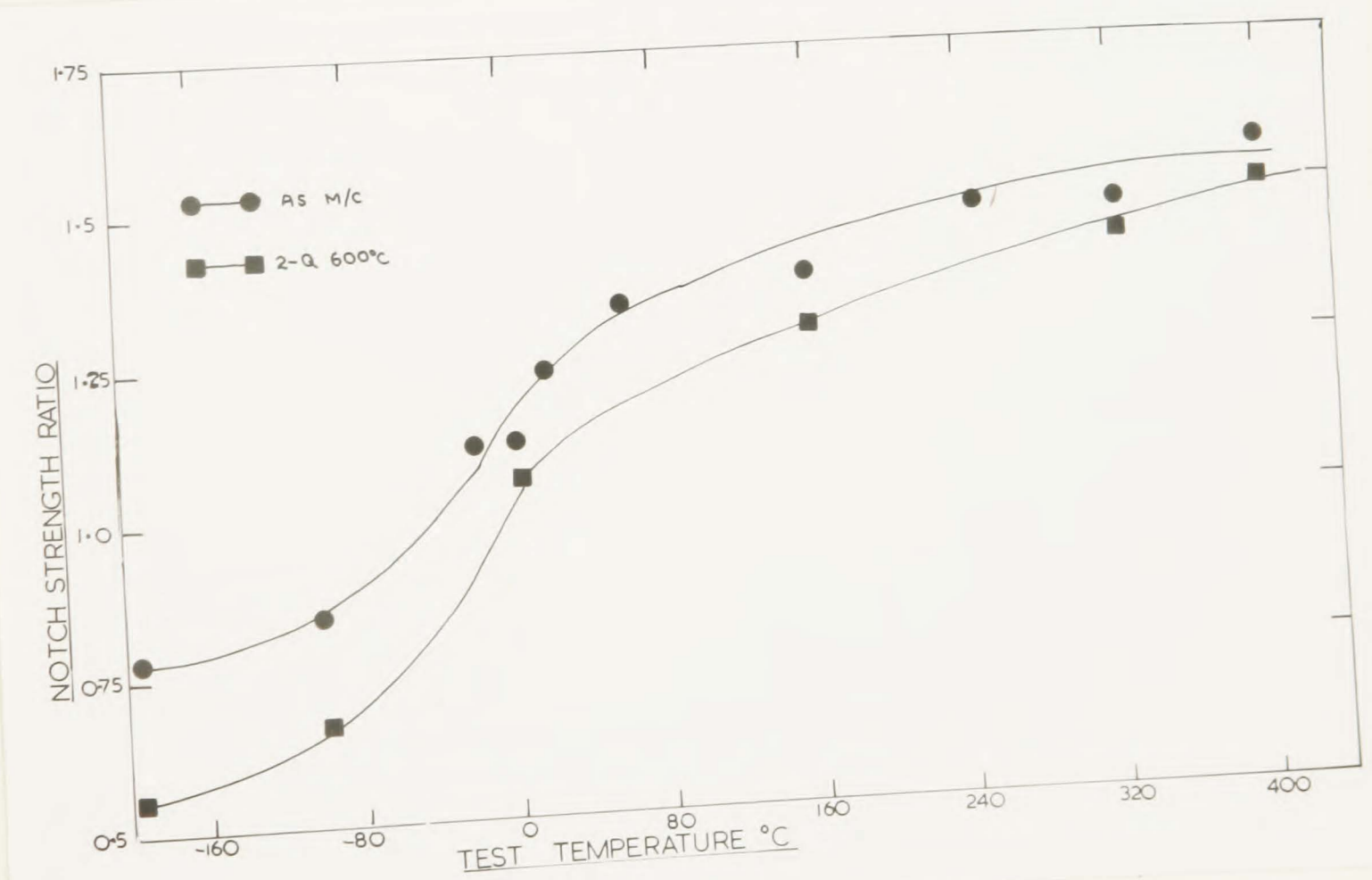


FIGURE 123

N.S.R. as a function of test temperature

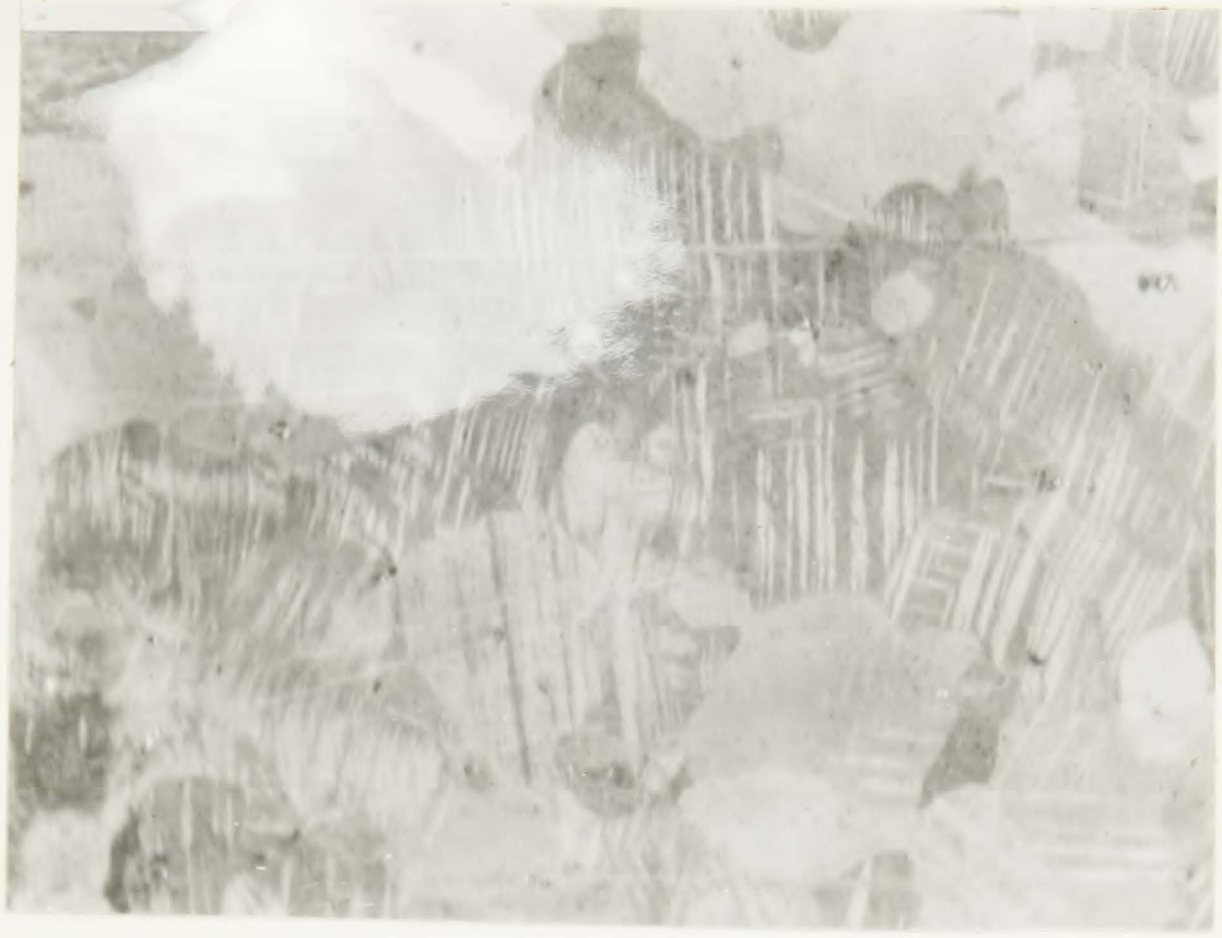


FIGURE 124 x175

Twinning near the shoulder of an alpha annealed specimen.
Note that twins are predominantly in one direction.

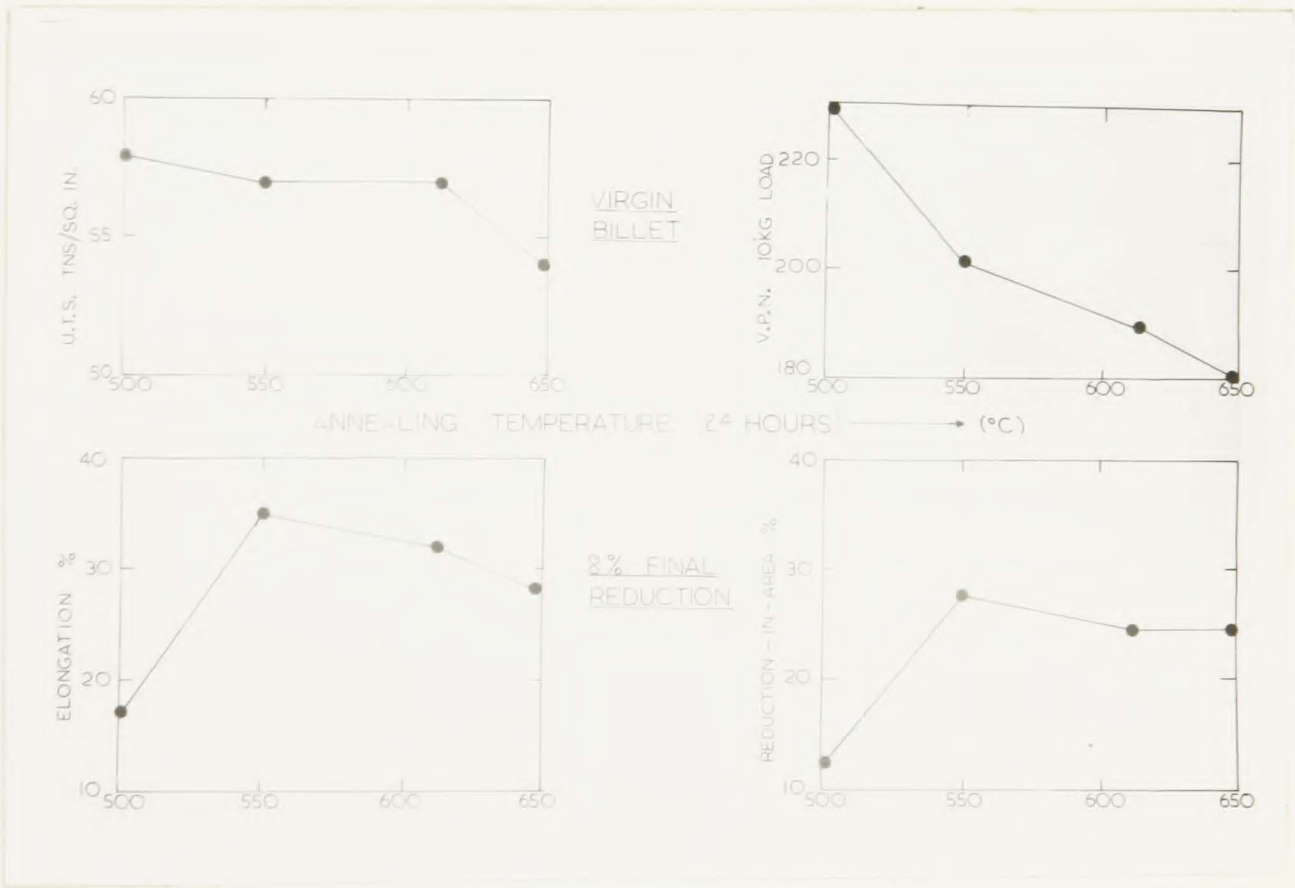


FIGURE 125

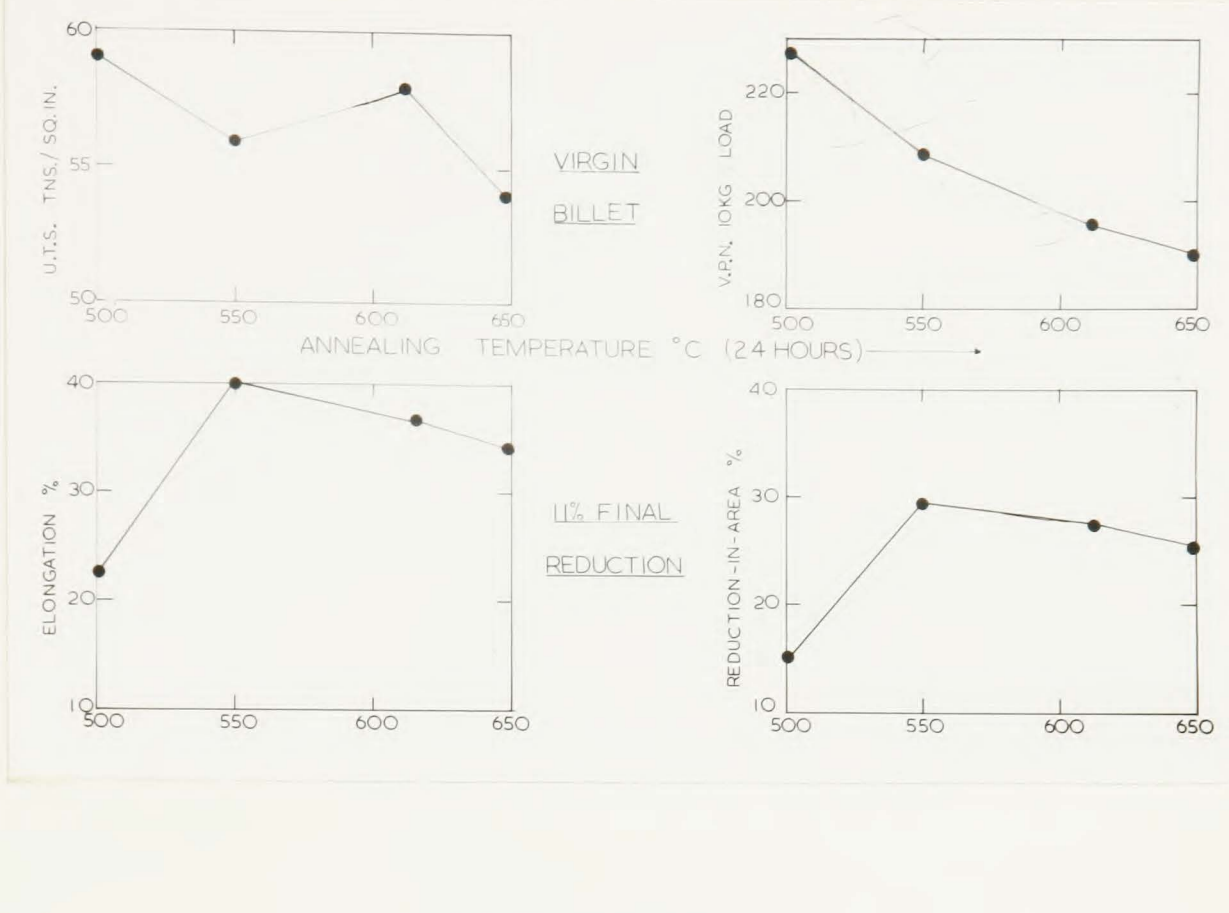


FIGURE 126

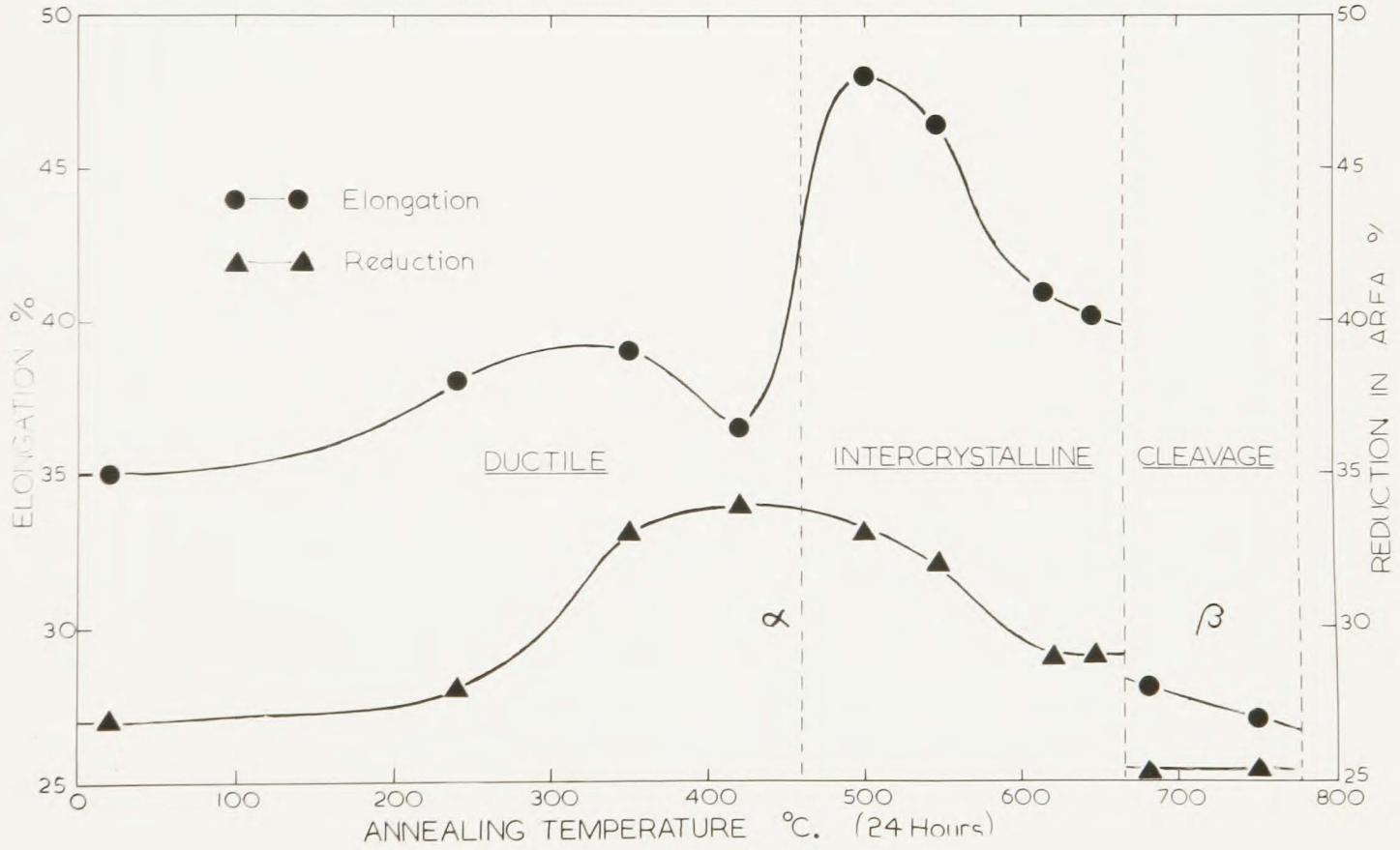


FIGURE 127

Elongation as a function of annealing temperature after 28% rolling reduction at 300°C.

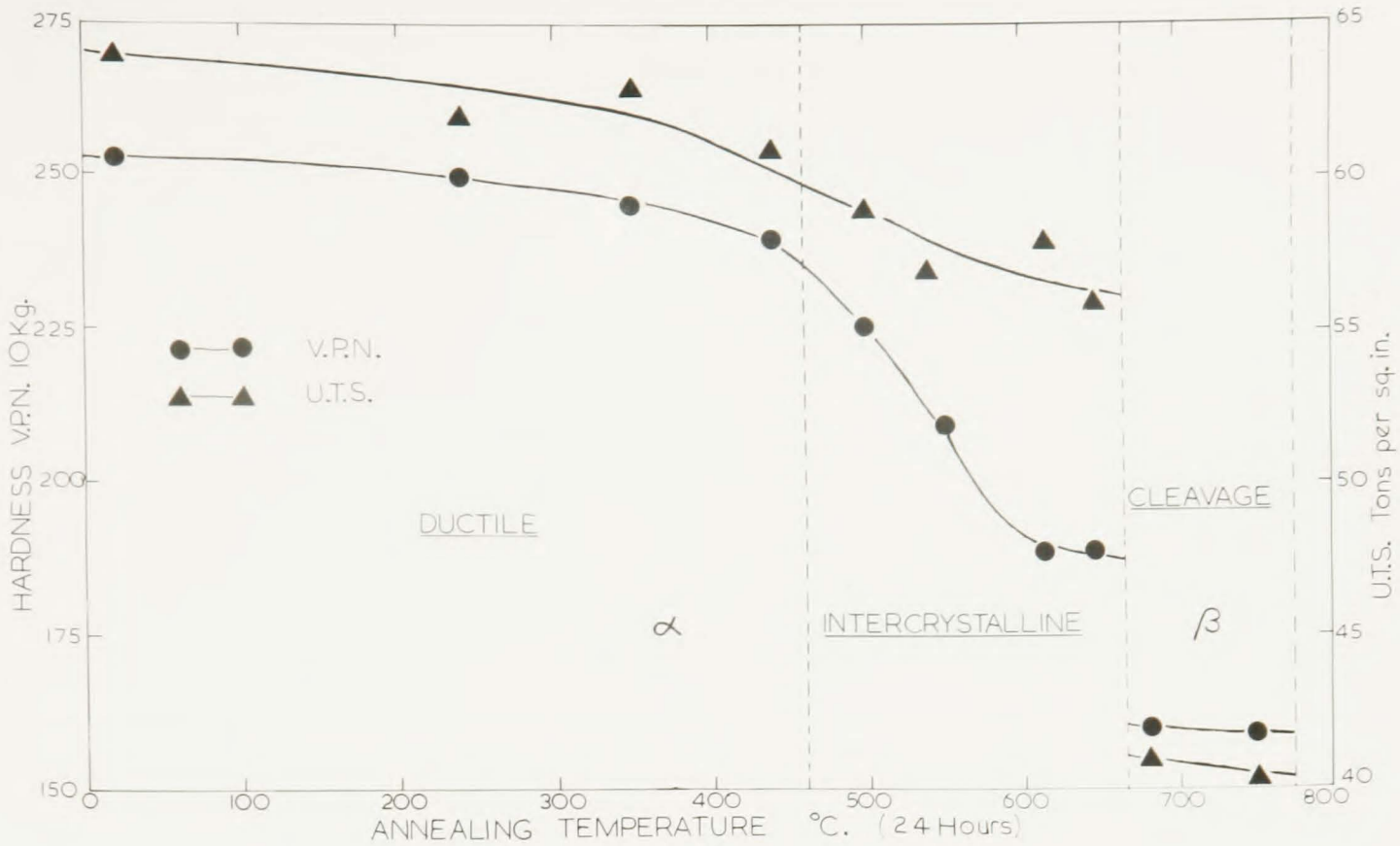


FIGURE 128

Hardness and U.T.S. as a function of annealing temperature after 28% rolling reduction at 300°C.

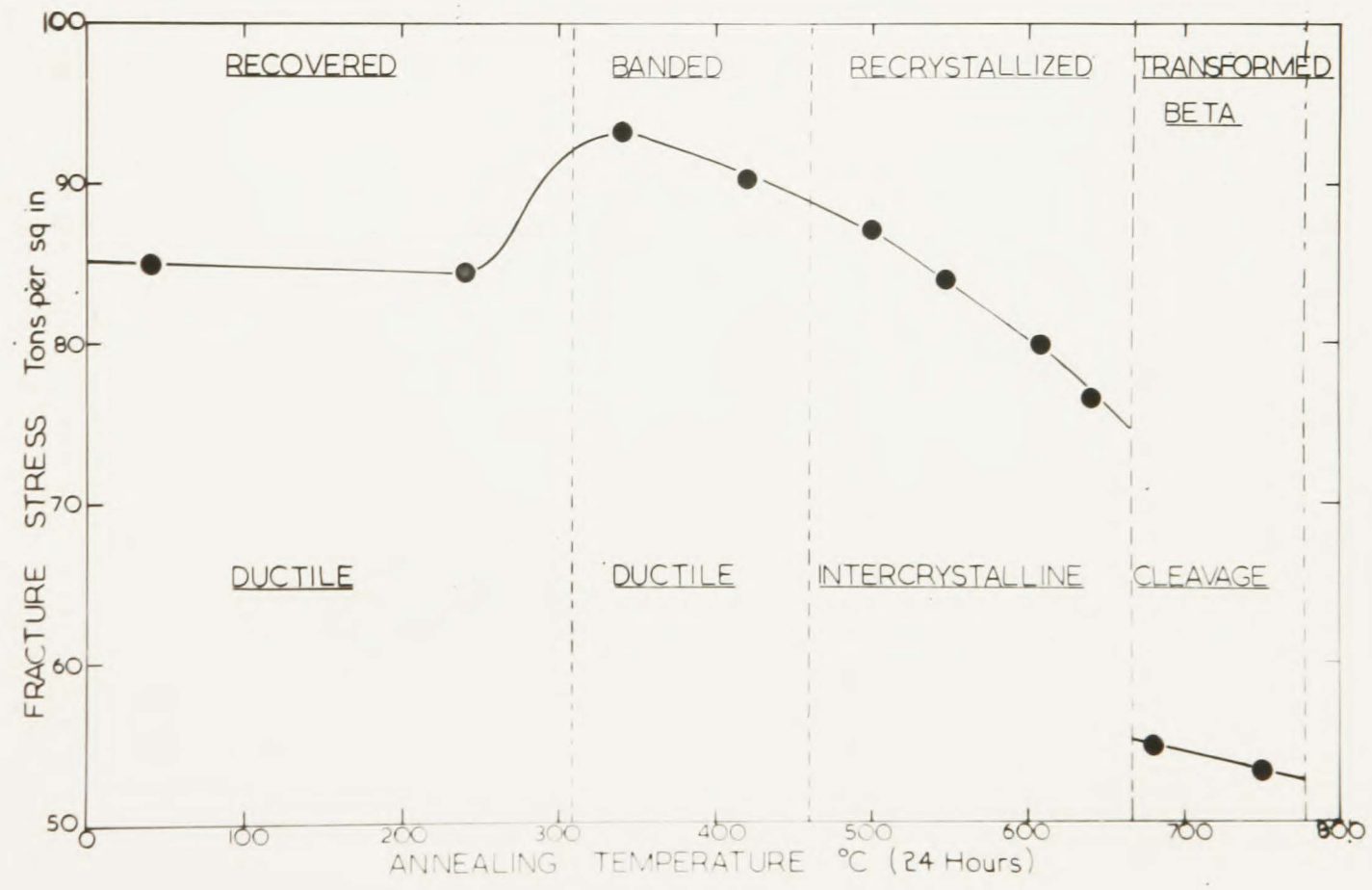


FIGURE 129

Fracture stress as a function of annealing temperature after 28% rolling reduction at 300°C.

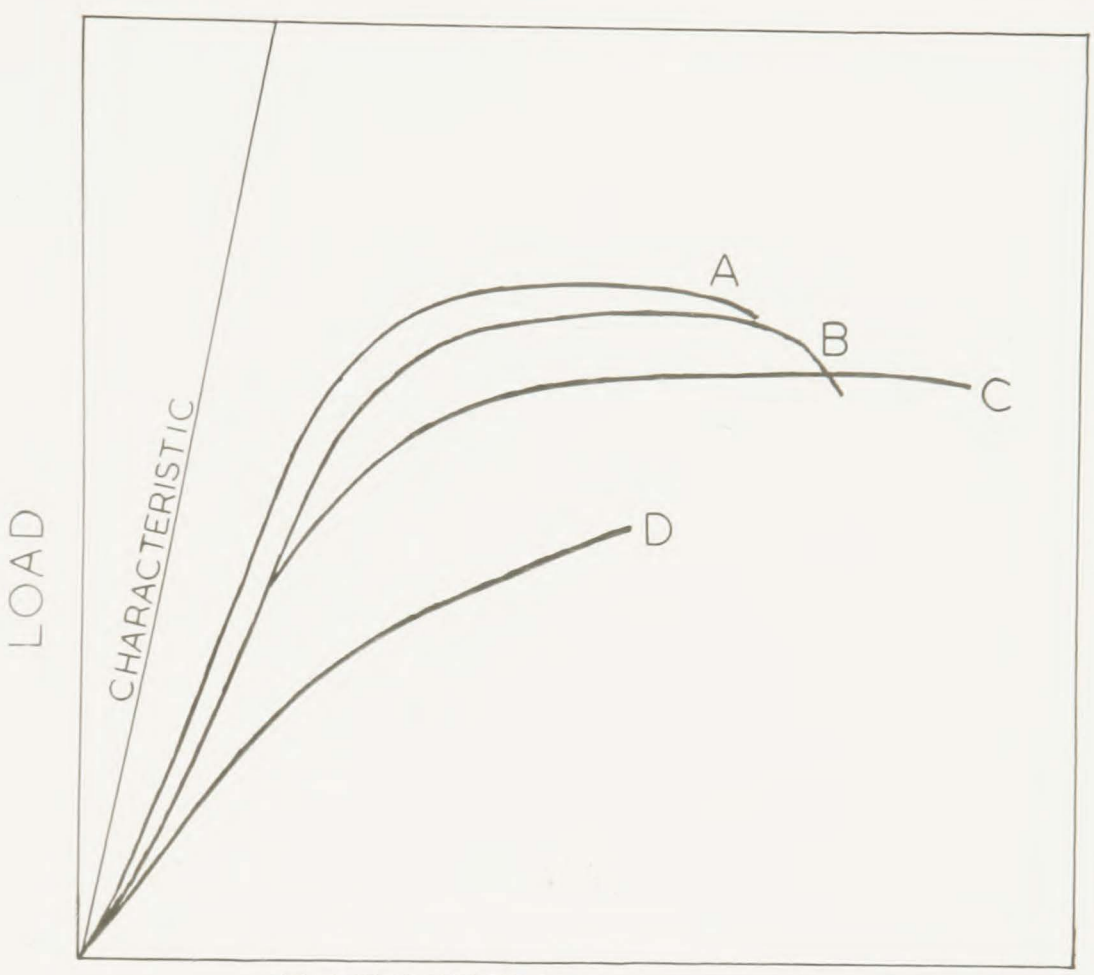


FIGURE 130

Some examples of load/extension curves obtained at room temperature after various treatments. 'A' is material rolled 28% reduction at 300°C (deformed structure); 'B' is rolled 28% and annealed at 348°C (banded structure); 'C' is annealed at 545°C after 28% reduction (fully recrystallized fine grain structure); and 'D' is rolled and annealed at 680°C (beta treated) which results in a very coarse grain structure.